MycoKeys 77: 1–25 (2021)
doi: 10.3897/mycokeys.77.60862
https://mycokeys.pensoft.net

RESEARCH ARTICLE

A peer-reviewed open-access journal
MycoKeys
Launched to accelerate biodiversity research

Novel species of *Cladosporium* from environmental sources in Spain

Isabel Iturrieta-González[1], Dania García[1], Josepa Gené[1]

1 *Unitat de Micologia, Facultat de Medicina i Ciències de la Salut and IISPV, Universitat Rovira i Virgili, 43201, Reus, Tarragona, Spain*

Corresponding author: Josepa Gené (josepa.gene@urv.cat)

Academic editor: T. Lumbsch | Received 17 November 2020 | Accepted 7 December 2020 | Published 5 January 2021

Citation: Iturrieta-González I, García D, Gené J (2021) Novel species of *Cladosporium* from environmental sources in Spain. MycoKeys 77: 1–25. https://doi.org/10.3897/mycokeys.77.60862

Abstract

Cladosporium is a monophyletic genus in *Cladosporiaceae* (*Cladosporiales*, *Dothideomycetes*) whose species are mainly found as saprobes and endophytes, but it also includes fungi pathogenic for plants, animals and human. Species identification is currently based on three genetic markers, viz., the internal transcribed spacer regions (ITS) of the rDNA, and partial fragments of actin (*act*) and the translation elongation factor 1-α (*tef1*) genes. Using this phylogenetic approach and from morphological differences, we have recognized six new species originating from soil, herbivore dung and plant material collected at different Spanish locations. They are proposed as *Cladosporium caprifimosum*, *C. coprophilum*, *C. fuscoviride* and *C. lentulum* belonging in the *C. cladosporioides* species complex, and *C. pseudotenellum* and *C. submersum* belonging in the *C. herbarum* species complex. This study revealed that herbivore dung represented a reservoir of novel lineages in the genus *Cladosporium*.

Keywords

Cladosporiales, *Cladosporiaceae*, hyphomycetes, phylogeny, Spain, taxonomy

Introduction

Cladosporium is a ubiquitous genus in the family *Cladosporiaceae* of the recently proposed order *Cladosporiales* in the *Dothideomycetes* (Abdollahzadeh et al. 2020). Their species inhabit a wide range of substrates and have been reported to be among the

most common fungi in both indoor and outdoor environments, including in extreme ecological niches (Flannigan et al. 2002; Bensch et al. 2010, 2012, 2018; Sandoval-Denis et al. 2015; Temperini et al. 2018; Chung et al. 2019). Most *Cladosporium* species are saprobic, but some have also been reported as endophytes, hyperparasites on other fungi and plant as well as animal pathogens, including humans (Heuchert et al. 2005; Sandoval-Denis et al. 2016; de Hoog et al. 2017; Marin-Felix et al. 2017). Certain species show the ability to produce compounds of medical interest or are relevant as potential biocontrol agents for plant disease (Köhl et al. 2015; Khan et al. 2016; Adorisio et al. 2019).

Cladosporium is morphologically characterized mainly by its asexual morph, which shows differentiated conidiophores producing acropetal chains of conidia from mono- or polyblastic conidiogenous cells. Both conidiogenous cells and conidia exhibit conidiogenous loci (scars) with a unique coronate structure, which is composed of a central convex dome surrounded by a raised periclinal rim, usually thickened, refractive and darkly pigmented (David 1997). Based on these features and DNA phylogeny derived from the LSU nrRNA gene, the genus has been well-delineated and distinguished from other cladosporium-like genera such as *Hyalodendriella*, *Ochrocladosporium*, *Rachicladosporium*, *Rhizocladosporium*, *Toxicocladosporium*, *Verrucocladosporium* and the recently described genus *Neocladosporium* (Crous et al. 2007; Bezerra et al. 2017). Phylogenetic relationships among species of *Cladosporium s. str.* have been studied extensively over the last decade by a multi-locus sequence analysis approach with sequences of the internal transcribed spacers (ITS) of the rDNA and of the two protein encoding genes, translation elongation factor 1-α (*tef1*) and actin (*act*). The molecular approach combined with morphological features have allowed recognition of more than 230 species within the genus, which are split into three species complexes, i.e., the *Cladosporium cladosporioides*, *Cladosporium herbarum* and *Cladosporium sphaerospermum* complex (Schubert et al. 2007; Bensch et al. 2010, 2012, 2015, 2018; Sandoval-Denis et al. 2016; Marin-Felix et al. 2017).

While aiming to explore the diversity of microfungi from Spain, several interesting *Cladosporium* isolates have been recovered from different environmental samples. Using the above mentioned polyphasic approach and following the Genealogical Phylogenetic Species Recognition (GCPSR) criterion (Taylor et al. 2000), the taxonomy of those isolates has been resolved in six novel species for science; four pertaining to the *C. cladosporioides* species complex and two to the *C. herbarum* complex.

Material and methods

Samples and isolates

Samples of soil, plant debris and herbivore dung were collected between 2016 and 2018 at various Spanish locations. Dilution plating methods were used for isolating fungi from soil and dung samples following the procedure described by Crous et al.

(2009) and a modified protocol described by Waksman (1922), respectively. In addition, soil samples were also processed by a baiting technique using small pieces of wood and filter paper as baits on the soil surface (Calduch et al. 2004). Samples of plant debris and also part of the herbivore dung were incubated in moist chambers following the procedures described by Castañeda-Ruiz et al. (2016) and Richardson (2001), respectively.

Among the cladosporium-like fungi found, we recovered eight isolates in pure culture which did not match any of the currently accepted species within the genus *Cladosporium* (Table 1). The isolates were deposited in the culture collection of the Universitat Rovira i Virgili (FMR, Reus, Spain) and, once phylogenetically and morphologically characterized, living cultures of the novel species and dry cultures for holotypes were also deposited in the Westerdijk Fungal Biodiversity Institute (CBS; Utrecht, the Netherlands). Nomenclatural novelties and descriptions were deposited in MycoBank (Crous et al. 2004).

DNA extraction, amplification and sequencing

Genomic DNA was extracted from cultures growing on potato dextrose agar (PDA; Pronadisa, Spain) after 7 days of incubation at 25 °C, following the modified protocol of Müller et al. (1998). Protocols listed previously in Sandoval-Denis et al. (2016) were used for amplification and sequencing. The primer pairs used were ITS5/ITS4 (White et al. 1990) to amplify the ITS region including the 5.8S gene of the rDNA, EF-728F/EF-986R to amplify a partial fragment of the *tef1* gene, and ACT-512F/ACT-783R to amplify a partial fragment of *act* gene (Carbone and Kohn 1999). PCR products were purified and stored at -20 °C until sequencing. The sequences were obtained using the same primers at Macrogen Europe (Macrogen Inc. Amsterdam, The Netherlands). Finally, the software SeqMan v. 7.0.0 (DNAStarLasergene, Madison, WI, USA) was used to assemble, edit and obtain the consensus sequences, which were then deposited in GenBank of the National Center for Biotechnology Information (NCBI) (Table 1).

Sequence alignment and phylogenetic analysis

The sequences obtained were compared with other fungal sequences deposited in the NCBI database through the BLASTn tool. Alignment of those sequences and the phylogenetic analysis for each locus were performed with the MEGA (Molecular Evolutionary Genetics Analysis) program v. 6.0. (Tamura et al. 2013), using ClustalW algorithm (Thompson et al. 1994) and refined with MUSCLE (Edgar 2004) or manually if necessary, on the same platform. Since the isolates under study were related to the *C. cladosporioides* and *C. herbarum* species complexes, we also carried out alignments including sequence data of ex-type and reference strains of all the species from both complexes retrieved from the GenBank and mainly published by Schubert et al. (2007, 2009), Bensch et al. (2010, 2012, 2015, 2018), Sandoval-Denis et al. (2016) and Marin-Felix et al. (2017) (Suppl. material 1: Table S1).

Table 1. *Cladosporium* species, strain information and GenBank accession numbers for sequences obtained in this study.

Species	Strain number[1]	Substrate	GenBank nucleotide accession no. for[2]:		
			ITS	*act*	*tef1*
C. caprifimosum	FMR 16532[T]	Goat dung	LR813198	LR813205	LR813210
C. coprophilum	FMR 16101	Unidentified herbivore dung	LR813199	LR813204	LR813211
	FMR 16164[T]	Unidentified herbivore dung	LR813201	LR813207	LR813213
C. fuscoviride	FMR 16385[T]	Garden soil	LR813200	LR813206	LR813212
C. lentulum	FMR 16288[T]	Unidentified leaf litter	LR813203	LR813209	LR813215
	FMR 16389	Unidentified herbivore dung	LR813202	LR813208	LR813214
C. pseudotenellum	FMR 16231[T]	Garden soil	LR813145	LR813146	LR813196
C. submersum	FMR 17264[T]	Submerged plant material	LR813144	LR813195	LR813197

[1] FMR: Facultat de Medicina i Ciències de la Salut, Reus, Spain. [T] indicate ex-type strains.
[2] ITS: Internal transcribed spacer regions of the rDNA and 5.8S region; *act*: partial actin gene; *tef1*: partial translation elongation factor 1-alpha gene.

Phylogenetic reconstructions were made with the three phylogenetic markers (ITS, *act* and *tef1*) recommended for an accurate identification at the species level (Bensch et al. 2010, 2018; Marin-Felix et al. 2017) using Maximum Likelihood (ML), Maximum Parsimony (MP), and Bayesian Inference (BI) analyses, with the Mega software v. 6.0. for the former two (Tamura et al. 2013) and with MrBayes v.3.2.6 for the latter one (Ronquist et al. 2012). Phylogenetic concordance of the three-locus datasets was evaluated through Incongruence Length Difference (ILD) implemented in the Winclada program (Farris et al. 1994) and also by visual comparison of the individual phylogenies in order to assess any incongruent results between nodes with high statistical support.

Determined by Mega software v. 6.0., the best nucleotide substitution model for ML analysis of the *C. cladosporioides* complex was General Time Reversible with Gamma distribution and invariant sites (GTR+G+I), and for the *C. herbarum* complex the best was the Kimura 2-parameter with Gamma distribution and invariant sites (K2+G+I). Bootstrap support value (MLBS) ≥ 70% was considered significant (Hillis and Bull 1993).

The MP analysis was performed using the heuristic search option with TBR (tree bisection and reconnection) branch swapping and 1,000 random sequence additions. Tree length (TL), consistency index (CI), retention index (RI), rescaled consistency index (RCI) were calculated. Bootstrap analysis was based on 1,000 replications. Maximum parsimony bootstrap support value (PBS) ≥ 70% was considered significant (Hillis and Bull 1993).

Determined by jModelTest (Posada 2008), the best nucleotide substitution models for the BI of the *C. cladosporioides* complex were Jukes Cantor with invariant sites (JC+I) for ITS, General Time Reversible with Gamma distribution (GTR+G) for *tef1* and Hasegawa-Kishino-Yano with Gamma distribution (HKY+G) for *act*; and for the *C. herbarum* complex the best were the Kimura 2-parameter with Gamma distribution (K80+G) for ITS, Hasegawa-Kishino-Yano with Gamma distribution (HKY+G) for *tef1* and *act.* The parameter settings used in these analyses were two simultaneous runs of 10,000,000 generations, and four Markov chains, sampled every 1,000 generations. The 50% majority rule consensus tree and posterior probability values (PP)

were calculated after discarding the first 25% of the samples. A PP value of ≥ 0.95 was considered significant (Hespanhol et al. 2019).

Final sequence alignments and trees generated in this study were registered in TreeBASE under the submission number S27350 (http://treebase.org).

Phenotypic studies

Microscopic features of the *Cladosporium* isolates were obtained from cultures growing on synthetic nutrient-poor agar (SNA; 1 g of KH_2PO_4, 1 g of KNO_3, 0.5 g of $MgSO_4 \times 7H_2O$, 0.5 g of KCl, 0.2 g of glucose, 0.2 g of sucrose, 14 g of bacteriological agar, 1 L of distilled water) after 7 to 14 days at 25 °C in the dark, mounted onto semi-permanent slides with Shear's solution (Bensch et al. 2018). At least 30 measurements were taken to calculate length and width ranges of the conidia and ramoconidia, given as the mean ± standard deviation in the descriptions. Macroscopic characterization of the colonies was made on PDA (Pronadisa, Spain), oatmeal agar (OA; 30 g of oatmeal, 13 g of bacteriological agar, 1 L distilled water) and SNA after 14 days of incubation at 25 °C in darkness. Colour notation of the colonies in descriptions were from Kornerup and Wanscher (1978). In addition, cardinal temperatures for the fungal growth were determined on PDA cultures after 14 days at temperatures ranging from 5 to 40 °C at intervals of 5 °C.

Results

Phylogeny

Three individual phylogenies (ITS, *tef1* and *act*), carried out for the *C. cladosporioides* and *C. herbarum* species complexes, were visually very similar and the ILD test showed that the three loci datasets were congruent in both complexes ($P = 0.16$) and could be combined. Phylogenies obtained by ML, MP and BI also showed a visual topological congruence and were similar to that obtained by other authors (Marin-Felix et al. 2017; Bensch et al. 2018). The combined alignment of the three mentioned loci datasets encompassed 101 sequences in the *C. cladosporioides* complex and 58 sequences in *C. herbarum* complex. The alignment for the former group comprised 1,060 bp (ITS 484 bp, *tef1* 313 bp and *act* 263 bp), which included 424 bp variable sites (ITS 47 bp, *tef1* 239 bp and *act* 138 bp) and 319 bp phylogenetically informative sites (ITS 25 bp, *tef1* 193 bp and *act* 101 bp). Two species of the *C. sphaerospermum* complex, *C. sphaerospermum* CBS 193.54 and *C. longissimum* CBS 300.96, were included as outgroup in this first multi-locus phylogeny (Fig. 1). For the maximum parsimony analysis the maximum of 1,000 equally most parsimonious trees were saved (Tree length = 1614; CI = 0.294; RI = 0.666; RCI = 0.214).

For the *C. herbarum* species complex, the alignment comprised 1,057 bp (ITS 503 bp, *tef1* 309 bp and *act* 245 bp) with 407 bp variable sites (ITS 101 bp, *tef1* 186 bp

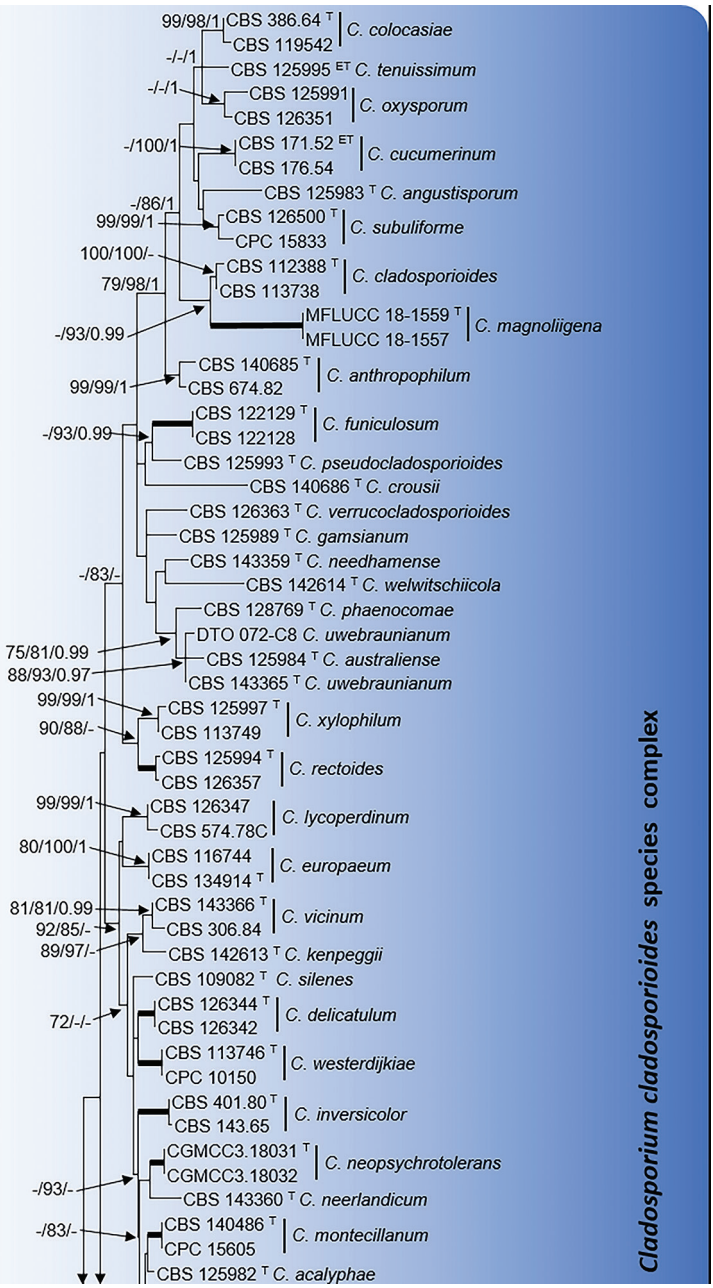

Figure 1. Maximum likelihood (ML) tree obtained from the combined analysis of ITS, *tef1* and *act* sequences of 101 strains from the *C. cladosporioides* complex. The tree is rooted with *C. sphaerospermum* CBS 193.54 and *C. longissimum* CBS 300.96. Numbers on the branches represent ML bootstrap support values (MLBS) ≥70%, followed by Maximum Parsimony bootstrap support values (PBS) ≥70% and Bayesian posterior probabilities (PP) ≥0.95, lower values are indicate as "-". Bold branches indicate MLBS/PBS/PP of 100/100/1. Names of species newly described are indicated in bold. Branch lengths are proportional to distance. ^{T} Ex-type strain. ^{ET} Ex-epitype strain.

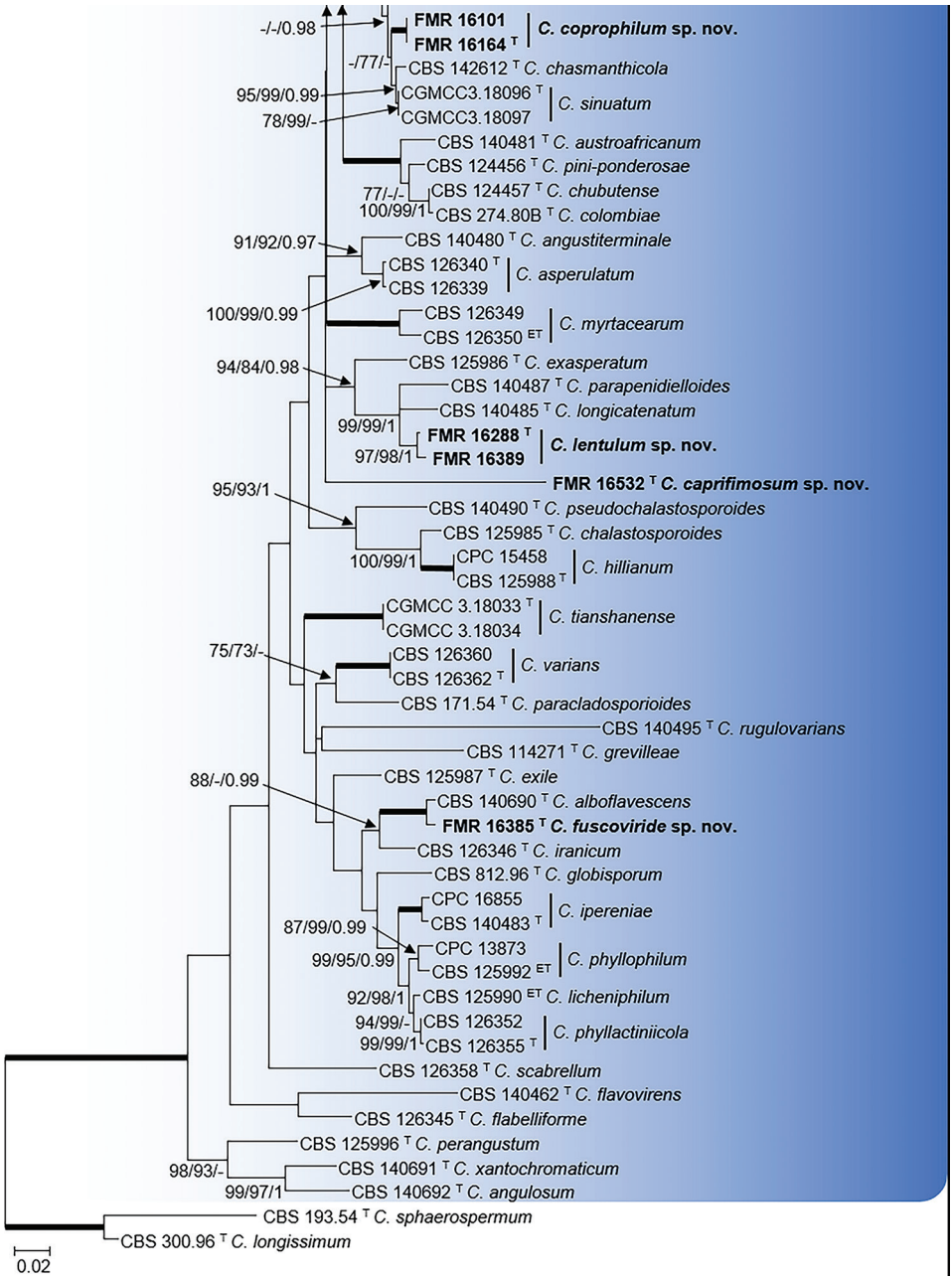

Figure 1. Continued.

and *act* 120 bp) and 240 bp phylogenetically informative sites (ITS 27 bp, *tef1* 123 bp and *act* 90 bp), using *Cercospora beticola* (CBS 116456) as outgroup (Fig. 2). For the maximum parsimony analysis the maximum of 1,000 equally most parsimonious trees were saved (Tree length = 898; CI = 0.537; RI = 0.661; RCI = 0.355).

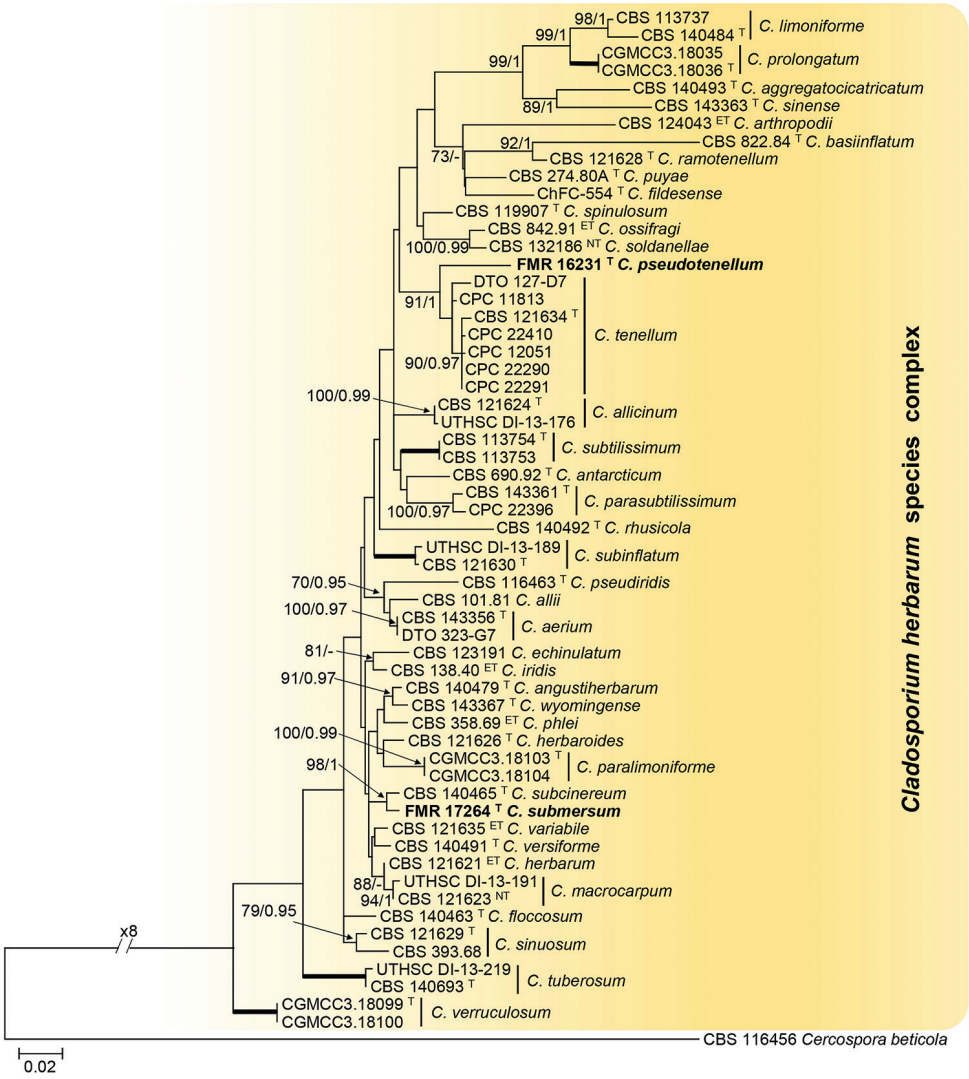

Figure 2. Maximum likelihood (ML) tree obtained from the combined analysis of ITS, *tef1* and *act* sequences of 58 strains from *C. herbarum* complex. The tree is rooted with *Cercospora beticola* CBS 116456. Numbers on the branches represent ML bootstrap support values (MLBS) ≥70%, followed by Maximum Parsimony bootstrap support values (PBS) ≥70% and Bayesian posterior probabilities (PP) ≥ 0.95, lower values are indicate as "-". Bold branches indicate MLBS/PBS/PP of 100/100/1. Names of species newly described are indicated in bold. Branch lengths are proportional to distance. ^{T} Ex-type strain. ^{ET} ex-epitype strain. ^{NT} ex-neotype strain.

The eight unidentified isolates did not match any known lineage of *Cladosporium* species, six were related to the *C. cladosporioides* species complex and two to the *C. herbarum* complex, and together they represented six new phylogenetic species in the genus.

In the combined phylogeny of the *C. cladosporioides* complex, 71 species were delineated (Fig. 1). The isolates FMR 16101 and FMR 16164 formed a strongly supported

terminal clade representative for a unique taxon, but with an uncertain phylogenetic position due to the low statistical support (- MLBS / 77 PBS / - PP) for the nearest lineages of *C. chasmanthicola* and *C. sinuatum*. Both unidentified isolates were genetically identical and showed a percentage of identity with the ex-type strains of these latter species of 97.22% and 97.65% for *act*, and 96.79% and 97.50% for *tef1*, respectively. A second undescribed monophyletic terminal clade included FMR 16288 and FMR 16389, which grouped with the lineages of *C. exasperatum*, *C. parapenidielloides* and *C. longicatenatum* in a clade with highly supported values (94 MLBS / 84 PBS / 0.98 PP). However, both isolates showed a sufficient genetic distance to be considered a distinct species from the closest, *C. longicatenatum* and , with a sequence similarity of 95.75% and 95.28% for *act* and 90.87% and 90.48% for *tef1* respect to the ex-type strains of these two known species. FMR 16532 and FMR 16385 formed two distinct monophyletic branches. The former showed an uncertain phylogenetic position with the species in the complex; the comparison of its sequences with those of the GenBank dataset through the BLASTn tool showed that the ITS was 100% similar with several species of the *C. cladosporioides* complex, while sequences of *act* and *tef1* were 99.12% and 89.02% similar with sequences belonging to *C. asperulatum* (UTHSC DI-13-216/GenBank LN834541 and CBS 113744/GenBank HM148237, respectively). FMR 16385 was closely related to the ex-type strain of *C. alboflavescens* (100 MLBS / 100 PBS / 1 PP). The percentages of identity between these latter two fungi (97.79% for *act* and 96.75% for *tef1*) together with morphological differences observed allow us to consider them distinct taxa.

In the *C. herbarum* complex, 40 species were phylogenetically well-delimited, including two novel lineages each represented by FMR 16231 and FMR 17264 (Fig. 2). Both were genetically and morphologically differentiated from their closest relatives, *C. tenellum* and *C. subcinereum*, respectively. The percentages of identity observed between the isolate FMR 16231 and the ex-type strain of *C. tenellum* (CBS 121634) were 97.78%, 83.76% and 100% for *act*, *tef1* and ITS, respectively, and between FMR 17264 and the ex-type strain of *C. subcinereum* (CBS 140465) were 98.57%, 95.98% and 100% for *act*, *tef1* and ITS, respectively.

The percentages of identity between the six putative new *Cladosporium* species and their relatives are summarized in Table 2. The novel taxa are described and illustrated in the taxonomy section below.

Taxonomy

Cladosporium caprifimosum **Iturrieta-González, Dania García, Gené, sp. nov.**
MycoBank No: 836074
Fig. 3

Etymology. The name refers to goat dung, the substrate where the species was isolated (capra = goat and fimus = dung, with the adjectival Latin suffix -osus, indicating abundance or full or marked development).

Table 2. Percentage of identity between the novel *Cladosporium* and their closest species.

Species	Closest taxa	Loci		
		ITS	*act*	*tef1*
C. caprifimosum (FMR 16532)	*C. asperulatum*[1]	100	99.12	89.02
C. coprophilum (FMR 16101 and 16164)	*C. chasmanthicola*	100	97.22	96.79
	C. sinuatum[1]	100	97.65	97.50
C. fuscoviride (FMR 16385)	*C. alboflavescens*	100	97.79	96.75
C. lentulum (FMR 16288 and 16389)	*C. exasperatum*	100	92.2	81.4–82.7
	C. longicatenatum	100	95.75	90.87
	C. parapenidielloides	100	95.28	90.48
C. pseudotenellum (FMR 16231)	*C. tenellum*[1]	100	97.5–100	83.2–84.1
C. submersum (FMR 17264)	*C. subcinereum*	100	98.57	95.98

[1] Species for which the percentage of identity was defined based on the ex-type strain and additional reference strains (see Figs 1 and 2).
[2] Species for which the percentage of identity was based on a NCBI BLAST search.

Type. Spain, Catalonia, Tarragona province, La Fatarella, from goat dung, Mar. 2017, *I. Iturrieta-González, M. Guevara-Suarez & J. Guarro* (holotype CBS H-24469; cultures ex-type FMR 16532, CBS 146918).

Description. *Mycelium* in vitro superficial and immersed, composed of septate, branched, subhyaline, smooth to verruculose hyphae, 1–2 µm wide. *Conidiophores* dimorphic, micronematous or macronematous, arising from lateral or terminal hyphae, erect to slightly flexuous, non-nodulose, septate, branched or unbranched, 8–137 µm long, 2–4 µm wide, pale brown, slightly verrucose. *Conidiogenous cells* integrated, terminal, cylindrical, sometimes geniculate at the apex, 22–44 × 3–4 µm, bearing up to four conidiogenous loci, darkened and refractive. *Ramoconidia* aseptate, almost cylindrical, 10–24 × 2–4 µm [av. (± SD) 15.8 (± 3.4) × 3.1 (± 0.45)], olive to pale brown, smooth. *Conidia* forming branched chains, with up to five conidia in the terminal unbranched part, aseptate, olive to pale brown, smooth; *small terminal conidia* ellipsoidal to obovoid, 3–7 × 2–3.5 µm [av. (± SD) 5.7 (± 0.83) × 2.4 (± 0.43)]; *intercalary conidia* ellipsoidal to somewhat fusiform, 6–11.5 × 2–3 µm [av. (± SD) 7.8 (± 1.06) × 2.6 (± 0.39)]; *secondary ramoconidia* ellipsoidal to almost cylindrical, 9–14 × 2.5–3.5 µm [av. (± SD) 11.3 (± 1.6) × 2.9 (± 0.26)].

Culture characteristics (14 d at 25 °C). Colonies on OA reaching 24–25 mm diam., dark green (30F8), flat, slightly dusty, aerial mycelium scarce, margin regular; reverse dark green (30F8) to black. On PDA attaining 34–35 mm diam., olive (3E6/3F4), slightly umbonate, radially folded, velvety, aerial mycelium scarce, margin slightly lobate; reverse dark green (30F8) to olive (3E4). On SNA reaching 25–26 mm diam., olive (3E8), flat, dusty, aerial mycelium scarce, margin regular; reverse dark green (30F8) to black.

Cardinal temperature for growth. Optimum 20 °C, maximum 30 °C, minimum 5 °C.

Distribution. Spain.

Notes. Although *C. caprifimosum* clearly belongs to the *C. cladosporioides* species complex, our multi-locus analysis did not reveal any phylogenetic relationship with other species in the complex. It is represented by a single branch placed distance from other *Cladosporium* species (Fig. 1). *Cladosporium caprifimosum* differs from the other novel species proposed here mainly by its aseptate and smooth conidia.

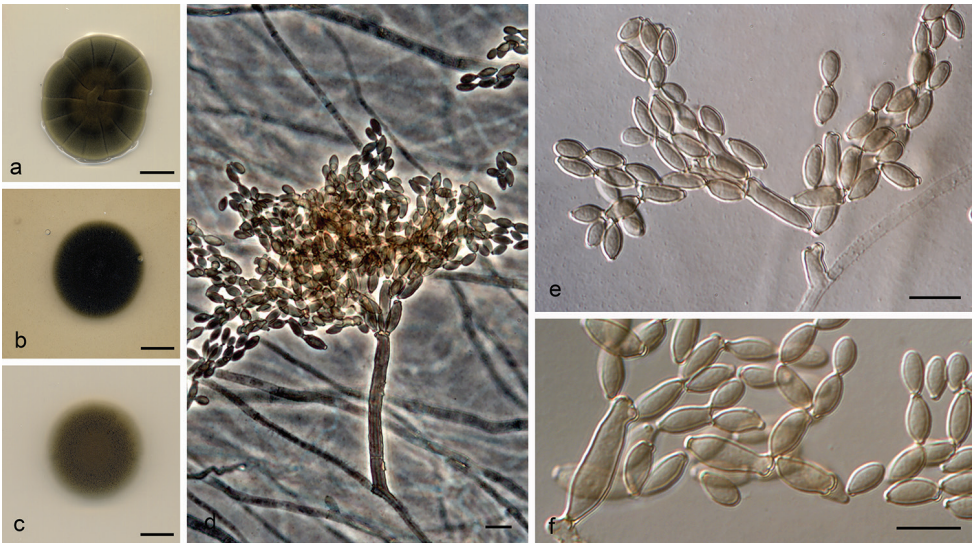

Figure 3. *Cladosporium caprifimosum* (ex-type FMR 16532) **a–c** colonies on PDA, OA and SNA after 14 days at 25 °C **d–e** conidiophores **f** ramoconidia and conidia. Scale bars: 10 mm (**a–c**); 10 µm (**d–f**).

Cladosporium coprophilum **Iturrieta-González, Dania García, Gené, sp. nov.**
MycoBank No: 836075
Fig. 4

Etymology. Name refers to the substrate where the species was isolated, unidentified herbivore dung (ancient Greek, kópros = dung + phílos = loving).

Type. Spain, Extremadura, Badajoz province, Granja de Torrehermosa, unidentified herbivore dung, Jan. 2017, *J. Cano* (holotype CBS H-24470; cultures ex-type FMR 16164, CBS 144919).

Description. *Mycelium* in vitro superficial and immersed, composed of septate, branched, pale brown, smooth hyphae, 3–5 µm wide. *Conidiophores* macronematous, arising laterally or terminally from hyphae, erect to slightly flexuous, non-nodulose, septate, unbranched, up to 124 µm long, 3–4 µm wide, pale brown, smooth. *Conidiogenous cells* integrated, terminal, rarely intercalary, cylindrical, (7–)14–33 × (2–)3–4 µm, bearing up to 3 conidiogenous loci, slightly darkened and refractive. *Ramoconidia* 0(–1)-septate, subcylindrical to cylindrical, 9–19 × 3–5 µm [av. (± SD) 12.3 (± 2.8) × 3.9 (± 0.54)], pale brown, smooth. *Conidia* forming branched chains, with up to five conidia in the terminal unbranched part, aseptate, pale brown, smooth to verruculose; *small terminal conidia* ellipsoidal to slightly obovoid, 4.5–7 × 2.5–4 µm [av. (± SD) 6 (± 0.64) × 3.1 (± 0.31)]; *intercalary conidia* ellipsoidal, 6–10.5 × 2.5–4 µm [av. (± SD) 7.7 (± 1.32) × 3.3 (± 0.37)]; *secondary ramoconidia* subcylindrical to cylindrical, 7–12.5 µm long × 3–5 µm [av. (± SD) 9.6 (± 1.7) × 4.2 (± 0.51)].

Culture characteristics (14 d at 25 °C). Colonies on OA reaching 21–22 mm diam., olive (2F6) to black, dark green margin (30F4), flat, slightly dusty at the center,

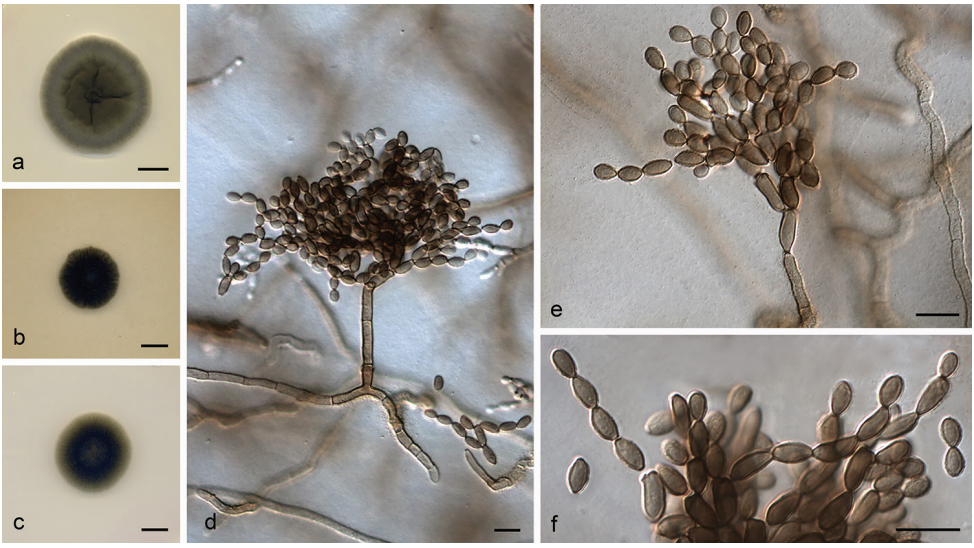

Figure 4. *Cladosporium coprophilum* (ex-type FMR 16164) **a–c** colonies on PDA, OA and SNA after 14 days at 25 °C **d–e** conidiophores **f** conidia. Scale bars: 10 mm (**a–c**); 10 µm (**d–f**).

aerial mycelium scarce, margin regular; reverse dark green (30F8) to black. On PDA attaining 36–37 mm diam., olive (2F6/2E3), greenish gray margin, slightly depressed and irregularly folded at the center, velvety, aerial mycelium scarce, margin regular; reverse dark green (30F8/27F3). On SNA reaching 27–28 mm diam., olive (3F6/2F8), flat, slightly dusty, aerial mycelium scarce, margin regular; reverse dark green (30F8) to black.

Cardinal temperature for growth. Optimum 20 °C, maximum 25 °C, minimum 5 °C.

Distribution. Spain.

Additional specimen examined. Spain, Extremadura, Badajoz province, Granja de Torrehermosa, unidentified herbivore dung, Mar. 2017, *J. Cano* (FMR 16101).

Notes. Based on the multi-locus analysis (Fig. 1), *C. coprophilum* is allocated to a terminal low-supported clade together with *C. chasmanthicola* and *C. sinuatum*, species recently described from leaf spots of *Chasmanthe aethiopica* in South Africa (Marin-Felix et al. 2017) and Alpine soil in China (Ma et al. 2017), respectively. The new species is distinguished from *C. chasmanthicola* by the production of smooth hyphae (smooth to distinctly verrucose or irregularly rough-walled in *C. chasmanthicola*), longer conidiogenous cells (up to 33 vs up to 24 µm), shorter ramoconidia (9–19 vs 15–33 µm) with fewer septa [(0(–1) vs 0–1(–3)-septate], and longer terminal conidia (4.5–7 vs 2.5–4.5 µm) (Marin-Felix et al. 2017). *Cladosporium coprophilum* differs from *C. sinuatum* by the production of aseptate intercalary conidia (0–1-septate in *C. sinuatum*). In addition, *C. sinuatum* is characterized by distinctive geniculate-sinuous conidiophores and a rather fast growth on OA (40–45 mm vs 21–22 mm in *C. coprophilum* after 14 d at 25 °C) (Ma et al. 2017).

Cladosporium fuscoviride **Iturrieta-González, Dania García, Gené, sp. nov.**
MycoBank No: 836076
Fig. 5

Etymology. Name refers to the dark green reverse of the colonies of the species growing in all agar media tested (fuscus = dark brown, blackish or figuratively dull and viridis = green).

Type. Spain, Catalonia, Tarragona province, Cambrils, Samà Park, garden soil, Feb. 2017, *I. Iturrieta-González* & *J. Gené* (holotype CBS H-24471; cultures ex-type FMR 16385, CBS 146920).

Description. *Mycelium* in vitro superficial and immersed, composed of septate, branched, subhyaline to pale brown, smooth to verruculose hyphae, 1–3 µm wide. *Conidiophores* semi-macronematous to macronematous, arising laterally and terminally from hyphae, sometimes reduced to conidiogenous cells, septate, erect to slightly flexuous, branched or unbranched, sometimes geniculate at the apex, up to 56 µm long, 3–4 µm wide, pale brown, smooth to verruculose. *Conidiogenous cells* terminal and subterminal, cylindrical to slightly clavate, 8–27 × 3–4 µm, bearing up to 4 conidiogenous loci, darkened and refractive. *Ramoconidia* 0–1(–3)-septate, subcylindrical to ellipsoidal, 7.5–22 × 2.5–4 µm [av. (± SD) 12.8 (± 3.9) × 3 (± 0.43)], pale brown, smooth to verruculose. *Conidia* in branched chains with up to 4 conidia in the terminal unbranched part, pale brown, smooth to verruculose, with protuberant, slightly darkened and refractive hila; *small terminal conidia* aseptate, globose, subglobose to obovoid, 3–6 × 2–3.5 µm [av. (± SD) 4.5 (± 0.66) × 3 (± 0.39)]; *intercalary conidia* aseptate, ellipsoidal to somewhat limoniform, 4.5–7 × 2.5–4 µm [av. (± SD) 5.7 (± 0.70) × 3.2 (± 0.36)]; *secondary ramoconidia* 0(–1)-septate, subcylindrical to ellipsoidal 6–11.5 × 2.5–4 µm [av. (± SD) 8.8 (± 1.64) × 3.1 (± 0.40)].

Culture characteristics (14 d at 25 °C). Colonies on OA reaching 31–32 mm diam., olive (3F8) to dark green (30F5), olive final edge (2F8), flat, velvety, aerial mycelium scarce, margin regular; reverse dark green (30F5) to black. On PDA attaining 44–46 mm diam., gray to olive to olive yellow (3D1/2E5/2C6), white at the final edge, flat, velvety, aerial mycelium scarce, margin regular; reverse dark green (30F8) to black, with a whitish final edge. On SNA reaching 34–35 mm diam., olive (3F8), flat, velvety, aerial mycelium scarce, margin regular; reverse dark green (30F8), olive final edge (3F3).

Cardinal temperature for growth. Optimum 25 °C, maximum 30 °C, minimum 5 °C.

Distribution. Spain.

Notes. *Cladosporium fuscoviride* is closely related to *C. alboflavescens* (Fig. 1), a monotypic species described from an animal respiratory specimen collected in California (Sandoval-Denis et al. 2016). The species can be distinguished by their colony and microscopic features; i.e., *C. fuscoviride* has darker colonies and faster growth rates at 25 °C after 2 wk on the three media tested (OA, 31–32 vs 20–23 mm; PDA, 44–46 vs 34–36 mm; SNA, 34–35 vs 20–25 mm), shorter conidiophores (up to 56 µm vs

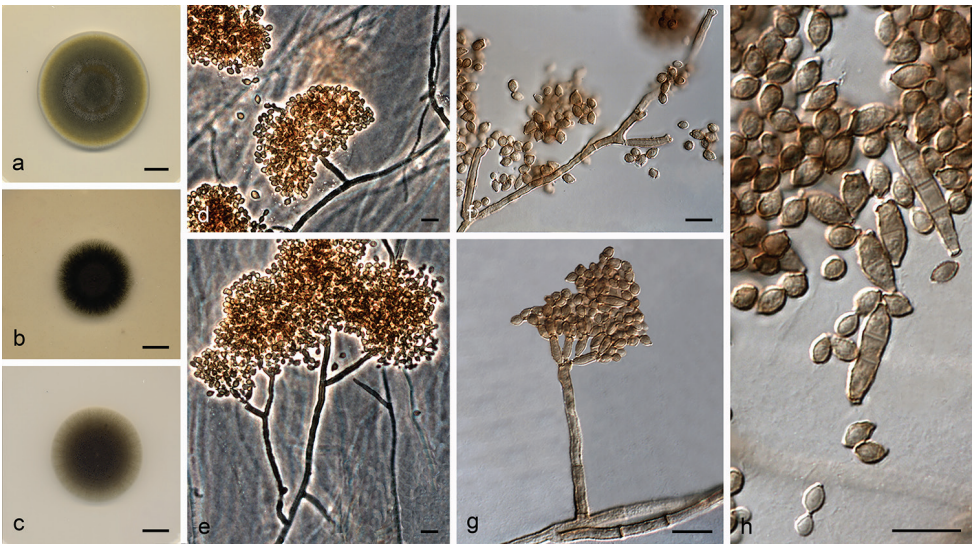

Figure 5. *Cladosporium fuscoviride* (ex-type FMR 16385) **a–c** colonies on PDA, OA and SNA after 14 days at 25 °C **d–g** conidiophores **h** ramoconidia and conidia. Scale bars: 10 mm (**a–c**); 10 µm (**d–h**).

up to 130 µm long in *C. alboflavescens*), and 0–3-septate (aseptate in *C. alboflavescens*) shorter (7.5–22 vs 11–36 µm) ramoconidia. *Cladosporium iranicum* is related with *C. fuscoviride* and *C. alboflavescens*, but can be easily distinguished from them by its larger conidiophores (40–180(–135) µm), with chains of up to 10 conidia in the terminal unbranched part, and a faster growth rate on PDA (56–60 mm after 14 d at 25 °C) (Bensch et al. 2010).

Cladosporium lentulum **Iturrieta-González, Dania García, Gené, sp. nov.**
MycoBank No: 836077
Fig. 6

Etymology. Name refers to its slower growth with respect to the phylogenetically related species (lentus = figuratively slow, with Latin adjectival suffix -ulus = diminutive).

Type. Spain, Catalonia, Tarragona province, Tarragona, unidentified leaf litter, Feb. 2017, *I. Iturrieta-González* (holotype CBS H-24472; cultures ex-type FMR 16288, CBS 146921).

Description. *Mycelium* in vitro superficial and immersed, composed of septate, branched, subhyaline to yellowish brown, smooth to verruculose hyphae, 1–4 µm wide. *Conidiophores* macronematous, arising laterally and terminally from hyphae, septate, erect to slightly flexuous, unbranched, sometimes geniculate at the apex, occasionally branched, up to 406 µm long, 3–4 µm wide, pale brown to brown, smooth to verrucose. *Conidiogenous cells* integrated, terminal and subterminal, cylindrical to subcylindrical, 11–27 × 2–4(–5) µm, bearing up to 5 conidiogenous loci, darkened and refractive.

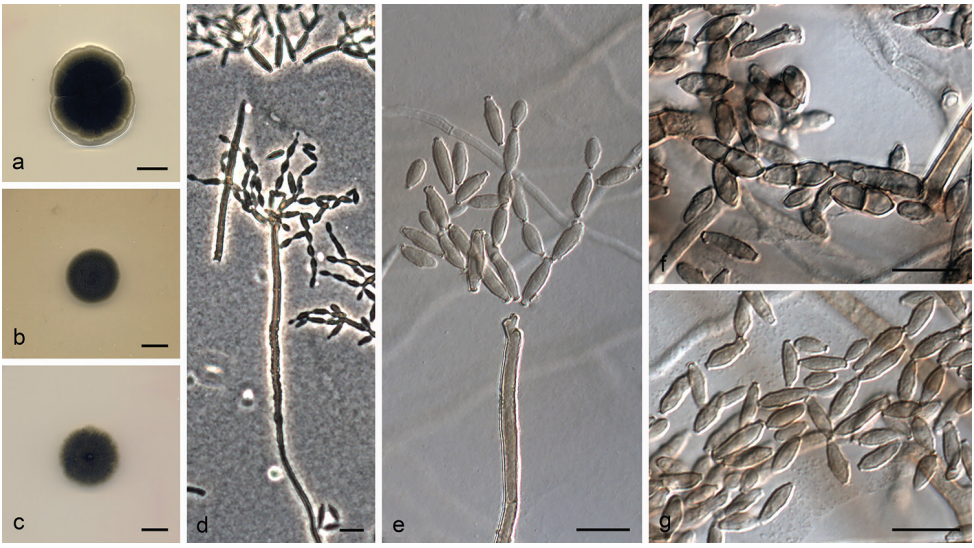

Figure 6. *Cladosporium lentulum* (ex-type FMR 16288) **a–c** colonies on PDA, OA and SNA after 14 days at 25 °C **d–e** conidiophores **f–g** conidia. Scale bars: 10 mm (**a–c**); 10 µm (**d–g**).

Ramoconidia 0(–2)-septate, subcylindrical to cylindrical, 10.5–23 × 2.5–4.5 µm [av. (± SD) 14.2 (± 2.61) × 3.2 (± 0.52)]; pale brown, smooth to verruculose. *Conidia* forming branched chains with up to 5 conidia in the unbranched part of the chain, pale brown, smooth to slightly verruculose, with protuberant, slightly darkened and refractive hila; *small terminal conidia* aseptate obovoidal to ellipsoidal, 4.5–7.5 × 1.5–2.5 µm [av. (± SD) 5.8 (± 0.81)) × 2.7 (± 0.29)]; *intercalary conidia* 0(–1)-septate, ellipsoidal to subcylindrical, 6–10.5 × 2–3 µm [av. (± SD) 8.4 (± 1.31) × 2.3 (± 0.34)]; *secondary ramoconidia* 0(–1)-septate, ellipsoidal to subcylindrical, slightly constricted at septum when present, 7.5–14.5 × 2–3 µm [av. (± SD) 10.5 (± 2.05) × 2.5 (± 0.30)].

Culture characteristics (14 d at 25 °C). Colonies on OA reaching 19–20 mm diam., olive (3F8), flat, velvety, aerial mycelium scarce, margin regular; reverse dark green (30F8) to black. On PDA attaining 28–36 mm diam., dark green (27F8), with a whitish final edge, slightly umbonate, radially folded, velvety, aerial mycelium scarce, margin slightly lobulate; reverse olive brown (4E4), whitish at the edge. On SNA reaching 22–23 mm diam., olive (3F5), flat, slightly dusty, aerial mycelium scarce, margin fimbriate; reverse dark green (30F8) to black.

Cardinal temperature for growth. optimum 20 °C, maximum 30 °C, minimum 5 °C.

Distribution. Spain.

Additional specimen examined. Spain, Catalonia, Tarragona province, Poblet, unidentified herbivore dung, Mar. 2017, *I. Iturrieta-González*, *M. Guevara-Suarez* & *J. Guarro* (FMR 16389).

Notes. Our phylogeny shows *C. lentulum* included in a well-supported terminal clade together with the ex-type strains of *C. exasperatum*, *C. parapenidielloides* and

C. longicatenatum, three species all described from plant material collected in Australia (Bensch et al. 2010, 2015). However, the genetic distance allows it to be considered a distinct species within the clade (Fig. 1). Phenotypically, *C. lentulum* can be distinguished from its counterparts mainly by its slower growth, especially on OA at 25 °C after 14 d (19–20 mm vs 39–54 mm for *C. exasperatum*, 42–55 mm for *C. parapenidielloides* and 43–54 mm for *C. longicatenatum*). In addition, our new species shows shorter ramoconidia (10.5–23 µm) than *C. exasperatum* and *C. longicatenatum* (19–40 µm and 22–42 µm, respectively); ramoconidia in *C. parapenidielloides* are absent; the conidia in *C. lentulum* are smooth or nearly so, while those of *C. exasperatum* and *C. longicatenatum* possess a unique verruculose-rugose conidial surface ornamentation, especially prominent in the former; and conidiophores in *C. parapenidielloides* are much shorter (up to 67 µm) than those observed in *C. lentulum* (up to 406 µm) (Bensch et al. 2010, 2015).

Cladosporium pseudotenellum **Iturrieta-González, Dania García, Gené, sp. nov.**
MycoBank No: 836078
Fig. 7

Etymology. The name refers to "*C. tenellum*", the closest phylogenetic species.

Type. Spain, Catalonia, Tarragona province, Reus, garden soil, Feb. 2017, *I. Iturrieta-González* (holotype CBS H-24473; cultures ex-type FMR 16231, CBS 146922).

Description. *Mycelium* in vitro superficial and immersed, composed of septate, branched, subhyaline to pale brown, smooth-walled, occasionally tuberculate and with abundant swellings, hyphae, 2–3(–4.5) µm wide. *Conidiophores* macronematous, arising laterally or terminally from hyphae, erect to slightly flexuous, non-nodulose, occasionally geniculate at the apex, septate, unbranched, occasionally branched, up to 146 µm long, 2.5–3 µm wide, pale brown, smooth to slightly verruculose. *Conidiogenous cells* integrated, terminal or intercalary, cylindrical, sometimes geniculate, 15–32 × 2.5–3 µm, with up to five conidiogenous loci, thickened, darkened and refractive, often crowded at the apex. *Ramoconidia* rarely formed, 0(–1)-septate, ellipsoidal to subcylindrical, 9–14.5 × 4–5.5 µm [av. (± SD) 11.6 (± 1.60) × 4.6 (± 0.44)], pale brown, verruculose. *Conidia* forming branched chains, with up to four conidia in the terminal unbranched part, aseptate, pale brown, verruculose to verrucose; *small terminal conidia* subglobose to obovoid, 4–7 × 3–5 µm [av. (± SD) 5.8 (± 0.77) × 3.9 (± 0.60)]; *intercalary conidia* ellipsoidal to limoniform, 6–8.5 × 3–5 µm [av. (± SD) 7.4 (± 0.73) × 3.8 (± 0.50)]; *secondary ramoconidia* 0(–2)-septate, ellipsoidal to subcylindrical, 7–12.5 × 4–5 µm [av. (± SD) 9.6 (± 1.76) × 4.4 (± 0.33)] with 1–3 distal hila.

Culture characteristics (14 d at 25 °C). Colonies on OA reaching 21–22 mm diam., olive (2F8/2F4), flat, velvety, aerial mycelium scarce, margin fimbriate; reverse dark green (30F8) to black. On PDA attaining 29–30 mm diam., olive gray (3E2/3F2), paler at the periphery, radially folded, velvety, aerial mycelium scarce, margin slightly lobate; reverse dark green (30F8) to black. On SNA reaching 21–22 mm diam., olive

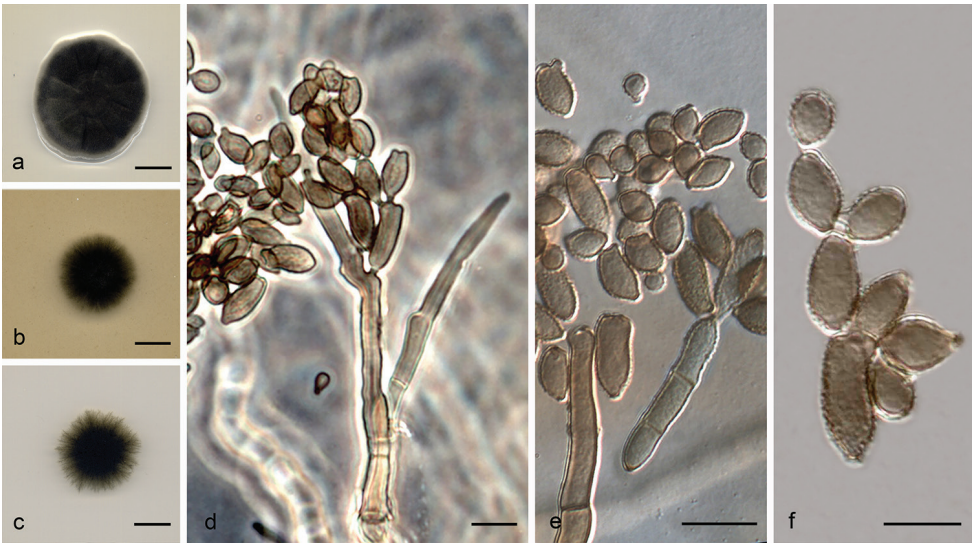

Figure 7. *Cladosporium pseudotenellum* (ex-type FMR 16231) **a–c** colonies on PDA, OA and SNA after 14 days at 25 °C **d–e** conidiophores **f** conidia. Scale bars: 10 mm (**a–c**); 10 µm (**d–f**).

(2F8), flat, slightly powdery, aerial mycelium scarce, margin fimbriate; reverse dark green (30F8) to black.

Cardinal temperature for growth. Optimum 20 °C, maximum 30 °C, minimum 5 °C.

Distribution. Spain.

Notes. Based on the phylogeny of the *C. herbarum* complex (Fig. 2), *C. pseudotenellum* is closely related with *C. tenellum*, a species originally described from hypersaline water in Israel, later found on *Phyllactinia* sp. (Erysiphaceae), and in indoor air samples collected in the USA (Schubert et al. 2007; Bensch et al. 2012, 2018). Our species differs from *C. tenellum* in the absence of micronematous conidiophores and in having shorter macronematous conidiophores (up to 146 µm vs up to 200 µm), shorter conidiogenous cells (15–32 µm vs 6–40 µm), with few conidiogenous loci (up to five vs up to 10 or more in *C. tenellum*), and shorter ramoconidia (9–14.5 vs up to 32 µm). In addition, terminal and intercalary conidia in *C. pseudotenellum* are aseptate, while those of *C. tenellum* are 0–1(–3)-septate (Schubert et al. 2007; Bensch et al. 2012).

Cladosporium submersum **Iturrieta-González, Dania García, Gené, sp. nov.**
MycoBank No: 836079
Fig. 8

Etymology. Name refers to the aquatic habitat where the substrate (submerged plant material) of the fungus was collected (submersus = submerged, verb in participle, from submergere).

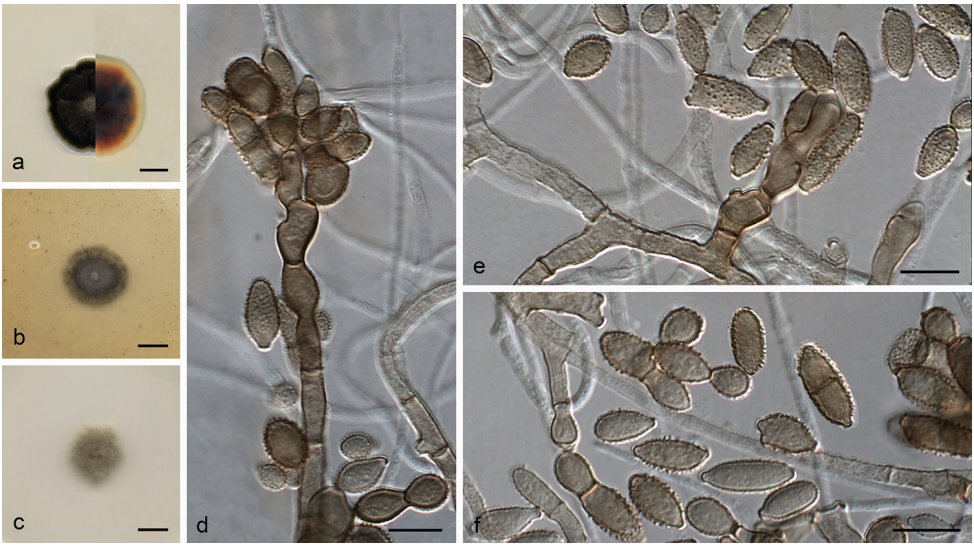

Figure 8. *Cladosporium submersum* (ex-type FMR 16264) **a–c** colonies on PDA (front at 25 °C and reverse at 20 °C), OA and SNA at 25 °C after 14 days **d, e** conidiophores and conidia **f** conidia. Scale bars: 10 mm (**a–c**); 10 µm (**d–f**).

Type. Spain, Catalonia, Tarragona province, Cornudella del Montsant, Siurana's swamp, submerged plant material, Feb. 2018, *I. Iturrieta-González, E. Carvalho & J. Gené* (holotype CBS H-24474; cultures ex-type FMR 17264, CBS 146923).

Description. *Mycelium* in vitro superficial and immersed, composed of septate, branched, subhyaline to pale brown, smooth-walled to verruculose hyphae, 1–3 µm wide. *Conidiophores* dimorphic, micronematous or macronematous, arising laterally and terminally from hyphae, erect to slightly flexuous, nodulose, geniculate at the apex, septate, unbranched, occasionally branched with small prolongations just below the septum, up to 77 µm long, 3–5 µm wide, pale brown to brown, smooth to verruculose. *Conidiogenous cells* integrated, terminal and intercalary, geniculate, nodulose, 11–28 × 3–6 µm, bearing up to five conidiogenous loci, darkened and refractive. *Ramoconidia* rarely formed, 0(–1)-septate, sometimes constricted at the septum when present, cylindrical to subcylindrical, 10.5–24 × 4.5–7 µm [av. (± SD) 16 (± 3.6) × 6.1 (± 1.03)], pale brown, verruculose to verrucose. *Conidia* forming short branched chains, pale brown, verrucose, occasionally verruculose, with protuberant and slightly darkened hila; *small terminal conidia* aseptate, ovoid to ellipsoidal, 6–12.5 × 3.5–7 µm [av. (± SD) 7.8 (± 1.63) × 4.8 (± 0.79)]; *intercalary conidia* and *secondary ramoconidia* 0–1-septate, ellipsoidal or subcylindrical, 7.5–16 × 4.5–8 µm [av. (± SD) 11 (± 2.18) × 5.7 (± 0.99)].

Culture characteristics (14 d at 25 °C). Colonies on OA reaching 22–23 mm diam., brownish gray to olive brown (4E2/4E4), umbonate, velvety, aerial mycelium scarce, margin slightly irregular and fimbriate; reverse dark green to olive brown (6F8/4E3). On PDA attaining 26–28 mm diam., olive (3F3/1F5), slightly umbonate, radially folded, velvety, aerial mycelium scarce, margin irregularly undulate; reverse

dark green (30F9) to black with brownish red (9C6) areas observed between 15 and 20 °C and a white edge. On SNA reaching 21–22 mm diam., olive (3E3), slightly umbonate, loosely cottony, margin fimbriate; reverse dark olive brown to golden gray (3E3/4C2).

Cardinal temperature for growth. Optimum 20 °C, maximum 35 °C, minimum 5 °C.

Distribution. Spain.

Notes. *Cladosporium submersum* is related to *C. subcinereum*, and morphologically differentiated by having shorter conidiophores (up to 77 µm vs up to 140 µm), shorter conidiogenous cells (11–28 vs 16–38 µm), shorter ramoconidia (10.5–24 vs 19–59 µm), and longer terminal conidia (6–12.5 vs 5–7 µm), which are ovoid to ellipsoidal in our species and globose to subglobose in *C. subcinereum* (Sandoval-Denis et al. 2016). In addition, *C. submersum* exhibited a colony reverse on PDA with brownish red areas, a feature that is absent in *C. subcinereum*.

Discussion

Cladosporium is a well-delineated genus, the taxonomic structure and phylogenetic relationships of its species have been investigated in several studies over the last decade, so far giving rise to a genus of more than two hundred well-established species (Zalar et al. 2007; Bensch et al. 2010, 2012, 2018; Sandoval-Denis et al. 2016; Marin-Felix et al. 2017; Crous et al. 2009, 2019; Jayasiri et al. 2019). However, this species number will continue to expand through the study of soil, which is a proven pool of fungal species that remains undescribed, and other substrates poorly investigated by molecular tools for fungal diversity (Tedersoo et al. 2017; Hyde et al. 2018). In this context, a set of *Cladosporium* isolates were obtained in pure culture from samples of soil, dung from different herbivorous animals, and plant debris collected during a survey of microfungi in various Spanish locations. Using the molecular approach for species delineation in *Cladosporium* (Bensch et al. 2012; Marin-Felix et al. 2017), eight of those isolates represented six novel lineages for the genus which are proposed as *C. caprifimosum*, *C. coprophilum*, *C. fuscoviride*, *C. lentulum*, *C. pseudotenellum* and *C. submersum*. Of note is that almost all the specimens in the present study (7/8) were isolated directly from the natural substratum incubated in moist chambers or from baiting technique plates. Although *Cladosporium* isolates are commonly detected by plating methods, the slow growth rate or the low spore concentration of some cladosporium-like fungi compared to other fungi present in a given substrate is probably a handicap to detection and/or isolation of uncommon *Cladosporium* species. Therefore, as recommended by Crous (1998) for similar fungi, techniques based on fungal isolation directly from the natural substratum should be considered a choice for future studies of *Cladosporium* species diversity.

To our knowledge, *Cladosporium* species as dung inhabiting fungi have been reported in a very few studies, *C. cladosporioides* and *C. herbarum* being the most reported species (Bell 1975; Seifert et al. 1983; Jeamjitt et al. 2006; Masunga et al. 2006; Piontelli et

al. 2006; Simões-Calaça et al. 2014; Thilagam et al. 2015). However, in all those studies, fungal identification was based exclusively on morphological features. Only *C. herbarum* has been reported recently from crown droppings and identified molecularly, but using only the ITS barcode (Torbati et al. 2016). In our case, the three new species isolated on herbivore dung (i.e., *C. caprifimosum*, *C. coprophilum*, and *C. lentulum*) showed the typical morphological features attributed to the *C. cladosporioides* species complex. However, their identifications would have been difficult with morphological features alone, even with the analysis of their ITS sequences (Table 2) since they are identical under the universal barcode for fungi as reported in previous studies for many other *Cladosporium* species (Bensch et al. 2010, 2012; Marin-Felix et al. 2017). Therefore, only sequence analysis with *act* and *tef1* will allow us to know the real diversity of *Cladosporium* species from this understudied substrate by molecular tools.

Although no temperature studies have been systematically applied to characterize most *Cladosporium* species (Bensch et al. 2012, 2015, 2018), we agree with Ma et al. (2017) that cardinal temperatures for growth can help to differentiate certain species in their respective complexes. While species in the *C. sphaerospermum* complex show a maximum temperature for growth of no more than 30–32 °C, *C. halotolerans* was able to grow at 35 °C (Sandoval-Denis et al. 2015). Similarly, although most species of the *C. cladosporioides* complex do not tolerate high temperatures, *C. angulosum*, *C. angustisporum*, *C. anthropophilum*, *C. flavovirens*, *C. funiculosum*, *C. pseudocladosporioides*, *C. subuliforme* and *C. tenuissimum* were able to grow at 35 °C (Sandoval-Denis et al. 2015, 2016). To date, no member of the *C. herbarum* complex was found to be able to grow above 30 °C; however, one of the novel species of the complex described here, *C. submersum*, had a maximum growth at 35 °C. On the contrary, the recently described species *C. neopsychrotolerans* and *C. tianshanense* from the complex *C. cladosporioides* and *C. psychrotolerans* from the complex *C. sphaerospermum* showed a psychrophilic behavior (Zalar et al. 2007; Ma et al. 2017), demonstrating in part the ability of *Cladosporium* species to adapt to different environmental conditions.

Acknowledgements

The authors are grateful to Lei Cai of Institute of Microbiology of the Chinese Academy of Sciences (Beijing, China) for sending the sequences of *C. tianshanense* included in this study. This study was supported in part by the Spanish Ministerio de Economía y Competitividad, grant CGL2017-88094-P.

References

Abdollahzadeh J, Groenewald JZ, Coetzee MPA, Wingfield MJ, Crous PW (2020) Evolution of lifestyles in *Capnodiales*. Studies in Mycology 95: 381–414. https://doi.org/10.1016/j.simyco.2020.02.004

Adorisio S, Fierabracci A, Muscari I, Liberati AM, Cannarile L, Thuy TT, Sung TV, Sohrab H, Hasan CM, Ayroldi E, Riccardi C, Mazid A, Delfino DV(2019) Fusarubin and Anhydrofusarubin isolated from a *Cladosporium* species inhibit cell growth in human cancer cell lines. Toxins 11(9): e503. https://doi.org/10.3390/toxins11090503

Bell A (1975) Fungal succession on dung of the brush-tailed opossum in New Zealand. New Zealand Journal of Botany 13: 437–462. https://doi.org/10.1080/0028825X.1975.10430336

Bensch K, Groenewald JZ, Dijksterhuis J, Starink-Willemse M, Andersen B, Starink-Willemse M, Andersen B, Summerell BA, Shin H-D, Dugan FM, Schroers H-J, Braun U, Crous PW (2010) Species and ecological diversity within the *Cladosporium cladosporioides* complex (*Davidiellaceae*, *Capnodiales*). Studies in Mycology 67: 1–94. https://doi.org/10.3114/sim.2010.67.01

Bensch K, Braun U, Groenewald JZ, Crous PW (2012) The genus *Cladosporium*. Studies in Mycology 72: 1–401. https://doi.org/10.3114/sim0003

Bensch K, Groenewald JZ, Braun U, Dijksterhuis J, Yañez-Morales M, Dijksterhuis J, Yáñez-Morales MJ, Crous PW (2015) Common but different: The expanding realm of *Cladosporium*. Studies in Mycology 82: 23–74. https://doi.org/10.1016/j.simyco.2015.10.001

Bensch K, Groenewald JZ, Meijer M, Dijksterhuis J, Jurjevic Ž, Dijksterhuis J, Jurjević Z, Andersen B, Houbraken J, Crous PW, Samson RA (2018) *Cladosporium* species in indoor environments. Studies in Mycology 89: 177–301. https://doi.org/10.1016/j.simyco.2018.03.002

Bezerra JDP, Sandoval-Denis M, Paiva LM, Silva GA, Groenewald JZ, Silva GA, Groenewald JZ, Souza-Motta CM, Crous PW(2017) New endophytic *Toxicocladosporium* species from cacti in Brazil, and description of *Neocladosporium* gen. nov. IMA Fungus 8: 77–97. https://doi.org/10.5598/imafungus.2017.08.01.06

Calduch M, Gené J, Stchigel AM, Cano JF, Guarro J (2004) *Ramophialophora*, a new anamorphic genus of Sordariales. Studies in Mycology 50: 83–88.

Carbone I, Kohn LM (1999) A method for designing primer sets for speciation studies in filamentous ascomycetes. Mycologia 91: 553–556. https://doi.org/10.1080/00275514.1999.12061051

Castañeda-Ruiz RF, Heredia G, Gusmao LFP, Li DW (2016) Fungal diversity of central and south America. In: De-Wei L (Ed.) Biology of Microfungi. Springer International Publishing, Switzerland, 197–218. https://doi.org/10.1007/978-3-319-29137-6_9

Chung D, Kim H, Choi HS (2019) Fungi in salterns. Journal of Microbiology 57: 717–724. https://doi.org/10.1007/s12275-019-9195-3

Crous PW (1998) *Mycosphaerella* spp. and their anamorphs associated with leaf spot diseases of Eucalyptus. Mycologia Memoir 21: 1–170.

Crous PW, Gams W, Stalpers JÁ, Robert V, Stegehuis G (2004) MycoBank: an online initiative to launch mycology into the 21st century. Studies in Mycology 50: 19–22.

Crous PW, Braun U, Schubert K, Groenewald JZ (2007) Delimiting *Cladosporium* from morphologically similar genera. Studies in Mycology 58: 33–56. https://doi.org/10.3114/sim.2007.58.02

Crous PW, Verkley GJM, Groenewald JZ, Samson RA (2009) Fungal Biodiversity. CBS Laboratory manual Series. Westerdijk Fungal Biodiversity Institute, Utrecht, The Netherlands, 269 pp.

Crous PW, Wingfield MJ, Lombard L, Roets F, Swart WJ, Roets F, Swart WJ, Alvarado P, Carnegie AJ, Moreno G, Luangsa-Ard J, Thangavel R, Alexandrova AV, Baseia IG, Bellanger J-M, Bessette AE, Bessette AR, Delapeña-Lastra S, García D, Gené J, Pham THG, Heykoop M, Malysheva E, Malysheva V, Martín MP, Morozova OV, Noisripoom W, Overton BE, Rea AE, Sewall BJ, Smith ME, Smyth CW, Tasanathai K, Visagie CM, Adamčík S, Alves A, Andrade JP, Aninat MJ, Araújo RVB, Bordallo JJ, Boufleur T, Baroncelli R, Barreto RW, Bolin J, Cabero J, Caboň M, Cafà G, Caffot MLH, Cai L, Carlavilla JR, Chávez R, Decastro RRL, Delgat L, Deschuyteneer D, Dios MM, Domínguez LS, Evans HC, Eyssartier G, Ferreira BW, Figueiredo CN, Liu F, Fournier J, Galli-Terasawa LV, Gil-Durán C, Glienke C, Gonçalves MFM, Gryta H, Guarro J, Himaman W, Hywel-Jones N, Iturrieta-González I, Ivanushkina NE, Jargeat P, Khalid AN, Khan J, Kiran M, Kiss L, Kochkina GA, Kolařík M, Kubátová A, Lodge DJ, Loizides M, Luque D, Manjón JL, Marbach PAS, Massolajr NS, Mata M, Miller AN, Mongkolsamrit S, Moreau P-A, Morte A, Mujic A, Navarro-Ródenas A, Németh MZ, Nóbrega TF, Nováková A, Olariaga I, Ozerskaya SM, Palma MA, Petters-Vandresen DAL, Piontelli E, Popov ES, Rodríguez A, Requejo Ó, Rodrigues ACM, Rong IH, Roux J, Seifert KA, Silva BDB, Sklenář F, Smith JA, Sousa JO, Souza HG, Desouza JT, Švec K, Tanchaud P, Tanney JB, Terasawa F, Thanakitpipattana D, Torres-Garcia D, Vaca I, Vaghefi N, Vaniperen AL, Vasilenko OV, Verbeken A, Yilmaz N, Zamora JC, Zapata M, Jurjevi Ž, Groenewald JZ (2019) Fungal Planet description sheets: 951–1041. Persoonia 43: 223–425. https://doi.org/10.3767/persoonia.2019.43.06

David JC (1997) A contribution to the systematics of *Cladosporium*. Revision of the fungi previously referred to *Heterosporium*. Mycological Papers 172: 1–157.

de Hoog GS, Guarro J, Gené J, Figueras MJ (2017) Atlas of clinical fungi. Electronic version 4.1.4. Westerdijk Fungal Biodiversity Institute / Universitat Rovira i Virgili, Utrecht / Reus. http://www.clinicalfungi.org/

Edgar RC (2004) MUSCLE: multiple sequence alignment with high accuracy and high throughput. Nucleic Acids Research 32: 1792–1797. https://doi.org/10.1093/nar/gkh340

Hespanhol L, Vallio CS, Costa LM, Saragiotto BT (2019) Understanding and interpreting confidence and credible intervals around effect estimates. Brazilian Journal of Physical Therapy 23(4): 290–301. https://doi.org/10.1016/j.bjpt.2018.12.006

Heuchert B, Braun U, Schubert K (2005) Morphotaxonomic revision of fungicolous *Cladosporium* species (Hyphomycetes). Schlechtendalia 13: 1–78.

Hillis DM, Bull JJ (1993) An empirical test of bootstrapping as a method for assessing confidence in phylogenetic analysis. Systematic Biology 42: 182–192. https://doi.org/10.1093/sysbio/42.2.182

Farris JS, Källersjö M, Kluge AG, Bult C (1994) Testing significance of incongruence. Cladistics 10: 315–319. https://doi.org/10.1111/j.1096-0031.1994.tb00181.x

Flannigan B, Samson RA, Miller JD (2002) Microorganisms in home and indoor work environments: diversity, health impacts, Investigation and control. London, United Kingdom, 504 pp. https://doi.org/10.1201/9780203302934

Hyde KD, Norphanphoun C, Chen J, Dissanayake AJ, Doilom M, Dissanayake AJ, Doilom M, Hongsanan S, Jayawardena RS, Jeewon R, Perera RH, Thongbai B, Wanasinghe DN, Wisitrassameewong K, Tibpromma S, Stadler M (2018) Thailand's amazing diversity: up

to 96% of fungi in northern Thailand may be novel. Fungal Diversity 93: 215–239. https://doi.org/10.1007/s13225-018-0415-7

Jayasiri SC, Hyde KD, Jones EBG, McKenzie EHC, Jeewon R, McKenzie EHC, Jeewon R, Phillips AJL, Bhat DJ, Wanasinghe DN2, Liu JK, Lu YZ, Kang JC, Xu J, Karunarathna SC (2019) Diversity, morphology and molecular phylogeny of Dothideomycetes on decaying wild seed pods and fruits. Mycosphere 10: 1–186. https://doi.org/10.5943/mycosphere/10/1/1

Jeamjitt O, Manoch L, Visarathanonth N, Chamswarng C (2006) Diversity and distribution of hyphomycetes from dung in Thailand. Witthayasan Kasetsat 40: 890–901.

Khan MIH, Sohrab MH, Rony SR, Tareq FS, Hasan CM, Mazid MA (2016) Cytotoxic and antibacterial naphthoquinones from an endophytic fungus, *Cladosporium* sp. Toxicology Reports 3: 861–865. https://doi.org/10.1016/j.toxrep.2016.10.005

Köhl J, Scheer C, Holb IJ, Masny S, Molhoek W (2015) Toward an integrated use of biological control by *Cladosporium cladosporioides* H39 in apple scab (*Venturia inaequalis*) management. Plant Disease 99: 535–543. https://doi.org/10.1094/PDIS-08-14-0836-RE

Kornerup A, Wanscher JH (1978) Methuen Handbook of Colour (3rd ed.). Methuen Publishing Ltd., London, 256 pp.

Ma R, Chen Q, Fan Y, Wang Q, Chen S, Wang Q, Chen S, Liu X, Cai L, Yao B (2017) Six new soil-inhabiting *Cladosporium* species from plateaus in China. Mycologia 109: 244–260. https://doi.org/10.1080/00275514.2017.1302254

Marin-Felix Y, Groenewald JZ, Cai L, Chen Q, Marincowitz S, Chen Q, Marincowitz S, Barnes I, Bensch K, Braun U, Camporesi E, Damm U, de Beer ZW, Dissanayake A, Edwards J, Giraldo A, Hernández-Restrepo M, Hyde KD, Jayawardena RS, Lombard L, Crous PW (2017) Genera of phytopathogenic fungi: GOPHY 1. Studies in Mycology 86: 99–216. https://doi.org/10.1016/j.simyco.2017.04.002

Masunga GS, Andersen Ø, Taylor JE, Dhillion SS (2006) Elephant dung decomposition and coprophilous fungi in two habitats of semi-arid Botswana. Mycological Research 110: 1214–1226. https://doi.org/10.1016/j.mycres.2006.07.004

Müller FM, Werner KE, Kasai M, Francesconi A, Chanock SJ, Francesconi A, Chanock SJ, Walsh TJ (1998) Rapid extraction of genomic DNA from medically important yeasts and filamentous fungi by high-speed cell disruption. Journal of Clinical Microbiology 36: 1625–1629. https://doi.org/10.1128/JCM.36.6.1625-1629.1998

Piontelli LE, Cruz CR, Toro SMMA (2006) Coprophilous fungal community of wild rabbit in a park of a hospital (Chile): a taxonomic approach. Boletín Micológico 21: 1–17. https://doi.org/10.22370/bolmicol.2006.21.0.239

Posada D (2008) jModelTest: phylogenetic Model Averaging. Molecular Biology and Evolution 25: 1253–1256. https://doi.org/10.1093/molbev/msn083

Richardson MJ (2001) Diversity and occurrence of coprophilous fungi. Mycological Research 105: 387–402. https://doi.org/10.1017/S0953756201003884

Ronquist F, Teslenko M, van der Mark P, Ayres DL, Darling A, Ayres DL, Darling S, Höhna S, Larget B, Liu L, Suchard MA, Huelsenbeck JP (2012) MrBayes 3.2: efficient Bayesian phylogenetic inference and model choice across a large model space. Systematic Biology 61: 539–542. https://doi.org/10.1093/sysbio/sys029

Sandoval-Denis M, Gené J, Sutton DA, Wiederhold NP, Cano-Lira JF, Wiederhold NP, Cano-Lira JF, Guarro J (2016) New species of *Cladosporium* associated with human and animal infections. Persoonia 36: 281–298. https://doi.org/10.3767/003158516X691951

Sandoval-Denis M, Sutton DA, Martin-Vicente A, Cano-Lira JF, Wiederhold N, Cano-Lira JF, Wiederhold N, Guarro J, Gené J (2015) *Cladosporium* species recovered from clinical samples in the United States. Journal of Clinical Microbiology 53: 2990–3000. https://doi.org/10.1128/JCM.01482-15

Schubert K, Groenewald JZ, Braun U, Dijksterhuis J, Starink M, Dijksterhuis J, Starink M, Hill CF, Zalar P, de Hoog GS, Crous PW (2007) Biodiversity in the *Cladosporium herbarum* complex (*Davidiellaceae*, *Capnodiales*), with standardisation of methods for *Cladosporium* taxonomy and diagnostics. Studies in Mycology 58: 105–156. https://doi.org/10.3114/sim.2007.58.05

Schubert K, Greslebin A, Groenewald JZ, Crous PW (2009) New foliicolous species of *Cladosporium* from South America. Persoonia 22: 111–122. https://doi.org/10.3767/003158509X449381

Seifert KA, Kendrick B, Murase G (1983) A Key to Hyphomycetes on Dung. Department of Biology, University of Waterloo, 62 pp.

Simões-Calaça FJ, Carvalho da Silva N, Xavier-Santos S (2014) A checklist of coprophilous fungi and other fungi recorded on dung from Brazil. Mycotaxon 128: 205–205. https://doi.org/10.5248/128.205

Tamura K, Stecher G, Peterson D, Filipski A, Kumar S (2013) MEGA6: Molecular evolutionary genetics analysis version 6.0. Molecular Biology and Evolution 30: 2725–2729. https://doi.org/10.1093/molbev/mst197

Taylor JW, Jacobson DJ, Kroken S, Kasugab T, Geiserc DM, Hibbettd DS, Fishera MS (2000) Phylogenetic species recognition and species concepts in fungi. Fungal Genetics and Biology 31: 21–32. https://doi.org/10.1006/fgbi.2000.1228

Tedersoo L, Bahram M, Puusepp R, Nilsson RH, James TY (2017) Novel soil-inhabiting clades fill gaps in the fungal tree of life. Microbiome 5: e42. https://doi.org/10.1186/s40168-017-0259-5

Temperini CV, Pardo AG, Pose GN (2018) Diversity of airborne *Cladosporium* species isolated from agricultural environments of northern Argentinean Patagonia: molecular characterization and plant pathogenicity. Aerobiologia 34: 227–239. https://doi.org/10.1007/s10453-018-9509-7

Thilagam L, Nayak BK, Nanda A (2015) Isolation and enumeration of saprophytic and coprophilous fungi from country cow dung. Journal of Chemical and Pharmaceutical Research 7: 474–477.

Thompson JD, Higgins DG, Gibson TJ (1994) CLUSTAL W: improving the sensitivity of progressive multiple sequence alignment through sequence weighting, position-specific gap penalties and weight matrix choice. Nucleic Acids Research 22: 4673–4680. https://doi.org/10.1093/nar/22.22.4673

Torbati M, Arzanlou M, Bakhshi M (2016) Morphological and molecular identification of ascomycetous coprophilous fungi occurring on feces of some bird species. Current Research in Environmental & Applied Mycology 6: 210–217. https://doi.org/10.5943/cream/6/3/9

Waksman SA (1922) A method for counting the number of fungi in the soil. Journal of Bacteriology 7: 339–341. https://doi.org/10.1128/JB.7.3.339-341.1922

White TJ, Bruns T, Lee S, Taylor JW (1990) Amplification and direct sequencing of fungal ribosomal RNA genes for phylogenetics. In: Innis MA, Gelfand DH, Sninsky JJ, White TJ (Eds) PCR protocols: a guide to methods and applications: Academic Press, New York, 315–322. https://doi.org/10.1016/B978-0-12-372180-8.50042-1

Zalar P, de Hoog GS, Schroers H-J, Crous PW, Groenewald JZ, Crous PW, Groenewald JZ, Gunde-Cimerman N (2007) Phylogeny and ecology of the ubiquitous saprobe *Cladosporium sphaerospermum*, with descriptions of seven new species from hypersaline environments. Studies in Mycology 58: 157–183. https://doi.org/10.3114/sim.2007.58.06

Supplementary material 1

Table S1

Authors: Isabel Iturrieta-González, Dania García, Josepa Gené

Data type: Species name and strains data

Explanation note: Species, strain information and GenBank accession numbers of the sequences included in the phylogenetic analyses.

Link: https://doi.org/10.3897/mycokeys.77.60862.suppl1

MycoKeys 77: 27–39 (2021)
doi: 10.3897/mycokeys.77.60077
https://mycokeys.pensoft.net

RESEARCH ARTICLE

A peer-reviewed open-access journal
MycoKeys
Launched to accelerate biodiversity research

Diversity of the genus *Sugiyamaella* and description of two new species from rotting wood in China

Cheng-Feng Shi[1], Kai-Hong Zhang[1], Chun-Yue Chai[1], Zhen-Li Yan[2], Feng-Li Hui[1]

1 *School of Life Science and Technology, Nanyang Normal University, Nanyang 473061, China* **2** *State Key Laboratory of Motor Vehicle Biofuel Technology, Henan Tianguan Enterprise Group Co., Ltd., Nanyang 473000, China*

Corresponding author: Feng-Li Hui (fenglihui@yeah.net)

Academic editor: T. Lumbsch | Received 27 October 2020 | Accepted 24 December 2020 | Published 12 January 2021

Citation: Shi C-F, Zhang K-H, Chai C-Y, Yan Z-L, Hui F-L (2021) Diversity of the genus *Sugiyamaella* and description of two new species from rotting wood in China. MycoKeys 77: 27–39. https://doi.org/10.3897/mycokeys.77.60077

Abstract

Species of the genus *Sugiyamaella* (Trichomonascaceae, Saccharomycetales), found in rotting wood in China, were investigated using morphology and the molecular phylogeny of a combined ITS and nrLSU dataset. Nine taxa were collected in China: two were new species (viz. *Sugiyamaella chuxiong* **sp. nov.** and *S. yunanensis* **sp. nov.**) and seven were known species, *S. americana*, *S. ayubii*, *S. novakii*, *S. paludigena*, *S. valenteae*, *S. valdiviana* and *S. xiaguanensis*. The two new species are illustrated and their morphology and phylogenetic relationships with other *Sugiyamaella* species are discussed. Our results indicate a potentially great diversity of *Sugiyamaella* spp. inhabiting rotting wood in China just waiting to be discovered.

Keywords

Phylogeny, rotted wood-inhabiting yeast, *Sugiyamaella*, taxonomy, Trichomonascaceae

Introduction

Sugiyamaella Kurtzman & Robnett (2007) is typified by *Sugiyamaella smithiae*, which was initially classified in the genus *Stephanoascus* (Giménez-Jurado et al. 1994). The genus *Sugiyamaella* belongs to the family Trichomonascaceae in the order Saccharomycetales and is closely related to the genera *Trichomonascus*, *Wickerhamiella* and *Zygoascus*, based on multigene phylogenetic analyses of LSU, MtSm and *COXII* nucleotide sequences (Kurtzman and Robnett 2007; Péter et al. 2012).

Kurtzman (2011) accepted four species in *Sugiyamaella* and proposed a key for this genus, based mainly on the reactions on standard growth and fermentation tests. Subsequently, *S. ayubii*, *S. bahiana*, *S. bonitensis*, *S. carassensis*, *S. ligni*, *S. mastotermitis*, *S. trypani*, *S. valenteae*, *S. xiaguanensis*, *S. xylolytica* and *S. xylanicola* were added to this genus (Morais et al. 2013; Handel et al. 2016; Sena et al. 2017; Huang et al. 2018; Crous et al. 2019). Within the same time frame, 14 *Candida* species in this clade were transferred to the genus *Sugiyamaella* as new combinations, based on their phylogeny (Urbina et al. 2013; Handel et al. 2016). Thus, 29 species were included in this genus before our study, 25 were asexual morphs and four had known ascosporic states, viz. *S. americana*, *S. chiloensis*, *S. japonica* and *S. smithiae* (Kurtzman 2007; Kurtzman and Robnett 2007; Morais et al. 2013; Handel et al. 2016; Sena et al. 2017; Huang et al. 2018; Crous et al. 2019). Morphologically, the sexual morph of *Sugiyamaella* is characterised by the production of globose to ellipsoidal asci with a single ellipsoidal or bacilliform ascospore. The asexual morph is characterised by multilateral budding and formation of blastoconidia. The other useful morphological feature is that pseudohyphae and true hyphae are commonly formed (Kurtzman and Robnett 2007; Kurtzman 2011; Sena et al. 2017).

The members of *Sugiyamaella* have been described in association with insects. They were isolated either directly from wood-ingesting insects and insect frass or from common insect habitats, such as rotting wood, forest soil, mushrooms and peat (Kurtzman 2007; Wang et al. 2010; Kurtzman 2011; Morais et al. 2013; Handel et al. 2016; Sena et al. 2017; Huang et al. 2018). Significantly, most species of *Sugiyamaella* have been reported as potential xylanase producers (Morais et al. 2013; Lara et al. 2014; Handel et al. 2016; Sena et al. 2017). Several species of *Sugiyamaella*, including *S. bahiana*, *S. bonitensis*, *S. boreocaroliniensis*, *S. lignohabitans*, *S. valenteae*, *S. xylanicola* and *S. xylolytica*, possess the ability to ferment D-xylose, which gives them economic potential for production of bioethanol and/or xylitol from plant waste residues (Morais et al. 2013; Sena et al. 2017). Therefore, *Sugiyamaella* species are important, not only for their wood-decaying activity, but also for their potential application in food, medicine and biofuels.

Sugiyamaella has a worldwide distribution and most of its species were originally found in Europe, North America and South America (Kurtzman 2007; Kurtzman 2011; Morais et al. 2013; Sena et al. 2017). The genus has not received as much attention in Asia, except for two novel species described from Japan (Kurtzman 2007; Kurtzman 2011). In China, two novel taxa have been described (Wang et al. 2010; Huang et al. 2018). To date, only four *Sugiyamaella* species have been reported in China, namely *S. lignohabitans*, *S. qingdaonensis*, *S. smithiae* and *S. xiaguanensis* (Wang et al. 2010; Zhai et al. 2019; Huang et al. 2018). In this study, we collected rotting wood samples from Yunnan Province in China. After isolation and examination, two new species and seven known species of *Sugiyamaella* were identified, based on morphology and molecular phylogenetic analysis, increasing the species diversity of *Sugiyamaella* in China.

Materials and methods

Sample collection, morphological studies and isolation

Rotting wood samples were collected in two areas of Yunnan Province, China. The areas were located in the Xishuangbanna Primeval Forest Park of Jinghong (21°98'N, 100°88'E) and Zixi Mountain of Chuxiong (25°03'N, 101°41'E). The predominant vegetation is characterised as tropical and subtropical forest biome. The climate is hot and humid, with annual precipitation between 1,000 to 1,600 mm and an average temperature that ranges from 14.8 to 21.9 °C. Sixty decayed wood samples were collected during July to August in 2016–2018. The samples were stored in sterile plastic bags and transported under refrigeration to the laboratory over a period of no more than 24 h. The yeast strains were isolated from rotting wood samples in accordance with the methods described by Morais et al. (2013) and Lopes et al. (2016). Each sample (1 g) was added to 20 ml sterile D-xylose medium (yeast nitrogen base 0.67%, D-xylose 0.5% and chloramphenicol 0.02%, pH 5.0 ± 0.2) in a 150 ml Erlenmeyer flask and then cultured for 3–10 days on a rotary shaker. Subsequently, 0.1 ml aliquots of the enrichment culture and appropriate decimal dilutions were spread on D-xylose agar plates and then incubated at 25 °C for 3–4 days. Different yeast colony morphotypes were then isolated by repeated plating on yeast extract-malt extract (YM) agar (1% glucose, 0.5% peptone, 0.3% yeast extract and 0.3% malt extract, pH 5.0 ± 0.2) and then stored on YM agar slants at 4 °C or in 15% glycerol at -80 °C.

The morphological, physiological and biochemical properties were determined according to those used by Kurtzman et al. (2011). The beginning of the sexual stage was determined by incubating single or mixed cultures of each of the two strains on cornmeal (CM) agar, 5% malt extract (ME) agar, dilute (1:9) V8 agar or yeast carbon base plus 0.01% ammonium sulphate (YCBAS) agar at 15 and 25 °C for 6 weeks (Kurtzman 2007; Huang et al. 2018). The assimilation of carbon and nitrogen compounds and related growth requirements were tested at 25 °C. The effects of temperature from 25–40 °C were examined in liquid and agar plate cultures.

DNA extraction, PCR amplification and sequencing

Genomic DNA was extracted from the yeast using an Ezup Column Yeast Genomic DNA Purification Kit, according to the manufacturer's instructions (Sangon Biotech, Shanghai, China). The nuc rDNA ITS1-5.8S-ITS2 (ITS) region was amplified using primer pairs ITS1/ITS4 (White et al. 1990). The D1/D2 domain of nrLSU rDNA (nrLSU) was amplified using the primer pairs NL1/NL4 (Kurtzman and Robnett 1998). The following thermal profile was used to amplify the ITS and D1/D2 nrLSU regions: an initial denaturation step of 2 min at 95 °C; followed by 35 cycles of 30 s at 95 °C, 30 s at 51 °C and 40 s at 72 °C; with a final extension of 10 min at 72 °C (Liu et al. 2016). PCR products were directly purified and sequenced by Sangon Biotech Inc.

(Shanghai, China). We confirmed the identity and accuracy of the resulting sequences by assembling them using BioEdit and comparing them to sequences in GenBank (Hall 1999). The sequences were then submitted to GenBank (https://www.ncbi.nlm.nih.gov/genbank/; Table 1).

Phylogenetic analysis

The sequences obtained from this study and the reference sequences downloaded from GenBank (Table 1) were aligned using MAFFT v. 6 (Katoh and Toh 2010) and manually edited using MEGA7 (Kumar et al. 2016). The best-fit nucleotide substitution models for each gene were selected using jModelTest v2.1.7 (Darriba et al. 2012) according to the Akaike Information Criterion. Phylogenetic analyses of combined gene regions (ITS and nrLSU) were performed using MEGA7 for Maximum Parsimony (MP) analysis (Kumar et al. 2016) and PhyML v3.0 for Maximum Likelihood (ML) analysis (Guindon et al. 2010). *Schizosaccharomyces pombe* NRRL Y-12796 was chosen as the outgroup after consulting Morais et al. (2013) and Sena et al. (2017).

Maximum Parsimony analysis was performed using a heuristic search option with tree-bisection reconnection (TBR) branch swapping (Nei and Kumar 2000) and 1,000 random sequence additions. Maximum Likelihood analysis was performed using GTR+I+G models for each partition (Nei and Kumar 2000) and a proportion of invariant sites with 1000 rapid bootstrap replicates. The phylogenies from MP and ML analyses were displayed using Mega7 and FigTree v1.4.3 (Rambaut 2016), respectively. Bootstrap support values ≥ 50% are shown at the nodes.

Results

Phylogenetic analyses

The alignment was based on the combined nuclear dataset (ITS and nrLSU), included 31 taxa and one outgroup taxon (*Schizosaccharomyces pombe* NRRL Y-12796) and was comprised of 976 characters including gaps (385 for ITS and 591 for nrLSU) in the aligned matrix. Of these characters, 452 were constant, 164 variable characters were parsimony-uninformative and 360 characters were parsimony-informative. The heuristic search, using MP analysis, generated the most parsimonious tree (TL = 1627, CI = 0.457, RI = 0.766, RC = 0.394). The best model applied in the ML analysis was GTR+I+G. The ML analysis yielded a best scoring tree with a final optimisation likelihood value of –8651.84. Two methods for phylogenetic tree construction resulted in a similar topology. Therefore, only the best scoring PhyML tree is shown with BS and BT values simultaneously in Fig. 1.

From the phylogenetic tree (Fig. 1), seven known species, including *S. americana*, *S. ayubii*, *S. novakii*, *S. paludigena*, *S. valenteae*, *S. valdiviana* and *S. xiaguanensis*, were absorbed in the genus *Sugiyamaella*. *Sugiyamaella chuxiong* and *S. yunanensis* are new

Table 1. Sequences used in molecular phylogenetic analysis. Entries in bold are newly generated for this study.

Species	Strain	Locality	Sample	ITS	D1/D2
Sugiyamaella americana	NRRL YB-2067^T	USA	Frass	NR_137759	DQ438193
S. americana	**NYNU 17714**	**China**	**Rotting wood**	**MT965698**	**MT965699**
S.ayubii	CBS 14108^T	Brazil	Rotting wood	NR_155796	KR184132
S. ayubii	**NYNU 177171**	**China**	**Rotting wood**	**MT965704**	**MT965705**
S. bahiana	CBS 13474^T	Brazil	Rotting wood	NR_155810	KC959941
S. bonitensis	CBS 14270^T	Brazil	Rotting wood	NR_155798	KT006004
S.boreocaroliniensis	NRRL YB-1835^T	USA	Frass	NR_165963	DQ438221
S. bullrunensis	CBS 11840^T	USA	Insect	NR_111543	HM208601
S. castrensis	NRRL Y-17329^T	Chile	Rotting wood	NR_111229	DQ438195
S. carassensis	CBS 14107^T	Brazil	Rotting wood	NR_155808	KX550111
S. chiloensis	NRRL Y-17643^T	Chile	Rotted wood	DQ911454	DQ438217
S. floridensis	NRRL YB-3827^T	USA	Frass	NR_111230	DQ438222
S. grinbergsii	NRRL Y-27117^T	Chile	Insect	KY102116	DQ438199
S. japonica	NRRL YB-2798^T	Japan	Frass	NR_111239	DQ438202
S. ligni	CBS 13482^T	Brazil	Rotting wood	KX550112	KX550112
S. lignohabitans	NRRL YB-1473^T	USA	Decayed log	NR_119622	DQ438198
S. marionensis	NRRL YB-1336^T	USA	Decayed log	NR_111237	DQ438197
S. marilandica	NRRL YB-1847^T	USA	Frass	NR_165965	DQ438219
S. mastotermitis	CBS 14182^T	Berlin	Termite	NR_156606	KU883286
S. neomexicana	CBS 10349^T	USA	Frass	NR_165966	DQ438201
S. novakii	NRRL Y-27346^T	Hungary	Rotting wood	NR_111235	DQ438196
S. novakii	**NYNU 17778**	**China**	**Rotting wood**	**MT965702**	**MT965703**
S. paludigena	NRRL Y-12697^T	Russia	Peat	NR_111236	DQ438194
S. paludigena	**NYNU 1771**	**China**	**Rotting wood**	**MT965696**	**MT965697**
S. paludigena	**NYNU 177116**	**China**	**Rotting wood**	**MT966075**	**MT966074**
S. pinicola	CBS 10348^T	USA	Frass	NR_165967	DQ438200
S. qingdaonensis	CBS 11390^T	China	Rotting wood	NR_151806	FJ613527
S. smithiae	NRRL Y-17850^T	Brazil	Soil	DQ911455	DQ438218
S. trypani	CBS 15876^T	Poland	Soil	MK388412	MK387312
S. valdiviana	NRRL Y-7791^T	Chile	Rotting wood	NR_111544	DQ438220
S. valdiviana	**NYNU17755**	**China**	**Rotting wood**	**MT965700**	**MT965701**
S. valenteae	CBS 14109^T	Brazil	Rotting wood	NR_155797	KT005999
S. valenteae	**NYNU 17795**	**China**	**Rotting wood**	**MT965706**	**MT965707**
S. xiaguanensis	NYNU 161041^T	China	Rotting wood	KY213802	KY213817
S. xiaguanensis	**NYNU 17753**	**China**	**Rotting wood**	**MT969346**	**MT969344**
S. xylanicola	CBS 12683^T	Brazil	Rotting wood	KC493642	KC493642
S. xylolytica	CBS 13493^T	Brazil	Rotting wood	KU214874	KF889433
S. yunanensis	**NYNU161059^T**	**China**	**Rotting wood**	**MT257259**	**MT257257**
S. yunanensis	**NYNU 16113**	**China**	**Rotting wood**	**MT257256**	**MT257261**
Candida sp.	W370	Taiwan	Forest soil	JN581120	JN581115
Candida sp.	GA2M09	Taiwan	Mushroom	FJ873591	FJ873521
S. chuxiongensis	**NYNU181038^T**	China	Rotting wood	**MK682800**	**MK682795**
S. chuxiongensis	**NYNU 18521**	China	Rotting wood	**MT257260**	**MT257255**
S. chuxiongensis	**NYNU 18634**	China	Rotting wood	**MT257258**	**MT257262**
Schizosaccharomyces pombe	NRRL Y-12796^T	–	–	KY105378	AY048171

Abbreviations: **CBS**: CBS-KNAW Collections, Westerdijk Fungal Biodiversity Institute, Utrecht, The Netherlands; **NRRL**: Agricultural Research Service Culture Collection, Peoria, IL, USA; **NYNU**: Microbiology Lab, Nanyang Normal University, Henan, China; **T**: type strain.

to science, based on the distinct and well-supported molecular phylogenetic placement and morphological differences with their closest described relatives. Phylogenetically, strains of *S. chuxiong* formed a unique lineage with 100% bootstrap support, while

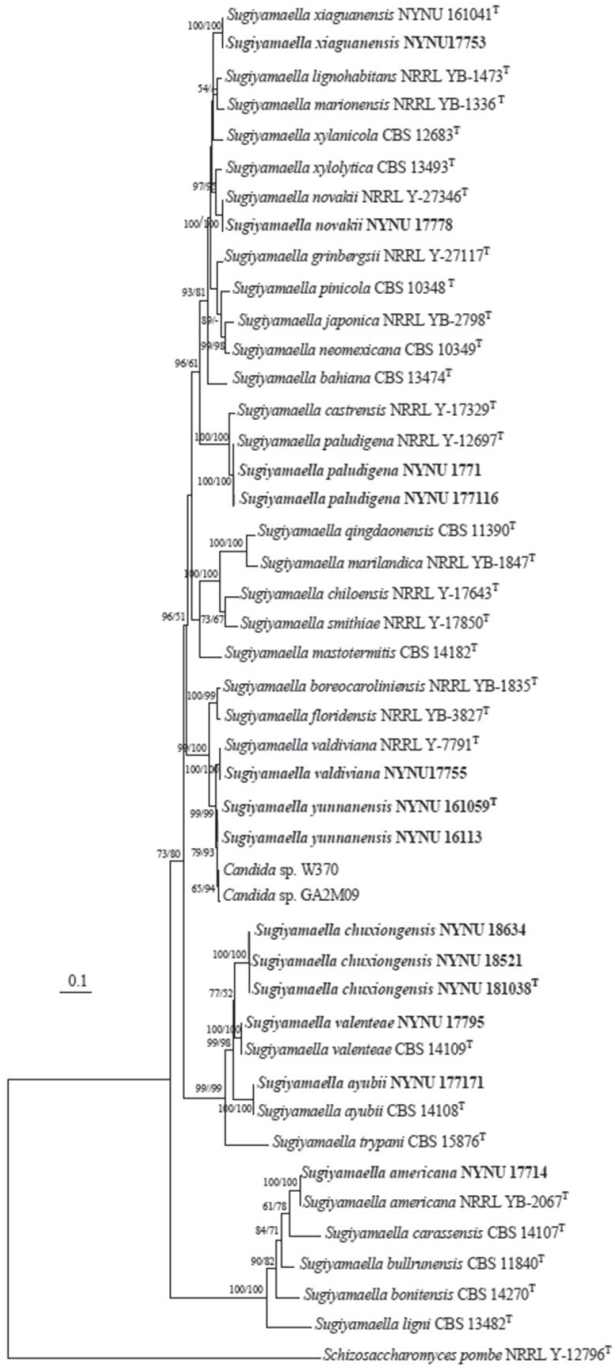

Figure 1. Maximum Likelihood phylogenetic tree of *Sugiyamaella* inferred from the combined ITS and nrLSU dataset and rooted with *Schizosaccharomyces pombe* NRRL Y-12796. The ML and MP bootstrap support values above 50% are shown at the first and second positions, respectively. Newly-sequenced collections are in black boldface.

S. yunanensis was closely related to *S. valdiviana* with high bootstrap support (99%). The collection, labelled *Candida* sp. (W370) from Taiwan, clustered together with S. *yunanensis* and another species labelled *Candida* sp. (GA2M09) from mushroom.

Taxonomy

***Sugiyamaella yunanensis* C.Y. Chai & F.L. Hui, sp. nov.**
MycoBank No: 835004
Figure 2

Type. China, Yunnan Province, Jinghong City, Mengyang Town, in rotting wood from a tropical rainforest, July 2016, K.F. Liu & L. Zhang (holotype NYNU 161059^T, culture ex-type CBS 14701).

Etymology. The species name *yunanensis* (N.L. fem. adj.) refers to the geographical origin of the type strain of this species.

Description. The cells are ovoid to elongate (2.5–5.5 × 3–7.5 μm) and occur singly or in pairs after being placed in YM broth for 3 days at 25 °C (Fig. 2A). Budding is multilateral. After 3 days of growth on YM agar at 25 °C, the colonies are white to cream-coloured, buttery and smooth, with entire margins. After 7 days at 25 °C on a Dalmau plate culture with CM agar, hyphae and blastoconidia are formed (Fig. 2B). Asci or signs of conjugation were not observed on sporulation media. Glucose and D-xylose are weakly fermented. Glucose, galactose, L-sorbose, D-glucosamine, D-xylose, L-arabinose, D-arabinose, sucrose, maltose, trehalose, methyl α-D-glucoside, cellobiose, salicin, arbutin, melibiose, raffinose, inulin, ribitol, D-glucitol, D-mannitol, D-gluco-no-1, 5-lactone, 2-keto-D-gluconate, D-gluconate, D-glucuronate, DL-lactate, succinate, citrate and ethanol are assimilated. No growth was observed in D-ribose, L-rhamnose, lactose, melezitose, glycerol, erythritol, xylitol, galactitol, myo-inositol or methanol. In nitrogen-assimilation tests, growth is present on nitrate, nitrite, L-lysine and glucosamine, while growth is absent on ethylamine, cadaverine, creatine, creatinine, imidazole and D-tryptophan. Growth is observed at 37 °C, but not at 40 °C. Growth in the presence of 0.01% cycloheximide is present, but growth in the presence of 10% sodium chloride (NaCl) with 5% glucose and 1% acetic acid is absent. Starch-like compounds are not produced. Urease activity and diazonium blue B reactions are negative.

Additional isolate examined. China, Yunnan Province, Jinghong City, Mengyang Town, in rotting wood from a tropical rainforest, July 2016, K.F. Liu & L. Zhang, NYNU 16113.

GenBank accession numbers. holotype NYNU 161059^T (ITS: MT257259; nrLSU D1/D2: MT257257); additional isolate NYNU 16113 (ITS: MT257256; nrLSU D1/D2: MT257261).

Notes. Two isolates, representing *S. yunanensis*, are retrieved in a well-supported clade and appear most closely related to *S. valdiviana* (Fig. 1). *Sugiyamaella yunanensis* can be distinguished from *S. valdiviana*, based on ITS and nrLSU D1/D2 loci (6/510 in ITS and 7/557 in nrLSU D1/D2). Physiologically, *S. yunanensis* differs from *S. val-*

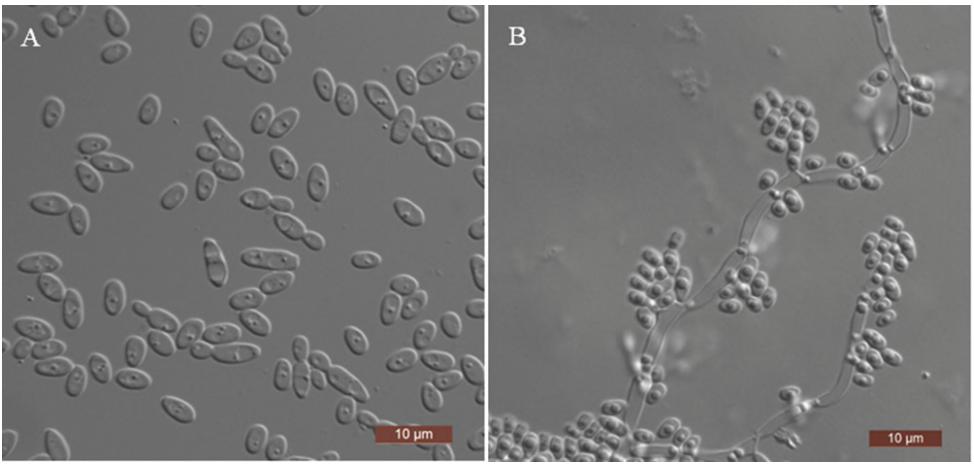

Figure 2. Morphology of *S. yunanensis* **A** budding cells after 3 days in YM broth at 25 °C **B** hyphae and blastoconidia on corn-meal agar after 7 days at 25 °C. Scale bars: 10 μm.

diviana by its ability to assimilate inulin and DL-lactate and its inability to assimilate melezitose, glycerol and myo-inositol. Additionally, *S. valdiviana* grows in the presence of 0.1% cycloheximide, while *S. yunanensis* does not (Kurtzman 2007).

***Sugiyamaella chuxiongensis* C.Y. Chai & F.L. Hui, sp. nov.**
MycoBank No: 835005
Figure 3

Type. China, Yunnan Province, Chuxiong City, Zixi Town, in rotting wood from Zixi Mountain, August 2018, K.F. Liu & Z.W. Xi (holotype NYNU 181038^{T}, culture ex-type CBS 16006, CICC 33361).

Description. The cells are ovoid to elongate (2.5–4 × 3–4.5 μm) and occur singly or in pairs after growth in a YM broth for 3 days at 25 °C (Fig. 3A). Budding is multilateral. After 3 days of growth on YM agar at 25 °C, the colonies are white to cream-coloured, buttery and smooth with entire margins. After 7 days at 25 °C, on a Dalmau plate culture with CM agar, hyphae and blastoconidia are formed (Fig. 3B). Asci or signs of conjugation were not observed on sporulation media. Fermentation of sugars is absent. Glucose, galactose, L-sorbose, D-glucosamine, D-ribose, D-xylose, L-arabinose, D-arabinose, sucrose, maltose, trehalose, methyl α-D-glucoside, cellobiose, salicin, arbutin, melibiose, raffinose, melezitose, inulin, erythritol, ribitol, xylitol, D-glucitol, D-mannitol, D-glucitol, D-mannitol, galactitol, myo-inositol, 2-keto-D-gluconate, succinate, citrate and ethanol are assimilated. No growth was observed in L-rhamnose, lactose, glycerol, D-gluconate, DL-lactate or methanol. In nitrogen-assimilation tests, growth is present on nitrate, nitrite, ethylamine, cadaverine, creatine, creatinine, glucosamine and D-tryptophan, while growth is absent on L-lysine and imidazole. Growth was observed at 35 °C, but not at 37 °C. Growth in the presence of 0.1%

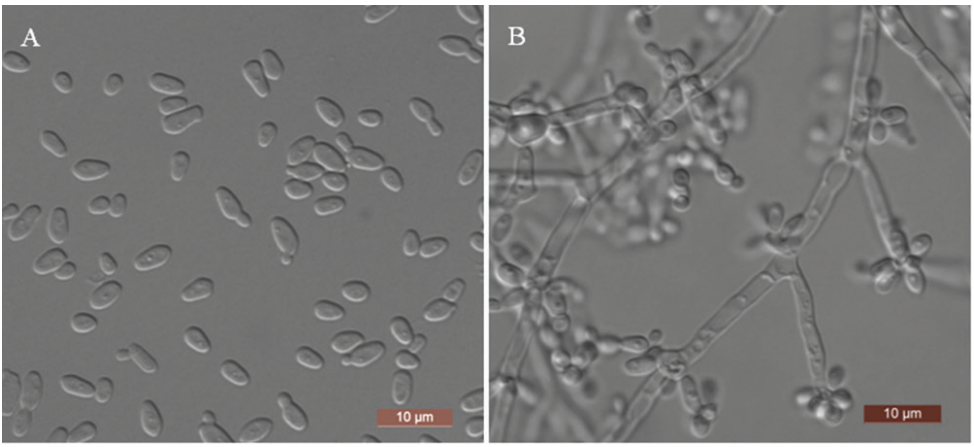

Figure 3. Morphology of *S. chuxiongensis* **A** budding cells after 3 days in YM broth at 25 °C **B** hyphae and blastoconidia on corn-meal agar after 7 days at 25 °C. Scale bars: 10 µm.

cycloheximide, 10% NaCl with 5% glucose and 1% acetic acid is present, but growth in the presence of 16% NaCl with 5% glucose is absent. Starch-like compounds are not produced. Urease activity and diazonium blue B reactions are negative.

Additional isolates examined. China, Yunnan Province, Chuxiong City, Zixi Town, in rotting wood from Zixi Mountain, August 2018, K.F. Liu & Z.W. Xi, NYNU 18521, NYNU 18634.

GenBank accession numbers. holotype NYNU 181038^{T} (ITS: MK682800; nrLSU D1/D2: MK682795); additional isolates NYNU 18521 (ITS: MT257260; nrLSU D1/D2: MT257255) and NYNU 18634 (ITS: MT257258; nrLSU D1/D2: MT257262).

Notes. We generated sequences for three isolates of *S. chuxiong*, NYNU 18521, NYNU 181038 and NYNU 18634. This new species is phylogenetically most closely related to *S. valenteae* and *S. ayubii* (Fig. 1). *Sugiyamaella chuxiong* can be distinguished from *S. valenteae*, based on ITS and nrLSU D1/D2 loci (33/454 in ITS and 15/513 in nrLSU D1/D2) and from *S. ayubii*, based on ITS and nrLSU D1/D2 (42/499 in ITS and 35/565 in nrLSU D1/D2). Physiologically, *S. chuxiong* can be differentiated from *S. valenteae* by its ability to assimilate D-arabinose, sucrose, salicin, melibiose, raffinose, melezitose and inulin and its inability to ferment glucose and grow at 37 °C (Sena et al. 2017). Similarly, the ability to assimilate salicin, inulin, erythritol and galactitol and the inability to assimilate L-rhamnose are the primary differences between *S. chuxiong* and *S. ayubii*. Additionally, *S. ayubii* can ferment glucose, while *S. chuxiong* cannot (Sena et al. 2017).

Discussion

In this study, nine *Sugiyamaella* species were identified, based on morphological and molecular phylogenetic analyses. All species were isolated from rotting wood collected in Yunnan Province, China. As a result, *S. chuxiong* and *S. yunanensis* are proposed as new species in *Sugiyamaella* for their distinct phylogenic positions and distinctive

physiological traits. In addition, identification of seven known species of *Sugiyamaella*, *S. americana*, *S. ayubii*, *S. novakii*, *S. paludigena*, *S. valenteae*, *S. valdiviana* and *S. xiaguanensis* were clearly distinguished by both morphological and molecular approaches.

Molecular phylogeny studies on *Sugiyamaella* and related genera have been carried out recently (Handel et al. 2016; Sena et al. 2017). Handel et al. (2016) determined that *Sugiyamaella* forms a well-supported monophyletic group, distinct from *Spencermartinsiella* and *Diddensiella*. However, Sena et al. (2017) indicated that *Sugiyamaella* is polyphyletic, where the species are intertwined with representatives of the genera *Trichomonascus* and *Spencermartinsiella*. The results of our phylogenetic analyses of combined gene sequences (ITS and nr LSU) with all currently-known species indicated that the genus is not monophyletic and grouped into a paraphyletic grade with three well-supported clades (Fig. 1): (i) *S. smithiae* (the type species), *S. lignohabitans* and *S. valdiviana* and their related species, (ii) *S. ayubii*, *S. trypani*, *S. valenteae* and *S. chuxiong* (described in this paper) and (iii) *S. americana*, *S. bullrunensis*, *S. carassensis* and *S. ligni*. These results suggest that the genus *Sugiyamaella* should be limited to species of the clade comprising the type species *S. smithiae*. The remaining two clades, which have previously been considered members of *Sugiyamaella*, could become two novel genera, although their phylogenetic relationships with other genera were not fully examined by this study (Fig. 1). As such, a careful phylogenetic analysis of *Sugiyamaella* species is required to clarify the possible heterogeneity of the genus.

Many new yeast species have been identified in the last ten years in China (Wang et al. 2010; Liu et al. 2016; Huang et al. 2018; Zhai et al. 2019). However, there is still a large number of undescribed yeast taxa in this country. This study indicates that there are at least 12 species of *Sugiyamaella* in China, including four species known previously to occur in China (*S. lignohabitans*, *S. qingdaonensis*, *S. smithiae* and *S. xiaguanensis*), new records of six species not known to occur in China (*S. americana*, *S. ayubii*, *S. novakii*, *S. paludigena*, *S. valenteae* and *S. valdiviana*) and two novel species (*S. chuxiong* and *S. yunanensis*). In China, there are still some species that need to be discovered, such as that listed under GenBank accession JN581116. To date, including the two novel species described in this study, there are thirty-one species of *Sugiyamaella* worldwide. Although the taxonomy of *Sugiyamaella* has received much attention in the past, many regions in China are under-sampled and more under-described indigenous *Sugiyamaella* species will undoubtedly be discovered in the future.

Sugiyamaella species have a worldwide distribution and are isolated from a wide range of substrates. Insect is their main habitat, but new species were also isolated from frass, rotting wood, decayed log, forest soil, mushrooms and peat (Kurtzman 2007; Wang et al. 2010; Kurtzman 2011; Morais et al. 2013; Handel et al. 2016; Sena et al. 2017; Huang et al. 2018). These studies expanded our knowledge on the substrates where *Sugiyamaella* species can occur, but on the other hand, demonstrated the complicated ecological function of this genus. In this study, seven known species and two new species were identified from rotting wood in China. Further research will focus on the *Sugiyamaella* diversity from a wide range of substrates.

Acknowledgements

We sincerely thank Dr. Lin Zhang, Dr. Kai-Fang Liu and Dr. Zhi-Wen Xi for their help with collecting specimens. This project was supported by Grant No. 31570021 from the National Natural Science Foundation of China, China, No. 2018001 from the State Key Laboratory of Motor Vehicle Biofuel Technology, Henan Tianguan Enterprise Group Co. Ltd., China.

References

Crous PW, Carnegie AJ, Wingfield MJ, Sharma R, Mughini G, Noordeloos ME, Santini A, Shouche YS, Bezerra JDP, Dima B, Guarnaccia V, Imrefi I, Jurjević Ž, Knapp DG, Kovács GM, Magistà D, Perrone G, Rämä T, Rebriev YA, Shivas RG, Singh SM, Souza-Motta CM, Thangavel R, Adhapure NN, Alexandrova AV, Alfenas AC, Alfenas RF, Alvarado P, Alves AL, Andrade DA, Andrade JP, Barbosa RN, Barili A, Barnes CW, Baseia IG, Bellanger JM, Berlanas C, Bessette AE, Bessette AR, Biketova AY, Bomfim FS, Brandrud TE, Bransgrove K, Brito ACQ, Cano-Lira JF, Cantillo T, Cavalcanti AD, Cheewangkoon R, Chikowski RS, Conforto C, Cordeiro TRL, Craine JD, Cruz R, Damm U, de Oliveira RJV, de Souza JT, de Souza HG, Dearnaley JDW, Dimitrov RA, Dovana F, Erhard A, Esteve-Raventós F, Félix CR, Ferisin G, Fernandes RA, Ferreira RJ, Ferro LO, Figueiredo CN, Frank JL, Freire KTLS, García D, Gené J, Gêsiorska A, Gibertoni TB, Gondra RAG, Gouliamova DE, Gramaje D, Guard F, Gusmão LFP, Haitook S, Hirooka Y, Houbraken J, Hubka V, Inamdar A, Iturriaga T, Iturrieta-González I, Jadan M, Jiang N, Justo A, Kachalkin AV, Kapitonov VI, Karadelev M, Karakehian J, Kasuya T, Kautmanová I, Kruse J, Kušan I, Kuznetsova TA, Landell MF, Larsson KH, Lee HB, Lima DX, Lira CRS, Machado AR, Madrid H, Magalhães OMC, Majerova H, Malysheva EF, Mapperson RR, Marbach PAS, Martín MP, Martín-Sanz A, Matočec N, McTaggart AR, Mello JF, Melo RFR, Mešić A, Michereff SJ, Miller AN, Minoshima A, Molinero-Ruiz L, Morozova OV, Mosoh D, Nabe M, Naik R, Nara K, Nascimento SS, Neves RP, Olariaga I, Oliveira RL, Oliveira TGL, Ono T, Ordoñez ME, Ottoni AM, Paiva LM, Pancorbo F, Pant B, Pawłowska J, Peterson SW, Raudabaugh DB, Rodríguez-Andrade E, Rubio E, Rusevska K, Santiago ALCMA, Santos ACS, Santos C, Sazanova NA, Shah S, Sharma J, Silva BDB, Siquier JL, Sonawane MS, Stchigel AM, Svetasheva T, Tamakeaw N, Telleria MT, Tiago PV, Tian CM, Tkalčec Z, Tomashevskaya MA, Truong HH, Vecherskii MV, Visagie CM, Vizzini A, Yilmaz N, Zmitrovich IV, Zvyagina EA, Boekhout T, Kehlet T, Læssøe T, Groenewald JZ (2019) Fungal Planet description sheets: 868–950. Persoonia 42: 291–473. https://doi.org/10.3767/persoonia.2019.42.11

Darriba D, Taboada GL, Doallo R, Posada D (2012) jModelTest 2: more models, new heuristics and parallel computing. Nature Methods 9: e772. https://doi.org/10.1038/nmeth.2109

Giménez-Jurado G, Cidadão AJ, Beijn-Van der Waaij A (1994) A novel heterothallic ascomycetous yeast species: *Stephanoascus smithiae*, teleomorph of *Candida edax*. Systematic and Applied Microbiology 17: 237–246. https://doi.org/10.1016/S0723-2020(11)80014-7

Guindon S, Dufayard JF, Lefort V, Anisimova M, Hordijk W, Gascuel O (2010) New algorithms and methods to estimate maximum-likelihood phylogenies: assessing the performance of PhyML 3.0. Systematic Biology 59: 307–321. https://doi.org/10.1093/sysbio/syq010

Hall TA (1999) Bioedit: a user-friendly biological sequence alignment editor and analysis program for Windows 95/98/NT. Nucleic Acids Symposium Series 41: 95–98.

Handel S, Wang T, Yurkov AM, König H (2016) *Sugiyamaella mastotermitis* sp. nov. and *Papiliotrema odontotermitis* f.a., sp. nov. from the gut of the termites *Mastotermes darwiniensis* and *Odontotermes obesus*. International Journal of Systematic and Evolutionary Microbiology 66: 4600–4608. https://doi.org/10.1099/ijsem.0.001397

Huang LN, Xi ZW, Li Y, Hui FL (2018) *Sugiyamaella xiaguanensis* f.a., sp. nov., a yeast species isolated from rotting wood. International Journal of Systematic and Evolutionary Microbiology 68: 3307–3310. https://doi.org/10.1099/ijsem.0.002988

Katoh K, Toh H (2010) Parallelization of the MAFFT multiple sequence alignment program. Bioinformatics 26: 1899–1900. https://doi.org/10.1093/bioinformatics/btq224

Kumar S, Stecher G, Tamura K (2016) MEGA7: molecular evolutionary genetics analysis version 7.0 for bigger datasets. Molecular Biology and Evolution 33: 1870–1874. https://doi.org/10.1093/molbev/msw054

Kurtzman CP (2007) Eleven new species of *Sugiyamaella* and *Candida* from forest habitats. FEMS Yeast Research 7: 1046–1063. https://doi.org/10.1111/j.1567-1364.2007.00224.x

Kurtzman CP (2011) *Sugiyamaella* Kurtzman & Robnett (2007). In: Kurtzman CP, Fell JW, Boekhout T (Eds) The Yeasts – a Taxonomic Study (5th edn, Vol. 2). Elsevier, Amsterdam, 817–822. https://doi.org/10.1016/B978-0-444-52149-1.00072-0

Kurtzman CP, Robnett CJ (1998) Identification and phylogeny of ascomycetous yeasts from analysis of nuclear large subunit (26S) ribosomal DNA partial sequences. Antonie van Leeuwenhoek 73: 331–371. https://doi.org/10.1023/A:1001761008817

Kurtzman CP, Robnett CJ (2007) Multigene phylogenetic analysis of the *Trichomonascus*, *Wickerhamiella* and *Zygoascus* yeast clades, and the proposal of *Sugiyamaella* gen. nov. and 14 new species combinations. FEMS Yeast Research 7: 141–151. https://doi.org/10.1111/j.1567-1364.2006.00157.x

Kurtzman CP, Fell JW, Boekhout T, Robert V (2011) Methods for isolation, phenotypic characterization and maintenance of yeasts. In: Kurtzman CP, Fell JW, Boekhout T (Eds) The Yeasts – a Taxonomic Study (5th edn, Vol. 1). Elsevier, Amsterdam, 87–110. https://doi.org/10.1016/B978-0-444-52149-1.00007-0

Lara CA, Santos RO, Cadete RM, Ferreira C, Marques S, Gírio F, Oliveira ES, Rosa CA, Fonseca C (2014) Identification and characterization of xylanolytic yeasts isolated from decaying wood and sugarcane bagasse in Brazil. Antonie van Leeuwenhoek International Journal of General and Molecular Microbiology 105: 1107–1119. https://doi.org/10.1007/s10482-014-0172-x

Liu XJ, Yi ZH, Ren YC, Li Y, Hui FL (2016) Five novel species in the Lodderomyces clade associated with insects. International Journal of Systematic and Evolutionary Microbiology 66: 4881–4889. https://doi.org/10.1099/ijsem.0.001446

Lopes MR, Batista TM, Franco GR, Ribeiro LR, Santos ARO, Furtado C, Moreira RG, Goes-Neto A, Vital MJS, Rosa LH, Lachance MA, Rosa CA (2018) *Scheffersomyces stambukii* f.a.,

sp. nov., a D-xylose-fermenting species isolated from rotting wood. International Journal of Systematic and Evolutionary Microbiology 68: 2306–2312. https://doi.org/10.1099/ijsem.0.002834

Morais CG, Lara CA, Marques S, Fonseca C, Lachance MA, Rosa CA (2013) *Sugiyamaella xylanicola* sp. nov., a xylan-degrading yeast species isolated from rotting wood. International Journal of Systematic and Evolutionary Microbiology 63: 2356–2360. https://doi.org/10.1099/ijs.0.050856-0

Nei M, Kumar S (2000) Molecular Evolution and Phylogenetics. Oxford University Press, New York.

Péter G, Dlauchy D, Price NPJ, Kurtzman CP (2012) *Diddensiella caesifluorescens* gen. nov., sp. nov., a riboflavin-producing yeast species of the family Trichomonascaceae. International Journal of Systematic and Evolutionary Microbiology 62: 3081–3087. https://doi.org/10.1099/ijs.0.042895-0

Rambaut A (2016) FigTree, version 1.4.3. University of Edinburgh, Edinburgh.

Sena LM, Morais CG, Lopes MR, Santos RO, Uetanabaro APT, Morais PB, Vital MJS, de Morais Jr MA, Lachance MA, Rosa CA (2017) D-Xylose fermentation, xylitol production and xylanase activities by seven new species of *Sugiyamaella*. Antonie van Leeuwenhoek International Journal of General and Molecular Microbiology 110: 53–67. https://doi.org/10.1007/s10482-016-0775-5

Urbina H, Frank R, Blackwell M (2013) *Scheffersomyces cryptocercus*: a new xylose-fermenting yeast associated with the gut of wood roaches and new combinations in the *Sugiyamaella* yeast clade. Mycologia 105: 650–660. https://doi.org/10.3852/12-094

Wang SA, Li FL, Bai FY (2010) *Candida laoshanensis* sp. nov. and *Candida qingdaonensis* sp. nov., anamorphic, ascomycetous yeast species isolated from decayed wood. International Journal of Systematic and Evolutionary Microbiology 60: 1697–1701. https://doi.org/10.1099/ijs.0.015230-0

White TJ, Bruns TD, Lee S, Taylor J (1990) Amplification and direct sequencing of fungal ribosomal RNA genes for phylogenetics. In: Innis MA, Gelfand DH, Sninsky JJ, White TJ (Eds) PCR protocols, a guide to methods and applications. Academic, San Diego, 315–322. https://doi.org/10.1016/B978-0-12-372180-8.50042-1

Zhai YC, Huang LN, Xi ZW, Chai CY, Hui FL (2019) *Candida yunanensis* sp. nov. and *Candida parablackwelliae* sp. nov., two yeast species in the *Candida albicans*/*Lodderomyces* clade. International Journal of Systematic and Evolutionary Microbiology 69: 2775–2780. https://doi.org/10.1099/ijsem.0.003552

MycoKeys 77: 41–64 (2021)
doi: 10.3897/mycokeys.77.59999
https://mycokeys.pensoft.net

RESEARCH ARTICLE

A peer-reviewed open-access journal
MycoKeys
Launched to accelerate biodiversity research

New species and records of *Diaporthe* from Jiangxi Province, China

Qin Yang[1,2,3], Ning Jiang[1], Cheng-Ming Tian[1]

1 *The Key Laboratory for Silviculture and Conservation of the Ministry of Education, Beijing Forestry University, Beijing 100083, China* **2** *Forestry Biotechnology Hunan Key Laboratories, Central South University of Forestry and Technology, Changsha 410004, China* **3** *The Key Laboratory for Non-Wood Forest Cultivation and Conservation of the Ministry of Education, Central South University of Forestry and Technology, Changsha 410004, China*

Corresponding author: Cheng-Ming Tian (chengmt@bjfu.edu.cn)

Academic editor: A. Miller | Received 25 October 2020 | Accepted 30 December 2020 | Published 14 January 2021

Citation: Yang Q, Jiang N, Tian C-M (2021) New species and records of *Diaporthe* from Jiangxi Province, China. MycoKeys 77: 41–64. https://doi.org/10.3897/mycokeys.77.59999

Abstract

Diaporthe species have often been reported as important plant pathogens, saprobes and endophytes on a wide range of plant hosts. Although several *Diaporthe* species have been recorded, little is known about species able to infect forest trees in Jiangxi Province. Hence, extensive surveys were recently conducted in Jiangxi Province, China. A total of 24 isolates were identified and analysed using comparisons of DNA sequence data for the nuclear ribosomal internal transcribed spacer (ITS), calmodulin (*cal*), histone H3 (*his3*), partial translation elongation factor-1α (*tef1*) and β-tubulin (*tub2*) gene regions, as well as their morphological features. Results revealed five novel taxa, *D. bauhiniae*, *D. ganzhouensis*, *D. schimae*, *D. verniciicola*, *D. xunwuensis* spp. nov. and three known species, *D. apiculatum*, *D. citri* and *D. multigutullata*.

Keywords

DNA phylogeny, five new taxa, forest trees, systematics, taxonomy

Introduction

The genus *Diaporthe* Nitschke (Sordariomycetes, Diaporthales) represents a cosmopolitan group of fungi occupying diverse ecological behaviour as plant pathogens, endophytes and saprobes (Muralli et al. 2006; Rossman et al. 2007; Udayanga et al. 2014,

2015; Fan et al. 2015, 2018; Guarnaccia and Crous 2017; Guarnaccia et al. 2018; Yang et al. 2018, 2020; Manawasinghe et al. 2019; Marin-Felix et al. 2019). *Diaporthe* species are responsible for diseases on a wide range of plant hosts, including agricultural crops, forest trees and ornamentals, some of which are economically important. Several symptoms, such as root and fruit rots, dieback, stem cankers, leaf spots, leaf and pod blights and seed decay are caused by *Diaporthe* spp. (Uecker 1988; Rehner and Uecker 1994; Mostert et al. 2001; Santos et al. 2011; Thompson et al. 2011; Udayanga et al. 2011).

Diaporthe was historically considered as monophyletic, based on its typical sexual morph and *Phomopsis* asexual morph (Gomes et al. 2013). However, Gao et al. (2017) recently revealed its paraphyletic nature, showing that *Mazzantia* (Wehmeyer 1926), *Ophiodiaporthe* (Fu et al. 2013), *Pustulomyces* (Dai et al. 2014), *Phaeocytostroma* and *Stenocarpella* (Lamprecht et al. 2011) are embedded in *Diaporthe* s. lat. Furthermore, Senanayake et al. (2017) recently included additional two genera in *Diaporthe* s. lat., namely *Paradiaporthe* and *Chiangraiomyces*.

Species identification criteria in *Diaporthe* were originally based on host association, morphology and culture characteristics (Mostert et al. 2001; Santos and Phillips 2009; Udayanga et al. 2011), which led to the description of over 200 species (Hyde et al. 2020). Some species of *Diaporthe* were reported to colonise a single host plant, while other species were found to be associated with different host plants (Santos and Phillips 2009; Diogo et al. 2010; Santos et al. 2011; Gomes et al. 2013). In addition, considerable variability of the phenotypic characters was found to be present within a species (Rehner and Uecker 1994; Mostert et al. 2001; Santos et al. 2010; Udayanga et al. 2011). During the past decade, a polyphasic approach, based on multi-locus DNA data, morphology and ecology, has been employed for species boundaries in the genus *Diaporthe* (Crous et al. 2012; Huang et al. 2015; Gao et al. 2016, 2017; Guarnaccia and Crous 2017; Guarnaccia et al. 2018; Yang et al. 2018, 2020). The classification of *Diaporthe* has been progressing and the basis for the species identification is a combination of morphological, cultural, phytopathological and phylogenetical analyses (Gomes et al. 2013; Udayanga et al. 2014, 2015; Fan et al. 2015; Huang et al. 2015; Gao et al. 2016, 2017; Guarnaccia and Crous 2017; Guarnaccia et al. 2018; Yang et al. 2018, 2020; Manawasinghe et al. 2019).

In Jiangxi Province, China, some forest trees were observed to be infected with fungal pathogens that cause dieback and leaf spots. Cankered branches and leaves with typical *Diaporthe* fruiting bodies were also found in the area. However, we found that only limited research had been undertaken regarding the fungal pathogens isolated from forest trees in Jiangxi Province. Hence, the present study was conducted to identify *Diaporthe* species that cause dieback and leaf spots disease in the forest trees in Jiangxi Province through morphological and multi-locus phylogenetic analyses, based on modern taxonomic concepts.

Materials and methods

Isolates

Fresh specimens of *Diaporthe* were isolated from the collected branches and leaves of six host plants during the collection trips conducted in Jiangxi Province (Table 1). A total of 24 isolates were established by removing a mucoid conidia mass from conidiomata, spreading the suspension on the surface of 1.8% potato dextrose agar (PDA) and incubating at 25 °C for up to 24 h. A single germinating conidium was plated on to fresh PDA plates. Specimens were deposited at the Museum of the Beijing Forestry University (**BJFC**). Axenic cultures were maintained at the China Forestry Culture Collection Centre (**CFCC**).

Morphological observation

Agar plugs (6 mm diam.) were taken from the edge of actively-growing cultures on PDA and transferred on to the centre of 9 cm diam. Petri dishes containing 2% tap water agar, supplemented with sterile pine needles (PNA; Smith et al. 1996) and potato dextrose agar (PDA) and incubated at 25 °C under a 12 h near-ultraviolet light/12 h dark cycle to induce sporulation, as described in recent studies (Gomes et al. 2013; Lombard et al. 2014). Colony characters and pigment production on PNA and PDA were noted in the 10-day culture. Colony features were rated according to the colour charts of Rayner (1970). Cultures were examined periodically for the development of conidiomata. The microscopic examination was based on the morphological features of conidiomata obtained from the fungal growth, mounted in clear lactic acid. At least 30 conidia were measured to calculate the mean size/length. Micro-morphological observations were done at 1000× magnification using a Leica compound microscope (DM 2500) with interference contrast (DIC) optics. Descriptions, nomenclature and illustrations of taxonomic novelties were deposited at MycoBank (www.MycoBank.org).

DNA extraction, PCR amplification and sequencing

Genomic DNA was extracted from colonies grown on cellophane-covered PDA, using a CTAB (cetyltrimethylammonium bromide) method (Doyle and Doyle 1990). DNA was estimated by electrophoresis in 1% agarose gel and the yield was measured using the NanoDrop 2000 (Thermo Scientific, Waltham, MA, USA), following the user manual (Desjardins et al. 2009). The PCR amplifications were performed in the DNA Engine Peltier Thermal Cycler (PTC-200; Bio-Rad Laboratories, Hercules, CA, USA). The primer set ITS1/ITS4 (White et al. 1990) was used to amplify the ITS region. The primer pair CAL228F/CAL737R (Carbone and Kohn 1999) was used to amplify the calmodulin gene (*cal*) and the primer pair CYLH4F (Crous et al. 2004) and H3-1b (Glass and Donaldson 1995) were used to amplify part of the histone H3 (*his3*) gene.

Table 1. Reference sequences included in molecular phylogenetic analyses of *Diaporthe*.

Species	Isolate	Host	Location	GenBank accession numbers				
				ITS	*cal*	*his3*	*tef1*	*tub2*
D. acericola	MFLUCC 17-0956	*Acer negundo*	Italy	KY964224	KY964137	NA	KY964180	KY964074
D. acerigena	CFCC 52554	*Acer tataricum*	China	MH121489	MH121413	MH121449	MH121531	NA
D. acutispora	CGMCC 3.18285	*Coffea* sp.	China	KX986764	KX999274	NA	KX999155	KX999195
D. alangii	CFCC 52556	*Alangium kurzii*	China	MH121491	MH121415	MH121451	MH121533	MH121573
D. alnea	CBS 146.46	*Alnus* sp.	Netherlands	KC343008	KC343250	KC343492	KC343734	KC343976
D. ampelina	STEU2660	*Vitis vinifera*	France	AF230751	AY745026	NA	AY745056	JX275452
D. amygdali	CBS 126679	*Prunus dulcis*	Portugal	KC343022	KC343264	KC343506	AY343748	KC343990
D. angelicae	CBS 111592	*Heracleum sphondylium*	Austria	KC343027	KC343269	KC343511	KC343753	KC343995
D. apiculatum	CGMCC 3.17533	*Camellia sinensis*	China	KP267896	NA	NA	KP267970	KP293476
	CFCC 53068	***Rhus chinensis***	**China**	**MK432651**	**MK442973**	**MK442998**	**MK578127**	**MK578054**
	CFCC 53069	***Rhus chinensis***	**China**	**MK432652**	**MK442974**	**MK442999**	**MK578128**	**MK578055**
	CFCC 53070	***Rhus chinensis***	**China**	**MK432653**	**MK442975**	**MK443000**	**MK578129**	**MK578056**
D. arctii	CBS 139280	*Arctium lappa*	Austria	KJ590736	KJ612133	KJ659218	KJ590776	KJ610891
D. arecae	CBS 161.64	*Areca catechu*	India	KC343032	KC343274	KC343516	KC343758	KC344000
D. arengae	CBS 114979	*Arenga enngleri*	Hong Kong	KC343034	KC343276	KC343518	KC343760	KC344002
D. aseana	MFLUCC 12-0299a	Unknown dead leaf	Thailand	KT459414	KT459464	NA	KT459448	KT459432
D. bauhiniae	**CFCC 53071**	***Bauhinia purpurea***	**China**	**MK432648**	**MK442970**	**MK442995**	**MK578124**	**MK578051**
	CFCC 53072		**China**	**MK432649**	**MK442971**	**MK442996**	**MK578125**	**MK578052**
	CFCC 53073		**China**	**MK432650**	**MK442972**	**MK442997**	**MK578126**	**MK578053**
D. beilharziae	BRIP 54792	*Indigofera australis*	Australia	JX862529	NA	NA	JX862535	KF170921
D. betulicola	CFCC 51128	*Betula albo-sinensis*	China	KX024653	KX024659	KX024661	KX024655	KX024657
D. biconispora	CGMCC 3.17252	*Citrus grandis*	China	KJ490597	KJ490539	KJ490539	KJ490476	KJ490418
D. biguttulata	CGMCC 3.17248	*Citrus limon*	China	KJ490582	NA	KJ490524	KJ490461	KJ490403
	CFCC 52584	*Juglans regia*	China	MH121519	MH121437	MH121477	MH121561	MH121598
D. bohemiae	CPC 28222	*Vitis vinifera*	Czech Republic	MG281015	MG281710	MG281361	MG281536	MG281188
D. brasiliensis	CBS 133183	*Aspidosperma tomentosum*	Brazil	KC343042	KC343284	KC343526	KC343768	KC344010
D. caatingaensis	CBS 141542	*Tacinga inamoena*	Brazil	KY085927	NA	NA	KY115603	KY115600
D. caryae	CFCC 52563	*Carya illinoensis*	China	MH121498	MH121422	MH121458	MH121540	MH121580
D. celeris	CPC 28262	*Vitis vinifera*	Czech Republic	MG281017	MG281712	MG281363	MG281538	MG281190
D. celastrina	CBS 139.27	*Celastrus* sp.	USA	KC343047	KC343289	KC343531	KC343773	KC344015
D. cercidis	CFCC 52565	*Cercis chinensis*	China	MH121500	MH121424	MH121460	MH121542	MH121582
D. charlesworthii	BRIP 54884m	*Rapistrum rugostrum*	Australia	KJ197288	NA	NA	KJ197250	KJ197268
D. cinnamomi	CFCC 52569	*Cinnamomum* sp.	China	MH121504	NA	MH121464	MH121546	MH121586
D. citri	AR 3405	*Citrus* sp.	USA	KC843311	KC843157	NA	KC843071	KC843187
	CFCC 53079	***Citrus sinensis***	**China**	**MK573940**	**MK574579**	**MK574595**	**MK574615**	**MK574635**
	CFCC 53080	***Citrus sinensis***	**China**	**MK573941**	**MK574580**	**MK574596**	**MK574616**	**MK574636**
	CFCC 53081	***Citrus sinensis***	**China**	**MK573942**	**MK574581**	**MK574597**	**MK574617**	**MK574637**
	CFCC 53082	***Citrus sinensis***	**China**	**MK573943**	**MK574582**	**MK574598**	**MK574618**	**MK574638**
D. citriasiana	CGMCC 3.15224	*Citrus unshiu*	China	JQ954645	KC357491	KJ490515	JQ954663	KC357459
D. citrichinensis	CGMCC 3.15225	*Citrus* sp.	China	JQ954648	KC357494	NA	JQ954666	NA
D. collariana	MFLU 17-2770	*Magnolia champaca*	Thailand	MG806115	MG783042	NA	MG783040	MG783041
D. conica	CFCC 52571	*Alangium chinense*	China	MH121506	MH121428	MH121466	MH121548	MH121588
D. cucurbitae	CBS 136.25	*Arctium* sp.	Unknown	KC343031	KC343273	KC343515	KC343757	KC343999
D. cuppatea	CBS 117499	*Aspalathus linearis*	South Africa	KC343057	KC343299	KC343541	KC343783	KC344025
D. discoidispora	ZJUD89	*Citrus unshiu*	China	KJ490624	NA	KJ490566	KJ490503	KJ490445
D. endophytica	CBS 133811	*Schinus terebinthifolius*	Brazil	KC343065	KC343307	KC343549	KC343791	KC343065
D. eres	AR5193	*Ulmus* sp.	Germany	KJ210529	KJ434999	KJ420850	KJ210550	KJ420799

Species	Isolate	Host	Location	GenBank accession numbers				
				ITS	*cal*	*his3*	*tef1*	*tub2*
D. fraxini-angustifoliae	BRIP 54781	*Fraxinus angustifolia*	Australia	JX862528	NA	NA	JX862534	KF170920
D. fraxinicola	CFCC 52582	*Fraxinus chinensis*	China	MH121517	MH121435	NA	MH121559	NA
D. fructicola	MAFF 246408	*Passiflora edulis* × *P. edulis* f. *flavicarpa*	Japan	LC342734	LC342738	LC342737	LC342735	LC342736
D. fukushii	MAFF 625034	*Pyrus pyrifolia*	Japan	JQ807469	NA	NA	JQ807418	NA
D. fusicola	CGMCC 3.17087	*Lithocarpus glabra*	China	KF576281	KF576233	NA	KF576256	KF576305
D. ganjae	CBS 180.91	*Cannabis sativa*	USA	KC343112	KC343354	KC343596	KC343838	KC344080
D. ganzhouensis	**CFCC 53087**	**Unknown dead wood**	**China**	**MK432665**	**MK442985**	**MK443010**	**MK578139**	**MK578065**
	CFCC 53088	**Unknown dead wood**	**China**	**MK432666**	**MK442986**	**MK443011**	**MK578140**	**MK578066**
D. garethjonesii	MFLUCC 12-0542a	Unknown dead leaf	Thailand	KT459423	KT459470	NA	KT459457	KT459441
D. guangxiensis	JZB320094	*Vitis vinifera*	China	MK335772	MK736727	NA	MK523566	MK500168
D. gulyae	BRIP 54025	*Helianthus annuus*	Australia	JF431299	NA	NA	KJ197271	JN645803
D. helicis	AR5211	*Hedera helix*	France	KJ210538	KJ435043	KJ420875	KJ210559	KJ420828
D. heterophyllae	CBS 143769	*Acacia heterohpylla*	France	MG600222	MG600218	MG600220	MG600224	MG600226
D. hispaniae	CPC 30321	*Vitis vinifera*	Spain	MG281123	MG281820	MG281471	MG281644	MG281296
D. hubeiensis	JZB320123	*Vitis vinifera*	China	MK335809	MK500235	NA	MK523570	MK500148
D. incompleta	CGMCC 3.18288	*Camellia sinensis*	China	KX986794	KX999289	KX999265	KX999186	KX999226
D. infecunda	CBS 133812	*Schinus terebinthifolius*	Brazil	KC343126	KC343368	KC343610	KC343852	KC344094
D. juglandicola	CFCC 51134	*Juglans mandshurica*	China	KU985101	KX024616	KX024622	KX024628	KX024634
D. kadsurae	CFCC 52586	*Kadsura longipedunculata*	China	MH121521	MH121439	MH121479	MH121563	MH121600
D. kochmanii	BRIP 54033	*Helianthus annuus*	Australia	JF431295	NA	NA	JN645809	NA
D. kongii	BRIP 54031	*Portulaca grandiflora*	Australia	JF431301	NA	NA	JN645797	KJ197272
D. litchicola	BRIP 54900	*Litchi chinensis*	Australia	JX862533	NA	NA	JX862539	KF170925
D. lithocarpus	CGMCC 3.15175	*Lithocarpus glabra*	China	KC153104	KF576235	NA	KC153095	KF576311
D. lonicerae	MFLUCC 17-0963	*Lonicera* sp.	Italy	KY964190	KY964116	NA	KY964146	KY964073
D. lusitanicae	CBS 123212	*Foeniculum vulgare*	Portugal	KC343136	KC343378	KC343620	KC343862	KC344104
D. masirevicii	BRIP 57892a	*Helianthus annuus*	Australia	KJ197277	NA	NA	KJ197239	KJ197257
D. middletonii	BRIP 54884e	*Rapistrum rugostrum*	Australia	KJ197286	NA	NA	KJ197248	KJ197266
D. miriciae	BRIP 54736j	*Helianthus annuus*	Australia	KJ197282	NA	NA	KJ197244	KJ197262
D. momicola	MFLUCC 16-0113	*Prunus persica*	China	KU557563	KU557611	NA	KU557631	KU55758
D. multigutullata	ZJUD98	*Citrus grandis*	China	KJ490633	NA	KJ490575	KJ490512	KJ490454
D. multigutullata	**CFCC 53095**	***Citrus maxima***	**China**	**MK432645**	**MK442967**	**MK442992**	**MK578121**	**MK578048**
	CFCC 53096	***Citrus maxima***	**China**	**MK432646**	**MK442968**	**MK442993**	**MK578122**	**MK578049**
	CFCC 53097	***Citrus maxima***	**China**	**MK432647**	**MK442969**	**MK442994**	**MK578123**	**MK578050**
D. musigena	CBS 129519	*Musa* sp.	Australia	KC343143	KC343385	KC343627	KC343869	KC344111
D. neilliae	CBS 144.27	*Spiraea* sp.	USA	KC343144	KC343386	KC343628	KC343870	KC344112
D. neoarctii	CBS 109490	*Ambrosia trifida*	USA	KC343145	KC343387	KC343629	KC343871	KC344113
D. oraccinii	CGMCC 3.17531	*Camellia sinensis*	China	KP267863	NA	KP293517	KP267937	KP293443
D. ovoicicola	CGMCC 3.17093	*Citrus* sp.	China	KF576265	KF576223	NA	KF576240	KF576289
D. pandanicola	MFLU 18-0006	*Pandanus* sp.	Thailand	MG646974	NA	NA	NA	MG646930
D. pascoei	BRIP 54847	*Persea americana*	Australia	JX862532	NA	NA	JX862538	KF170924
D. passifloricola	CBS 141329	*Passiflora foetida*	Malaysia	KX228292	NA	KX228367	NA	KX228387
D. penetriteum	CGMCC 3.17532	*Camellia sinensis*	China	KP714505	NA	KP714493	KP714517	KP714529
D. perjuncta	CBS 109745	*Ulmus glabra*	Austria	KC343172	KC343414	KC343656	KC343898	KC344140

Species	Isolate	Host	Location	GenBank accession numbers				
				ITS	*cal*	*his3*	*tef1*	*tub2*
D. perseae	CBS 151.73	*Persea gratissima*	Netherlands	KC343173	KC343415	KC343657	KC343899	KC344141
D. pescicola	MFLUCC 16-0105	*Prunus persica*	China	KU557555	KU557603	NA	KU557623	KU557579
D. podocarpi-macrophylli	CGMCC 3.18281	*Podocarpus macrophyllus*	China	KX986774	KX999278	KX999246	KX999167	KX999207
D. pseudomangiferae	CBS 101339	*Mangifera indica*	Dominican Republic	KC343181	KC343423	KC343665	KC343907	KC344149
D. pseudophoe-nicicola	CBS 462.69	*Phoenix dactylifera*	Spain	KC343184	KC343426	KC343668	KC343910	KC344152
D. psoraleae-pinnatae	CBS 136413	*Psoralea pinnata*	South Africa	KF777159	NA	NA	NA	KF777252
D. pterocarpicola	MFLUCC 10-0580a	*Pterocarpus indicus*	Thailand	JQ619887	JX197433	NA	JX275403	JX275441
D. pulla	CBS 338.89	*Hedera helix*	Yugoslavia	KC343152	KC343394	KC343636	KC343878	KC344120
D. pyracanthae	CAA483	*Pyracantha coccinea*	Portugal	KY435635	KY435656	KY435645	KY435625	KY435666
D. racemosae	CBS 143770	*Euclea racemosa*	South Africa	MG600223	MG600219	MG600221	MG600225	MG600227
D. rostrata	CFCC 50062	*Juglans mandshurica*	China	KP208847	KP208849	KP208851	KP208853	KP208855
D. sackstonii	BRIP 54669b	*Helianthus annuus*	Australia	KJ197287	NA	NA	KJ197249	KJ197267
D. sambucusii	CFCC 51986	*Sambucus williamsii*	China	KY852495	KY852499	KY852503	KY852507	KY852511
D. schimae	**CFCC 53103**	***Schima superba***	**China**	**MK432640**	**MK442962**	**MK442987**	**MK578116**	**MK578043**
	CFCC 53104	***Schima superba***	**China**	**MK432641**	**MK442963**	**MK442988**	**MK578117**	**MK578044**
	CFCC 53105	***Schima superba***	**China**	**MK432642**	**MK442964**	**MK442989**	**MK578118**	**MK578045**
D. schini	CBS 133181	*Schinus terebinthifolius*	Brazil	KC343191	KC343433	KC343675	KC343917	KC344159
D. schisandrae	CFCC 51988	*Schisandra chinensis*	China	KY852497	KY852501	KY852505	KY852509	KY852513
D. schoeni	MFLU 15-1279	*Schoenus nigricans*	Italy	KY964226	KY964139	NA	KY964182	KY964109
D. sennae	CFCC 51636	*Senna bicapsularis*	China	KY203724	KY228875	NA	KY228885	KY228891
D. serafiniae	BRIP 55665a	*Helianthus annuus*	Australia	KJ197274	NA	NA	KJ197236	KJ197254
D. siamensis	MFLUCC 10-573a	*Dasymaschalon* sp.	Thailand	JQ619879	NA	NA	JX275393	JX275429
D. sojae	FAU635	*Glycine max*	USA	KJ590719	KJ612116	KJ659208	KJ590762	KJ610875
D. sterilis	CBS 136969	*Vaccinium corymbosum*	Italy	KJ160579	KJ160548	MF418350	KJ160611	KJ160528
D. subclavata	ICMP20663	*Citrus unshiu*	China	KJ490587	NA	KJ490529	KJ490466	KJ490408
D. subellipicola	MFLU 17-1197	Dead wood	China	MG746632	NA	NA	MG746633	MG746634
D. subordinaria	CBS 464.90	*Plantago lanceolata*	New Zealand	KC343214	KC343456	KC343698	KC343940	KC344182
D. taoicola	MFLUCC 16-0117	*Prunus persica*	China	KU557567	NA	NA	KU557635	KU557591
D. tectonae	MFLUCC 12-0777	*Tectona grandis*	China	KU712430	KU749345	NA	KU749359	KU743977
D. tectonendophytica	MFLUCC 13-0471	*Tectona grandis*	China	KU712439	KU749354	NA	KU749367	KU749354
D. tectonigena	MFLUCC 12-0767	*Tectona grandis*	China	KU712429	KU749358	NA	KU749371	KU743976
D. terebinthifolii	CBS 133180	*Schinus terebinthifolius*	Brazil	KC343216	KC343458	KC343700	KC343942	KC344184
D. ternstroemia	CGMCC 3.15183	*Ternstroemia gymnanthera*	China	KC153098	NA	NA	KC153089	NA
D. thunbergii	MFLUCC 10-576a	*Thunbergia laurifolia*	Thailand	JQ619893	JX197440	NA	JX275409	JX275449
D. tibetensis	CFCC 51999	*Juglandis regia*	China	MF279843	MF279888	MF279828	MF279858	MF279873
D. tulliensis	BRIP 62248a	*Theobroma cacao*	Australia	KR936130	NA	NA	KR936133	KR936132
D. ukurunduensis	CFCC 52592	*Acer ukurunduense*	China	MH121527	MH121445	MH121485	MH121569	NA
D. unshiuensis	CGMCC 3.17569	*Citrus unshiu*	China	KJ490587	NA	KJ490529	KJ490408	KJ490466
	CFCC 52594	*Carya illinoensis*	China	MH121529	MH121447	MH121487	MH121571	MH121606
D. undulata	CGMCC 3.18293	Leaf of unknown host	China-Laos border	KX986798	NA	KX999269	KX999190	KX999230
D. vawdreyi	BRIP 57887a	*Psidium guajava*	Australia	KR936126	NA	NA	KR936129	KR936128

Species	Isolate	Host	Location	GenBank accession numbers				
				ITS	*cal*	*his3*	*tef1*	*tub2*
D. verniciicola	**CFCC 53109**	***Vernicia montana***	**China**	**MK573944**	**MK574583**	**MK574599**	**MK574619**	**MK574639**
	CFCC 53110	***Vernicia montana***	**China**	**MK573945**	**MK574584**	**MK574600**	**MK574620**	**MK574640**
	CFCC 53111	***Vernicia montana***	**China**	**MK573946**	**MK574585**	**MK574601**	**MK574621**	**MK574641**
	CFCC 53112	***Vernicia montana***	**China**	**MK573947**	**MK574586**	**MK574602**	**MK574622**	**MK574642**
D. viniferae	JZB320071	*Vitis vinifera*	China	MK341551	MK500107		MK500119	MK500112
D. virgiliae	CMW40748	*Virgilia oroboides*	South Africa	KP247566	NA	NA	NA	KP247575
D. xishuangbanica	CGMCC 3.18282	*Camellia sinensis*	China	KX986783	NA	KX999255	KX999175	KX999216
D. xunwuensis	**CFCC 53085**	**Unknown dead wood**	**China**	**MK432663**	**MK442983**	**MK443008**	**MK578137**	**MK578063**
	CFCC 53086	**Unknown dead wood**	**China**	**MK432664**	**MK442984**	**MK443009**	**MK578138**	**MK578064**
D. yunnanensis	CGMCC 3.18289	*Coffea* sp.	China	KX986796	KX999290	KX999267	KX999188	KX999228
Diaporthella corylina	CBS 121124	*Corylus* sp.	China	KC343004	KC343246	KC343488	KC343730	KC343972

Newly sequenced material is indicated in bold type. NA, not applicable.

The primer pair EF1-728F/EF1-986R (Carbone and Kohn 1999) was used to amplify a partial fragment of the translation elongation factor 1-α gene (*tef1*). The primer sets T1 (O'Donnell and Cigelnik 1997) and Bt2b (Glass and Donaldson 1995) were used to amplify the beta-tubulin gene (*tub2*); the additional combination of Bt2a/Bt2b (Glass and Donaldson 1995) was used in case of amplification failure of the T1/Bt2b primer pair. The PCR amplifications of the genomic DNA with the phylogenetic markers were done using the same primer pairs and conditions as in Yang et al. (2018). The PCR products were assayed via electrophoresis in 2% agarose gels, while the DNA sequencing was performed using an ABI PRISM 3730XL DNA Analyser with a Big-Dye Terminater Kit v.3.1 (Inv-itrogen, USA) at the Shanghai Invitrogen Biological Technology Company Limited (Beijing, China).

Phylogenetic analyses

The quality of the amplified nucleotide sequences was checked and combined using SeqMan v.7.1.0 and reference sequences were retrieved from the National Center for Biotechnology Information (NCBI), based on recent publications on the genus *Diaporthe* (Guarnaccia et al. 2018; Yang et al. 2018, 2020). Sequences were aligned using MAFFT v. 6 (Katoh and Toh 2010) and corrected manually using Bioedit 7.0.9.0 (Hall 1999). The best-fit nucleotide substitution models for each gene were selected using jModelTest v. 2.1.7 (Darriba et al. 2012) under the Akaike Information Criterion.

The phylogenetic analyses of the combined gene regions were performed using Maximum Likelihood (ML) and Bayesian Inference (BI) methods. ML was conducted using PhyML v. 3.0 (Guindon et al. 2010), with 1000 bootstrap replicates while BI was performed using a Markov Chain Monte Carlo (MCMC) algorithm in MrBayes v. 3.0 (Ronquist et al. 2003). Two MCMC chains, started from random trees for 1,000,000 generations and trees, were sampled every 100th generation, resulting in a

total of 10,000 trees. The first 25% of trees were discarded as burn-in of each analysis. Branches with significant Bayesian Posterior Probabilities (BPP) were estimated in the remaining 7500 trees. Phylogenetic trees were viewed with FigTree v.1.3.1 (Rambaut and Drummond 2010) and processed by Adobe Illustrator CS5. Sequence alignment and phylogenetic trees were deposited in TreeBASE (submission ID: S25213). The nucleotide sequence data of the new taxa were deposited in GenBank (Table 1).

Results

The phylogenetic position of the 24 isolates of *Diaporthe* was determined by the phylogenetic analysis of the combined ITS, *cal*, *his3*, *tef1* and *tub2* sequences data. Reference sequences of the representative species used in the analysis were selected from Yang et al. (2018) and supplemented with sequences from GenBank. The ITS, *cal*, *his3*, *tef1 tub2* and combined data matrices contained 522, 541, 529, 520, 535 and 2 659 characters with gaps, respectively. The alignment comprised of 142 strains together with *Diaporthella corylina* (culture CBS 121124) which was selected as the outgroup. The best nucleotide substitution model used for the analysis of ITS, *his3* and *tub2* was TrN+I+G, while HKY+I+G was used for *cal* and *tef1*. The topologies resulting from ML and BI analyses of the concatenated dataset were congruent (Fig. 1) and the sequences from the 24 *Diaporthe* isolates formed eight distinct clades as shown in Fig. 1, representing five undescribed species and three known species.

Taxonomy

Diaporthe apiculatum **Y.H. Gao & L. Cai, in Gao, Liu & Cai, Syst. Biodiv. 14: 106. 2016.**
Figure 2

Description. Conidiomata pycnidial, discoid, immersed in bark, scattered, slightly erumpent through bark surface, with a solitary undivided locule. Ectostromatic disc yellowish to grey, one ostiole per disc, (300–)305–357(–368) µm diam. Ostiole medium black, up to level of disc. Locule undivided, (338–)357–450(–464) µm diam. Conidiophores reduced to conidiogenous cells. Conidiogenous cells cylindrical, hyaline, densely aggregated, phiailidic, unbranched, straight or slightly curved. Beta conidia hyaline, aseptate, filiform, hamate, eguttulate, base subtruncate, tapering towards one apex, (26.5–)30–39.5(–43) × 1.5–2 µm. Alpha conidia not observed.

Culture characters. Colony originally flat with white fluffy aerial mycelium, becoming yellowish to pale green mycelium with age, marginal area irregular, conidiomata absent.

Specimens examined. China. Jiangxi Province: Ganzhou City, Fengshan Forest Park, on branches of *Rhus chinensis*, 25°45'12"N, 115°00'41"E, 23 Jul 2018, *Q. Yang*, *Y. Liu*, *Y.M. Liang* & *C.M. Tian* (BJFC-S1680; living culture: CFCC 53068, CFCC 53069 and CFCC 53070).

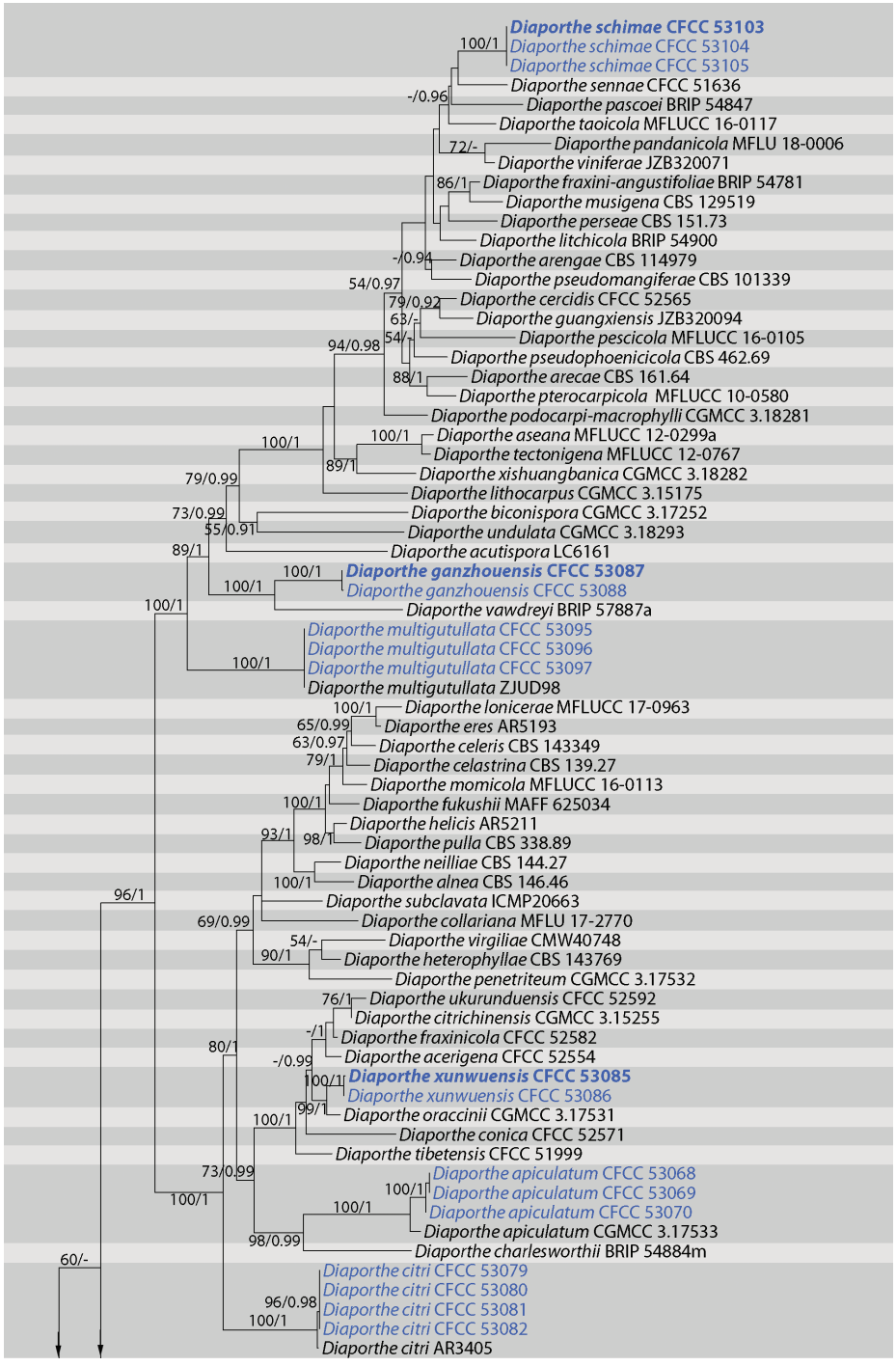

Figure 1. Phylogram of *Diaporthe* from a Maximum Likelihood analysis based on combined ITS, *cal*, *his3*, *tef1* and *tub2*. Values above the branches indicate Maximum Likelihood bootstrap (left, ML BP ≥ 50%) and Bayesian probabilities (right, BI PP ≥ 0.90). The tree is rooted with *Diaporthella corylina*. Strains in current study are in blue font and the ex-type cultures are in bold font.

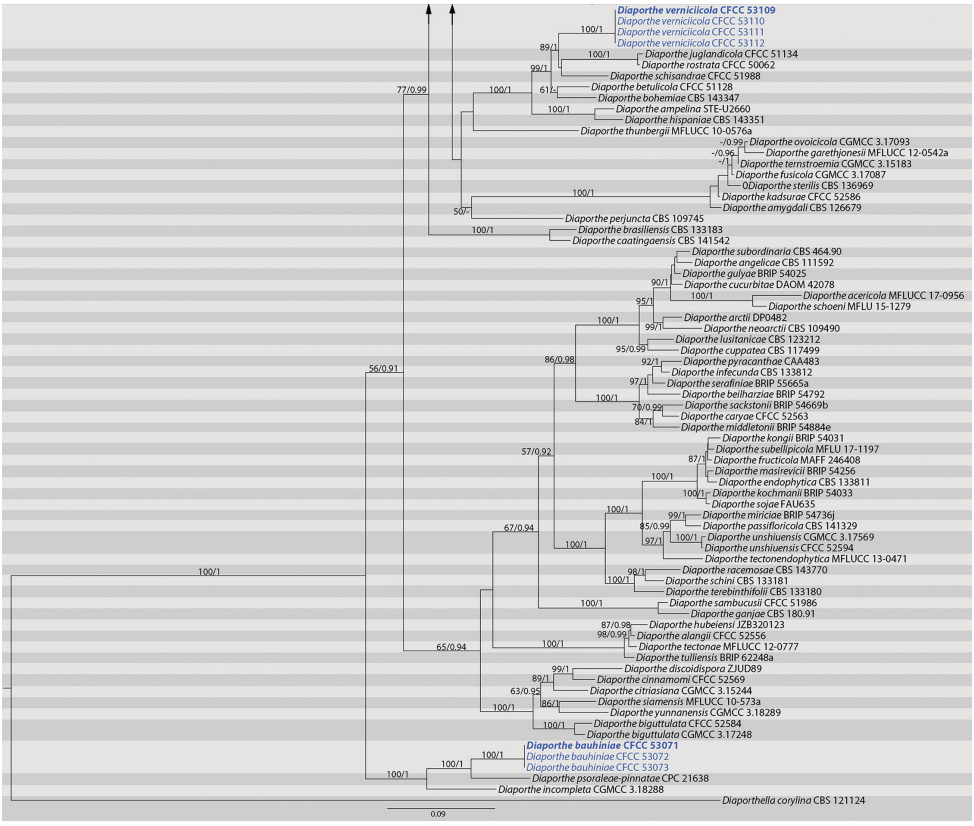

Figure 1. Continued.

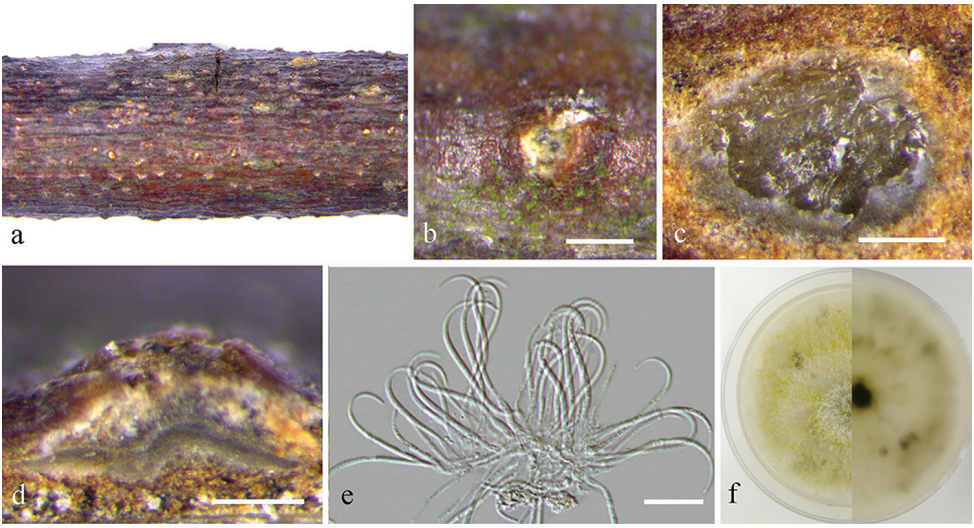

Figure 2. *Diaporthe apiculatum* on *Rhus chinensis* (BJFC-S1680) **a, b** habit of conidiomata in wood **c** transverse section of conidiomata **d** longitudinal section through conidiomata **e** conidiogenous cells attached with beta conidia **f** the colony on PDA. Scale bars: 200 μm (**b–d**); 10 μm (**e**).

Notes. *Diaporthe apiculatum* was originally described as an endophyte from healthy leaves of *Camellia sinensis* in Jiangxi Province, China (Gao et al. 2015). In the present study, three isolates (CFCC 53068, CFCC 53069 and CFCC 53070) from symptomatic branches of *Rhus chinensis* were found congruent with *D. apiculatum*, based on DNA sequence and morphological data (Fig. 1). The clade was, therefore, confirmed to be *D. apiculatum* and was found to be both an endophyte and a pathogen.

Diaporthe bauhiniae **C.M. Tian & Q. Yang, sp. nov.**
MycoBank No: 829519
Figure 3

Diagnosis. Distinguished from the phylogenetically closely-related species *D. psoraleae-pinnatae* in alpha and beta conidia.

Etymology. Named after *Bauhinia*, the host genus where the fungus was isolated.

Description. Conidiomata pycnidial, immersed in bark, scattered, slightly erumpent through bark surface, nearly flat, discoid, with a solitary undivided locule. Ectostromatic disc grey to brown, one ostiole per disc. Locule circular, undivided, (180–)200–290(–300) µm diam. Conidiophores reduced to conidiogenous cells. Conidiogenous cells hyaline, cylindrical, unbranched, straight, tapering towards the apex. Alpha conidia hyaline, aseptate, ellipsoidal to fusiform, biguttulate to multi-guttulate, (7.5–)9–13(–14) × (1.5–)2–2.5(–3) µm. Beta conidia hyaline, aseptate, filiform, straight to sinuous, eguttulate, (25–)28.5–40(–43) × 1 µm.

Culture characters. Colony at first white, becoming wine-red in the centre with age. Aerial mycelium white, dense, fluffy, conidiomata absent.

Specimens examined. China. Jiangxi Province: Ganzhou City, on branches of *Bauhinia purpurea*, 25°52'21"N, 114°56'44"E, 11 May 2018, *Q. Yang*, *Y. Liu* & *Y.M. Liang* (holotype BJFC-S1621; ex-type living culture: CFCC 53071; living culture: CFCC 53072 and CFCC 53073).

Notes. Three isolates representing *D. bauhiniae* cluster in a well-supported clade and appear most closely related to *D. psoraleae-pinnatae*. *Diaporthe bauhiniae* can be distinguished from *D. psoraleae-pinnatae*, based on ITS and *tub2* (38/458 in ITS and 11/418 in *tub2*). Morphologically, *D. bauhiniae* differs from *D. psoraleae-pinnatae* in having narrower alpha conidia (2–2.5 vs. 2.5–3 µm) and the beta conidia of *D. psoraleae-pinnatae* were not observed (Crous et al. 2013).

Diaporthe citri **(H.S. Fawc.) F.A. Wolf, J. Agric. Res., Washington 33(7): 625, 1926.**
Figure 4

Description. Leaf spots subcircular to irregular, pale brown, with dark brown at margin. Pycnidia solitary, scattered on the leaf surface. Pycnidial conidiomata in culture, globose, erumpent, single or clustered in groups of 3–5 pycnidia, coated with hyphae, cream to yellowish translucent conidial droplets exuded from ostioles. Conidiophores

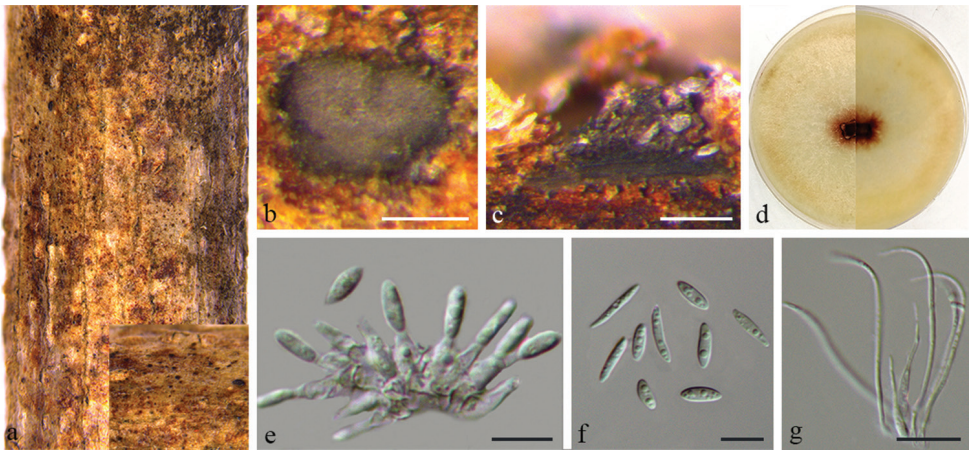

Figure 3. *Diaporthe bauhiniae* on *Bauhinia purpurea* (BJFC-S1621) **a** habit of conidiomata in wood **b** transverse section of conidiomata **c** longitudinal section through conidiomata **d** the colony on PDA **e** conidiogenous cells attached with alpha conidia **f** Alpha conidia **g** Beta conidia. Scale bars: 100 μm (**b, c**); 10 μm (**e–h**).

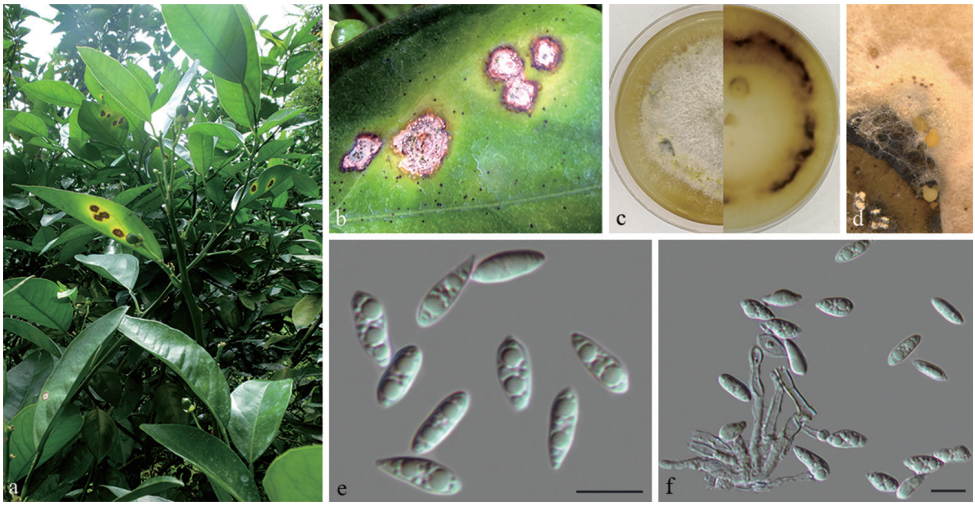

Figure 4. *Diaporthe citri* on *Citrus sinensis* (BJFC-S1658) **a, b** symptoms on leaves of host plant **c** culture on PDA (30d) **d** conidiomata **e** alpha conidia **f** conidiophores and alpha conidia. Scale bars: 10 μm (**e, f**).

reduced to conidiogenous cells. Conidiogenous cells hyaline, unbranched, septate, straight, slightly tapering towards the apex, 14.5–25 × 2–3 μm. Alpha conidia hyaline, aseptate, rounded at one end, apex at the other end, usually with two large guttulate, (9.5–)10.5–12 × 3.5–4.5 μm. Beta conidia not observed.

Culture characters. Colony originally flat with white fluffy aerial mycelium, becoming greyish mycelium with age, with yellowish-cream conidial drops exuding from the ostioles.

Specimens examined. China. Jiangxi Province: Ganzhou City, on leaves of *Citrus sinensis*, 24°59'44"N, 115°31'01"E, 13 May 2018, *Q. Yang*, *Y. Liu* & *Y.M.*

Liang (BJFC-S1658; living culture: CFCC 53079 and CFCC 53080); 24°59'45"N, 115°31'02"E, 13 May 2018, *Q. Yang*, *Y. Liu* & *Y.M. Liang* (BJFC-S1659; living culture: CFCC 53081 and CFCC 53082).

Notes. *Diaporthe citri* is a widely distributed species in citrus-growing regions. In the present study, four isolates (CFCC 53079, CFCC 53080, CFCC 53081 and CFCC 53082) from symptomatic leaves of *Citrus sinensis* were congruent with *D. citri*, based on DNA sequence and morphological data (Fig. 1). The clade was, therefore, confirmed to be *D. citri*.

Diaporthe ganzhouensis **C.M. Tian & Q. Yang, sp. nov.**
MycoBank No: 829522
Figure 5

Diagnosis. Distinguished from the phylogenetically closely-related species *D. vawdreyi* in having longer conidiophores and wider alpha conidia.

Etymology. Named after Ganzhou City where the species was first collected.

Description. On PDA: Conidiomata pycnidial, subglobose, solitary, deeply embedded in the medium, erumpent, dark brown to black. Pale yellow conidial drops exuding from ostioles. Conidiophores (12–)15.5–21 × 1.5–2 μm, cylindrical, hyaline, phiailidic, branched, straight or slightly curved. Alpha conidia 6.5–8.5(–9) × 2–2.5(–3) μm, aseptate, hyaline, ellipsoidal to fusiform, rounded at one end, slightly apex at the other end, biguttulate. Beta conidia hyaline, aseptate, filiform, sinuous at one end, eguttulate, (21.5–)25.5–31(–33) × 1 μm.

Culture characters. Colony at first white, becoming yellowish with age. Aerial mycelium white, dense, fluffy, with visible solitary conidiomata at maturity.

Specimens examined. China. Jiangxi Province: Ganzhou City, unknown dead wood, 25°45'17"N, 115°00'41"E, 23 Jul 2018, *Q. Yang*, *Y. Liu*, *Y.M. Liang* & *C.M. Tian* (holotype BJFC-C004; ex-type culture: CFCC 53087; living culture: CFCC 53088).

Notes. *Diaporthe ganzhouensis* comprises the isolates CFCC 53087 and CFCC 53088, revealed to be closely related to *D. vawdreyi* in the combined phylogenetic tree (Fig. 1). *Diaporthe ganzhouensis* can be distinguished, based on ITS, *tef1-a* and *tub2* loci from *D. vawdreyi* (6/456 in ITS, 63/357 in *tef1-a* and 40/469 in *tub2*). *Diaporthe ganzhouensis* differs morphologically from *D. vawdreyi* in having longer conidiopores (15.5–21 vs. 6–15 μm) and wider alpha conidia (2–2.5 vs. 1.5–2 μm) (Crous et al. 2015).

Diaporthe multiguttulata **F. Huang, K.D. Hyde & Hong Y. Li, in Huang et al., Fungal Biology 119(5): 343. 2015.**
Figure 6

Description. Conidiomata pycnidial, 692–750(–800) μm diam., solitary and with single necks erumpent through host bark. Tissue around neck is cylindrical. Locule circular, undivided, 450–565(–600) μm diam. Conidiophores reduced to conidiogenous cells. Con-

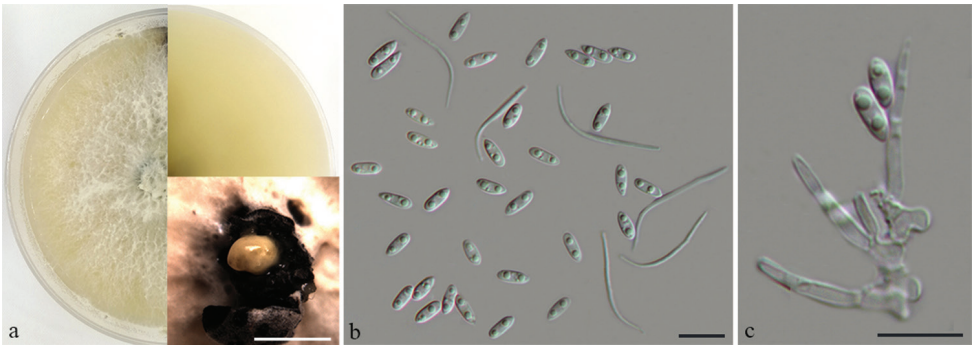

Figure 5. *Diaporthe ganzhouensis* on unknown host (BJFC-S1678) **a** the colony on PDA and conidiomata **b** alpha and beta conidia **c** conidiogenous cells and alpha conidia. Scale bars: 10 μm (**b, c**).

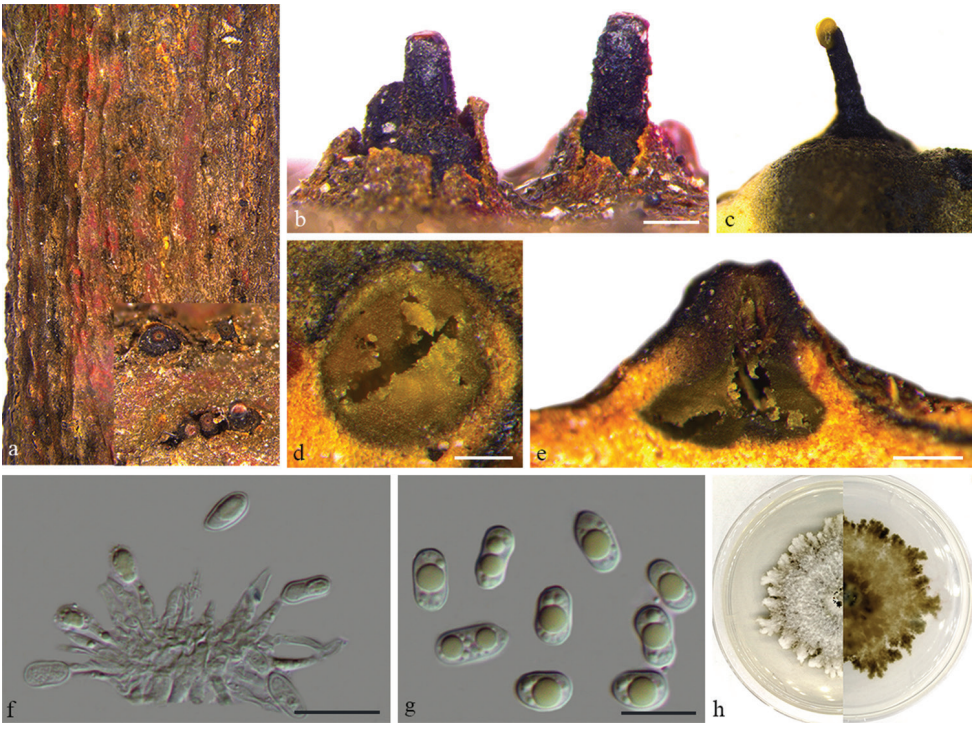

Figure 6. *Diaporthe multiguttulata* on *Citrus maxima* (BJFC-S1614) **a, b** habit of conidiomata on twig **c** conidiomata on PDA **d** transverse section through conidiomata **e** longitudinal section through conidiomata **f** conidiogenous cells attached with alpha conidia **g** alpha conidia **h** the colony on PDA. Scale bars: 200 μm (**b, d, e**); 10 μm (**f, g**).

idiogenous cells unbranched, straight or slightly curved, apical or base sometimes swelling, (8.5–)9–10.5(–11) × 1.5–2 μm. Alpha conidia hyaline, aseptate, ellipsoidal, biguttulate or with one large guttulate, rounded at one end, slightly apex at the other end, occasionally submedian constriction, (7.5–)8–9(–10.5) × 4–5(–5.5) μm. Beta conidia not observed.

Culture characters. Colony originally flat with white felty aerial mycelium, becoming pale green mycelium with age, margin area irregularly, with visible solitary conidiomata at maturity.

Specimens examined. China. Jiangxi Province: Ganzhou City, on branches of *Citrus maxima*, 25°51'28"N, 114°55'19"E, 11 May 2018, *Q. Yang*, *Y. Liu* & *Y.M. Liang* (BJFC-S1614; living culture: CFCC 53095, CFCC 53096 and CFCC 53097).

Notes. *Diaporthe multiguttulata* was originally described as an endophyte from a healthy branch of *Citrus grandis* in Fujian Province, China (Huang et al. 2015). In the present study, three isolates (CFCC 53095, CFCC 53096 and CFCC 53097) from symptomatic branches of *Citrus maxima* were congruent with *D. multigutullata*, based on DNA sequence data and confirmed from the morphological analysis (Fig. 1). The clade, therefore, was verified as *D. multigutullata* which could exist both as an endophyte and a pathogen.

Diaporthe schimae **C.M. Tian & Q. Yang, sp. nov.**
MycoBank No: 829526
Figure 7

Diagnosis. Distinguished from the phylogenetically closely-related species *D. sennae* in having larger alpha conidia and longer beta conidia.

Etymology. Named after the host genus *Schima* on which the fungus was isolated.

Description. Leaf spots subcircular to irregular, pale brown, with dark brown at margin. Pycnidia solitary, scattered on the leaf surface. Pycnidial conidiomata in culture, globose, (150–)173–357(–373) µm in its widest diam., erumpent, single or clustered in groups of 3–5 pycnidia, coated with hyphae, cream to yellowish translucent conidial droplets exuded from ostioles. Conidiophores reduced to conidiogenous cells. Conidiogenous cells hyaline, unbranched, septate, straight, slightly tapering towards the apex. Alpha conidia scarce, hyaline, aseptate, ellipsoidal to spindle-shaped, four small guttulate, (7.5–)8–8.5(–9) × 2.5–3 µm. Beta conidia abundant, hyaline, aseptate, filiform, straight to sinuous at one end, eguttulate, (25–)27.5–38.5(–40.5) × 1–1.5 µm.

Culture characters. Colony entirely white, with fluffy aerial mycelium, concentric zonation, margin fimbricate, reverse slightly yellowish.

Specimens examined. China. Jiangxi Province: Ganzhou City, Fengshan Forest Park, on leaves of *Schima superba*, 25°44'22"N, 114°59'40"E, 15 May 2018, *Q. Yang*, *Y. Liu* & *Y.M. Liang* (holotype BJFC-S1661; ex-type culture: CFCC 53103); 24°40'51"N, 115°34'36"E, 15 May 2018, *Q. Yang*, *Y. Liu* & *Y.M. Liang* (BJFC-S1662; living culture: CFCC 53104); 24°40'52"N, 115°34'54"E, 15 May 2018, *Q. Yang*, *Y. Liu* & *Y.M. Liang* (BJFC-S1663; living culture: CFCC 53105).

Notes. *Diaporthe schimae* occurs in an independent clade (Fig. 1) and was revealed to be phylogenetically distinct from *D. sennae*. *Diaporhe schimae* can be distinguished with *D. sennae* by 41 nucleotides in concatenated alignment, in which three were

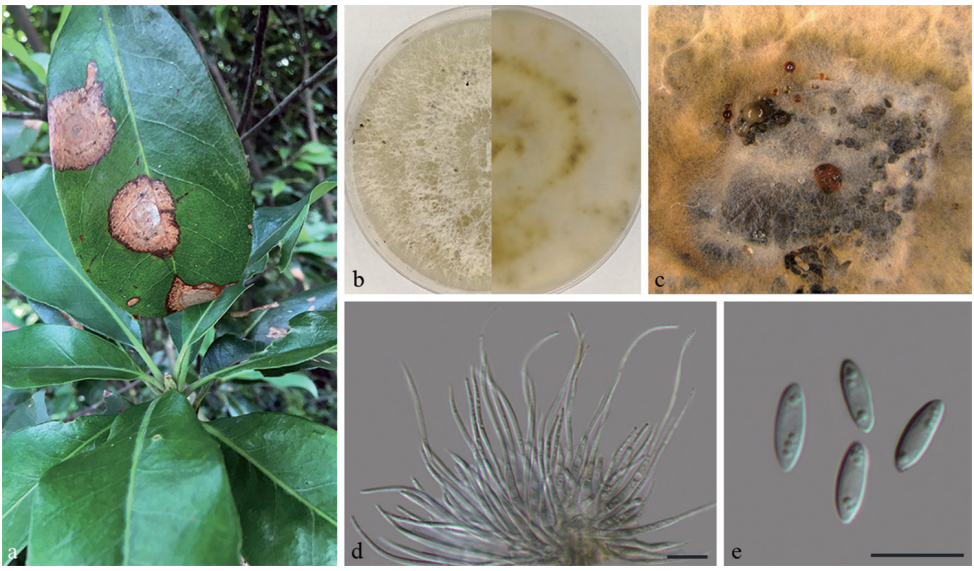

Figure 7. *Diaporthe schimae* on *Schima superba* (BJFC-S1661) **a** symptoms on leaves of host plant **b** the colony on PDA **c** conidiomata on PDA **d** conidiophores cells attached with beta conidia **e** Alpha conidia. Scale bars: 10 μm (**d, e**).

distinct in the ITS region, 20 in the *tef1-a* region and 18 in the *tub2* region. *Diaporthe schimae* differs morphologically from *D. sennae* in having larger alpha conidia and longer beta conidia (8–8.5 × 2.5–3 vs. 5.5–6.3 × 1.5–1.7 μm in alpha conidia; 27.5–38.5 vs. 18.4–20 μm in beta conidia) (Yang et al. 2017a).

Diaporthe verniciicola **C.M. Tian & Q. Yang, sp. nov.**
MycoBank No: 832921
Figure 8

Diagnosis. Distinguished from the phylogenetically closely-related species *D. rostrata* in having smaller alpha conidia; and from *D. juglandicola* in having wider alpha conidia.

Etymology. Named after the host genus *Vernicia* on which the fungus was isolated.

Description. Conidiomata pycnidial, 825–1050 × 445–500 μm diam., solitary and with single necks erumpent through host bark. Tissue around neck is conical. Locule circular, undivided, 400–665 μm diam. Conidiophores reduced to conidiogenous cells. Conidiogenous cells unbranched, straight or sinuous, 14.5–21.5 × 1–1.5 μm. Alpha conidia hyaline, aseptate, ellipsoidal to fusiform, with 1–2-guttulate, 7–8.5 × 3–3.5 μm. Beta conidia not observed.

Culture characters. Colony white to yellowish, with dense and felted mycelium in the centre, lacking aerial mycelium, conidiomata absent.

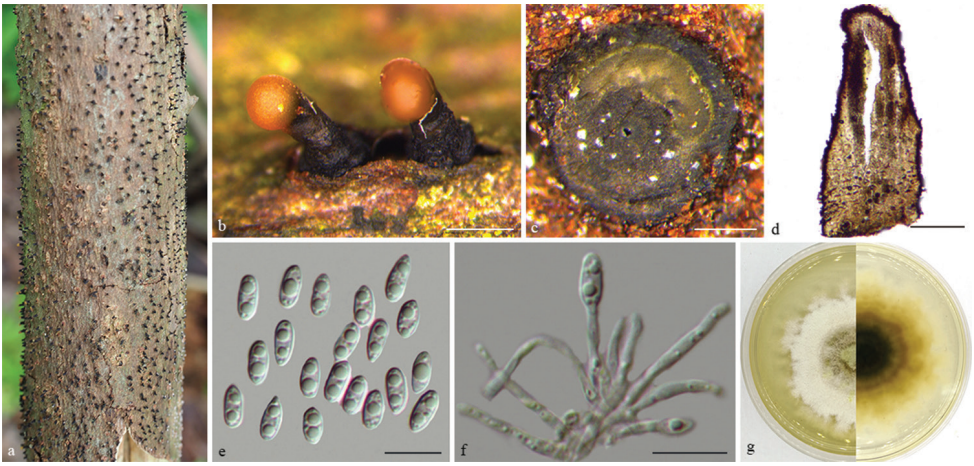

Figure 8. *Diaporthe verniciicola* on *Vernicia montana* (BJFC-S1622) **a, b** habit of conidiomata on twig **c** transverse section through conidiomata **d** longitudinal section through conidiomata **e** alpha conidia **f** conidiophores **g** culture on PDA (30d). Scale bars: 500 μm (**b**); 200 μm (**c**); 10 μm (**e, f**).

Specimens examined. China. Jiangxi Province: Ganzhou City, on branches of *Vernicia montana*, 24°40'51"N, 115°34'52"E, 12 May 2018, *Q. Yang*, *Y. Liu* & *Y.M. Liang* (holotype BJFC-S1622; ex-type culture: CFCC 53109); 24°40'52"N, 115°34'50"E, 12 May 2018, *Q. Yang*, *Y. Liu* & *Y.M. Liang* (BJFC-S1623; living culture: CFCC 53110); 24°45'14"N, 115°34'00"E, 12 May 2018, *Q. Yang*, *Y. Liu* & *Y.M. Liang* (BJFC-S1624; living culture: CFCC 53111); 25°44'15"N, 114°59'32"E, 15 May 2018, *Q. Yang*, *Y. Liu* & *Y.M. Liang* (BJFC-S1624; living culture: CFCC 53112).

Notes. Two isolates of *D. verniciicola* clustered in a well-supported clade (ML/BI = 100/1) and appeared closely related to *D. rostrata* and *D. juglandicola* (Fig. 1). Morphologically, *D. verniciicola* is similar to *D. rostrata* characterised by conidiomata with single necks erumpent through the host bark. However, the new taxon can be distinguished from *D. rostrata* in having smaller alpha conidia (7–8.5 × 3–3.5 vs. 8.5–11.5 × 4–5 μm) (Fan et al. 2015) and *D. verniciicola* differs from *D. juglandicola* in having wider alpha conidia (3–3.5 vs. 2.5–3 μm) (Yang et al. 2017b). This is the first discovery of a *Diaporthe* species isolated from infected branches or twigs on *Vernicia montana* and was confirmed as a new species, based on phylogeny and morphology.

Diaporthe xunwuensis **C.M. Tian & Q. Yang, sp. nov.**
MycoBank No: 829521
Figure 9

Diagnosis. Distinguished from the phylogenetically closely-related species *D. oraccinii* in having longer conidiophores and larger alpha conidia.

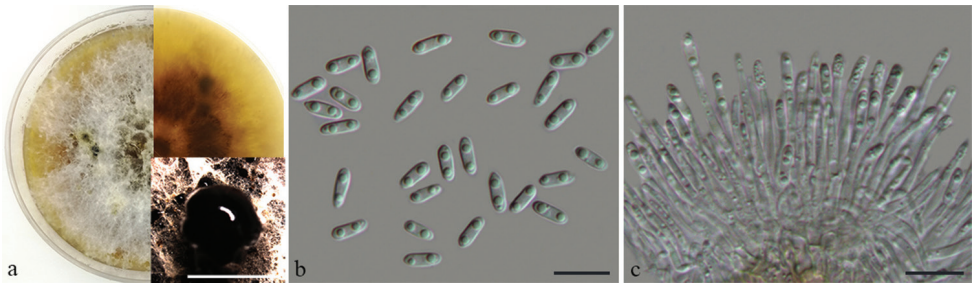

Figure 9. *Diaporthe xunwuensis* on unknown host (BJFC-S1679) **a** the colony on PDA and conidiomata **b** alpha conidia **c** conidiogenous cells attached with alpha conidia. Scale bars: 10 μm (**a–c**).

Etymology. Named after the county (Xunwu) where the species was first collected.

Description. On PDA: Conidiomata pycnidial, globose, solitary or aggregated, deeply embedded in the medium, erumpent, dark brown to black. Hyaline conidial drops exuding from ostioles. Conidiophores (18.5–)21.5–30(–32.5) × 1–1.5(–2) μm, cylindrical, hyaline, phiailidic, unbranched, straight to sinuous. Alpha conidia (6.5–)7–8.5 × 2–3 μm, aseptate, hyaline, ellipsoidal to fusiform, rounded at one end, slightly apex at the other end, usually with 2-guttulate. Beta conidia not observed.

Culture characters. Colony at first white, becoming dark brown in the centre with age. Aerial mycelium white, dense, fluffy, with black conidial drops exuding from the ostioles.

Specimens examined. China. Jiangxi Province: Ganzhou City, unknown dead wood, 25°45'17"N, 115°00'41"E, 23 Jul 2018, *Q. Yang*, *Y. Liu*, *Y.M. Liang* & *C.M. Tian* (holotype BJFC-C003; ex-type culture: CFCC 53085; living culture: CFCC 53086).

Notes. Two isolates representing *D. xunwuensis* clustered in a well-supported clade and appear most closely related to *D. oraccinii*. *Diaporthe xunwuensis* can be distinguished from *D. oraccinii*, based on ITS, *his3* and *tef1-a* loci (5/471 in ITS, 5/432 in *his3* and 5/325 in *tef1-a*). Morphologically, *D. xunwuensis* differs from *D. oraccinii* in having longer conidiopores (21.5–30 vs. 10.5–22.5 μm) and larger alpha conidia (7–8.5 × 2–3 vs. 5.5–7.5 × 0.5–2 μm) (Gao et al. 2016).

Discussion

The current study described eight *Diaporthe* species from 24 strains, based on a large set of freshly-collected specimens. It includes five new species and three known species, which were sampled from six host genera distributed in Jiangxi Province of China (Table 1). In this study, 142 reference sequences (including outgroup) were selected, based on BLAST searches of NCBIs GenBank nucleotide database and included in the phylogenetic analyses (Table 1). Phylogenetic analyses, based on five combined loci (ITS, *cal*, *his3*, *tef1* and *tub2*), as well as morphological characters, revealed the diversity of *Diaporthe* species in Jiangxi Province, mainly focusing on diebacks from major ecological or economic forest trees.

The identification and characterisation of novel taxa and new host records indicate the high potential of *Diaporthe* to evolve rapidly. In the present study, five species were first reported in China as pathogens. Amongst these species, *D. bauhiniae* was characterised by having longer alpha conidia (9–13 × 2–2.5 μm). *Diaporthe ganzhouensis* and *D. xunwuensis* were isolated from unknown dead wood, but *D. ganzhouensis* can be distinguish from *D. xunwuenesis* in having beta conidia and was supported by analysis of the sequence data. *Diaporthe schimae* was identified as the most widespread species from isolates collected in Jiangxi Province. *Diaporthe verniciicola* have conidiomata with single necks erumpent through the host bark. Furthermore, two new host records were described, *D. apiculatum* from *Rhus chinensis* and *D. multiguttulata* from *Citrus maxima*.

Recent plant pathological studies have revealed that several *Diaporthe* species cause disease, particularly to important plant hosts on a wide range of economically-significant agricultural crops, such as blueberries, citrus, grapes, oaks, sunflowers, soybeans, tea plants, tropical fruits, vegetables and various trees (van Rensburg et al. 2006; Santos and Phillips 2009; Santos et al. 2011; Thompson et al. 2011; Grasso et al. 2012; Lombard et al. 2014; Huang et al. 2015; Udayanga et al. 2015; Gao et al. 2016; Guarnaccia et al. 2018; Yang et al. 2020). For example, research conducted by Huang et al. (2015) revealed seven endophytic *Diaporthe* species on *Citrus*; Gao et al. (2016) demonstrated that *Diaporthe* isolates associated with *Camellia* spp. could be assigned to seven species and two species complexes; Guarnaccia et al. (2018) explored the occurrence, diversity and pathogenicity of *Diaporthe* species associated with *Vitis vinifera* and revealed four new *Diaporthe* species; Yang et al. (2018) provided the first molecular phylogenetic framework of *Diaporthe* diversity associated with dieback diseases in China. Following the adoption of DNA sequence-based methods, *Diaporthe* taxonomy is actively changing, with numerous species being described each year.

The present study is the first evaluation of *Diaporthe* species, associated with dieback diseases in Jiangxi Province using the combined morphology and molecular data and provided useful information for evaluating the pathogenicity of various species. Multiple strains from different locations should also be subjected to multi-locus phylogenetic analysis to determine intraspecific variation and redefine species boundaries. The descriptions and molecular data of *Diaporthe* species, provided in this study, represent a resource for plant pathologists, plant quarantine officials and taxonomists for identification of *Diaporthe*.

Acknowledgements

This study is financed by the National Natural Science Foundation of China (Project No.: 31670647). We are grateful to Chungen Piao and Minwei Guo (China Forestry Culture Collection Center (CFCC), Chinese Academy of Forestry, Beijing) for support of strain preservation during this study.

References

Carbone I, Kohn LM (1999) A method for designing primer sets for speciation studies in filamentous ascomycetes. Mycologia 3: 553–556. https://doi.org/10.1080/00275514.1999.12061051

Crous PW, Gams W, Stalpers JA, Robert V, Stegehuis G (2004) MycoBank: an online initiative to launch mycology into the 21st century. Studies in Mycology 50: 19–22.

Crous PW, Summerell BW, Shivas RG, Burgess TI, Decock CA, Dreyer LL, Granke LL, Guest DI, Hardy GESTJ, Hausbeck MK, Hüberli D, Jung T, Koukol O, Lennox CL, Liew ECY, Lombard L, McTaggart AR, Pryke JS, Roets F, Saude C, Shuttleworth LA, Stukely MJC, Vánky K, Webster BJ, Windstam ST, Groenewald JZ (2012) Fungal Planet description sheets: 107–127. Persoonia 28: 138–182. https://doi.org/10.3767/003158512X652633

Crous PW, Wingfield MJ, Guarro J, Cheewangkoon, R, van der Bank, M, Swart WJ, Stchigel AM, Cano-Lira JF, Roux J, Madrid H, Damm U, Wood AR, Shuttleworth LA, Hodges CS, Munster, M, de Jesús Yáñez-Morales M, Zúñiga-Estrada L, Cruywagen EM, De Hoog GS, Silvera C, Najafzadeh J, Davison EM, Davison PJN, Barrett MD, Barrett RL, Manamgoda DS, Minnis AM, Kleczewski NM, Flory SL, Castlebury LA, Clay K, Hyde KD, Maússe-Sitoe SND, Shuaifei C, Lechat C, Hairaud M, Lesage-Meessen L, Pawłowska J, Wilk M, Śliwińska-Wyrzychowska A, Mętrak M, Wrzosek M, Pavlic-Zupanc D, Maleme HM, Slippers B, Mac Cormack WP, Archuby DI, Grünwald NJ, Tellería MT, Dueñas M, Martín MP, Marincowitz S, de Beer ZW, Perez CA, Gené J, Marin-Felix Y, Groenewald JZ (2013) Fungal Planet description sheets: 154–213. Persoonia 31: 188–296. https://doi.org/10.3767/003158513X675925

Crous PW, Wingfield MJ, Le Roux JJ, Richardson DM, Strasberg D, Shivas RG, Alvarado P, Edwards J, Moreno G, Sharma R, Sonawane MS, Tan YP, Altés A, Barasubiye T, Barnes CW, Blanchette RA, Boertmann D, Bogo A, Carlavilla JR, Cheewangkoon R, Daniel R, de Beer ZW, Yáñez-Morales M de Jesús, Duong TA, Fernández-Vicente J, Geering ADW, Guest DI, Held BW, Heykoop M, Hubka V, Ismail AM, Kajale SC, Khemmuk W, Kolařík M, Kurli R, Lebeuf R, Lévesque CA, Lombard L, Magista D, Manjón JL, Marincowitz S, Mohedano JM, Nováková A, Oberlies NH, Otto EC, Paguigan ND, Pascoe IG, Pérez-Butrón JL, Perrone G, Rahi P, Raja HA, Rintoul T, Sanhueza RMV, Scarlett K, Shouche YS, Shuttleworth LA, Taylor PWJ, Thorn RG, Vawdrey LL, Solano-Vidal R, Voitk A, Wong PTW, Wood AR, Zamora JC, Groenewald JZ (2015) Fungal Planet description sheets: 371–399. Persoonia 35: 264–327. https://doi.org/10.3767/003158515X690269

Dai DQ, Wijayawardene NN, Bhat DJ, Chukeatirote E, Bahkali AH, Zhao R-L, Xu J-C, Hyde KD (2014) *Pustulomyces* gen. nov. accommodated in Diaporthaceae, Diaporthales, as revealed by morphology and molecular analyses. Cryptogamie, Mycologie 35: 63–72. https://doi.org/10.7872/crym.v35.iss1.2014.63

Darriba D, Taboada GL, Doallo R, Posada D (2012) jModelTest 2: more models, new heuristics and parallel computing. Nature Methods 9: e772. https://doi.org/10.1038/nmeth.2109

Desjardins P, Hansen JB, Allen M (2009) Microvolume protein concentration determination using the NanoDrop 2000c spectrophotometer. Journal of Visualized Experiments: JoVE 33: 1–3. https://doi.org/10.3791/1610

Diogo E, Santos JM, Phillips AJ (2010) Phylogeny, morphology and pathogenicity of Diaporthe and Phomopsis species on almond in Portugal. Fungal Diversity 44: 107–115. https://doi.org/10.1007/s13225-010-0057-x

Doyle JJ, Doyle JL (1990) Isolation of plant DNA from fresh tissue. Focus 12: 13–15. https://doi.org/10.2307/2419362

Fan XL, Hyde KD, Udayanga D, Wu XY, Tian CM (2015) *Diaporthe rostrata*, a novel ascomycete from *Juglans mandshurica* associated with walnut dieback. Mycological Progress 14: 1–8. https://doi.org/10.1007/s11557-015-1104-5

Fan XL, Yang Q, Bezerra JDP, Alvarez LV, Tian CM (2018) *Diaporthe* from walnut tree (*Juglans regia*) in China, with insight of *Diaporthe eres* complex. Mycological Progress 1–13. https://doi.org/10.1007/s11557-018-1395-4

Fu CH, Hsieh HM, Chen CY, Chang TT, Huang YM, Ju YM (2013) *Ophiodiaporthe cyatheae* gen. et sp. nov., a diaporthalean pathogen causing a devastating wilt disease of *Cyathea lepifera* in Taiwan. Mycologia 105: 861–872. https://doi.org/10.3852/12-346

Gao YH, Liu F, Cai L (2016) Unravelling *Diaporthe* species associated with *Camellia*. Systematics and Biodiversity 14: 102–117. https://doi.org/10.1080/14772000.2015.1101027

Gao YH, Liu F, Duan W, Crous PW, Cai L (2017) *Diaporthe* is paraphyletic. IMA Fungus 8: 153–187. https://doi.org/10.5598/imafungus.2017.08.01.11

Gao YH, Su YY, Sun W, Cai L (2015) *Diaporthe* species occurring on *Lithocarpus glabra* in China, with descriptions of five new species. Fungal Biology 115: 295–309. https://doi.org/10.1016/j.funbio.2014.06.006

Glass NL, Donaldson GC (1995) Development of primer sets designed for use with the PCR to amplify conserved genes from filamentous ascomycetes. Applied and Environmental Microbiology 61: 1323–1330. https://doi.org/10.1128/AEM.61.4.1323-1330.1995

Gomes RR, Glienke C, Videira SIR, Lombard L, Groenewald JZ, Crous PW (2013) *Diaporthe*: a genus of endophytic, saprobic and plant pathogenic fungi. Persoonia 31: 1–41. https://doi.org/10.3767/003158513X666844

Grasso FM, Marini M, Vitale A, Firrao G, Granata G (2012) Canker and dieback on *Platanus* × *acerifolia* caused by *Diaporthe scabra*. Forest Pathology 42: 510–513. https://doi.org/10.1111/j.1439-0329.2012.00785.x

Guarnaccia V, Crous PW (2017) Emerging citrus diseases in Europe caused by species of *Diaporthe*. IMA Fungus 8: 317–334. https://doi.org/10.5598/imafungus.2017.08.02.07

Guarnaccia V, Groenewald JZ, Woodhall J, Armengol J, Cinelli T, Eichmeier A, Ezra D, Fontaine F, Gramaje D, Gutierrez-Aguirregabiria A, Kaliterna J, Kiss L, Larignon P, Luque J, Mugnai L, Naor V, Raposo R, Sándor E, Váczy KZ, Crous PW (2018) *Diaporthe* diversity and pathogenicity revealed from a broad survey of grapevine diseases in Europe. Persoonia 40: 135–153. https://doi.org/10.3767/persoonia.2018.40.06

Guindon S, Dufayard JF, Lefort V, Anisimova M, Hordijk W, Gascuel O (2010) New algorithms and methods to estimate maximum-likelihood phylogenies: assessing the performance of PhyML 3.0. Systematic Biology 59: 307–321. https://doi.org/10.1093/sysbio/syq010

Hall T (1999) BioEdit: a user-friendly biological sequence alignment editor and analysis program for Windows 95/98/NT. Nucleic Acids Symposium Series 41: 95–98.

Huang F, Udayanga D, Wang X, Hou X, Mei X, Fu Y, Hyde KD, Li HY (2015) Endophytic *Diaporthe* associated with *Citrus*: A phylogenetic reassessment with seven new species from China. Fungal Biology 119: 331–347. https://doi.org/10.1016/j.funbio.2015.02.006

Hyde KD, Dong Y, Phookamsak R, Jeewon R, Jayarama Bhat D, Gareth Jones EB, Liu N-G, Abeywickrama PD, Mapook A, Wei D, Perera RH, Manawasinghe IS, Pem D, Bundhun D, Karunarathna A, Ekanayaka AH, Bao D-F, Li J, Samarakoon MC, Chaiwan N, Chuan-Gen Lin, Phutthacharoen K, Zhang S-N, Senanayake IC, Goonasekara ID, Thambugala KM, Phukhamsakda C, Tennakoon DS, Jiang H-B, Yang J, Zeng M, Huanraluek N, Liu J-K, Wijesinghe SN, Tian Q, Tibpromma S, Brahmanage RS, Boonmee S, Huang S-K, Thiyagaraja V, Lu Y-Z, Jayawardena RS, Dong W, Yang E-F, Singh SK, Singh MS, Rana S, Lad SS, Anand G, Devadatha B, Niranjan M, Sarma VV, Liimatainen K, Aguirre-Hudson B, Niskanen T, Overall A, Alvarenga LRM, Gibertoni BT, Pfliegler WP, Horváth E, Imre A, Alves LA, da Silva Santos CA, Tiago VP, Bulgakov TS, Wanasinghe DN, Bahkali AH, Doilom M, Elgorban AM, Maharachchikumbura SSN, Rajeshkumar KC, Haelewaters D, Mortimer PE, Zhao Q, Lumyong S, Xu J, Sheng J (2020) Fungal diversity notes 1151–1276: taxonomic and phylogenetic contributions on genera and species of fungal taxa. Fungal Diversity 100: 5–277. https://doi.org/10.1007/s13225-020-00439-5

Katoh K, Toh H (2010) Parallelization of the MAFFT multiple sequence alignment program. Bioinformatics 26: 1899–1900. https://doi.org/10.1093/bioinformatics/btq224

Lamprecht SC, Crous PW, Groenewald JZ, Tewoldemedhin YT, Marasas WFO (2011) Diaporthaceae associated with root and crown rot of maize. IMA Fungus 2: 13–24. https://doi.org/10.5598/imafungus.2011.02.01.03

Lombard L, Van Leeuwen GCM, Guarnaccia V, Polizzi G, Van Rijswick PC, Karin Rosendahl KC, Gabler J, Crous PW (2014) *Diaporthe* species associated with *Vaccinium*, with specific reference to Europe. Phytopathologia Mediterranea 53: 287–299. https://doi.org/10.14601/Phytopathol_Mediterr-14034

Manawasinghe IS, Dissanayake A, Liu M, Liu M, Wanasinghe DN, Xu J, Zhao W, Zhang W, Zhou Y, Hyde KD, Brooks S, Yan J (2019) High genetic diversity and species complexity of *Diaporthe* associated with grapevine dieback in China. Frontiers in Microbiology 10: e1936. https://doi.org/10.3389/fmicb.2019.01936

Marin-Felix Y, Hernández-Restrepo M, Wingfield M J, Akulov A, Carnegie AJ, Cheewangkoon R, Gramaje D, Groenewald JZ, Guarnaccia V, Halleen F, Lombard L, Luangsa-ard J, Marincowitz S, Moslemi A, Mostert L, Quaedvlieg W, Schumacher RK, Spies CFJ, Thangavel R, Taylor PWJ, Wilson AM, Wingfield BD, Wood AR, Crous PW (2019) Genera of phytopathogenic fungi: GOPHY 2. Studies in Mycology 92: 47–133. https://doi.org/10.1016/j.simyco.2018.04.002

Mostert L, Crous PW, Kang JC, Phillips AJ (2001) Species of *Phomopsis* and a *Libertella* sp. occurring on grapevines with specific reference to South Africa: morphological, cultural, molecular and pathological characterization. Mycologia 93: 146–167. https://doi.org/10.1080/00275514.2001.12061286

Muralli TS, Suryanarayanan TS, Geeta R (2006) Endophytic *Phomopsis* species: host range and implications for diversity estimates. Canadian Journal of Microbiology 52: 673–680. https://doi.org/10.1139/w06-020

O'Donnell K, Cigelnik E (1997) Two divergent intragenomic rDNA ITS2 types within a monophyletic lineage of the fungus *Fusarium* are nonorthologous. Molecular Phylogenetics and Evolution 7: 103–116. https://doi.org/10.1006/mpev.1996.0376

Rambaut A, Drummond A (2010) FigTree v.1.3.1. Institute of Evolutionary Biology, University of Edinburgh, Edinburgh.

Rayner RW (1970) A mycological colour chart. Commonwealth Mycological Institute, Kew, 34 pp.

Rehner SA, Uecker FA (1994) Nuclear ribosomal internal transcribed spacer phylogeny and host diversity in the coelomycete *Phomopsis*. Canadian Journal of Botany 72: 1666–1674. https://doi.org/10.1139/b94-204

Ronquist F, Huelsenbeck JP (2003) MrBayes 3: Bayesian phylogenetic inference under mixed models. Bioinformatics 19: 1572–1574. https://doi.org/10.1093/bioinformatics/btg180

Rossman AY, Farr DF, Castlebury LA (2007) A review of the phylogeny and biology of the Diaporthales. Mycoscience 48: 135–144. https://doi.org/10.1007/S10267-007-0347-7

Santos JM, Correia VG, Phillips AJL (2010) Primers for mating-type diagnosis in *Diaporthe* and *Phomopsis*, their use in teleomorph induction in vitro and biological species definition. Fungal Biology 114: 255–270. https://doi.org/10.1016/j.funbio.2010.01.007

Santos JM, Phillips AJL (2009) Resolving the complex of *Diaporthe* (*Phomopsis*) species occurring on *Foeniculum vulgare* in Portugal. Fungal Diversity 34: 111–125.

Santos JM, Vrandečić K, Ćosić J, Duvnjak T, Phillips AJL (2011) Resolving the *Diaporthe* species occurring on soybean in Croatia. Persoonia 27: 9–19. https://doi.org/10.3767/003158511X603719

Senanayake IC, Crous PW, Groenewald JZ, Senanayake IC, Crous PW, Groenewald JZ, Maharachchikumbura SSN, Jeewon R, Phillips AJL, Bhat JD, Perera RH, Li QR, Li WJ, Tangthirasunun N, Norphanphoun C, Karunarathna SC, Camporesi E, Manawasighe IS, Al-Sadi AM, Hyde KD (2017) Families of Diaporthales based on morphological and phylogenetic evidence. Studies in Mycology 86: 217–296. https://doi.org/10.1016/j.simyco.2017.07.003

Smith H, Wingfeld MJ, Coutinho TA, Crous PW (1996) *Sphaeropsis sapinea* and *Botryosphaeria dothidea* endophytic in *Pinus* spp. and *Eucalyptus* spp. in South Africa. South African Journal of Botany 62: 86–88. https://doi.org/10.1016/S0254-6299(15)30596-2

Thompson SM, Tan YP, Young AJ, Neate SM, Aitken EAB, Shivas RG (2011) Stem cankers on sunflower (*Helianthus annuus*) in Australia reveal a complex of pathogenic *Diaporthe* (*Phomopsis*) species. Persoonia 27: 80–89. https://doi.org/10.3767/003158511X617110

Udayanga D, Castlebury LA, Rossman AY, Chukeatirote E, Hyde KD (2014) Insights into the genus *Diaporthe*: phylogenetic species delimitation in the *D. eres* species complex. Fungal Diversity 67: 203–229. https://doi.org/10.1007/s13225-014-0297-2

Udayanga D, Castlebury LA, Rossman AY, Chukeatirote E, Hyde KD (2015) The *Diaporthe sojae* species complex: Phylogenetic re-assessment of pathogens associated with soybean, cucurbits and other field crops. Fungal Biology 119: 383–407. https://doi.org/10.1016/j.funbio.2014.10.009

Udayanga D, Liu X, McKenzie EH, Chukeatirote E, Bahkali AH, Hyde KD (2011) The genus *Phomopsis*: biology, applications, species concepts and names of common phytopathogens. Fungal Diversity 50: 189–225. https://doi.org/10.1007/s13225-011-0126-9

Uecker FA (1988) A world list of *Phomopsis* names with notes on nomenclature, morphology and biology. Mycological Memoirs 13: 1–231.

van Rensburg JCJ, Lamprecht SC, Groenewald JZ, Castlebury LA, Crous PW (2006) Characterization of *Phomopsis* spp. associated with die-back of rooibos (*Aspalathus linearis*) in South Africa. Studies in Mycology 55: 65–74. https://doi.org/10.3114/sim.55.1.65

Wehmeyer LE (1926) A biologic and phylogenetic study of stromatic Sphaeriales. American Journal of Botany 13: 575–645. https://doi.org/10.1002/j.1537-2197.1926.tb05903.x

White TJ, Bruns T, Lee S, Taylor J (1990) Amplification and direct sequencing of fungal ribosomal RNA genes for phylogenetics. PCR Protocols: A Guide to Methods and Applications 18: 315–322. https://doi.org/10.1016/B978-0-12-372180-8.50042-1

Yang Q, Fan XL, Du Z, Tian CM (2017b) *Diaporthe juglandicola* sp. nov. (Diaporthales, Ascomycetes), evidenced by morphological characters and phylogenetic analysis. Mycosphere 8: 817–826. https://doi.org/10.5943/mycosphere/8/5/3

Yang Q, Fan XL, Guarnaccia V, Tian CM (2018) High diversity of *Diaporthe* species associated with dieback diseases in China, with twelve new species described. MycoKeys 39: 97–149. https://doi.org/10.3897/mycokeys.39.26914

Yang Q, Fan XL, Du Z, Tian CM (2017a) *Diaporthe* species occurring on *Senna bicapsularis* in southern China, with descriptions of two new species. Phytotaxa 302: 145–155. https://doi.org/10.11646/phytotaxa.302.2.4

Yang Q, Jiang N, Tian CM (2020) Three new *Diaporthe* species from Shaanxi Province, China. Mycokeys 67: 1–18. https://doi.org/10.3897/mycokeys.67.49483

MycoKeys 77: 65–95 (2021)
doi: 10.3897/mycokeys.77.59852
https://mycokeys.pensoft.net

REVIEW ARTICLE

A peer-reviewed open-access journal
MycoKeys
Launched to accelerate biodiversity research

Morphological and molecular identification of *Diaporthe* species in south-western China, with description of eight new species

Wenxiu Sun[1], Shengting Huang[1], Jiwen Xia[2], Xiuguo Zhang[2], Zhuang Li[2]

1 *College of Life Sciences, Yangtze University, Jingzhou 434025, Hubei, China* **2** *Shandong Provincial Key Laboratory for Biology of Vegetable Diseases and Insect Pests, College of Plant Protection, Shandong Agricultural University, Taian, Shandong, 271018, China*

Corresponding author: Zhuang Li (junwuxue@126.com)

Academic editor: H. Raja | Received 20 October 2020 | Accepted 17 December 2020 | Published 14 January 2021

Citation: Sun W, Huang S, Xia J, Zhang X, Li Z (2021) Morphological and molecular identification of *Diaporthe* species in south-western China, with description of eight new species. MycoKeys 77: 65–95. https://doi.org/10.3897/mycokeys.77.59852

Abstract

Diaporthe species have often been reported as plant pathogens, endophytes and saprophytes, commonly isolated from a wide range of infected plant hosts. In the present study, twenty strains obtained from leaf spots of twelve host plants in Yunnan Province of China were isolated. Based on a combination of morphology, culture characteristics and multilocus sequence analysis of the rDNA internal transcribed spacer region (ITS), translation elongation factor 1-α (*TEF*), β-tubulin (*TUB*), calmodulin (*CAL*), and histone (*HIS*) genes, these strains were identified as eight new species: *Diaporthe camelliae-sinensis, D. grandiflori, D. heliconiae*, *D. heterostemmatis*, *D. litchii*, *D. lutescens*, *D. melastomatis*, *D. pungensis* and two previously described species, *D. subclavata* and *D. tectonendophytica*. This study showed high species diversity of *Diaporthe* in tropical rain forests and its hosts in south-western China.

Keywords

Diaporthaceae, Diaporthales, phylogeny, taxonomy, 8 new taxa

Introduction

Diaporthe is a genus in the Diaporthaceae family (Diaporthales), with the asexual morph previously known as *Phomopsis* and type species *Diaporthe eres* Nitschke collected from *Ulmus* sp. in Germany (Nitschke 1870). Nevertheless, with the implementation of "one fungus one name" nomenclature, the generic names *Diaporthe* and *Phomopsis* are no longer used for both morphs of this genus, and Rossman et al. (2015) gave priority to the older name *Diaporthe* Nitschke over *Phomopsis* (Sacc.) Bubák because it was published first, encountered commonly in literatures and represents the majority of species. The sexual morph of *Diaporthe* is characterized by: immersed perithecial ascomata and an erumpent pseudostroma with more or less elongated perithecial necks; unitunicate clavate to cylindrical asci; fusoid, ellipsoid to cylindrical, septate or aseptate, hyaline ascospores, biseriately to uniseriately arranged in the ascus, sometimes having appendages (Udayanga et al. 2011; Senanayake et al. 2017, 2018). The asexual morph is characterized by ostiolate conidiomata, with cylindrical phialides producing three types of hyaline, aseptate conidia (Udayanga et al. 2011; Gomes et al. 2013): type I: α-conidia, hyaline, fusiform, straight, guttulate or eguttulate, aseptate, smooth-walled; type II: β-conidia, hyaline, filiform, straight or hamate, aseptate, smooth-walled, eguttulate; type III: γ-conidia, rarely produced, hyaline, multiguttulate, fusiform to subcylindrical with an acute or rounded apex, while the base is sometimes truncate. The gamma conidia rarely produced and observed, those species described, having a third type of spores are *D. ampelina* (Berk. & M.A. Curtis) R.R. Gomes, Glienke & Crous, *D. cinerascens* Sacc., *D. eres* Nitschke, *D. hongkongensis* R.R. Gomes, C. Glienke & Crous, *D. limonicola* Guarnaccia & Crous, *D. oncostoma* (Duby) Fuckel, *D. perseae* (Zerova) R.R. Gomes, C. Glienke & Crous, *D. raonikayaporum* R.R. Gomes, C. Glienke & Crous (Gomes et al. 2013; Guarnaccia and Crous 2017; Guo et al. 2020).

Currently, more than 1100 epithets of *Diaporthe* are listed in Index Fungorum (http://www.indexfungorum.org/; accessed 1 June 2020), but only one-fifth of these taxa have been studied with molecular data (Guo et al. 2020; Yang et al. 2020; Zapata et al. 2020). They are widely distributed and have a broad range of hosts from economically significant agricultural crops to ornamental plants including *Camellia*, *Castanea*, *Citrus*, *Glycine*, *Helianthus*, *Juglans*, *Persea*, *Pyrus*, *Vaccinium* and *Vitis* (van Rensburg et al. 2006; Santos and Phillips 2009; Crous et al. 2011a, b, 2016; Santos et al. 2011; Thompson et al. 2011; Grasso et al. 2012; Huang et al. 2013; Lombard et al. 2014; Gao et al. 2015, 2016, 2017; Udayanga et al. 2012, 2015; Guarnaccia et al. 2016; Dissanayake et al. 2017; Guarnaccia and Crous 2017; Fan et al. 2018; Senanayake et al. 2018; Guo et al. 2020). Many *Diaporthe* species have been reported as destructive plant pathogens, innocuous endophytes and saprobes (Murali et al. 2006; Udayanga et al. 2012; Gomes et al. 2013; Ménard et al. 2014; Guarnaccia et al. 2016; Torres et al. 2016; Senanayake et al. 2018). However, the biology and lifestyle of some of them remain unclear (Vilka and Volkova 2015).

From previous studies, the methods of species identification and classification in genus *Diaporthe* were based on criteria such as morphological characters like the size and shape of ascomata (Udayanga et al. 2011) and conidiomata (Rehner and Uecker 1994). However, in recent studies, determining species boundaries only by morphological characters was demonstrated to be not always informative due to their variability under changing environmental conditions (Gomes et al. 2013). As for phylogenetic analysis for *Diaporthe* species, the use of a five-locus dataset (ITS-*TUB*-*TEF*-*CAL*-*HIS*) is the optimal combination for species delimitation as revealed by Santos et al. (2017). Thus, in recent years, many *Diaporthe* species have been described based on a polyphasic approach combined with morphological characterization and their host associations (Guarnaccia and Crous 2017; Gao et al. 2017; Yang et al. 2018, 2020; Crous et al. 2020; Dayarathne et al. 2020; Guo et al. 2020; Hyde et al. 2020; Li et al. 2020; Zapata et al. 2020).

In this study, we propose eight novel species and two previously described species of *Diaporthe*, collected in Yunnan Province of China on twelve plant host genera, based on their morphological characters in culture, and molecular phylogenetic analysis.

Materials and methods

Isolation and morphological studies

The leaves of samples were collected from Yunnan Province, China. Isolations from surface sterilized leaf tissues were conducted following the protocol of Gao et al. (2014). Tissue fragments (5 × 5 mm) were taken from the margin of leaf lesions and surface-sterilized by consecutively immersing in 75% ethanol solution for 1 min, 5% sodium hypochlorite solution for 30 s, and finally rinsed in sterile distilled water for 1 min. The pieces were dried with sterilized paper towels and transferred on potato dextrose agar (PDA) in petri plates (Cai et al. 2009). All the PDA plates were incubated at biochemical incubator at 25 °C for 2–4 days, and hyphae were picked out of the periphery of the colonies and inoculated onto new PDA plates.

Following 2–3 weeks of incubation, photographs of the fungal colonies were taken at 7 days and 15 days using a Powershot G7X mark II digital camera. Micromorphological characters were observed and documented in distilled water from microscope slides under Olympus SZX10 stereomicroscope and Olympus BX53 microscope, both supplied with Olympus DP80 HD color digital cameras to photodocument fungal structures. All fungal strains were stored in 10% sterilized glycerin at 4 °C for further studies. Voucher specimens were deposited in the Herbarium of Plant Pathology, Shandong Agricultural University (**HSAUP**). Living strain cultures were deposited in the Shandong Agricultural University Culture Collection (**SAUCC**). Taxonomic information on the new taxa was submitted to MycoBank (http://www.mycobank.org).

DNA extraction and amplification

Genomic DNA was extracted from fungal mycelia on PDA, using a modified cetyltrimethylammonium bromide (CTAB) protocol as described in Guo et al. (2000). The internal transcribed spacer regions with intervening 5.8S nrRNA gene (ITS), part of the beta-tubulin gene region (*TUB*), partial translation elongation factor 1-alpha (*TEF*), histone H3 (*HIS*) and calmodulin (*CAL*) genes were amplified and sequenced by using primers pairs ITS4/ITS5 (White et al. 1990), Bt2a/Bt2b (Glass and Donaldson 1995), EF1-728F/EF1-986R (Carbone and Kohn 1999), CAL-228F/CAL-737R (Carbone and Kohn 1999) and CYLH3F/H3-1b (Glass and Donaldson 1995; Crous et al. 2004), respectively.

PCR was performed using an Eppendorf Master Thermocycler (Hamburg, Germany). Amplification reactions were performed in a 25 μL reaction volume which contained 12.5 μL Green Taq Mix (Vazyme, Nanjing, China), 1 μL of each forward and reverse primer (10 μM) (Biosune, Shanghai, China), and 1 μL template genomic DNA in amplifier, and were adjusted with distilled deionized water to a total volume of 25 μL.

PCR parameters were as follows: 95 °C for 5 min, followed by 35 cycles of denaturation at 95 °C for 30 s, annealing at a suitable temperature for 30 s, extension at 72 °C for 1 min and a final elongation step at 72 °C for 10 min. Annealing temperature for each gene was 55 °C for ITS, 60 °C for *TUB*, 52 °C for *TEF*, 54 °C for *CAL* and 57 °C for *HIS*. The PCR products were visualized on 1% agarose electrophoresis gel. Sequencing was done bi-directionally, conducted by the Biosune Company Limited (Shanghai, China). Consensus sequences were obtained using MEGA 7.0 (Kumar et al. 2016). All sequences generated in this study were deposited in GenBank (Table 1).

Phylogenetic analyses

Novel sequences generated from twenty strains in this study, and all reference available sequences of *Diaporthe* species downloaded from GenBank were used for phylogenetic analyses. Alignments of the individual locus were determined using MAFFT v. 7.110 by default settings (Katoh et al. 2017) and manually corrected where necessary. To establish the identity of the isolates at species level, phylogenetic analyses were conducted first individually for each locus and then as combined analyses of five loci (ITS, *TUB*, *TEF*, *CAL* and *HIS* regions). Phylogenetic analyses were based on maximum likelihood (ML) and Bayesian inference (BI) for the multi-locus analyses. For BI, the best evolutionary model for each partition was determined using MrModeltest v. 2.3 (Nylander 2004) and incorporated into the analyses. ML and BI were run on the CIPRES Science Gateway portal (https://www.phylo.org/) (Miller et al. 2012) using RaxML-HPC2 on XSEDE (8.2.12) (Stamatakis 2014) and MrBayes on XSEDE (3.2.7a) (Huelsenbeck and Ronquist 2001; Ronquist and Huelsenbeck 2003; Ronquist et al. 2012), respectively. For ML analyses the default parameters were used and

Table 1. Species and GenBank accession numbers of DNA sequences used in this study with new sequences in bold.

Species	Strain/Isolate	Host/Substrate	GenBank accession number				
			ITS	*TUB*	*TEF*	*CAL*	*HIS*
Diaporthe alnea	CBS 146.46*	*Alnus* sp.	KC343008	KC343976	KC343734	KC343250	KC343492
D. anacardii	CBS 720.97*	*Anacardium occidentale*	KC343024	KC343992	KC343750	KC343266	KC343508
D. baccae	CBS 136972*	*Vaccinium corymbosum*	KJ160565	–	KJ160597	–	–
D. batatas	CBS 122.21	*Ipomoea batatas*	KC343040	KC344008	KC343766	KC343282	KC343524
D. camelliae-sinensis	**SAUCC194.92***	***Camellia sinensis***	**MT822620**	**MT855817**	**MT855932**	**MT855699**	**MT855588**
	SAUCC194.103	***Castanea mollissima***	**MT822631**	**MT855828**	**MT855943**	**MT855710**	**MT855599**
	SAUCC194.104	***Castanea mollissima***	**MT822632**	**MT855829**	**MT855944**	**MT855711**	**MT855600**
	SAUCC194.108	***Machilus pingii***	**MT822636**	**MT855833**	**MT855948**	**MT855715**	**MT855603**
D. canthii	CBS 132533*	*Canthium inerme*	JX069864	KC843230	KC843120	KC843174	–
D. chamaeropis	CBS 753.70	*Spartium junceum*	KC343049	KC344017	KC343775	KC343291	KC343533
D. cinerascens	CBS 719.96	*Ficus carica*	KC343050	KC344018	KC343776	KC343292	KC343534
D. cissampeli	CPC 27302	*Cissampelos capensis*	KX228273	KX228384	–	–	KX228366
D. citri	CBS 230.52	*Citrus sinensis*	KC343052	KC344020	KC343778	KC343294	KC343536
D. collariana	MFLUCC 17-2636*	*Magnolia champaca*	MG806115	MG783041	MG783040	MG783042	–
D. convolvuli	CBS 124654	*Convolvulus arvensis*	KC343054	KC344022	KC343780	KC343296	KC343538
D. cytosporella	AR 5149	*Citrus sinensis*	KC843309	KC843223	KC843118	KC843143	–
D. destruens	SPPD-1	*Solanum tuberosum*	JN848791	JX421691	–	–	–
D. dorycnii	MFLU 17-1015*	*Dorycnium hirsutum*	KY964215	KY964099	KY964171	–	–
D. elaeagni	CBS 504.72	*Elaeagnus* sp.	KC343064	KC344032	KC343790	KC343306	KC343548
D. elaeagni-glabrae	LC4802*	*Elaeagnus glabra*	KX986779	KX999212	KX999171	KX999281	KX999251
D. endophytica	CBS 133811*	*Schinus terebinthifolius*	KC343065	KC344033	KC343791	KC343307	KC343549
D. eres	AR5193*	*Ulmus laevis*	KJ210529	KJ420799	KJ210550	KJ434999	KJ420850
D. foeniculina	CBS 123208	*Foeniculum vulgare*	KC343104	KC344072	KC343830	KC343346	KC343588
D. fructicola	MAFF 246408	*Passiflora edulis*	LC342734	LC342736	LC342735	LC342738	LC342737
D. grandiflori	**SAUCC194.84***	***Heterostemma grandiflorum***	**MT822612**	**MT855809**	**MT855924**	**MT855691**	**MT855580**
D. heliconiae	**SAUCC194.75**	***Heliconia metallica***	**MT822603**	**MT855800**	**MT855915**	**MT855682**	**MT855571**
	SAUCC194.77*	***Heliconia metallica***	**MT822605**	**MT855802**	**MT855917**	**MT855684**	**MT855573**
D. heterophyllae	CPC 26215	*Acacia heterophylla*	MG600222	MG600226	MG600224	MG600218	MG600220
D. heterostemmatis	**SAUCC194.85***	***Heterostemma grandiflorum***	**MT822613**	**MT855810**	**MT855925**	**MT855692**	**MT855581**
	SAUCC194.102	***Camellia sinensis***	**MT822630**	**MT855827**	**MT855942**	**MT855709**	**MT855598**
D. hickoriae	CBS 145.26*	*Carya glabra*	KC343118	KC344086	KC343844	KC343360	KC343602
D. inconspicua	CBS 133813*	*Maytenus ilicifolia*	KC343123	KC344091	KC343849	KC343365	KC343607
D. kongii	T12509H*	*Helianthus annuus*	JF431301	KJ197272	JN645797	–	–
D. litchii	**SAUCC194.12**	***Elaeagnus conferta***	**MT822540**	**MT855737**	**MT855854**	**MT855625**	**MT855509**
	SAUCC194.22*	***Litchi chinensis***	**MT822550**	**MT855747**	**MT855863**	**MT855635**	**MT855519**
D. longicolla	FAU599	*Glycine max*	KJ590728	KJ610883	KJ590767	KJ612124	KJ659188
D. lutescens	**SAUCC194.36***	***Chrysalidocarpus lutescens***	**MT822564**	**MT855761**	**MT855877**	**MT855647**	**MT855533**
D. macintoshii	BRIP 55064a*	*Rapistrum rugostrum*	KJ197289	KJ197269	KJ197251	–	–
D. masirevicii	BRIP 57330	*Chrysanthemoides monilifera subsp. rotundata*	KJ197275	KJ197255	KJ197237	–	–
	BRIP 57892a*	*Helianthus annuus*	KJ197276	KJ197257	KJ197239	–	–
D. melastomatis	**SAUCC194.55***	***Melastoma malabathricum***	**MT822583**	**MT855780**	**MT855896**	**MT855664**	**MT855551**
	SAUCC194.80	***Millettia reticulata***	**MT822608**	**MT855805**	**MT855920**	**MT855687**	**MT855576**
	SAUCC194.88	***Camellia sinensis***	**MT822616**	**MT855813**	**MT855928**	**MT855695**	**MT855584**
D. melonis	CBS 507.78*	*Cucumis melo*	KC343142	KC344110	KC343868	KC343384	KC343626
D. miriciae	BRIP 54736j*	*Helianthus annuus*	KJ197282	KJ197262	KJ197244	–	–
D. neilliae	CBS 144.27	*Spiraea* sp.	KC343144	KC344112	KC343870	KC343386	KC343628
D. nigra	JZBH320170	*Ballota nigra*	MN653009	MN887113	MN892277	–	–

Species	Strain/Isolate	Host/Substrate	GenBank accession number				
			ITS	*TUB*	*TEF*	*CAL*	*HIS*
D. nomurai	CBS 157.29	*Morus* sp.	KC343154	KC344122	KC343880	KC343396	KC343638
D. oncostoma	CBS 100454	*Robinia pseudoacacia*	KC343160	KC344128	KC343886	KC343402	KC343644
	CBS 109741	*Robinia pseudoacacia*	KC343161	KC344129	KC343887	KC343403	KC343645
D. ovalispora	ZJUD93*	*Citrus limon*	KJ490628	KJ490449	KJ490507	–	KJ490570
D. parapterocarpi	CPC 22729	*Pterocarpus brenanii*	KJ869138	KJ869248	–	–	–
D. parvae	PSCG 034*	*Pyrus bretschneideri*	MK626919	MK691248	MK654858	–	MK726210
D. passifloricola	CPC 27480*	*Passiflora foetida*	KX228292	KX228387	–	–	KX228367
D. penetriteum	LC3353*	*Camellia sinensis*	KP714505	KP714529	KP714517	–	KP714493
	LC3394	*Camellia sinensis*	KP267893	KP293473	KP267967	–	KP293544
D. phaseolorum	CBS 116019	*Caperonia palustris*	KC343175	KC344143	KC343901	KC343417	KC343659
	CBS 116020	*Aster exilis*	KC343176	KC344144	KC343902	KC343418	KC343660
D. phillipsii	CAA 817*	Dead twig	MK792305	MN000351	MK828076	MK883831	MK871445
D. poincianellae	URM 7932	*Poincianella pyramidalis*	MH989509	MH989537	MH989538	MH989540	MH989539
D. pseudoinconspicua	G26	*Poincianella pyramidalis*	MH122538	MH122524	MH122533	MH122528	MH122517
D. psoraleae	CPC 21634	*Psoralea pinnata*	KF777158	KF777251	KF777245	–	–
D. pterocarpi	MFLUCC 10-0571	*Pterocarous indicus*	JQ619899	JX275460	JX275416	JX197451	–
	MFLUCC 10-0575	*Pterocarous indicus*	JQ619901	JX275462	JX275418	JX197453	–
D. pungensis	**SAUCC194.89**	***Camellia sinensis***	**MT822617**	**MT855814**	**MT855929**	**MT855696**	**MT855585**
	SAUCC194.112*	***Elaeagnus pungens***	**MT822640**	**MT855837**	**MT855952**	**MT855719**	**MT855607**
D. ravennica	MFLUCC 17-1029	*Tamarix* sp.	KY964191	KY964075	KY964147	–	–
D. rosae	MFLUCC 17-2658	*Rosa* sp.	MG828894	MG843878	–	MG829273	–
D. rumicicola	MFLUCC18-0739	*Rumex* sp.	MH846233	MK049555	MK049554	–	–
D. saccarata	CBS 116311*	*Protea repens*	KC343190	KC344158	KC343916	KC343432	KC343674
D. shennongjiaensis	CNUCC 201905	*Juglans regia*	MN216229	MN227012	MN224672	MN224551	MN224560
D. sojae	CBS 100.87*	*Glycine soja*	KC343196	KC344164	KC343922	KC343438	KC343680
D. stictica	CBS 370.54	*Buxus sampervirens*	KC343212	KC344180	KC343938	KC343454	KC343696
D. subclavata	ZJUD95*	*Citrus unshiu*	KJ490630	KJ490451	KJ490509	–	KJ490572
	SAUCC194.66	***Pometia pinnata***	**MT822594**	**MT855791**	**MT855906**	**MT855674**	**MT855562**
D. subellipicola	KUMCC 17-0153	on dead wood	MG746632	MG746634	MG746633	–	–
D. tectonendophytica	MFLUCC 13-0471*	*Tectona grandis*	KU712439	KU743986	KU749367	KU749354	–
	SAUCC194.11	***Elaeagnus conferta***	**MT822539**	**MT855736**	**MT855853**	**MT855624**	**MT855508**
	SAUCC194.63	***Pometia pinnata***	**MT822591**	**MT855788**	**MT855903**	**MT855672**	**MT855559**
D. ueckerae	FAU656*	*Cucumis melo*	KJ590726	KJ610881	KJ590747	KJ612122	KJ659215
D. unshiuensis	CFCC 52595	*Carya illinoensis*	MH121530	MH121607	MH121572	MH121448	MH121488
D. vangueriae	CPC 22703	*Vangueria infausta*	KJ869137	KJ869247	–	–	–
D. velutina	LC4419*	*Neolitsea* sp.	KX986789	KX999222	KX999181	KX999286	KX999260
D. virgiliae	CMW40755*	*Virgilia oroboides*	KP247573	KP247582	–	–	–
	CMW40748	*Virgilia oroboides*	KP247566	KP247575	–	–	–
D. zaobaisu	PSCG 031*	*Pyrus bretschneideri*	MK626922	MK691245	MK654855	–	MK726207
Diaporthella corylina	CBS 121124	*Corylus* sp.	KC343004	KC343972	KC343730	KC343246	KC343488

Isolates marked with "*" are ex-type or ex-epitype strains.

BI was carried out using the rapid bootstrapping algorithm with the automatic halt option. Bayesian analyses included five parallel runs of 5,000,000 generations, with the stop rule option and a sampling frequency of 500 generations. The burn-in fraction was set to 0.25 and posterior probabilities (PP) were determined from the remaining trees. The resulting trees were plotted using FigTree v. 1.4.2 (http://tree.bio.ed.ac.uk/software/figtree) and edited with Adobe Illustrator CS5.1. New sequences generated in this study were deposited at GenBank (https://www.ncbi.nlm.nih.gov; Table 1), the alignments and trees were deposited in TreeBASE (http://treebase.org/treebase-web/home.html).

Results

Phylogenetic analyses

Twenty fungal strains of *Diaporthe* isolates from 15 plant hosts were sequenced (Table 1). These were analyzed by using multilocus data (ITS, *TUB*, *TEF*, *CAL* and *HIS*) composed of 87 isolates of *Diaporthe*, with *Diaporthella corylina* (CBS 121124) as an outgroup taxon. A total of 2856 characters including gaps were obtained in the phylogenetic analysis, viz. ITS: 1–650, *TUB*: 651–1263, *TEF*: 1264–1705, *CAL*: 1706–2279, *HIS*: 2280–2856. Of these characters, 1395 were constant, 475 were variable and parsimony-uninformative, and 986 were parsimony-informative. For the BI and ML analyses, the substitution model GTR+I+G for ITS, HKY+I+G for *TUB*, *TEF* and *CAL*, GTR+G for *HIS* were selected and incorporated into the analyses. The ML tree topology confirmed the tree topologies obtained from the BI analyses, and therefore, only the ML tree is presented (Fig. 1).

ML bootstrap support values (≥ 50%) and Bayesian posterior probability (≥ 0.90) are shown as first and second position above nodes, respectively. Based on the five-locus phylogeny and morphology, 20 strains isolated in this study were assigned to 10 species, 8 of them are proposed and described here as new species (Fig. 1). Strains (SAUCC194.92, SAUCC194.103, SAUCC194.104 and SAUCC194.108) are *D. camelliae-sinensis*, strain (SAUCC194.84) – *Diaporthe grandiflori*, strains (SAUCC194.75 and SAUCC194.77) – *D. heliconiae*, strains (SAUCC194.85 and SAUCC194.102) – *D. heterostemmatis*, strains (SAUCC194.12 and SAUCC194.22) – *D. litchii*, strain (SAUCC194.36) – *D. lutescens*, strains (SAUCC194.55, SAUCC194.80 and SAUCC194.88) – *D. melastomatis*, strains (SAUCC194.89 and SAUCC194.112) – *D. pungensis*. One strain (SAUCC194.66) is of a previously described *D. subclavata*, and strains (SAUCC194.11 and SAUCC194.63) – of previously described *D. tectonendophytica*.

Taxonomy

Diaporthe camelliae-sinensis **S.T. Huang, J.W. Xia, X.G. Zhang & Z. Li, sp. nov.**
MycoBank No: 837600
Figure 2

Etymology. Named after the host *Camellia sinensis* on which it was collected.

Diagnosis. *Diaporthe camelliae-sinensis* can be distinguished from the closely related species *D. macintoshii* R.G. Shivas et al. and *D. vangueriae* Crous based on ITS, *TUB* and *TEF* loci. *Diaporthe camelliae-sinensis* differs from *D. macintoshii* in smaller α-conidia and from *D. vangueriae* in shorter β-conidia.

Type. China, Yunnan Province: Xishuangbanna Tropical Botanical Garden, Chinese Academy of Sciences, on infected leaves of *Camellia sinensis*. 19 April 2019, S.T. Huang, HSAUP194.92, holotype, ex-holotype living culture SAUCC194.92.

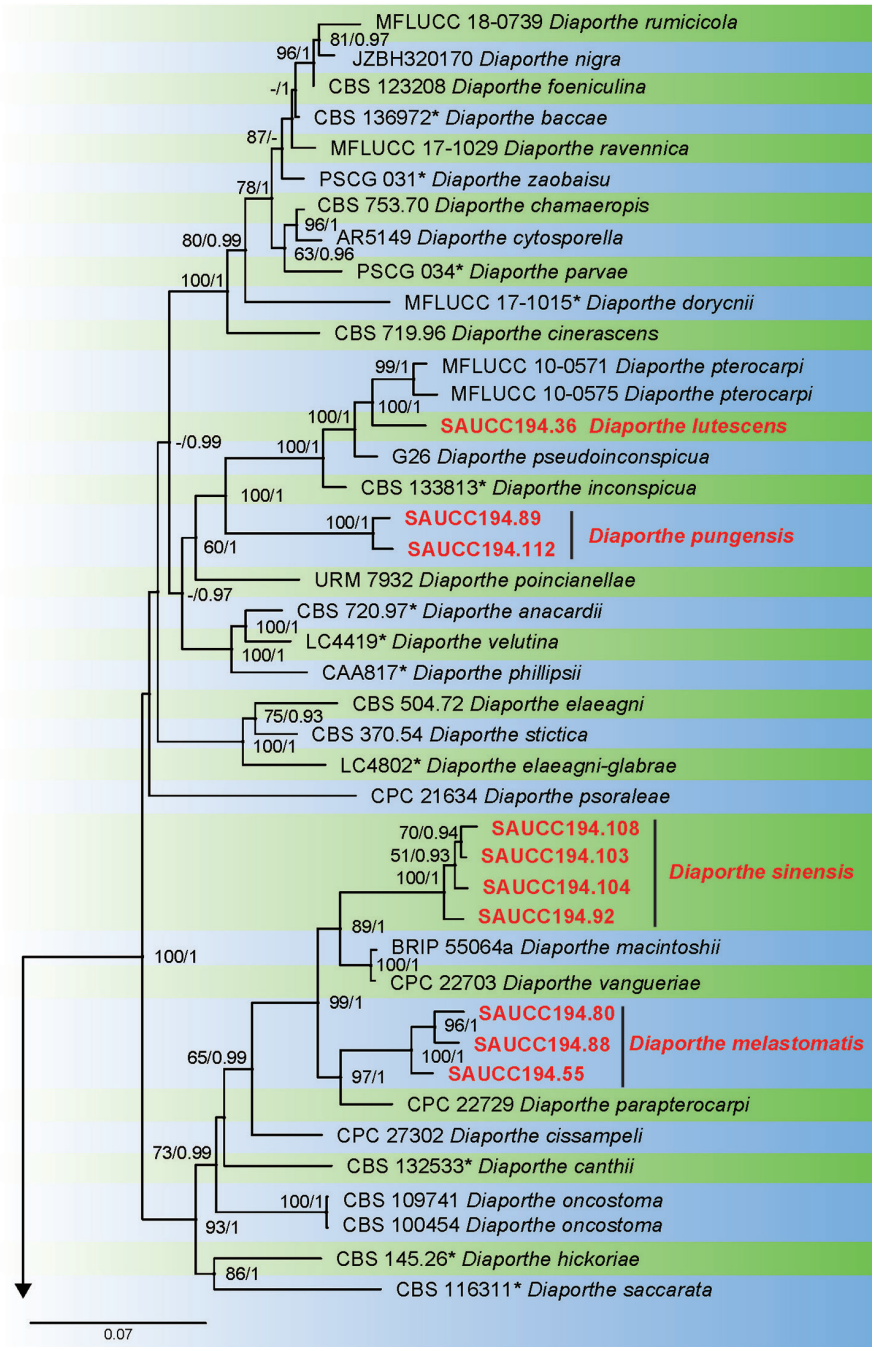

Figure 1. Phylogram of *Diaporthe* based on combined ITS, *TUB*, *TEF*, *CAL* and *HIS* genes. The ML and BI bootstrap support values above 50% and 0.90 BYPP are shown at the first and second position, respectively. Strains marked with "*" are ex-type or ex-epitype. Strains from this study are shown in red. Three branches were shortened to fit the page size – these are indicated by symbol (//) with indication number showing how many times they are shortened.

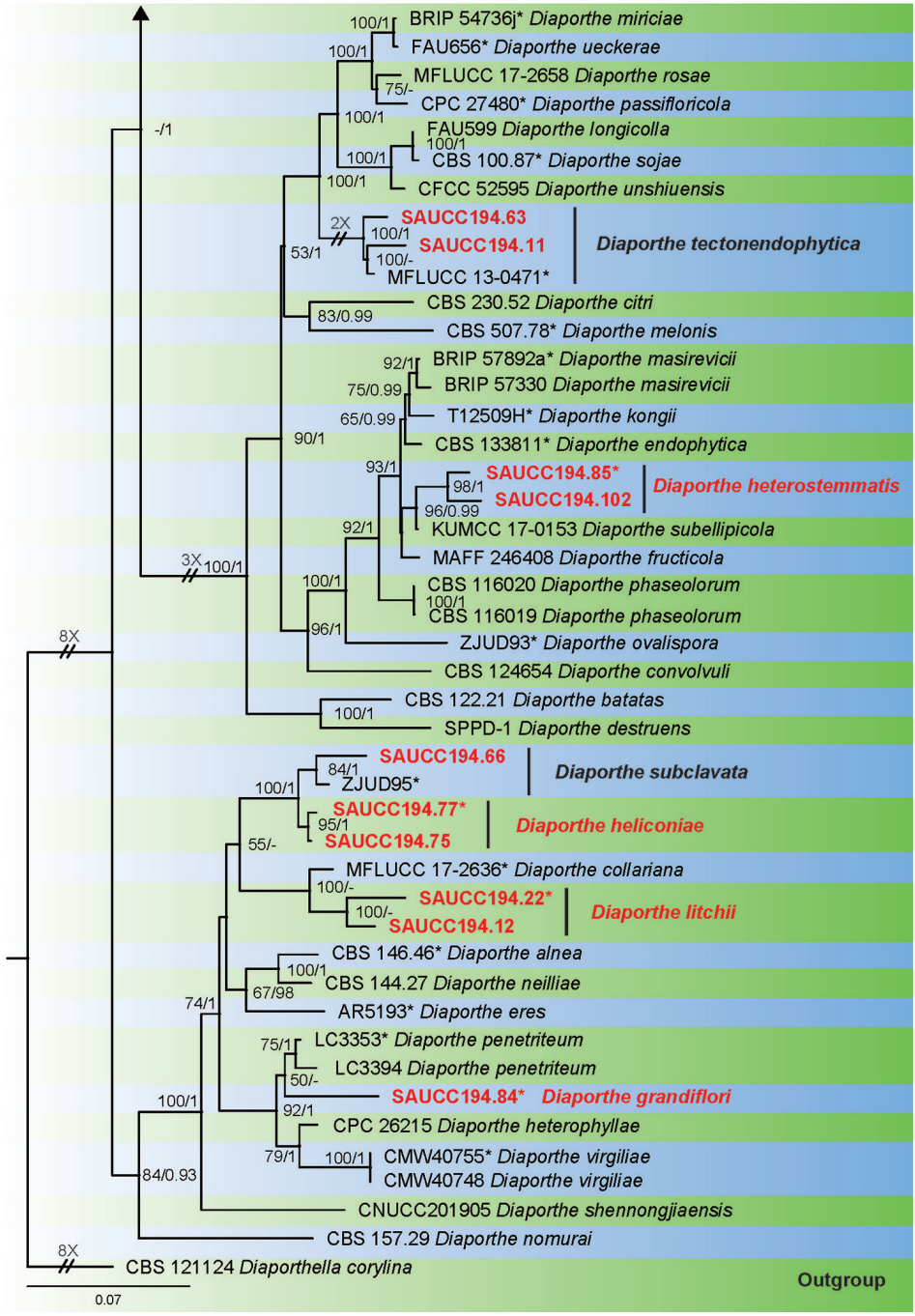

Figure 1. Continued.

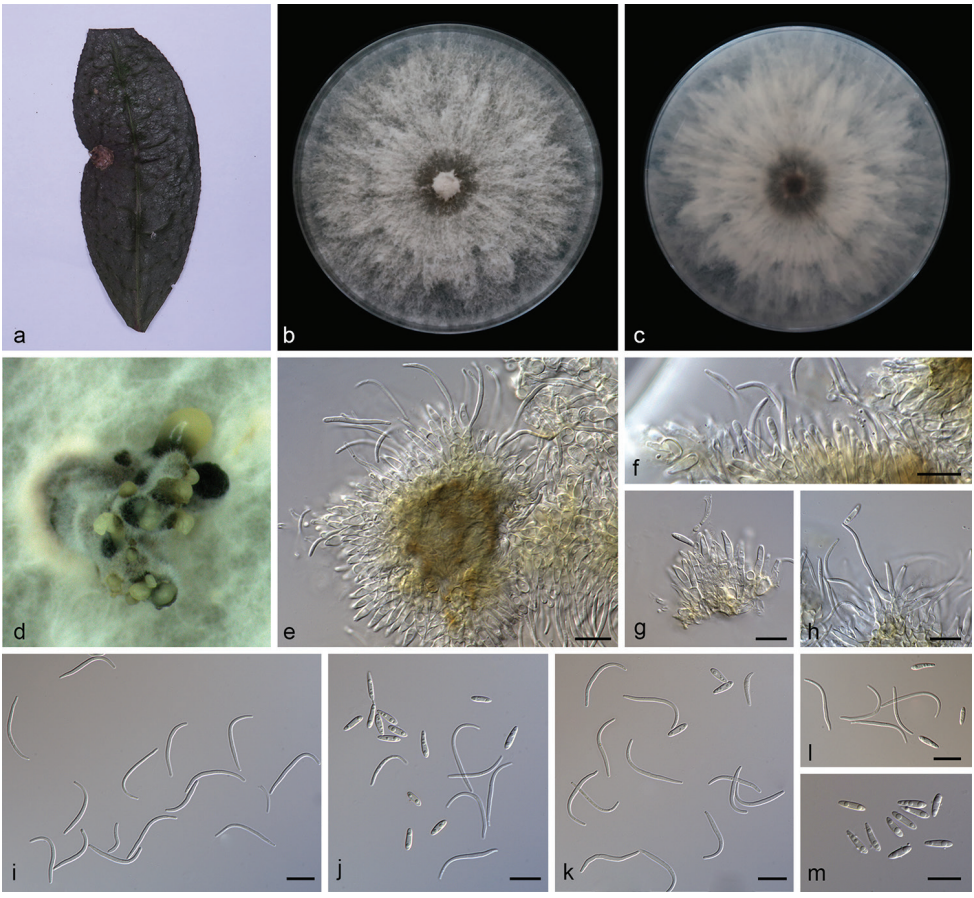

Figure 2. *Diaporthe camelliae-sinensis* (SAUCC194.92) **a** leaf of host plant **b, c** surface (**b**) and reverse (**c**) sides of colony after incubation for 15 days on PDA **d** conidiomata **e–h** conidiophores and conidiogenous cells **i** beta conidia **j–l** alpha conidia and beta conidia **m** alpha conidia. Scale bars: 10 μm (**e–m**).

Description. Asexual morph: Conidiomata pycnidial, multi-pycnidia grouped together, globose, black, erumpent, coated with white hyphae, thick-walled, exuding creamy to yellowish conidial droplets from central ostioles. Conidiophores hyaline, smooth, septate, branched, densely aggregated, cylindrical, straight to sinuous, swelling at the base, tapering towards the apex, 10–15 × 1.5–2 μm. Conidiogenous cells 8.5–12 × 2–2.8 μm, phialidic, cylindrical, terminal, slightly tapering towards the apex. Alpha conidia, hyaline, smooth, aseptate, ellipsoidal to fusoid, 2–4 guttulate, apex subobtuse, base subtruncate, 7.5–10 × 1.8–2.5 μm (mean = 8.5 × 2.2 μm, n = 20). Beta conidia hyaline, aseptate, filiform, sigmoid to lunate, mostly curved through 90–180°, tapering towards the apex, base truncate, 20–30 × 1.2–1.6 μm (mean = 25.6 × 1.3 μm, n = 20). Gamma conidia and sexual morph not observed.

Culture characteristics. Pure culture was isolated by subbing hyphal tips growing from surface sterilized diseased material. Colonies on PDA cover the Petri dish

diameter after incubation for 15 days in dark conditions at 25 °C, cottony and radially with abundant aerial mycelium, sparse in the margin. With a tanned concentric ring of dense hyphae, white on surface side, white to pale yellow on reverse side.

Additional specimens examined. China, Yunnan Province: Xishuangbanna Tropical Botanical Garden, Chinese Academy of Sciences, 19 April 2019, S.T. Huang. On infected leaves of *Castanea mollissima*, HSAUP194.103 and HSAUP194.104 paratype, living culture SAUCC194.103 and SAUCC194.104; on diseased leaves of *Machilus pingii*, HSAUP194.108 paratype, living culture SAUCC194.108.

Notes. Four isolates are clustered in a clade distinct from its closest phylogenetic neighbor, *D. macintoshii* and *D. vangueriae*. *Diaporthe camelliae-sinensis* can be distinguished from *D. macintoshii* in ITS, *TUB* and *TEF* loci (23/558 in ITS, 2/463 in *TUB* and 20/328 in *TEF*); from *D. vangueriae* in ITS and *TUB* loci (23/558 in ITS and 1/423 in *TUB*). Morphologically, *Diaporthe camelliae-sinensis* differs from *D. macintoshii* in having guttulate alpha conidia and smaller alpha conidia (7.5–10 × 1.8–2.5 vs. 8.0–11.0 × 2.0–3.0 μm) (Thompson et al. 2015). Furthermore, *Diaporthe camelliae-sinensis* differs from *D. vangueriae* in shorter beta conidia (20–30 × 1.2–1.6 vs. 28–35 × 1.5–2.0 μm) and *D. camelliae-sinensis* can produce alpha conidia, but *D. vangueriae* could not (Crous et al. 2014).

***Diaporthe grandiflori* S.T. Huang, J.W. Xia, X.G. Zhang & Z. Li, sp. nov.**
MycoBank No: 837591
Figure 3

Etymology. Named after the host *Heterostemma grandiflorum* on which it was collected.

Diagnosis. *Diaporthe grandiflori* can be distinguished from the phylogenetically closely related species *D. penetriteum* Y.H. Gao & L. Cai in larger α-conidia and β-conidia.

Type. China, Yunnan Province: Xishuangbanna Tropical Botanical Garden, Chinese Academy of Sciences, on infected leaves of *Heterostemma grandiflorum*. 19 April 2019, S.T. Huang, HSAUP194.84, holotype, ex-holotype living culture SAUCC194.84.

Description. Asexual morph: Conidiomata pycnidial, subglobose to globose, solitary or aggregated in groups, black, erumpent, coated with white hyphae, thick-walled, exuding golden yellow spiral conidial cirrus from ostiole. Conidiophores hyaline, smooth, septate, branched, densely aggregated, cylindrical, straight to slightly sinuous, 9.5–16.5 × 1.9–2.8 μm. Conidiogenous cells 19.0–22.8 × 1.4–2.4 μm, cylindrical, multi-guttulate, terminal, tapering towards the apex. Alpha conidia abundant in culture, biguttulate, hyaline, smooth, aseptate, ellipsoidal, apex subobtuse, base subtruncate, 6.3–8.3 × 2.8–3.3 μm (mean = 7.5 × 2.9 μm, n = 20). Beta conidia, not numerous, hyaline, aseptate, filiform, slightly curved, tapering towards the apex, 21.5–30.5 × 1.5–2.1 μm (mean = 24.0 × 1.7 μm, n = 20). Gamma conidia not observed. Sexual morph not observed.

Culture characteristics. Pure culture was isolated by subbing hyphal tips growing from surface sterilized plant material. Colonies on PDA cover the Petri dish after

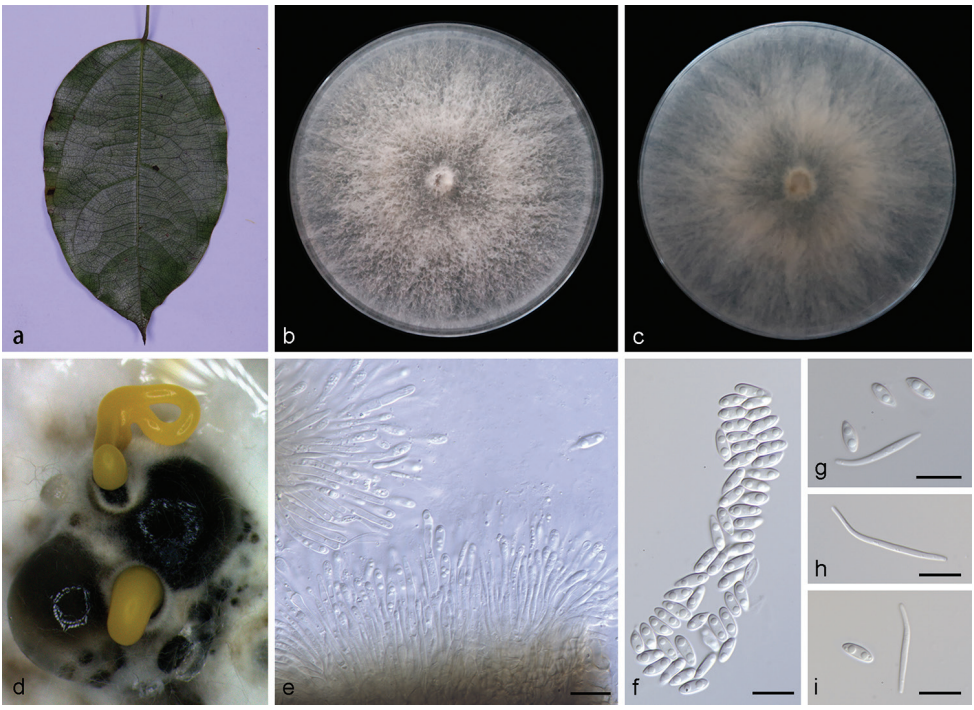

Figure 3. *Diaporthe grandiflori* (SAUCC194.84) **a** leaf of *Heterostemma grandiflorum* **b, c** surface (**b**) and reverse (**c**) sides of colony after incubation for 15 days on PDA **d** conidiomata **e** conidiophores and conidiogenous cells **f** alpha conidia **g, i** alpha conidia and beta conidia **h** beta conidia. Scale bars: 10 μm (**e–i**).

15 days kept in dark conditions at 25 °C, cottony with abundant aerial mycelium, white on surface side, white to grayish on reverse.

Notes. Phylogenetic analysis of a combined five loci showed that *D. grandiflori* (strain SAUCC194.84) formed an independent clade (Fig. 1) and is phylogenetically distinct from *D. penetriteum*. This species can be easily distinguished from *D. penetriteum* by 87 nucleotides difference concatenated alignment (24 in the ITS region, 1 *TUB*, 41 *CAL* and 21 *HIS*). Morphologically, *D. grandiflori* differs from *D. penetriteum* in larger α-conidia (6.3–8.3 × 2.8–3.3 vs. 4.5–5.5 × 1.5–2.5 μm) and longer β-conidia (21.5–30.5 × 1.5–2.1 vs. 16.5–27.5 × 1.0–2.0 μm) (Gao et al. 2016).

Diaporthe heliconiae **S.T. Huang, J.W. Xia, X.G. Zhang & Z. Li, sp. nov.**
MycoBank No: 837592
Figure 4

Etymology. Named after the host *Heliconia metallica* on which it was collected.

Diagnosis. *Diaporthe heliconiae* can be distinguished from the phylogenetically closely related species *D. subclavata* F. Huang, K.D. Hyde & Hong Y. Li in smaller α-conidia.

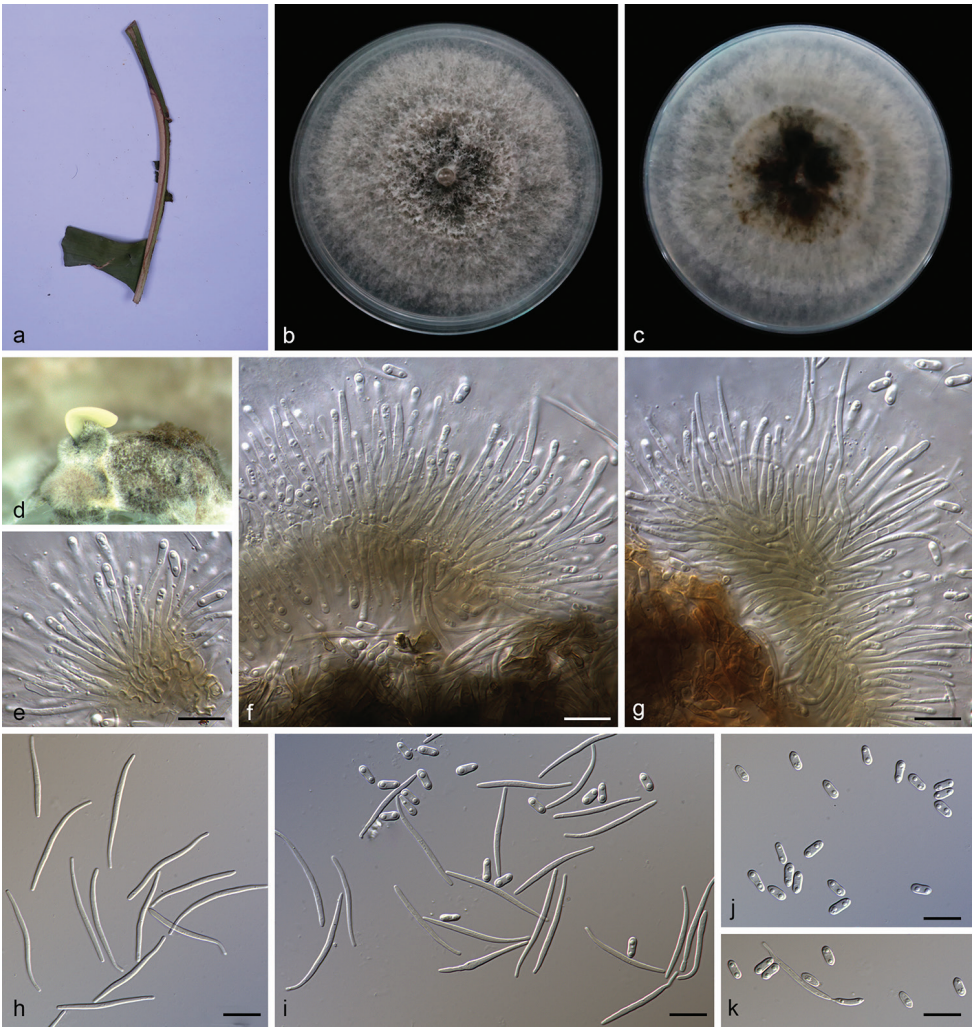

Figure 4. *Diaporthe heliconiae* (SAUCC194.77) **a** petiole of *Heliconia metallica* **b, c** surface (**b**) and reverse (**c**) sides of colony after incubation for 15 days on PDA **d** conidiomata on PDA **e–g** conidiophores and conidiogenous cells **h** beta conidia **i** alpha conidia and beta conidia **j** alpha conidia **k** alpha conidia and germinating conidia. All in water. Scale bars: 10 μm (**e–k**).

Type. China, Yunnan Province: Xishuangbanna Tropical Botanical Garden, Chinese Academy of Sciences, on the symptomatic petiole of *Heliconia metallica*. 19 April 2019, S.T. Huang, HSAUP194.77, holotype, ex-holotype living culture SAUCC194.77.

Description. Asexual morph: Conidiomata pycnidial, solitary or aggregated in groups, erumpent, thin-walled, superficial to embedded on PDA, dark brown to black, globose or subglobose, exuding creamy yellowish spiral conidial cirrus from the ostioles. Conidiophores hyaline, aseptate, cylindrical, straight to sinuous, branched, 16.5–25.0 × 1.3–1.8 μm. Alpha conidiogenous cells, cylindric-clavate, terminal, few guttu-

late, 11.5–18.0 × 1.0–1.5 μm. Beta conidiogenous cells, prismatic, terminal, few guttulate, 10.0–14.1 × 1.0–1.2 μm. Alpha conidia, hyaline, smooth, aseptate, ellipsoidal, 2–4 guttulate, apex subobtuse, base subtruncate, 5.0–6.5 × 2.0–2.5 μm (mean = 6.1 × 2.3 μm, n = 20). Beta conidia hyaline, aseptate, filiform, slightly curved, tapering towards the apex, 25.0–33.5 × 1.0–1.5 μm (mean = 29.4 × 1.3 μm, n = 20). Gamma conidia and sexual morph not observed.

Culture characteristics. Pure culture was isolated by subbing hyphal tips growing from surface sterilized infected plant material. Colonies on PDA cover the Petri dish diameter after incubation for 15 days in dark conditions at 25 °C. Aerial mycelium abundant, cottony, white, dense in the center, sparse near the margin. White on surface side, white to tanned on reverse side.

Additional specimen examined. China, Yunnan Province: Xishuangbanna Tropical Botanical Garden, Chinese Academy of Sciences, on the symptomatic petiole of *Heliconia metallica*. 19 April 2019, S.T. Huang, HSAUP194.75 paratype; living culture SAUCC194.75.

Notes. *Diaporthe heliconiae* clade comprises strains SAUCC194.75 and SAUCC194.77, closely related to *D. subclavata* in the combined phylogenetic tree (Fig. 1). *Diaporthe heliconiae* can be distinguished based on ITS, *TUB* and *HIS* loci from *D. subclavata* (16/489 in ITS, 8/357 in *TUB* and 3/470 in *HIS*). Morphologically, *Diaporthe heliconiae* differs from *D. subclavata* in its smaller α-conidia (5.0–6.5 × 2.0–2.5 vs. 5.5–7.2 × 2.2–2.9 μm). Furthermore, in *Diaporthe heliconiae* β-conidia were obtained size 25.0–33.5 × 1.0–1.5 μm, while in *D. subclavata* β-conidia were not obtained (Huang et al. 2015).

Diaporthe heterostemmatis **S.T. Huang, J.W. Xia, X.G. Zhang & Z. Li, sp. nov.**
MycoBank No: 837593
Figure 5

Etymology. Named after the host *Heterostemma grandiflorum* on which it was collected.

Diagnosis. *Diaporthe heterostemmatis* differs from its closest phylogenetic species *D. subellipicola* S.K. Huang & K.D. Hyde in ITS, *TUB* and *TEF* loci based on the alignments deposited in Tree-BASE.

Type. China, Yunnan Province: Xishuangbanna Tropical Botanical Garden, Chinese Academy of Sciences, on infected leaves of *Heterostemma grandiflorum*. 19 April 2019, S.T. Huang, HSAUP194.85, holotype, ex-holotype living culture SAUCC194.85.

Description. Asexual morph: Conidiomata pycnidial, 3–5 pycnidia grouped together, globose, black, erumpent, exuding creamy to yellowish conidial droplets from ostioles. Conidiophores hyaline, septate, branched, elliptical or cylindrical, straight to sinuous, 6.5–10.5 × 2.5–4.5 μm. Conidiogenous cells 5.3–11.8 × 1.5–3.2 μm, phialidic, cylindrical, enlarged towards the base, tapering towards the apex, slightly curved, neck up to 5.5 μm long, 2.0 μm wide. Alpha conidia, hyaline, smooth, aseptate, ellipsoidal,

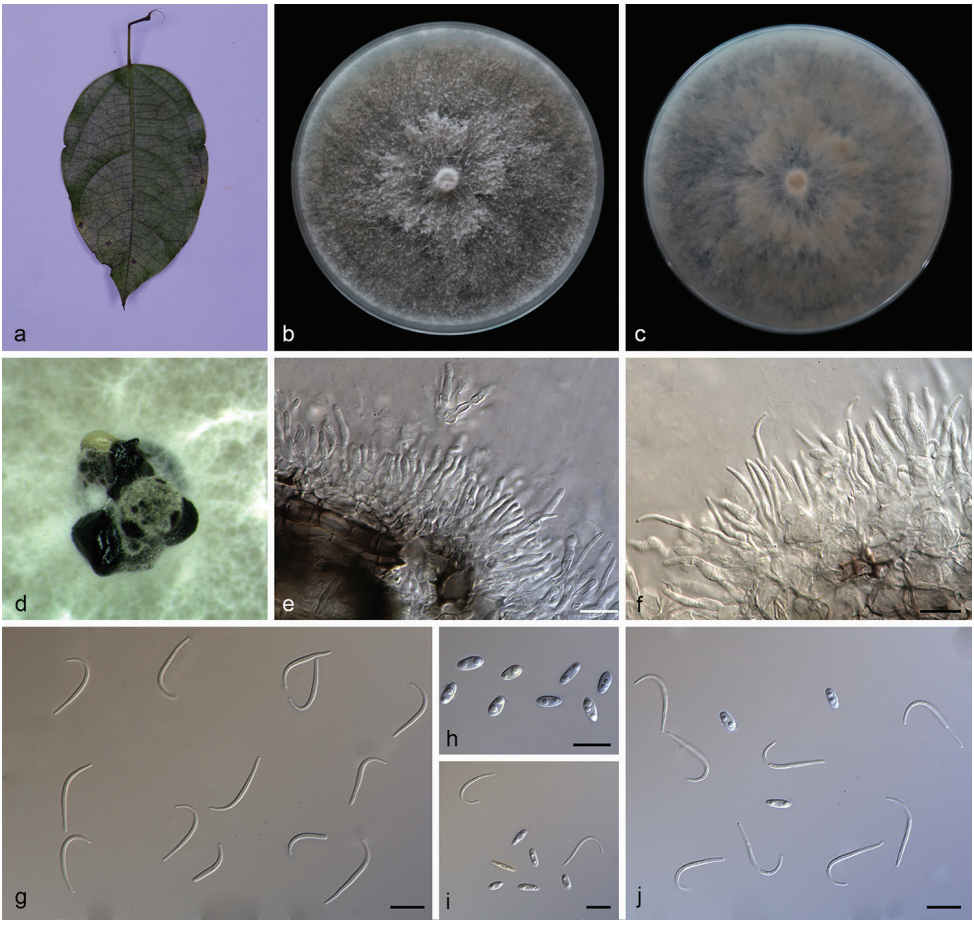

Figure 5. *Diaporthe heterostemmatis* (SAUCC194.85) **a** leaf of host plant **b, c** surface (**b**) and reverse (**c**) sides of colony, after incubation for 15 days on PDA **d** conidiomata on PDA **e, f** conidiophores and conidiogenous cells **g** beta conidia **h** Alpha conidia **i, j** alpha conidia and beta conidia. Scale bars: 10 μm (**e–j**).

biguttulate, apex subobtuse, base subtruncate, 5.8–7.5 × 2.5–3.3 μm (mean = 6.5 × 3.0 μm, n = 20). Beta conidia hyaline, aseptate, filiform, few guttulate, hooked and mostly curved through 90–180°, tapering towards both ends, 16.0–22.7 × 1.0–1.5 μm (mean = 20.4 × 1.2 μm, n = 20). Gamma conidia and sexual morph not observed.

Culture characteristics. Pure culture was isolated by subbing hyphal tips growing from surface sterilized plant material. Colonies on PDA cover the Petri dish diameter after incubation for 15 days in dark conditions at 25 °C. Aerial mycelium white, cottony, feathery, with concentric zonation, white on surface side, pale brown to black on reverse side.

Additional specimen examined. China, Yunnan Province: Xishuangbanna Tropical Botanical Garden, Chinese Academy of Sciences, on infected leaves of *Camellia sinensis*. 19 April 2019, S.T. Huang, HSAUP194.102 paratype; living culture SAUCC194.102.

Notes. This new species is proposed as the molecular data showed it forms a distinct clade with high support (ML/BI=98/1) and it appears most closely related to *D. subellipicola*. *Diaporthe heterostemmatis* can be distinguished from *D. subellipicola* by 57 nucleotides in concatenated alignment, in which 8 were distinct in the ITS region, 28 in the *TUB* region and 21 in the *TEF* region. Morphologically, *D. subellipicola* was observed only on the basis of the sexual morph and culture characteristics (Hyde et al. 2018).

Diaporthe litchii **S.T. Huang, J.W. Xia, X.G. Zhang, Z. Li, sp. nov.**
MycoBank No: 837595
Figure 6

Etymology. Named after the host *Litchi chinensis* on which it was collected.

Diagnosis. *Diaporthe litchii* differs from *D. collariana* R.H. Perrera & K.D. Hyde in smaller alpha conidia and shorter conidiophores.

Type. China, Yunnan Province: Xishuangbanna Tropical Botanical Garden, Chinese Academy of Sciences, on infected leaves of *Litchi chinensis*. 19 April 2019, S.T. Huang, HSAUP194.22, holotype, ex-holotype living culture SAUCC194.22.

Description. Asexual morph: Conidiomata pycnidial, 3–5 pycnidia grouped together, globose, black, erumpent, coated with white hyphae, creamy to yellowish conidial droplets exuded from central ostioles. Conidiophores hyaline, branched, densely aggregated, cylindrical, 10.5–15.0 × 1.8–2.5 μm. Conidiogenous cells 7.5–9.5 × 1.5–2.0 μm, cylindrical, terminal, straight to sinuous. Alpha conidia, hyaline, smooth, aseptate, ellipsoidal to fusiform, biguttulate, 3.8–5.0 × 1.5–2.3 μm (mean = 4.7 × 2.0 μm, n = 20). Beta conidia hyaline, aseptate, filiform, few guttulate, slightly curved, tapering towards both ends, 20.0–28.0 × 1.2–1.8 μm (mean = 23.2 × 1.2 μm, n = 20). Gamma conidia and sexual morph not observed.

Culture characteristics. Pure culture was isolated by subbing hyphal tips growing from surface sterilized plant material. Colonies on PDA cover the Petri dish diameter after incubation for 15 days in dark conditions at 25 °C. Aerial mycelium abundant, white, cottony on surface, reverse white to pale brown with two concentric zonation.

Additional specimen examined. China, Yunnan Province: Xishuangbanna Tropical Botanical Garden, Chinese Academy of Sciences, on diseased leaves of *Elaeagnus conferta*. 19 April 2019, S.T. Huang, HSAUP194.12 paratype; living culture SAUCC194.12.

Notes. *Diaporthe litchii* comprises strains SAUCC194.12 and SAUCC194.22 can be distinguished from the closely related species *D. collariana* by 63 nucleotides difference in the concatenated alignment (9 in the ITS region, 34 *TUB*, 5 *TEF* and 15 *CAL*). *Diaporthe litchii* differs from *D. collariana* in smaller alpha conidia (3.8–5.0 × 1.5–2.3 vs. 4.7–5.6 × 1.7–2.2 μm) and shorter conidiophores (10.5–15.0 × 1.8–2.5 vs. 12–20 × 2.4–3.2 μm) (Perera et al. 2018).

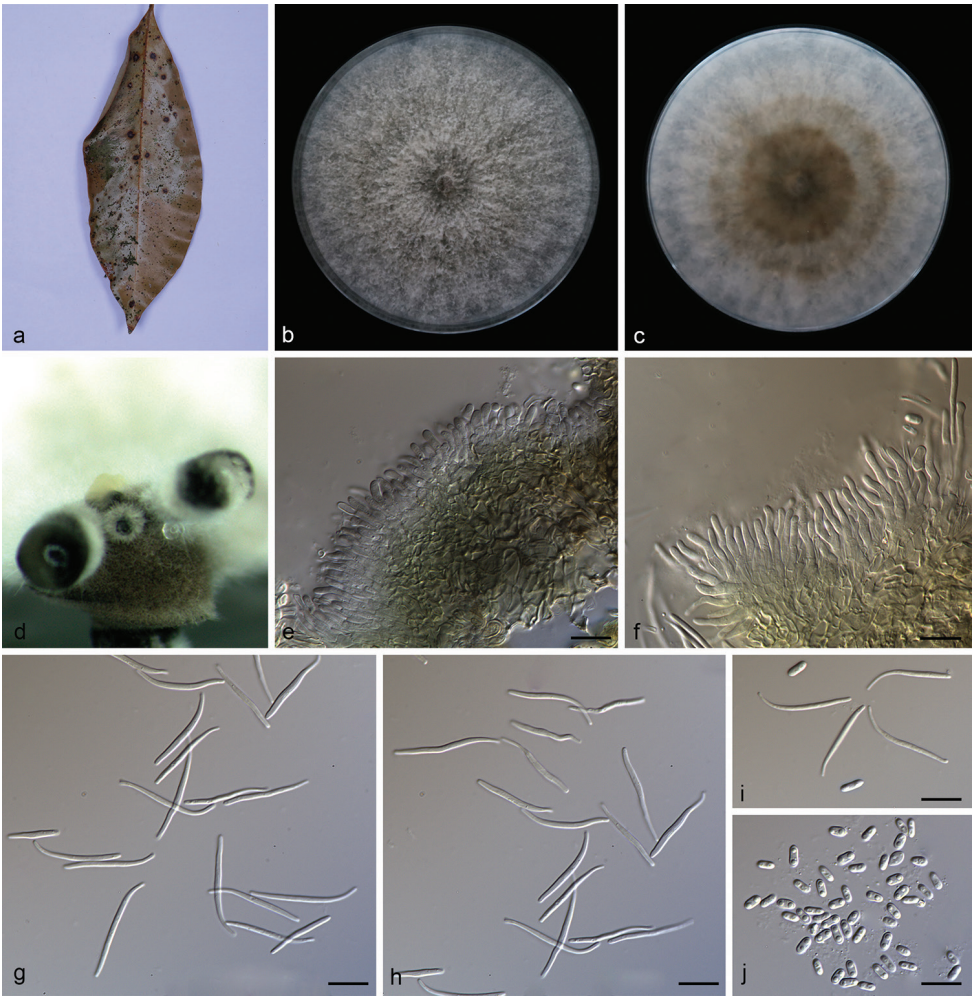

Figure 6. *Diaporthe litchii* (SAUCC194.22) **a** leaf of host plant **b, c** surface (**b**) and reverse (**c**) sides of colony after incubation for 15 days on PDA **d** conidiomata **e, f** conidiophores and conidiogenous cells **g, h** beta conidia **i** alpha conidia and beta conidia **j** alpha conidia. Scale bars: 10 μm (**e–j**).

Diaporthe lutescens **S.T. Huang, J.W. Xia, X.G. Zhang & Z. Li, sp. nov.**
MycoBank No: 837597
Figure 7

Etymology. Named after the host *Chrysalidocarpus lutescens* on which it was collected.

Diagnosis. *Diaporthe lutescens* differs from *D. pterocarpi* (S. Hughes) D. Udayanga et al. and *D. pseudoinconspicua* T.G.L. Oliveira et al. in longer beta conidia and the types of conidia.

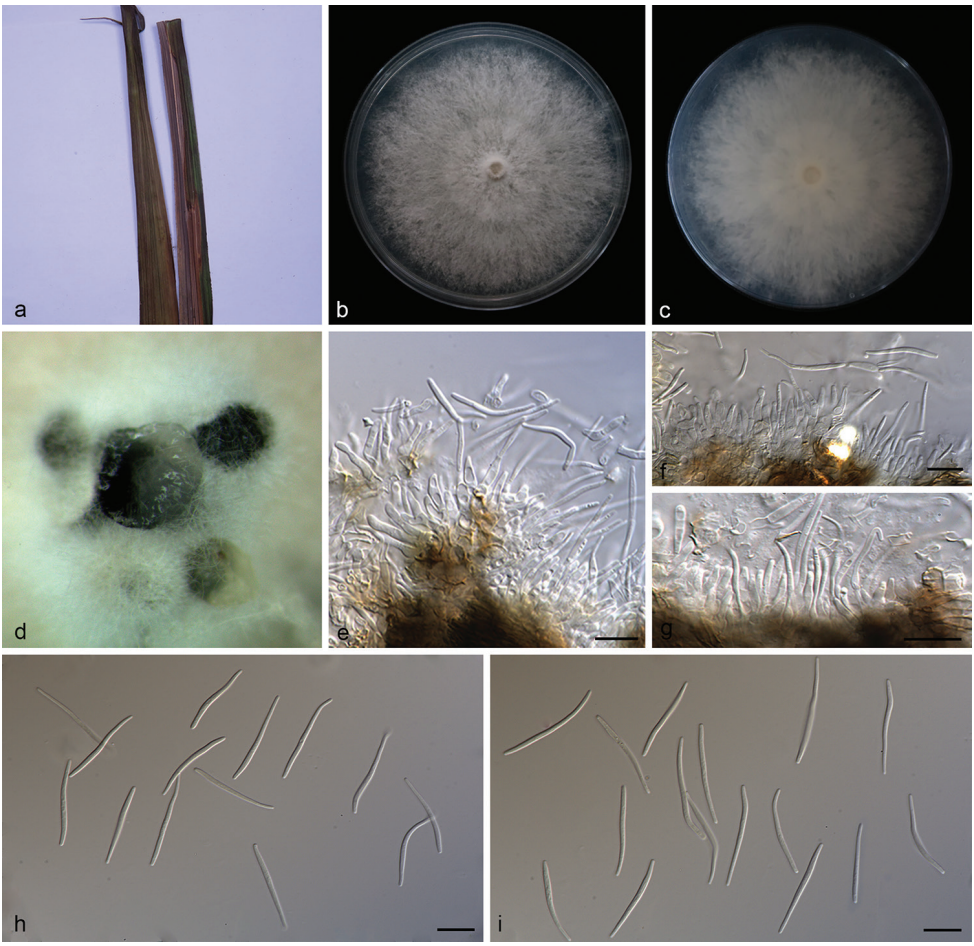

Figure 7. *Diaporthe lutescens* (SAUCC194.36) **a** leaves of host plant **b, c** surface (**b**) and reverse (**c**) sides of colony after incubation for 15 days on PDA **d** conidiomata **e–g** conidiophores and conidiogenous cells **h, i** beta conidia. Scale bars: 10 μm (**e–i**).

Type. China, Yunnan Province: Xishuangbanna Tropical Botanical Garden, Chinese Academy of Sciences, on leaves of *Chrysalidocarpus lutescens*. 19 April 2019, S.T. Huang, HSAUP194.36, holotype, ex-holotype living culture SAUCC194.36.

Description. Asexual morph: Conidiomata pycnidial, scattered or aggregated, black, erumpent, slightly raised above the surface of the culture medium, subglobose, exuding white creamy conidial droplets from central ostioles after 30 days incubation in light condition at 25 °C on PDA; pycnidial wall consists of black to dark brown, thin-walled cells. Conidiophores 10.2–17.0 × 1.8–3.0 μm, hyaline, unbranched, subcylindrical, septate, smooth, straight or slightly curved, obtuse at the apex, widened at base. Conidiogenous cells 5.7–9.1 × 1.4–2.6 μm, phialidic, cylindrical, terminal, straight to sinuous, tapering towards the apex. Beta conidia 20.8–28.8 × 1.2–2.0 μm (mean =

25.3 × 1.4 µm, n = 20), filiform, hyaline, straight or slightly curved, aseptate, base subtruncate, enlarged towards the apex. Alpha conidia and gamma conidia not observed.

Culture characteristics. Pure culture was isolated by subbing hyphal tips growing from surface sterilized infected plant material. Colonies on PDA cover the petri plate diameter after incubation for 15 days in dark conditions at 25 °C, initially white, becoming grayish, reverse pale brown, with concentric rings of dense and sparse hyphae, irregular margin, fluffy aerial mycelium. Pycnidia formed in 15 days.

Notes. From the phylotree, seen on Fig. 1, *Diaporthe lutescens* forms an independent clade and is phylogenetically distinct from *D. pterocarpi* and *D. pseudoinconspicua*. *Diaporthe lutescens* can be distinguished from *D. pterocarpi* in ITS, *TUB*, *TEF* and *CAL* loci by 77 nucleotide differences in concatenated alignment (43 in ITS, 2 in *TUB*, 29 in *TEF* and 17 in *CAL*), and from *D. pseudoinconspicua* in ITS, *TUB*, *TEF*, *CAL* and *HIS* loci by 65 nucleotide differences (18 in ITS, 3 in *TUB*, 23 in *TEF*, 8 in *CAL* and 13 in *HIS*). Moreover, *D. lutescens* differs from *D. pterocarpi* and *D. pseudoinconspicua* in having longer beta conidia (20.8–28.8 × 1.2–2.0 vs. 16.0–23.4 × 1.0–1.4 µm, and 20.8–28.8 × 1.2–2.0 vs. 18.0–21.0 × 1.0–1.5 µm). Furthermore, *Diaporthe pterocarpi* and *D. pseudoinconspicua* can produce α-conidia, but *D. lutescens* cannot (Crous et al. 2018a; Broge et al. 2020).

Diaporthe melastomatis **S.T. Huang, J.W. Xia, X.G. Zhang & Z. Li, sp. nov.**
MycoBank No: 837598
Figure 8

Etymology. Named after the host *Melastoma malabathricum* on which it was collected.

Diagnosis. *Diaporthe melastomatis* differs from *D. parapterocarpi* Crous in smaller α-conidia and the types of conidia.

Type. China, Yunnan Province: Xishuangbanna Tropical Botanical Garden, Chinese Academy of Sciences, on diseased leaves of *Melastoma malabathricum*. 19 April 2019, S.T. Huang, HSAUP194.55, holotype, ex-holotype living culture, SAUCC194.55.

Description. Asexual morph: Conidiomata pycnidial, subglobose to globose, black, erumpent, coated with white hyphae, thick-walled, yellowish spiral conidial cirrus exuded from ostioles. Conidiophores hyaline, smooth, septate, branched, densely aggregated, cylindric-clavate, straight to slightly sinuous, tapering towards the apex, 14.5–21.0 × 2.0–3.2 µm. Conidiogenous cells 9.5–13.0 × 1.5–2.5 µm, cylindrical, guttulate, terminal, tapering towards the base. Alpha conidia, hyaline, smooth, aseptate, oblong ellipsoidal, 2–4 guttulate, apex subobtuse, base subtruncate, 5.5–8.5 × 1.7–2.5 µm (mean = 6.8 × 2.1 µm, n = 20). Beta conidia abundant in the culture, hyaline, aseptate, filiform, multi-guttulate, sigmoid to lunate, mostly curved through 90–180°, tapering towards both ends, 25.0–33.5 × 1.1–2.0 µm (mean = 27.6 × 1.4 µm, n = 20). Gamma conidia and sexual morph not observed.

Culture characteristics. Pure culture was isolated by subbing hyphal tips growing from surface sterilized diseased material. Colonies on PDA cover the Petri diameter

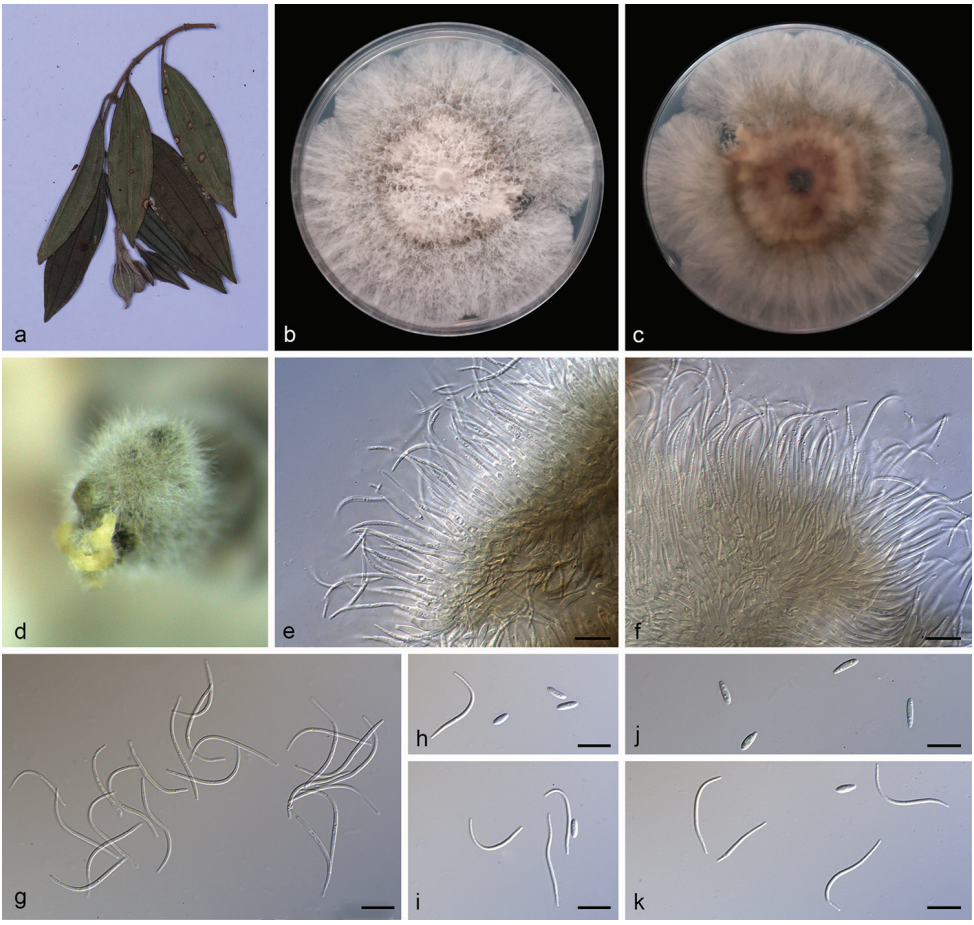

Figure 8. *Diaporthe melastomatis* (SAUCC194.55) **a** branch with leaves of host plant **b, c** surface (**b**) and reverse (**c**) sides of colony after incubation for 15 days on PDA **d** conidiomata **e, f** conidiophores and conidiogenous cells **g** beta conidia **h, i, k** alpha conidia and beta conidia **j** alpha conidia. Scale bars: 10 μm (**e–k**).

after incubation for 15 days in dark conditions at 25 °C, cottony and lobate with abundant aerial mycelium, hyphae white in the margin on surface side, with pale brown concentric ring of dense hyphae on reverse side.

Additional specimens examined. China, Yunnan Province: Xishuangbanna Tropical Botanical Garden, Chinese Academy of Sciences, 19 April 2019, S.T. Huang. On diseased leaves of *Millettia reticulata*, HSAUP194.80 paratype, living culture SAUCC194.80; on infected leaves of *Camellia sinensis*, HSAUP194.88 paratype, living culture SAUCC194.88.

Notes. *Diaporthe melastomatis* is introduced based on the multi-locus phylogenetic analysis, with three isolates clustering separately in a well-supported clade (ML/BI = 100/1). *Diaporthe melastomatis* is most closely related to *D. parapterocarpi*, but

distinguished based on ITS and *TUB* loci from *D. parapterocarpi* by 32 nucleotides difference in the concatenated alignment, in which 20 are distinct in the ITS region, 12 in the *TUB* region. Morphologically, *Diaporthe melastomatis* differs from *D. parapterocarpi* in its smaller alpha conidia (5.5–8.5 × 1.7–2.5 vs. 8.0–10.0 × 2.5–3.0 μm). Furthermore, *Diaporthe melastomatis* can produce beta conidia, but *D. parapterocarpi* cannot (Crous et al. 2014).

Diaporthe pungensis **S.T. Huang, J.W. Xia, X.G. Zhang, Z. Li, sp. nov.**
MycoBank No: 837599
Figure 9

Etymology. Named after the host *Elaeagnus pungens* on which it was collected.

Diagnosis. *Diaporthe pungensis* differs from its closest phylogenetic species *D. inconspicua* R.R. Gomes et al. and *D. poincianellae* T.G.L. Oloveira et al. in ITS, *TUB*, *TEF*, *CAL* and *HIS* loci based on the alignments deposited in Tree-BASE.

Type. China, Yunnan Province: Xishuangbanna Tropical Botanical Garden, Chinese Academy of Sciences, on diseased leaves of *Elaeagnus pungens*. 19 April 2019, S.T. Huang, HSAUP194.112, holotype, ex-holotype living culture SAUCC194.112.

Description. Asexual morph: Conidiomata pycnidial, 3–5 pycnidia grouped together, superficial to embedded on PDA, erumpent, thin-walled, dark brown to black, globose or subglobose, exuding white creamy conidial mass from the ostioles. Conidiophores hyaline, aseptate, cylindrical, smooth, straight to sinuous, unbranched, 11.0–14.5 × 1.5–2.3 μm. Conidiogenous cells phialidic, cylindrical, terminal, 8.0–9.5 × 1.0–2.5 μm. Alpha conidia, hyaline, smooth, aseptate, ellipsoidal to fusoid, 2–3 guttulate, apex subobtuse, base subtruncate, 6.0–8.5 × 2.0–3.3 μm (mean = 6.6 × 2.5 μm, n = 20). Beta conidia hyaline, aseptate, eguttulate, filiform, slightly curved, tapering towards the apex, base truncate, some conidia are in the immature stage swollen in the middle, 24.0–28.9 × 1.0–2.0 μm (mean = 26.9 × 1.4 μm, n = 20). Gamma conidia not observed, sexual morph not observed.

Culture characteristics. Pure culture was isolated by subbing hyphal tips growing from surface sterilized plant material. Colonies on PDA cover the 3/4 of Petri dish diameter after incubation for 15 days in dark conditions at 25 °C, flat, cottony in the center with medium developed aerial mycelium, sparse in the outer region. With several concentric rings of dense and sparse hyphae, irregular margin, white on surface side, white to pale yellow and cinnamon speckle on reverse side.

Additional specimen examined. China, Yunnan Province: Xishuangbanna Tropical Botanical Garden, Chinese Academy of Sciences, on infected leaves of *Camellia sinensis*. 19 April 2019, S.T. Huang, HSAUP194.89 paratype, living culture SAUCC194.89.

Notes. *Diaporthe pungensis* forms a distinct clade with high support (ML/BI = 100/1), and differed with the closely related species (*D. inconspicua* and *D. poincianellae*) on ITS, *TUB*, *CAL* and *HIS* loci (94% in ITS, 92% in *TUB*, 70% in *TEF*, 92% in *CAL* and 92% in *HIS*; and 95% in ITS, 94% in *TUB*, 80% in *TEF*, 94% in *CAL* and 89% in *HIS*, respectively). Moreover, *Diaporthe pungensis* differs from *D. inconspicua*,

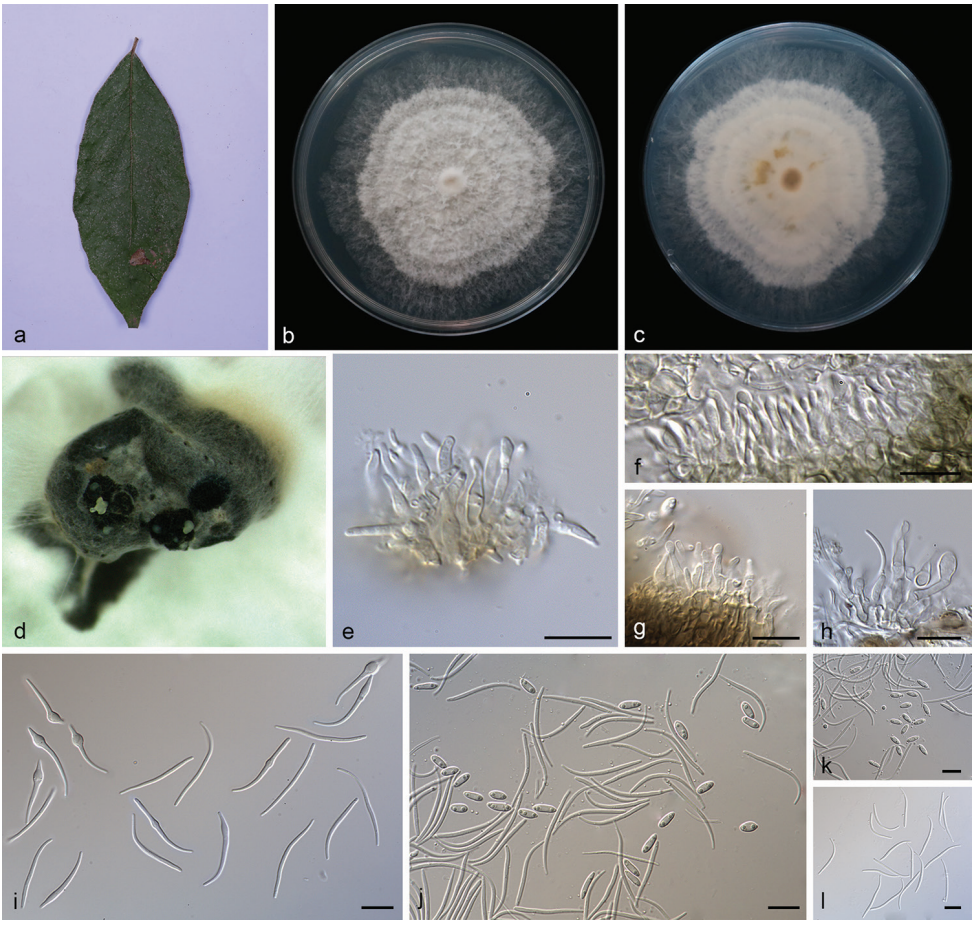

Figure 9. *Diaporthe pungensis* (SAUCC194.112) **a** leaf of host plant **b, c** surface (**b**) and reverse (**c**) sides of colony after incubation for 15 days on PDA **d** conidiomata on PDA **e–h** conidiophores and conidiogenous cells **i, l** beta conidia **j, k** alpha conidia and beta conidia. Scale bars: 10 μm (**e–l**).

in having guttulate of alpha conidia, and having larger alpha conidia (6.0–8.5 × 2.0–3.3 vs. 5.5–6.5 × 1.5–2 μm) (Bezerra et al. 2018). Furthermore, *Diaporthe pungensis* can produce two types of conidia (α-conidia and β-conidia), but *D. poincianellae* only produce a α-conidia(Crous et al. 2018b).

Diaporthe subclavata F. Huang, K.D. Hyde & H.Y. Li, Fung. Biol. 119: 343, 2015

Figure 10

Description. Asexual morph: Conidiomata pycnidial, multi-pycnidia grouped together, globose, black, erumpent, coated with white hyphae, creamy to yellowish conidial drop-

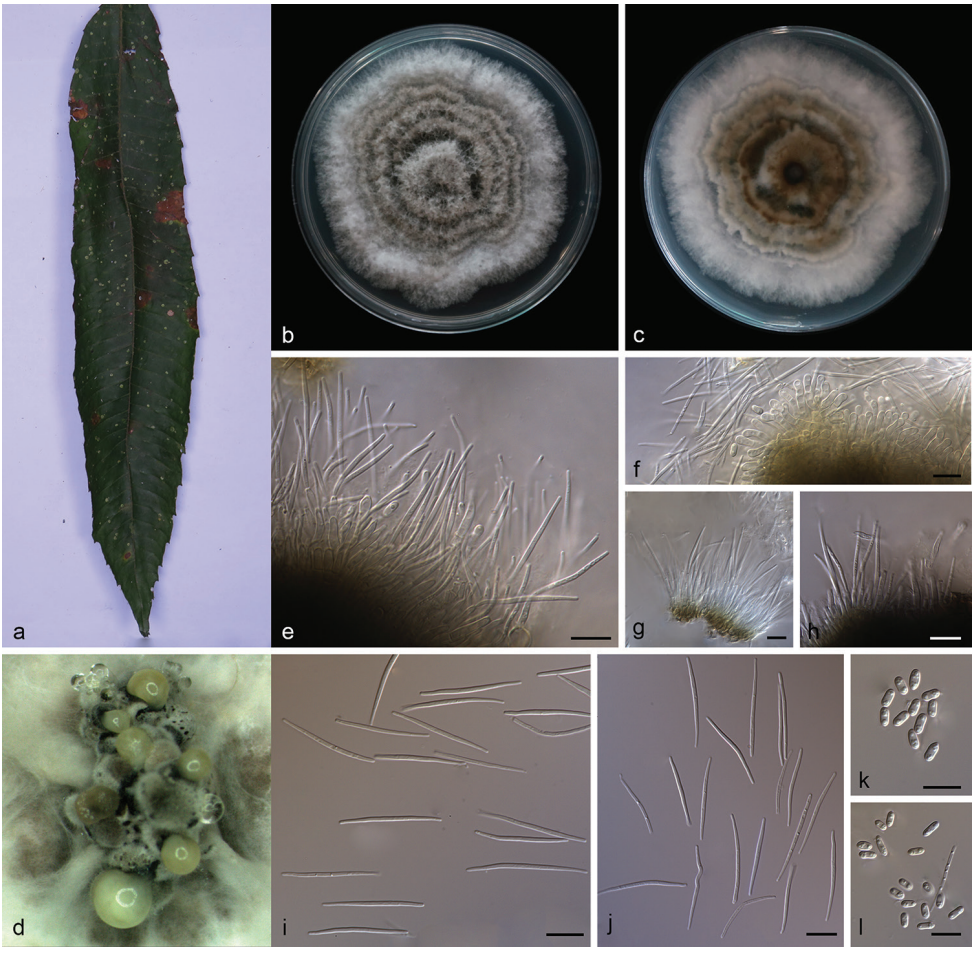

Figure 10. *Diaporthe subclavata* (SAUCC194.66) **a** leaf of *Pometia pinnata* **b, c** surface (**b**) and reverse (**c**) sides of colony after incubation for 15 days on PDA **d** conidiomata **e–h** conidiophores and conidiogenous cells **i, j** Beta conidia **k, l** Alpha conidia. Scale bars: 10 μm (**e–l**).

lets exuded from central ostioles. Conidiophores hyaline, densely aggregated, cylindrical, straight to sinuous, tapering towards the apex, 13.5–23.0 × 2.0–3.0 μm. Alpha conidiogenous cells 7.0–10 × 1.8–2.5 μm, cylindrical, terminal, slightly curved. Beta conidiogenous cells 10.5–13.5 × 0.9–1.5 μm, cylindrical, hyaline, tapering towards the apex. Alpha conidia, hyaline, smooth, aseptate, ellipsoidal, multi-guttulate, apex subobtuse, base subtruncate, 4.7–5.8 × 2.4–2.9 μm (mean = 5.3 × 2.6 μm, n = 20). Beta conidia hyaline, aseptate, filiform, few guttulate, slightly curved, tapering towards the both ends, 25.5–32.0 × 1.0–1.6 μm (mean = 27.5 × 1.3 μm, n = 20). Gamma conidia and sexual morph not observed.

Culture characteristics. Pure culture was isolated by subbing hyphal tips growing from surface sterilized diseased material. Colonies on PDA cover the Petri dish diam-

eter after incubation for 15 days in dark conditions at 25 °C. Aerial mycelium white, cottony, feathery, with concentric zonation, white on surface side, pale brown to black on reverse side.

Specimen examined. China, Yunnan Province: Xishuangbanna Tropical Botanical Garden, Chinese Academy of Sciences, on infected leaves of *Pometia pinnata*. 19 April 2019, S.T. Huang, HSAUP194.66, living culture SAUCC194.66.

Notes. *Diaporthe subclavata* was originally described from the leaf with citrus scab of *Citrus unshiu* in Fujian Province, China (Huang et al. 2015). In the present study, isolated strain SAUCC194.66 from symptomatic leaves of *Pometia pinnata* was congruent with *D. subclavata* based on morphology and DNA sequences data (Fig. 1). We therefore present a description and illustration of *D. subclavata* as a known species for this clade, found on new host.

Diaporthe tectonendophytica **M. Doilom, A. J. Dissanayake & K.D. Hyde, Fung. Div., 82: 163, 2016**

Figure 11

Description. Asexual morph: Conidiomata pycnidial, aggregated, brownish to black, erumpent, subglobose, exuding white creamy conidial droplets from central ostioles after being kept for 30 days in light at 25 °C. Conidiophores 17.4–35.0 × 2.2–3.5 µm, hyaline, branched, subcylindrical, septate, straight or slightly curved, guttulate. Conidiogenous cells 11.3–15.0 × 1.7–2.5 µm (mean = 12.3 × 2.1 µm, n = 20), cylindric-clavate, hyaline, straight to slightly sinuous, tapering towards the apex. Beta conidia 25.0–31.8 × 0.9–1.8 µm (mean = 28.2 × 1.2 µm, n = 20), filiform, hyaline, guttulate, aseptate, hooked and mostly curved through 90–180°, swollen in the middle. Alpha conidia and Gamma conidia not observed.

Culture characteristics. Pure culture was isolated by subbing hyphal tips growing from surface sterilized diseased material. Colonies on PDA cover the Petri dish diameter after incubation for 15 days in dark conditions at 25 °C, aerial mycelium abundant, white to grayish on surface side, pale yellow on reverse with concentric zonation. Pycnidia are formed on 15th day or later.

Specimens examined. China, Yunnan Province: Xishuangbanna Tropical Botanical Garden, Chinese Academy of Sciences, 19 April 2019, S.T. Huang. On diseased leaves of *Elaeagnus conferta* HSAUP194.11, living culture SAUCC194.11; on diseased leaves of *Pometia pinnata* HSAUP194.63, living culture SAUCC194.63.

Notes. *Diaporthe tectonendophytica* was originally described from the asymptomatic branches of *Tectona grandis* in Thailand (Doilom et al. 2017). In the present study, two strains (SAUCC194.11 and SAUCC194.63) from symptomatic leaves of *Elaeagnus conferta* and *Pometia pinnata* were congruent with *D. tectonendophytica* based on morphology and DNA sequences data (Fig. 1). We therefore describe *D. tectonendophytica* as a known species for this clade.

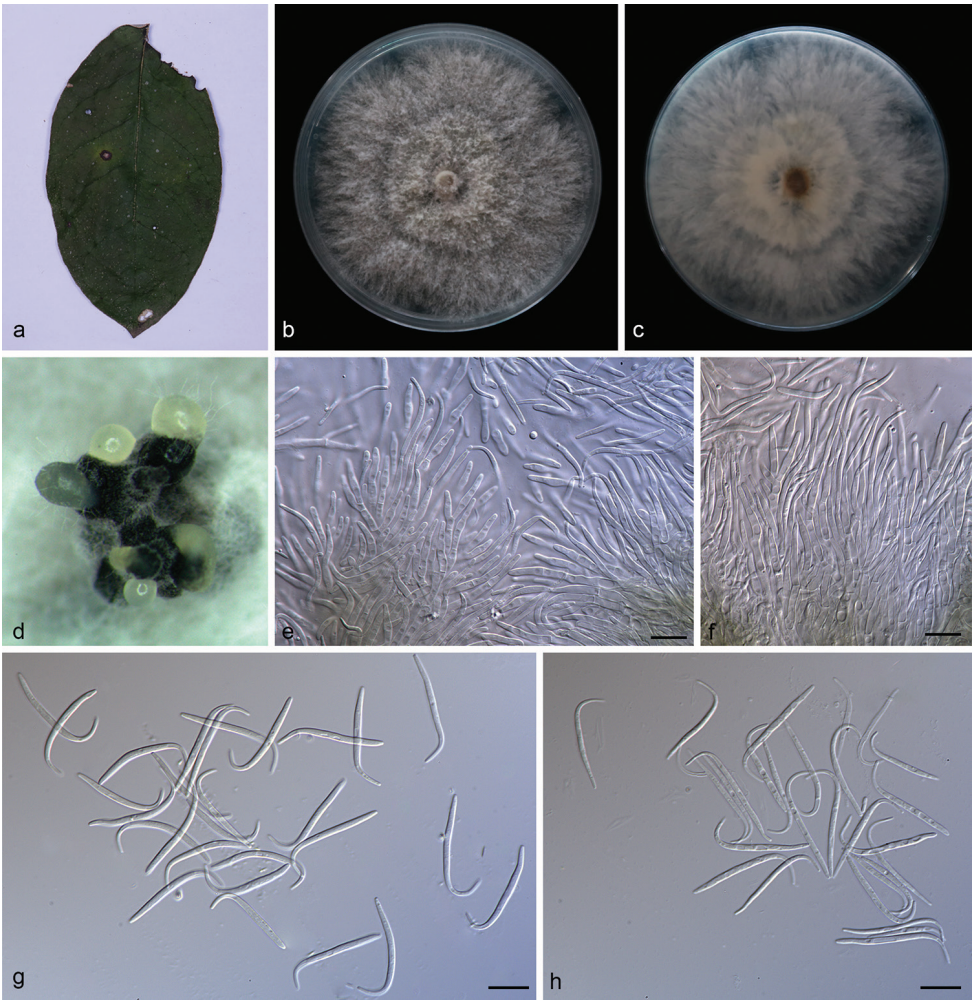

Figure 11. *Diaporthe tectonendophytica* (SAUCC194.11) **a** leaf of host plant **b, c** surface (**b**) and reverse (**c**) side of colony after incubation for 15 days on PDA **d** conidiomata on PDA **e, f** conidiophores and conidiogenous cells **g, h** beta conidia. Scale bars: 10 μm (**e–h**).

Discussion

In the current study, 87 reference sequences (including an outgroup taxon) were selected based on BLAST searches of NCBIs GenBank nucleotide database and were included in the phylogenetic analyses (Table 1). Phylogenetic analyses based on five combined loci (ITS, *TUB*, *TEF*, *CAL* and *HIS*), as well as morphological characters of the non-sexual morph obtained in culture, contributed to knowledge of the diversity of *Diaporthe* species in Yunnan Province. Based on a large set of freshly collected specimens from Yunnan province, China, 20 strains of *Diaporthe* species were isolated from 12 host genera (Table 1). As a result, eight new species are proposed: *Diaporthe*

camelliae-sinensis, *D. grandiflori*, *D. heliconiae*, *D. heterostemmatis*, *D. litchii*, *D. lutescens*, *D. melastomatis*, *D. pungensis* and two previously described species were described and illustrated, *D. subclavata* and *D. tectonendophytica*.

Previously, species identification of *Diaporthe* was largely referred to the assumption of host-specificity, leading to the proliferation of names (Gomes et al. 2013). However, based on a polyphasic approach and known morphology, more than one species of *Diaporthe* can colonize a single host, while one species can be associated with different hosts (Gomes et al. 2013; Gao et al. 2017; Guarnaccia and Crous 2017; Guarnaccia et al. 2018; Guo et al. 2020). Our study can well support this phenomenon. On the one hand, *Diaporthe grandiflori* (SAUCC194.84) and *D. heterostemmatis* (SAUCC194.85) were collected from *Heterostemma grandiflorum*; *D. camelliae-sinensis* (SAUCC194.92), *D. heterostemmatis* (SAUCC194.102), *D. melastomatis* (SAUCC194.88), and *D. pungensis* (SAUCC194.89) and were isolated from *Camellia sinensis*; *D. litchii* (SAUCC194.12) and *D. tectonendophytica* (SAUCC194.11) were known on *Elaeagnus conferta*. On the other hand, the species of *D. camelliae-sinensis* collected from three hosts (*Camellia sinensis*, *Castanea mollissima*, *Machilus pingii*) *D. melastomatis* sampled from three hosts (*Camellia sinensis*, *Melastoma malabathricum*, *Millettia reticulata*) and *D. litchii* sampled from two hosts (*Elaeagnus conferta*, *Litchi chinensis*). These studies revealed a high diversity of *Diaporthe* species from different hosts. The descriptions and molecular data of *Diaporthe* represent an important resource for plant pathologists, plant quarantine officials and taxonomists.

Acknowledgements

This work was jointly supported by the National Natural Science Foundation of China (no. 31770016, 31750001, and 31900014) and the China Postdoctoral Science Foundation (no. 2018M632699).

References

Bezerra JDP, Machado AR, Firmino AL, Rosado AWC, de Souza CAF, de Souza-Motta CM, de Sousa Freire KTL, Paiva LM, Magalhães OMC, Pereira OL (2018) Mycological diversity description I. Acta Botanica Brasilica 32(4): 656–666. https://doi.org/10.1590/0102-33062018abb0154

Broge M, Howard A, Biles CL, Udayanga D, Taff H, Dudley L, Bruton BD (2020) First report of *Diaporthe* fruit rot of melons caused by *D. Pterocarpi* in Costa Rica. Plant Disease 104(5): 1550–1550. https://doi.org/10.1094/PDIS-08-19-1655-PDN

Cai L, Hyde KD, Taylor PWJ, Weir B, Waller J, Abang MM, Zhang ZJ, Yang YL, Phoulivong S, Liu ZY, Prihastuti H, Shivas RG, McKenzie EHC, Johnston PR (2009) A polyphasic approach for studying *Colletotrichum*. Fungal Diversity 39: 183–204.

Carbone I, Kohn LM (1999) A method for designing primer sets for speciation studies in filamentous Ascomycetes. Mycologia 91(3): 553–556. https://doi.org/10.1080/00275514.1999.12061051

Crous PW, Groenewald JZ, Risède JM, Simoneau P, Hywel-Jones NL (2004) *Calonectria* species and their *Cylindrocladium* anamorphs: species with sphaeropedunculate vesicles. Studies in Mycology 50: 415–430.

Crous PW, Groenewald JZ, Shivas RG, Edwards J, Seifert KA, Alfenas AC, Alfenas RF, Burgess TI, Carnegie AJ, Hardy GEStJ (2011a) Fungal planet description sheets: 69–91. Persoonia 26(1): 108–156. https://doi.org/10.3767/003158511X581723

Crous PW, Summerell BA, Swart L, Denman S, Taylor JE, Bezuidenhout CM, Palm ME, Marincowitz S, Groenewald JZ (2011b) Fungal pathogens of Proteaceae. Persoonia 27(1): 20–45. https://doi.org/10.3767/003158511X606239

Crous PW, Shivas RG, Quaedvlieg W, van der Bank M, Zhang Y, Summerell BA, Guarro J, Wingfield MJ, Wood AR, Alfenas AC (2014) Fungal planet description sheets: 214–280. Persoonia 32(1): 184–306. https://doi.org/10.3767/003158514X682395

Crous PW, Wingfield MJ, Richardson DM, Roux JJL, Strasberg D, Edwards J, Roets F, Hubka V, Taylor PWJ, Heykoop M (2016) Fungal planet description sheets: 400–468. Persoonia 36(1): 316–458. https://doi.org/10.3767/003158516X692185

Crous PW, Wingfield MJ, Burgess TI, Hardy GEStJ, Gene J, Guarro J, Baseia IG, Garcia D, Gusmao LFP, Souza-Motta CM (2018a) Fungal planet description sheets: 716–784. Persoonia 40(1): 240–393.

Crous PW, Luangsa-ard JJ, Wingfield MJ, Carnegie AJ, Hernández-Restrepo M, Lombard L, Roux J, Barreto RW, Baseia IG, Cano-Lira JF (2018b) Fungal planet description sheets: 785–867. Persoonia 41(1): 238–417.

Crous PW, Wingfield MJ, Schumacher RK, Akulov A, Bulgakov TS, Carnegie AJ, Jurjević Ž, Decock C, Denman S, Lombard L (2020) New and interesting fungi. 3. Fungal Systematics and Evolution 6: 157–231. https://doi.org/10.3114/fuse.2020.06.09

Dayarathne MC, Jones EBG, Maharachchikumbura SSN, Devadatha B, Sarma VV (2020) Morpho-molecular characterization of microfungi associated with marine based habitats. Mycosphere 11(1): 1–188. https://doi.org/10.5943/mycosphere/11/1/1

Dissanayake AJ, Phillips AJL, Hyde KD, Yan JY, Li XH (2017) The current status of species in *Diaporthe*. Mycosphere 8: 1106–1156. https://doi.org/10.5943/mycosphere/8/5/5

Doilom M, Dissanayake AJ, Wanasinghe DN, Boonmee S, Liu JK, Bhat DJ, Taylor JE, Bahkali AH, McKenzie EHC, Hyde KD (2017) Microfungi on *Tectona Grandis* (Teak) in Northern Thailand. Fungal Diversity 82(1): 107–182. https://doi.org/10.1007/s13225-016-0368-7

Fan XL, Bezerra JDP, Tian CM, Crous PW (2018) Families and genera of diaporthalean fungi associated with canker and dieback of tree hosts. Persoonia 40: 119–134. https://doi.org/10.3767/persoonia.2018.40.05

Gao YH, Sun W, Su YY, Cai L (2014) Three new species of *Phomopsis* in Gutianshan Nature Reserve in China. Mycological Progress 13(1): 111–121. https://doi.org/10.1007/s11557-013-0898-2

Gao YH, Su YY, Sun W, Cai L (2015) *Diaporthe* species occurring on *Lithocarpus glabra* in China, with descriptions of five new species. Fungal Biology 119(5): 295–309. https://doi.org/10.1016/j.funbio.2014.06.006

Gao YH, Liu F, Cai L (2016) Unravelling *Diaporthe* species associated with *Camellia*. Systematics and Biodiversity 14(1): 102–117. https://doi.org/10.1080/14772000.2015.1101027

Gao YH, Liu F, Duan W, Crous PW, Cai L (2017) *Diaporthe* is paraphyletic. IMA fungus 8: 153–187. https://doi.org/10.5598/imafungus.2017.08.01.11

Glass NL, Donaldson GC (1995) Development of primer sets designed for use with the PCR to amplify conserved genes from filamentous ascomycetes. Applied and Environmental Microbiology 61(4): 1323–1330. https://doi.org/10.1128/AEM.61.4.1323-1330.1995

Gomes RR, Glienke C, Videira SIR, Lombard L, Groenewald JZ, Crous PW (2013) *Diaporthe*: a genus of endophytic, saprobic and plant pathogenic fungi. Persoonia: Molecular Phylogeny and Evolution of Fungi 31(1): 1–41. https://doi.org/10.3767/003158513X666844

Grasso FM, Marini M, Vitale A, Firrao G, Granata G (2012) Canker and dieback on *Platanus* × *acerifolia* caused by *Diaporthe scabra*. Forest Pathology 42(6): 510–513. https://doi.org/10.1111/j.1439-0329.2012.00785.x

Guarnaccia V, Vitale A, Cirvilleri G, Aiello D, Susca A, Epifani F, Perrone G, Polizzi G (2016) Characterisation and pathogenicity of fungal species associated with branch cankers and stem-end rot of avocado in Italy. European Journal of Plant Pathology 146(4): 963–976. https://doi.org/10.1007/s10658-016-0973-z

Guarnaccia V, Crous PW (2017) Emerging *citrus* diseases in Europe caused by *Diaporthe* spp. IMA Fungus 8: 317–334. https://doi.org/10.5598/imafungus.2017.08.02.07

Guarnaccia V, Groenewald JZ, Woodhall J, Armengol J, Cinelli T, Eichmeier A, Ezra D, Fontaine F, Gramaje D, Gutierrez-Aguirregabiria A (2018) *Diaporthe* diversity and pathogenicity revealed from a broad survey of grapevine diseases in europe. Persoonia 40(6): 135–153. https://doi.org/10.3767/persoonia.2018.40.06

Guo LD, Hyde KD, Liew ECY (2000) Identification of endophytic fungi from *Livistona chinensis* based on morphology and rDNA sequences. New Phytologist 147(3): 617–630. https://doi.org/10.1046/j.1469-8137.2000.00716.x

Guo YS, Crous PW, Bai Q, Fu M, Yang MM, Wang XH, Du YM, Hong N, Xu WX, Wang GP (2020) High diversity of *Diaporthe* species associated with pear shoot canker in China. Persoonia 45: 132–162. https://doi.org/10.3767/persoonia.2020.45.05

Huang F, Hou X, Dewdney MM, Fu Y, Chen GQ, Hyde KD, Li HY (2013) *Diaporthe* species occurring on *citrus* in China. Fungal Diversity 61(1): 237–250. https://doi.org/10.1007/s13225-013-0245-6

Huang F, Udayanga D, Wang XH, Hou X, Mei XF, Fu YS, Hyde KD, Li HY (2015) Endophytic *Diaporthe* associated with *Citrus*: A phylogenetic reassessment with seven new species from China. Fungal Biology 119(5): 331–347. https://doi.org/10.1016/j.funbio.2015.02.006

Huelsenbeck JP, Ronquist F (2001) MRBAYES: bayesian inference of phylogeny. Bioinformatics 17(17): 754–755. https://doi.org/10.1093/bioinformatics/17.8.754

Hyde KD, Chaiwan N, Norphanphoun C, Boonmee S, Camporesi E, Chethana KWT, Dayarathne MC, de Silva IN, Dissanayake AJ, Ekanayaka AH (2018) Mycosphere notes 169–224. Mycosphere 9(2): 271–430. https://doi.org/10.5943/mycosphere/9/2/8

Hyde KD, Dong Y, Phookamsak R, Jeewon R, Bhat DJ, Gareth Jones EB, Liu NG, Abeywickrama PD, Mapook A, Wei D (2020) Fungal diversity notes 1151–1276: Taxonomic and phylogenetic contributions on genera and species of fungal taxa. Fungal Diversity 100(1): 1–273. https://doi.org/10.1007/s13225-020-00439-5

Katoh K, Rozewicki J, Yamada KD (2017) MAFFT online service: multiple sequence alignment, interactive sequence choice and visualization. Briefings in Bioinformatics 20(4): 1160–1166. https://doi.org/10.1093/bib/bbx108

Kumar S, Stecher G, Tamura K (2016) MEGA7: Molecular evolutionary genetics analysis version 7.0 for bigger datasets. Molecular Biology and Evolution 33(7): 1870–1874. https://doi.org/10.1093/molbev/msw054

Li WJ, McKenzie EHC, Liu JK, Bhat DJ, Dai DQ, Camporesi E, Tian Q, Maharachchikumbura SSN, Luo ZL, Shang QJ (2020) Taxonomy and phylogeny of hyaline-spored coelomycetes. Fungal Diversity 100(1): 279–801. https://doi.org/10.1007/s13225-020-00440-y

Lombard L, van Leeuwen GCM, Guarnaccia V, Polizzi G, van Rijswick PCJ, Rosendahl KCHM, Gabler J, Crous PW (2014) *Diaporthe* species associated with *Vaccinium*, with specific reference to Europe. Phytopathologia Mediterranea 53(2): 287–299.

Ménard L, Brandeis PE, Simoneau P, Poupard P, Sérandat I, Detoc J, Robbes L, Bastide F, Laurent E, Gombert J, Morel E (2014) First report of umbel browning and stem necrosis caused by *Diaporthe angelicae* on carrot in France. Plant Disease 98(3): 421–422. https://doi.org/10.1094/PDIS-06-13-0673-PDN

Miller MA, Pfeiffer W, Schwartz T (2012) The CIPRES science gateway: enabling high-impact science for phylogenetics researchers with limited resources. Proceedings of the 1st Conference of the Extreme Science and Engineering Discovery Environment. Bridging from the extreme to the campus and beyond. Association for Computing Machinery 39: 1–8. https://doi.org/10.1145/2335755.2335836

Murali TS, Suryanarayanan TS, Geeta R (2006) Endophytic *Phomopsis* species: host range and implications for diversity estimates. Canadian Journal of Microbiology 52(7): 673–680. https://doi.org/10.1139/w06-020

Nitschke T (1870) Pyrenomycetes Germanici (2nd ed.). Eduard Trewendt, Germany, Breslau, 161–320.

Nylander JAA (2004) MrModeltest v. 2. Program distributed by the author. Evolutionary Biology Centre, Uppsala University.

Perera RH, Hyde KD, Dissanayake AJ, Jones EBG, Liu JK, Wei D, Liu ZY (2018) *Diaporthe collariana* sp. nov., with prominent collarettes associated with *Magnolia champaca* fruits in Thailand. Studies in Fungi 3(1): 141–151. https://doi.org/10.5943/sif/3/1/16

Rehner SA, Uecker FA (1994) Nuclear ribosomal internal transcribed spacer phylogeny and host diversity in the coelomycete *Phomopsis*. Botany 72(11): 1666–1674. https://doi.org/10.1139/b94-204

Ronquist F, Huelsenbeck JP (2003) MrBayes 3: bayesian phylogenetic inference under mixed models. Bioinformatics 19(12): 1572–1574. https://doi.org/10.1093/bioinformatics/btg180

Ronquist F, Teslenko M, van der Mark P, Ayres DL, Darling A, Höhna S, Larget B, Liu L, Suchard MA, Huelsenbeck JP (2012) MrBayes 3.2: Efficient Bayesian phylogenetic inference and model choice across a large model space. Systematic Biology 61(3): 539–542. https://doi.org/10.1093/sysbio/sys029

Rossman AY, Adams GC, Cannon PF, Castlebury LA, Crous PW, Gryzenhout M, Jaklitsch WM, Mejia LC, Stoykov D, Udayanga D (2015) Recommendations of generic names in

Diaporthales competing for protection or use. IMA Fungus 6(1): 145–154. https://doi.org/10.5598/imafungus.2015.06.01.09

Santos JM, Phillips AJL (2009) Resolving the complex of *Diaporthe* (*Phomopsis*) species occurring on *Foeniculum vulgare* in Portugal. Fungal Diversity 34: 111–125.

Santos JM, Vrandečić K, Ćosić J, Duvnjak T, Phillips AJL (2011) Resolving the *Diaporthe* species occurring on soybean in Croatia. Persoonia 27(1): 9–19. https://doi.org/10.3767/003158511X603719

Santos L, Alves A, Alves R (2017) Evaluating multi-locus phylogenies for species boundaries determination in the genus *Diaporthe*. PeerJ 5: e3120. https://doi.org/10.7717/peerj.3120

Senanayake IC, Crous PW, Groenewald JZ, Maharachchikumbura SSN, Jeewon R, Phillips AJL, Bhat DJ, Perera RH, Li QR, Li WJ (2017) Families of Diaporthales based on morphological and phylogenetic evidence. Studies in Mycology 86: 217–296. https://doi.org/10.1016/j.simyco.2017.07.003

Senanayake IC, Jeewon R, Chomnunti P, Wanasinghe DN, Norphanphoun C, Karunarathna A, Pem D, Perera RH, Camporesi E, McKenzie EHC (2018) Taxonomic circumscription of Diaporthales based on multigene phylogeny and morphology. Fungal Diversity 93(1): 241–443. https://doi.org/10.1007/s13225-018-0410-z

Stamatakis A (2014) RAxML Version 8: A tool for phylogenetic analysis and post-analysis of large phylogenies. Bioinformatics 30(9): 1312–1313. https://doi.org/10.1093/bioinformatics/btu033

Thompson SM, Tan YP, Young AJ, Neate SM, Aitken EAB, Shivas RG (2011) Stem cankers on sunflower (*Helianthus annuus*) in Australia reveal a complex of pathogenic *Diaporthe* (*Phomopsis*) species. Persoonia 27(1): 80–89. https://doi.org/10.3767/003158511X617110

Thompson SM, Tan YP, Shivas RG, Neate SM, Morin L, Bissett A, Aitken EAB (2015) Green and brown bridges between weeds and crops reveal novel *Diaporthe* species in Australia. Persoonia 35(1): 39–49. https://doi.org/10.3767/003158515X687506

Torres C, Camps R, Aguirre R, Besoain XA (2016) First report of *Diaporthe rudis* in Chile causing stem-end rot on hass avocado fruit imported from California, USA. Plant Disease 100(9): 1951–1951. https://doi.org/10.1094/PDIS-12-15-1495-PDN

Udayanga D, Liu X, McKenzie EH, Chukeatirote E, Bahkali AH, Hyde KD (2011) The genus *Phomopsis*: biology, applications, species concepts and names of common phytopathogens. Fungal Diversity 50(1): 189–225. https://doi.org/10.1007/s13225-011-0126-9

Udayanga D, Liu XZ, Crous PW, McKenzie EHC, Chukeatirote E, Hyde KD (2012) A multilocus phylogenetic evaluation of *Diaporthe* (*Phomopsis*). Fungal Diversity 56(1): 157–171. https://doi.org/10.1007/s13225-012-0190-9

Udayanga D, Castlebury LA, Rossman AY, Chukeatirote E, Hyde KD (2015) The *Diaporthe sojae* species complex: Phylogenetic re-assessment of pathogens associated with soybean, cucurbits and other field crops. Fungal Biology 119(5): 383–407. https://doi.org/10.1016/j.funbio.2014.10.009

van Rensburg JCJ, Lamprecht SC, Groenewald JZ, Castlebury LA, Crous PW (2006) Characterization of *Phomopsis* spp. associated with die-back of rooibos (*Aspalathus linearis*) in South Africa. Studies in Mycology 55: 65–74. https://doi.org/10.3114/sim.55.1.65

Vilka L, Volkova J (2015) Morphological diversity of *Phomopsis vaccinii* isolates from cranberry (*Vaccinium macrocarpon* Ait.) in Latvia. Proceedings of the Latvia University of Agriculture 33: 8–18. https://doi.org/10.1515/plua-2015-0002

White T, Bruns T, Lee S, Taylor FJRM, White TJ, Lee SH, Taylor L, Shawe-Taylor J (1990) Amplification and direct sequencing of fungal ribosomal RNA genes for phylogenetics. PCR Protocols: A guide to methods and applications. Academic Press 18: 315–322. https://doi.org/10.1016/B978-0-12-372180-8.50042-1

Yang Q, Du Z, Tian CM (2018) Phylogeny and morphology reveal two new species of *Diaporthe* from Traditional Chinese Medicine in Northeast China. Phytotaxa 336(2): 159–170. https://doi.org/10.11646/phytotaxa.336.2.3

Yang Q, Jiang N, Tian CM (2020) Three new *Diaporthe* species from Shaanxi Province, China. MycoKeys 67: 1–18. https://doi.org/10.3897/mycokeys.67.49483

Zapata M, Palma MA, Aninat MJ, Piontelli E (2020) Polyphasic studies of new species of *Diaporthe* from native forest in Chile, with descriptions of *Diaporthe araucanorum* sp. nov., *Diaporthe foikelawen* sp. nov. and *Diaporthe patagonica* sp. nov. International Journal of Systematic and Evolutionary Microbiology 70(5): 3379–3390. https://doi.org/10.1099/ijsem.0.004183

MycoKeys 77: 97–116 (2021)
doi: 10.3897/mycokeys.77.60084
https://mycokeys.pensoft.net

RESEARCH ARTICLE

A peer-reviewed open-access journal
MycoKeys
Launched to accelerate biodiversity research

Three new species of *Inosperma* (Agaricales, Inocybaceae) from Tropical Africa

Hyppolite L. Aïgnon[1], Sana Jabeen[2], Arooj Naseer[3], Nourou S. Yorou[1], Martin Ryberg[4]

1 *Research Unit Tropical Mycology and Plant-Soil Fungi Interactions, Faculty of Agronomy, University of Parakou, 03 BP 125, Parakou, Benin* **2** *Department of Botany, Division of Science and Technology, University of Education, Lahore, Pakistan* **3** *Department of Botany, University of the Punjab, Quaid-e-Azam Campus-54590, Lahore, Pakistan* **4** *Systematic Biology Programme, Department of Organismal Biology, Uppsala University, Norbyvägen 18D, 752 36, Uppsala, Sweden*

Corresponding author: Hyppolite L. Aïgnon (hyppoliteaignon@yahoo.com)

Academic editor: Zai-Wei Ge | Received 28 October 2020 | Accepted 11 January 2021 | Published 28 January 2021

Citation: Aïgnon HL, Jabeen S, Naseer A, Yorou NS, Ryberg M (2021) Three new species of *Inosperma* (Agaricales, Inocybaceae) from Tropical Africa. MycoKeys 77: 97–116. https://doi.org/10.3897/mycokeys.77.60084

Abstract

Here, we describe three new species of *Inosperma* from Tropical Africa: *Inosperma africanum*, *I. bulbomarginatum* and *I. flavobrunneum*. Morphological and molecular data show that these species have not been described before, hence need to be described as new. The phylogenetic placements of these species were inferred, based on molecular evidence from sequences of 28S and RPB2. Additional analysis using ITS dataset shows interspecific variation between each species. Phylogenetic analyses resolve *I. flavobrunneum* in Old World Tropical clade 1 with weak support, *I. bulbomarginatum* is sister of Old World Tropical clade 1 and *I. africanum* is indicated as sister to the rest of *Inosperma*. Complete description and illustrations, including photographs and line drawings, are presented for each species. A new combination of *Inocybe shawarensis* into *Inosperma* is also proposed.

Keywords

Ectomycorrhizal, molecular systematics, phylogeny, taxonomy, West Africa

Introduction

Inocybaceae Jülich (Basidiomycota, Agaricales) is a family of ectomycorrhizal species, forming symbiotic association with more than 23 families of vascular plants (Matheny et al. 2020). The family is diverse with an estimated 1050 species distributed worldwide (Matheny and Kudzma 2019; Matheny et al. 2020). The number of species described will continue to increase as new habitats are explored (Matheny and Watling 2004; Esteve-Raventós 2014; Latha and Manimohan 2015, 2016; Matheny et al. 2017; Naseer et al. 2018; Jabeen and Khalid 2020).

Recently, Inocybaceae was revised to include seven genera, *Auritella* Matheny & Bougher, *Inocybe* (Fr.) Fr., *Inosperma* (Kühner) Matheny & Esteve-Rav., *Mallocybe* (Kuyper) Matheny, Vizzini & Esteve-Rav., *Nothocybe* Matheny & K.P.D. Latha, *Pseudosperma* Matheny & Esteve-Rav. and *Tubariomyces* Esteve-Rav. & Matheny (Matheny et al. 2020). *Inosperma* is represented by more than 70 known species that are distributed in Africa, Asia, Australasia, Europe, North America and northern South America (Matheny et al. 2020). Typically, the species of the genus are characterised by a radially fibrillose and rimose or squamulose pileus; smooth, ellipsoid or phaseoliform basidiospores; and absence of metuloid hymenial cystidia. In addition, many species of *Inosperma* have odours that are fruity, pleasant, like honey, fishy, pelargonium or otherwise distinct (Matheny et al. 2020). Phylogenetically the genus is monophyletic with four major clades: the Maculata clade (Larsson et al. 2009), *I.* sect. *Inosperma* and two clades from the Old World tropics (Pradeep et al. 2016; Matheny et al. 2020).

In this study, we describe three new species of *Inosperma* from West Africa, based on morphological characters, as well as analysing their phylogenetic position using multigene molecular analysis of 28S and RPB2 sequences data.

Material and methods

Study area and specimen sampling

Specimens were collected in Benin in Okpara Forest (9°15.13'N, 2°43.05'E), N'dali Forest Reserve (09°45.73'N, 2°19.93'E), Toui-Kilibo Forest Reserve (8°32.74'N, 2°40.42'E) and Alibori Superieur Forest Reserve (10°23.76'N, 2°5.15'E). Additionally, specimens were collected in, Burkina Faso in the Forest Reserve of Kou (10°55.86'N,4°51.83'W); Ivory Coast in Gbeke Region (7°40.52'N, 4°54.48'W), Guinea in National Park of Haut Niger (10°30.76'N, 9°57.68'W) and Togo in Central Region (09°20.38'N, 1°14.44'E).

The habitats are woodland dominated by *Isoberlinia doka* Craib & Stapf, *I. tomentosa* (Harms) Craib et Stapf, *Uapaca togoensis* Pax or gallery forest dominated by *Berlinia grandiflora* (Vahl) Hutch. Specimens were preserved by drying on an electric dryer (type Stöckli Dörrex) for 24 hours at 45 °C. All studied materials are deposited at the Mycological Herbarium of Parakou University (UNIPAR).

Morphological analyses

Specimens were photographed in the field with a digital camera Sony FE. Colour codes are described using Kornerup and Wanscher (1978). For anatomical analyses, samples of specimens were rehydrated and examined directly in 3% potassium hydroxide (KOH) and Congo red. Drawings of microscopic characters were made with the aid of a drawing tube attached to a Leica DM2700. Microscopic characters were drawn at magnification 1000×. Spore measurements were made from 40 spores for each species. We measured length (L) and width (W) of the basidiospores and calculated the ratio Q = L / W. Measurements of basidiospores and basidia excluded the apiculus and sterigmata, respectively and are given as (a–)b–c(–d), where (a) = extreme minimum value, range b–c contains minimum of 90% of the calculated values and (d) = extreme maximum value as used in Aïgnon et al. (2021).

Molecular analyses

DNA extraction, PCR and sequencing

Genomic DNA was extracted from dried specimens by QIAGEN® plant mini kit following the manufacturer's instructions and PCR products were cleaned using ExoSAP-IT (Bell 2018). The internal transcribed spacer regions (ITS), portions of the nuclear large subunit ribosomal RNA gene (28S) and DNA-directed RNA polymerase II subunit (RPB2) were amplified. For sequencing of the ITS region, we used the primers ITS1F and ITS4 (White et al. 1990; Gardes and Bruns 1993), for LSU we used LR0R, LR7 and internal primers LR5 and LR3R (Vilgalys and Hester 1990; Cubeta et al. 1991; Rehner and Samuels 1995) and for RPB2, we used primer pairs b6F and b7.1R (Matheny 2005). PCR products were cleaned and sequenced at Macrogen Inc. (Macrogen Europe B.V., Amsterdam, Netherlands) using the same primers as those used for PCR.

Sequence alignments and phylogenetic analyses

Nineteen new sequences were generated (Table 1). Sequences were BLAST searched against NCBI and similar sequences were retrieved from GenBank (Benson et al. 2010). The sequences of ITS, 28S and RPB2 were aligned separately in MAFFT V7.464 (Katoh et al. 2019). Alignment is available online in TreeBase under accession number 27445 (http://purl.org/phylo/treebase/phylows/study/TB2:S27445).

For phylogenetic analysis, the dataset of 28S and RPB2 was generated using Geneious 7.0.2 (Drummond et al. 2010) and partitioned in 28S, RPB2 codon position 1, RPB2 codon position 2, RPB2 codon position 3 and the intron in RPB2 separately (Suppl. material 1). We tested for the best partitioning scheme and best model for each partition using Modelfinder (Kalyaanamoorthy et al. 2017). It was indicated that keeping all the

Table 1. List of species, geographic origin and GenBank accession numbers of ITS, 28S and RPB2 sequences used in the molecular analysis; the new species and new combinations are in bold.

Species	Voucher	Country	ITS	28S	RPB2	References
Auritella brunnescens Matheny & Bougher	PBM3174	Australia	KJ702344	JQ313571	KJ702349	Matheny et al. (2017)
Auritella dolichocystis Matheny, Trappe & Bougher	Trappe 24844	New South Wales		AY380371	AY337371	Matheny (2005)
Auritella fulvella Matheny & Bougher	BRI:AQ669485	Australia	KJ702355	KJ702353	KJ702357	Matheny et al. (2017)
Auritella hispida Matheny & T.W. Henkel	TH1009, TH10379	Cameroon	KT378203	KT378208	KT378215	Matheny et al. (2017)
Auritella serpentinocystis Matheny, Trappe &Bougher ex Matheny & Bougher	PBM3188	Australia	KJ729858	JQ313559	KJ756402	Matheny et al. (2017)
Auritella spiculosa Matheny & T.W. Henkel	MCA7031, TH9866	Cameroon	MF374763	KT378206	KT378214	Matheny et al. (2017)
Inosperma adaequatum (Britzelm.) Matheny & Esteve-Rav.	JV 16501F, JV11290F	Finland	JQ801381	JQ815407	AY333771	Matheny et al. (2020)
***I. africanum* Aïgnon, Yorou & Ryberg**	**MR00387**	**Togo**	**MN096189**	**MN097881**	**MT770739**	**This study**
	HLA0361	**Benin**	**MT534295**	**MT560735**		
	HLA0383	**Benin**	**MT534298**	**MT560733**		
	HLA0353	**Benin**	**MT534299**			
	BRF4157	Benin		MK908843		Unpublished
I. akirnum (K.P.D. Latha & Manimohan) Matheny & Esteve-Rav.	CAL 1358	India		NG_057279	KY553236	Latha and Manimohan (2016)
I. apiosmotum (Grund& D.E. Stuntz) Matheny & Esteve-Rav.	AU10560, TENN:062779	Canada, USA	HQ201336	JN975022	JQ846463	Ryberg and Matheny (2012)
I. bongardii (Weinm.) Matheny & Esteve-Rav.	EL9406	Sweden	FN550943	FN550943		Unpublished
***I. bulbomarginatum* Aïgnon, Yorou & Ryberg**	**MR00357**	**Benin**	**MN096190**	**MN097882**	**MN200775**	**This study**
	HLA0373	**Benin**	**MT534301**			
	HLA0389	**Benin**	**MT534302**			
	HLA0417	**Benin**	**MT534300**	**MT560734**		
	PC96082	Zambia	JQ801412	JN975027		Ryberg and Matheny (2012)
I. calamistratoides (E. Horak) Matheny & Esteve-Rav.	PBM3384	Australia		JQ815415	KJ729949	Latha and Manimohan (2016)
I. calamistratum (Fr.) Matheny & Esteve-Rav.	PBM1105	USA	JQ801386	JQ815409	JQ846466	Pradeep et al. (2016)
I. carnosibulbosum (C.K. Pradeep & Matheny) Matheny & Esteve-Rav.	TBGT:12047	India	KT329448	KT329454	KT32944	Pradeep et al. (2016)
I. cervicolor (Pers.) Matheny & Esteve-Rav.	SJ04024, TURA:4761	Sweden, Finland	AM882939	AM882939	JQ846474	Ryberg et al. (2008)
I. cookei (Bres.) Matheny & Esteve-Rav.	EL70A03	Sweden	AM882953	AM882953		Ryberg et al. (2008)
I. cyanotrichium (Matheny, Bougher& G.M. Gates) Matheny & Esteve-Rav	TENN:065729	Australia		JQ815418	KJ729948	Unpublished
***I. flavobrunneum* Aïgnon, Yorou & Ryberg**	**HLA0367**	**Benin**	**MN096199**	**MT536754**		**This study**
	HLA0372	**Benin**	**MT534290**	**MT536756**		
I. geraniodorum (J. Favre) Matheny & Esteve-Rav.	EL10606	Sweden	FN550945	FN550945		Latha and Manimohan (2016)
I. gregarium (K.P.D. Latha & Manimohan) Matheny & Esteve-Rav.	CAL 1309	India	KX852305	KX852306	KX852307	Latha and Manimohan (2016)
I. lanatodiscum (Kauffman) Matheny & Esteve-Rav.	PBM2451	USA	JQ408759	JQ319688	JQ846483	Latha and Manimohan (2016)
I. maculatum (Boud.) Matheny & Esteve-Rav.	MR00020	Sweden	AM882958	AM882958		Ryberg et al. (2008)
I. maximum (A.H. Sm.) Matheny & Esteve-Rav.	PBM 2222,UBC F33244	USA,Canada	MG953983	EU569854		Matheny et al. (2009)
I. misakaense (Matheny & Watling) Matheny &Esteve-Rav.	96234 (PC)	Zambia	JQ801409	EU569874	EU569873	Pradeep et al. (2016)

Species	Voucher	Country	ITS	28S	RPB2	References
I. mutatum (Peck) Matheny & Esteve-Rav.	PBM4108, PBM2953	USA	MG773837	JQ994476	JQ846488	Matheny et al. (2020)
I. neobrunnescens (Grund & D.E. Stuntz) Matheny &Esteve-Rav.	PBM 2452	USA		EU569868	EU569867	Matheny et al. (2009)
I. quietiodor (Bon) Matheny & Esteve-Rav.	PAM01091310	France	FJ936168	FJ936168		Larsson et al. (2009)
I. rhodiolum (Bres.) Matheny & Esteve-Rav.	PAM00090117	France	FJ904176	FJ904176		Larsson et al. (2009)
I. rimosoides (Peck) Matheny & Esteve-Rav.	PBM 2459, PBM3311	USA	JQ801414	JQ815426	DQ385884	Latha and Manimohan (2016)
I. rubricosum (Matheny & Bougher) Matheny & Esteve-Rav.	PBM3784	Australia		NG_057260	KM406230	Horak et al. (2015)
***I. shawarense* (Naseer & Khalid) Aïgnon & Naseer**	**FLAS-FS9456**	**Pakistan**	**KY616965**	**KY616966**		**Naseer et al. (2018)**
Inosperma sp.	DB166	Democratic Republic of the Congo	KT461385			Bauman et al. (2016)
Inosperma sp.	PC 96013	Zambia	JQ801383	JQ815408	EU600882	Matheny et al. (2009)
Inosperma sp.	BB3233	Zambia	JQ801415	EU600885		Matheny et al.(2009)
Inosperma sp.	G1842	Zambia		MK278245		Unpublished
Inosperma sp.	TR220_06	Papua New Guinea	JQ801416	JN975017	JQ846496	Ryberg and Matheny (2012)
Inosperma sp.	L-GN3a	Papua New Guinea	JX316732			Tedersoo and Põlme (2012)
Inosperma sp.	Zam07	Zambia	FR731653			Tedersoo et al. (2011)
Inosperma sp.	PBM3406	Australia		JQ815431	JQ846498	Unpublished
Inosperma sp.	TJB10045	Thailand	KT600658	KT600659	KT600660	Pradeep et al. (2016)
Inosperma sp.	PC 96073	Zambia	JQ801417	EU600870	EU600869	Matheny et al. (2009)
Inosperma sp.	PC:96080	Zambia	JQ801382			Unpublished
I. vinaceobrunneum (Matheny, Ovrebo & Kudzma) Haelew.	TENN:062709, PBM 2951	USA	FJ601813	NG_067775	JQ846478	Matheny and Kudzma (2019)
I. viridipes (Matheny, Bougher & G.M. Gates) Matheny & Esteve-Rav.	PBM3767	Australia	NR_153168	KP171094	KM656138	Latha and Manimohan (2016)
I. virosum (K.B. Vrinda, C.K. Pradeep, A.V. Joseph & T.K. Abraham ex C.K. Pradeep, K.B. Vrinda& Matheny) Matheny & Esteve-Rav.	TBGT:753	India	KT329452	KT329458	KT329446	Pradeep et al. (2016)
Mallocybe myriadophylla (Vauras & E. Larss.) Matheny & Esteve-Rav.	JV19652F	Finland	DQ221106	AY700196	AY803751	Matheny et al. (2007)
M. subdecurrens (Ellis & Everh.) Matheny & Esteve-Rav.	REH10168	USA	MH024850	MH024886	MH577503	Matheny et al. (2020)
M. terrigena (Fr.) Matheny, Vizzini & Esteve-Rav.	EL11704, JV 16431	Sweden	AM882864	AY380401	AY333309	Matheny and Ammirati (2003); Matheny (2005)
M. tomentosula Matheny & Esteve-Rav.	PBM4138	USA	MG773814	MK421969	MH577506	Matheny et al. (2020)
M. unicolor (Peck) Matheny & Esteve-Rav.	PBM 1481	USA		AY380403	AY337409	Matheny (2005)
Pseudosperma lepidotellum (Matheny & Aime) Matheny & Esteve-Rav.	TENN066442	Guyana	JN642233	NG_042597	MH577508	Matheny et al. (2012)
P. pluviorum (Matheny & Bougher) Matheny & Esteve-Rav.	BRI:AQ794010, PERTH:08556466	Australia		NG_057259	KM406221	Horak et al. (2015)
Pseudosperma sp.	PBM3751	Australia	KP636851	KP171053	KM555145	Pradeep et al. (2016)
Pseudosperma sp.	TR194-02 (M)	Papua New Guinea	JQ408793	JN975032	JQ421080	Ryberg and Matheny (2012)
Tubariomyces inexpectatus (M. Villarreal, Esteve-Rav., Heykoop & E. Horak) Esteve-Rav. & Matheny	AH25500 AH20390	Spain	GU907095	EU569855	GU907088	Matheny et al. (2009), Alvarado et al. (2010)
T. similis Della Magg., Tolaini & Vizzini	RFS0805	Spain	GU907096	GU907092	GU907089	Alvarado et al. (2010)
T. hygrophoroides Esteve-Rav., P.-A. Moreau & C.E. Hermos.	P05112008	France	GU907097	GU907094	GU907090	Pradeep et al. (2016)

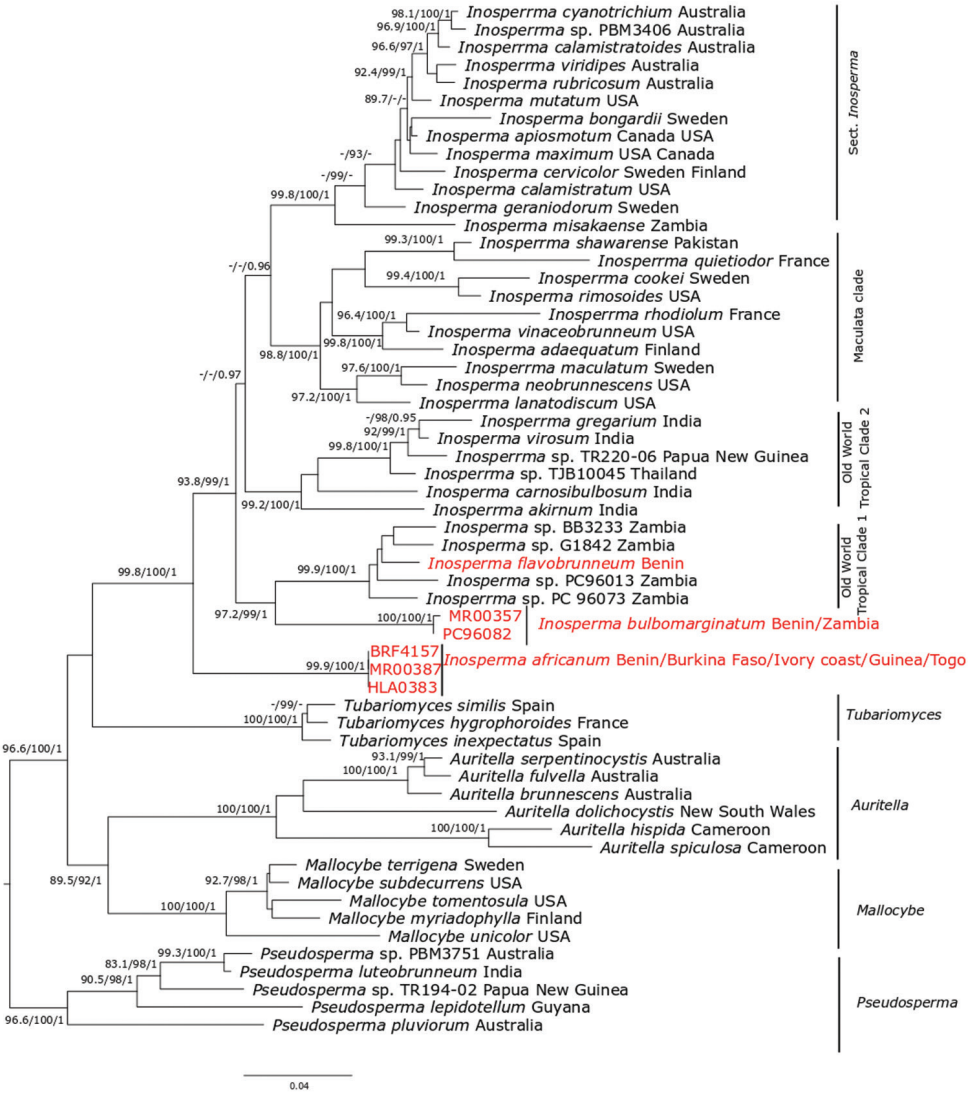

Figure 1. ML tree of 28S and RPB2 sequences showing the placement of *Inosperma africanum*, *I. bulbomarginatum* and *I. flavobrunneum*. Values above or below branches indicate bootstrap proportions SH-aLRT support ≥ 80% / ultrafast bootstrap support ≥ 95% / Bayesian posterior probabilities > 0.95 as shown. Origin of species is given after the name of each taxon. The new species are in red.

partitions was the best way to proceed. Maximum Likelihood (ML) analysis was performed with IQTREE 1.6.12 (Nguyen et al. 2015). Branch support was assessed with 1000 replicates of ultrafast bootstrap replicates and approximate likelihood ratio test [aLRT] and Shimodaira-Hasegawa [SH]-aLRT (SH-Alrt) test with 1000 replicates (Hoang et al. 2017).

For Bayesian Inference (BI) analyses, GTR models with gamma-distributed rate heterogeneity and a proportion of invariant sites parameter were assigned to each

partition as indicated above, using MrBayes 3.2.7 (Ronquist et al. 2012), set as follows: lset applyto = (all), nst = 6, rates = invgamma, ngammacat = 4, sampling frequency = 1000 and the command "unlink" was used to unlink parameters across characters on partitioned datasets. Two independent Markov Chain Monte Carlo (MCMC) processes were executed, each in four chains for 20 million generations. Posterior probabilities (BPP) were calculated after burning the first 25% of the posterior sample and ensuring that this threshold met the convergence factors described above. The sequences from *Pseudosperma lepidotellum* (Matheny & Aime) Matheny & Esteve-Rav., *P. pluviorum* (Matheny & Bougher) Matheny & Esteve-Rav., *Pseudosperma* sp. PBM3751 and *Pseudosperma* sp. TR194-02 were used as outgroup taxa. We also produced trees using ITS database only to show interspecific variation between each species.

Results

Phylogenetic analyses

Inosperma is indicated as monophyletic with full bootstrap support. All three of the species described here, *Inosperma africanum I. bulbomarginatum* and *I. flavobrunneum*, are members of this genus. Phylogenetically, *I. africanum* is indicated as sister to the rest of *Inosperma*, with full support (99.9% SH-aLRT values, 100% ML ultrafast bootstrap, 1 BPP). The Old World Tropical clade 1 is retrieved with strong support (93.8% SH-aLRT values, 99% ML bootstrap, 1 BPP) and *I. bulbomarginatum* is indicated as the sister of Old World Tropical clade 1 with full bootstrap support (100% SH-aLRT values, 100% ML Ultrafast bootstrap, 1 BPP). The sequences of collection PC96082 are very similar to the sequences of *I. bulbomarginata* that we infer to be of the same species. *Inosperma flavobrunneum* is nested in Old World Tropical clade 1 as sister species to three undescribed collections, BB3233, G1842 and PC96013, all from Zambia with weak support.

Taxonomy

1. *Inosperma africanum* Aïgnon, Yorou & Ryberg, sp. nov.
MycoBank No: 836199
Figs 2a, 3

Diagnosis. *Inosperma africanum* is distinct from all species of *Inosperma* and truly outstanding by its vinaceous to red colouration.

Type. *Holotype*. Benin, Collines Region, Kilibo: 8°32.74'N, 2°40.42'E, on soil in Forest Reserve of Toui-Kilibo in Woodland dominated by *Isoberlinia doka* and *I. tomentosa*, 11 August 2017, leg. AIGNON L.H, Voucher (HLA0383) GenBank accession: ITS (MN096193); LSU (MN097885) and RPB2 (MT770739).

Description. Pileus 8.5–15 mm diam., convex to plane, uniform, surface fibrillose, vinaceous to red (8F8), surface rimose, dry. Lamellae moderately close, subven-

Figure 2. Macromorphology of: **A** *Inosperma africanum* (HLA0383) **B** *Inosperma bulbomarginatum* (MR00357) **C, D** *Inosperma flavobrunneum* (HLA0367). Scale bar: 1 cm.

tricose, narrowly attached, 0.5–1 mm deep; vinaceous, sometimes light pinkish (8F8), edges fimbriate, vinaceous (8B8). Stipe 15–23 × 0.5–1 mm, cylindrical, central, fibrillose, swollen, bulbous at the base, veil none with the lower two thirds pinkish-white (8A3) and the upper third light vinaceous (8A5). Odour and taste not distinctive. Basidiospores (6.2) 8–10 (10.3) × (3.8) 4–6.8 (7) µm, avl × avw = 8.3 × 5.3 µm, Q = (1.2) 1.1–2.1 (2.2), avQ = 1.6, smooth, (sub) globose to cylindrical, sometimes ellipsoid. Basidia 18–47 × 7–10 µm, clavate, 3–4 sterigmate, hyaline. Cheilocystidia 22–54 × 8–12 µm, cylindrical to clavate, thin-walled, hyaline. Pleurocystidia absent. Pileipellis a cutis with cylindrical, smooth, thin-walled hyphae, 6–20 µm diam., negative reaction of pileus surface in KOH. Stipitipellis a cutis radially arranged, hyphae 5–13 µm diam., parallel, sometimes septate, filamentous. Caulocystidia 22–63 × 8–13 µm, fusiform sometimes utriform, observed on the upper third of the stipe. Clamp connections present.

Distribution. Currently known from Benin, Burkina Faso, Guinea, Ivory Coast, Togo.

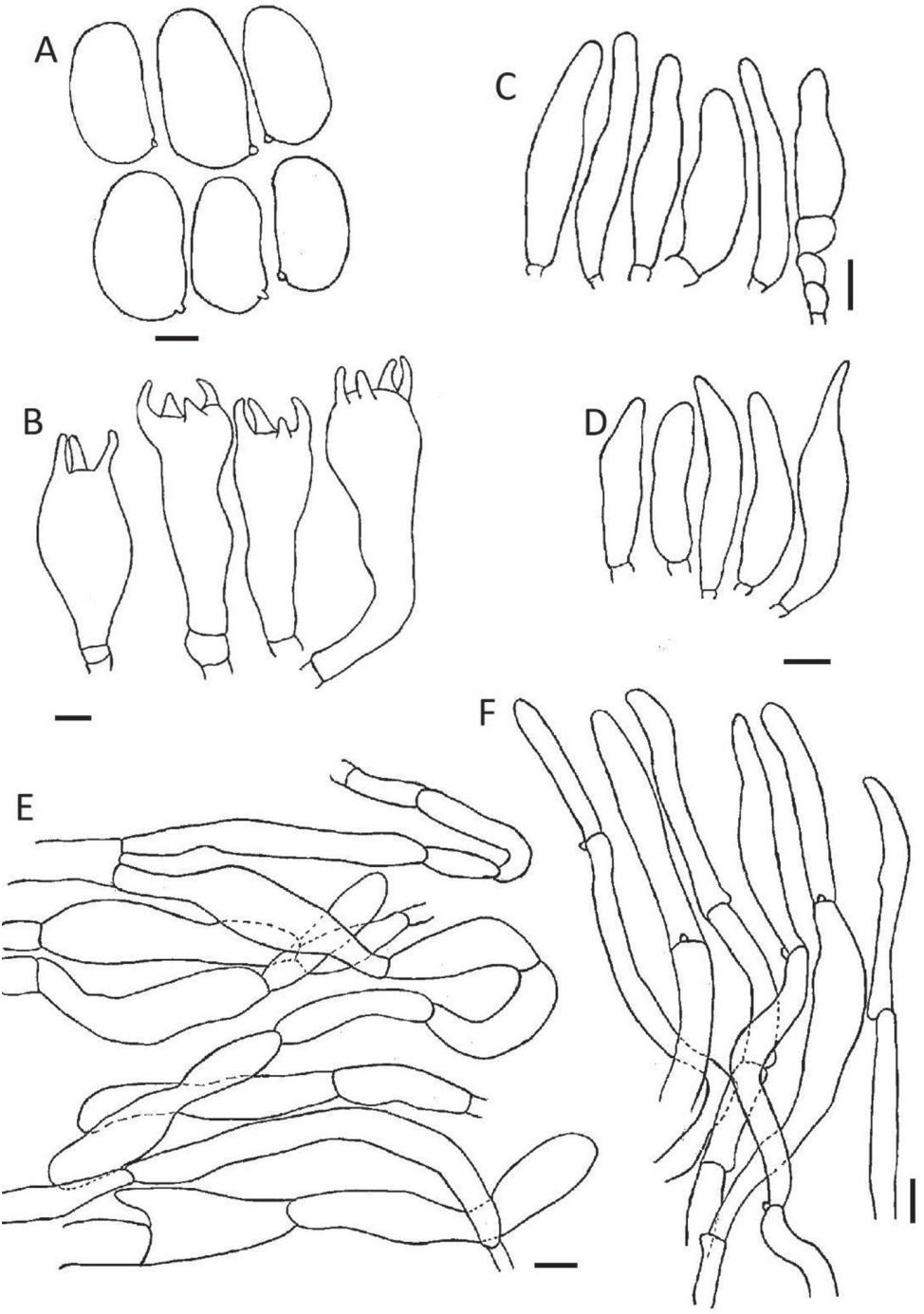

Figure 3. Microscopic structures of *Inosperma africanum* (HLA0383) **A** basidiospores **B** basidia **C** cheilocystidia **D** caulocystidia **E** pileipellis **F** stipitipellis. Scale bars: 3 µm (**A**); 5 µm (**B**); 10 µm (**C–F**).

Ecology. Scattered in Tropical Woodlands dominated by *Isoberlinia doka* and *I. tomentosa* or gallery forests dominated by *Berlinia grandiflora.*

Etymology. *africanum*, referring to the distribution in Africa.

Additional specimens examined. Benin, Borgou Province, N'dali Region: 8°32.74'N, 2°40.42'E, on soil in Woodland dominated by *Isoberlinia doka*, 30 August 2017 in Forest Reserve of N'dali, Leg. Aïgnon HL., Voucher (HLA0461) GenBank accession: ITS (MT534297) and LSU (MT560732). Benin, Borgou Province, Tchaorou Region: 9°15.28'N, 2°43.38'E, on soil in forest of Okpara in woodland dominated by *I. doka*, 7 June 2017, leg. Aïgnon HL., Voucher (HLA0353) GenBank accession: ITS (MT534299). Benin, Borgou Province, N'dali Region: 8°45.73'N, 2°19.93'E, on soil in Woodland dominated by *Isoberlinia doka*, 8 July 2013, leg. Ryberg M., Voucher (MR00361). Benin, Province, Boukoumbe, North Region: 10°14.45'N, 1°7.00'E, on soil in Woodland dominated by *Isoberlinia doka*, 25 July 2020 in Koussoukouangou waterfall, Leg. Aïgnon HL., Voucher (HLA0736). Burkina Faso, Kenedougou Province, Toussiambandougou Region: 10°55.86'N, 4°51.83'W, on soil in gallery forest dominated by *Berlinia grandiflora*, 27 June 2018, leg. Aïgnon HL., Voucher (HLA0353). Ivory Coast, Kekrekouakoukro Province, Bouake, Gbeke Region: 7°40.52'N, 4°54.48'W, on soil in Woodland dominated by *B. grandiflora*, 11 July 2018, leg. Aïgnon HL., Voucher (HLA0562). Guinea, Faranah Province, Upper Guinea Region, National Park of Haut Niger: 10°30.76'N, 9°57.68'W, on soil in Woodland dominated by *B. grandiflora*, 4 July 2018, leg. Aïgnon HL., Voucher (HLA0532). Togo, Central Region, Prefecture of Assoli, on the road between Bafilo and Aledjo: 09°20.38'N, 1°14.44'E in Woodlands dominated by *I. tomentosa*, 7 August 2013, leg. Martin Ryberg, Voucher (MR00387) GenBank accession: ITS (MN096189); LSU (MN097881), RPB2 (MT770739).

Notes. *Inosperma africanum* is nested in *Inosperma* and indicated as sister to the rest of the genus in our phylogenetic analyses and is very distinct by its small size and a vinaceous to red pileus. It has a wide distribution in West Africa.

2. *Inosperma bulbomarginatum* Aïgnon, Yorou & Ryberg, sp. nov.

MycoBank No: 836198

Figs 2b, 4

Diagnosis. *Inosperma bulbomarginatum* differs from *I. flavobrunneum* by the smaller size of its basidiomata and larger basidiospores. It is phylogenetically distinct from all other undescribed African *Inosperma* in Old World Tropical clade 2

Type. *Holotype*. Benin, Borgou Province, N'dali Region: 09°45.73'N, 2°19.93'E, on soil in Woodland dominated by *Isoberlinia doka* and *I. tomentosa*, 8 July 2013, leg. Martin Ryberg, Voucher (MR00357), GenBank accession: ITS (MN096190); LSU (MN097882) and RPB2 (MN200775).

Description. Pileus 13–18 mm diam., undulating plane, fibrillose, margin rimose, orange-brown to somewhat cinnamon, greyish-white (8E5), splitting at edge. Lamellae

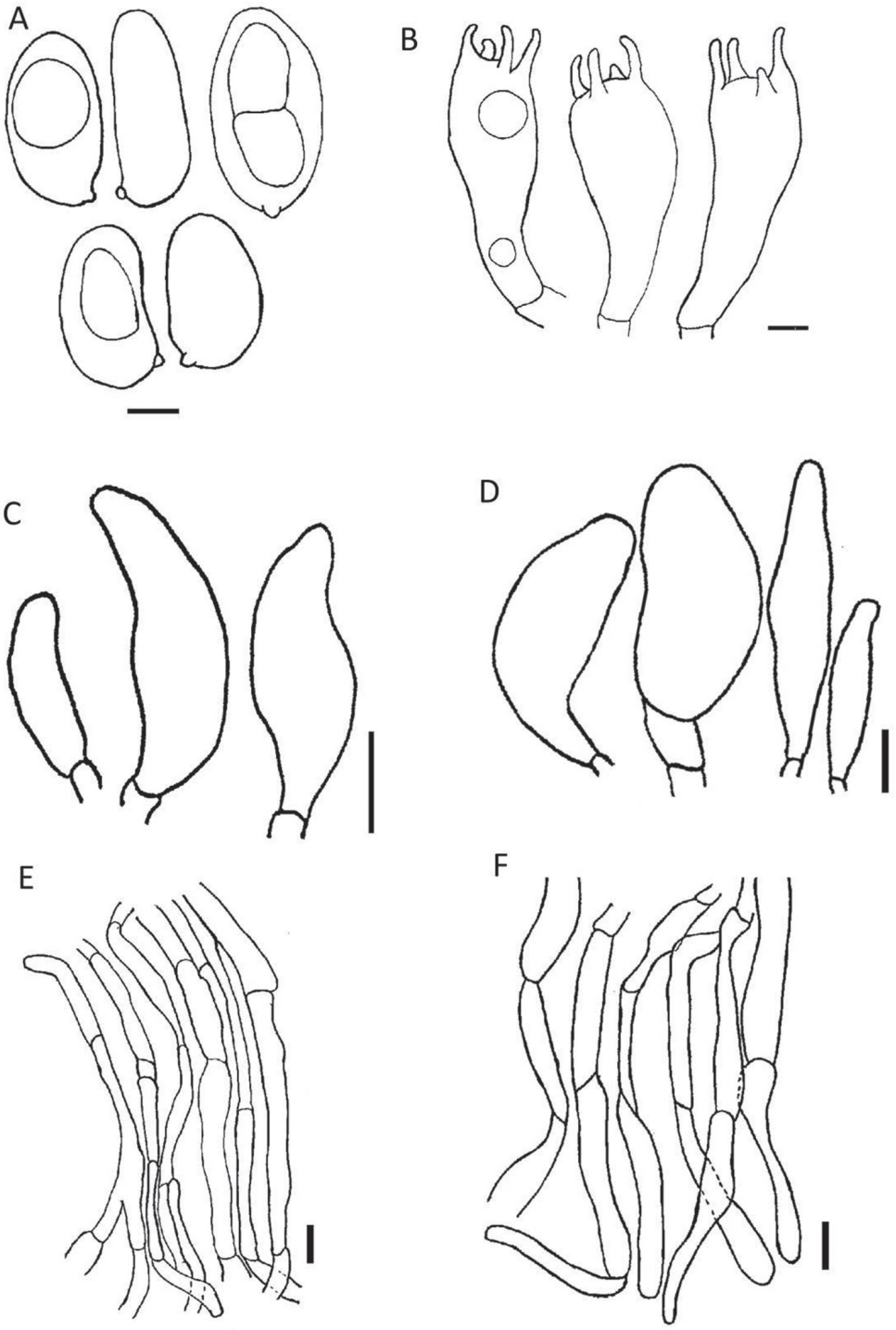

Figure 4. Microscopic structures of *Inosperma bulbomarginatum* (MR00357) **A** basidiospores **B** basidia **C** cheilocystidia **D** caulocystidia **E** pileipellis **F** stipitipellis. Scale bars: 3 µm (**A**); 5 µm (**B**); 10 µm (**C–F**).

2–2.5 mm deep, moderately close, narrowly attached, pale grey brown (9B5) to dark brown (9D5), sinuate. Stipe 10–22 × 2–2.5 mm, central, equal, marginate bulb, white to pinkish-buff (7A2), velar remnants. Odour and taste not distinctive. Basidiospores (7.1) 8–12.1 (14) × (4) 4.2–6.7(7) µm, avl × avw = 9.6 × 5.4 µm, Q = (1.3) 1.2–2.3(2.6), avQ = 1.8, smooth, elongate, thick-walled. Basidia (25) 28–40 × 6–12 µm, tetrasporic. Cheilocystidia 20–25 × 10–12 µm, clavate, thin-walled hyaline. Pleurocystidia absent. Pileipellis a cutis, thin-walled hyphae, 3–12 µm diam., cylindrical. Stipitipellis a cutis with subparallel hyphae 3–15 µm diam., septate, filamentous, subhymenium of compact hyphae, any reaction of pileus surface in KOH not observed. Caulocystidia 25–60 × 7–20 µm, ovoid to obovoid, sometimes utriform, observed on the upper third of the stipe.

Distribution. Currently known from Benin and Zambia.

Ecology. Scattered in Woodland dominated by *Isoberlinia doka* and *I. tomentosa*.

Etymology. *bulbomarginatum* referring to the presence of a marginate bulb at the base of the stipe.

Additional specimens examined. Benin, Collines Province, Kilibo Region: 8°32.74'N, 2°40.42'E, on soil in Woodland dominated by *Isoberlinia doka*, 22 June 2017 in the Forest Reserve of Toui-Kilibo, leg. Aïgnon HL., Voucher (HLA0389) GenBank accession: ITS (MT534302). Benin, Tchaorou, Borgou Prov, Okpara Forest: 9°15.28'N, 2°43.38'E, on soil in Woodland dominated by *Isoberlinia doka*, 13 June 2017, leg. Aïgnon HL., Voucher (HLA0373) GenBank accession: ITS (MT534301). Benin, Alibori Borgou Prov, Alibori Superieur Forest Reserve: 10°23.76'N, 2°5.15'E on soil in Woodland dominated by *Isoberlinia doka*, 11 July 2017, in Forest Reserve of Alibori Supérieur leg. Aïgnon HL., Voucher (HLA0417), GenBank accession: ITS (MT534300) and LSU (MT560734).

Notes. *Inosperma bulbomarginatum* is similar to *Inosperma cervicolor* (Pers.) Matheny & Esteve-Rav., by its orange-brown pileus, but differs from it by the smaller size of the basidiomata and basidiospores, as well as its ecological association with Fabaceae Lindley and/or Phyllanthaceae Martynov and extensive distribution in Tropical Africa. *I. cervicolor* is associated with Pinaceae Spreng. ex F. Rudolphi and distributed in Europe and North America.

3. *Inosperma flavobrunneum* Aïgnon, Yorou & Ryberg, sp. nov.

MycoBank No: 836197
Figs 2c, d, 5

Diagnosis. Characterised by yellow to orange-brown pileus, 7–12 × 4–7 µm smooth, thick-walled, ellipsoid basidiospores with cheilocystidia measuring 23–41 × 7–10 µm, clavate, thin-walled.

Type. *Holotype*. Benin, Borgou Province, Tchaorou, Okpara Forest: 9°15.13'N, 2°43.05'E on soil in Woodland dominated by *Isoberlinia doka* 12 June 2017, leg. AIGNON L.H, Voucher (HLA0367), GenBank accession: ITS (MN096199); LSU (MT536754).

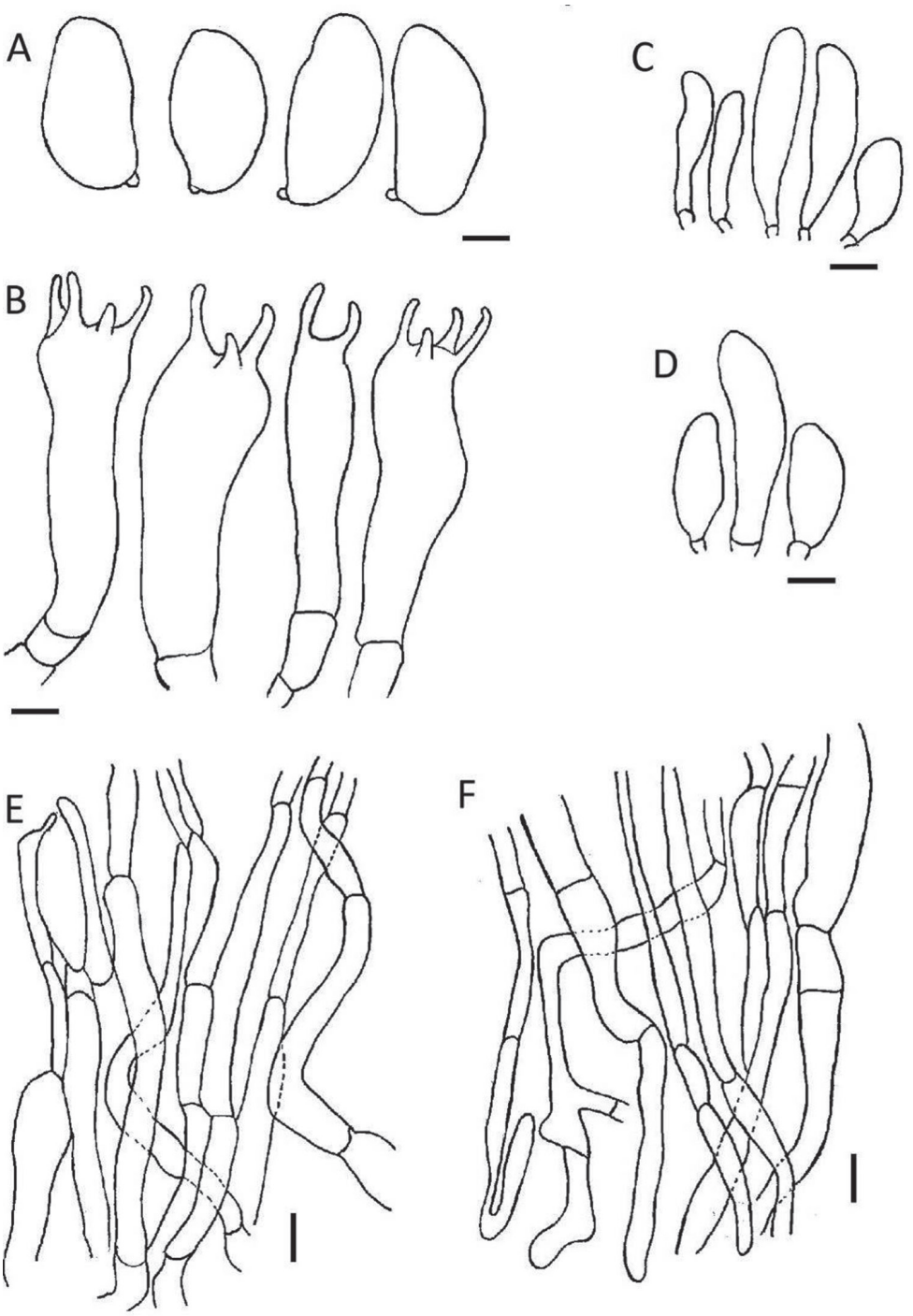

Figure 5. Microscopic structures of *Inosperma flavobrunneum* (HLA0367) **A** basidiospores **B** basidia **C** cheilocystidia **D** caulocystidia **E** pileipellis and **F** stipitipellis. Scale bars: 3 μm(**A**); 4 μm (**B**); 10 μm (**C–F**).

Description. Pileus 28–38 mm diam., umbonate, yellow (5A3) to orange brown (5C5), dark brown in middle, convex when young, plane at maturity, hard, surface rimose, dry. Lamellae emarginated, adnexed and decurrent, yellow brown (5B5). Stipe 27–39 × 5–6 mm, central, cylindrical, uniform; white, equal, solid, hard, base slightly swollen to bulbous, pruinose at the apex. Basidiospores (7.1) 9.2–11.2 (12) × (4.1) 5.7–7 (7.2) µm, avl × avw = 9.2 × 5.7 µm, Q = (1.2) 1.6–2.1 (2.5), avQ = 1.6, smooth, ellipsoid. Basidia 24–40 × 6–14 µm, clavate, 2–4 spored. Cheilocystidia 23–41 × 7–10 µm, clavate, thin walled. Pleurocystidia absent. Pileipellis a cutis thin-walled hyphae 4–16 µm diam., subparallel, compact hyphae, negative reaction of pileus surface in KOH. Stipitipellis a cutis hyphae 5–10 µm diam., septate, filamentous, thick, subparallel, compact. Caulocystidia 23–52 × 9–10 µm, utriform, rare, observed on the upper third of the stipe.

Distribution. Currently known only from Benin in Soudano-Guinean zone.

Ecology. Gregarious under Woodland dominated by *Isoberlinia doka*, *I. tomentosa and Monotes kerstingii* Gilg.

Etymology. *flavobrunneum* referring to yellow to dark brown pileus.

Additional specimens examined. Benin, Tchaorou, Borgou Province, Okpara Forest: 9°15.27'N, 2°43.40'E on soil in Woodland dominated by *Isoberlinia doka*, *I. tomentosa* 13 June 2017, leg. AIGNON L.H, HLA0372, GenBank accession: ITS (MT534290); LSU (MT536756).

Notes. In the phylogenetic tree (Figure 1), *Inosperma flavobrunneum* is a sister of *Inosperma* sp. PC96013, an undescribed species from Zambia in Miombo woodland. Morphologically, *I. flavobrunneum* is similar to *I. lanatodiscum* by its yellow to orange-brown pileus, but differs from it by the smaller size of the basidiomata, larger basidiospores, ecological association with Fabaceae / Dipterocarpaceae Blume and distribution in West Africa. *I. lanatodiscum* is associated with a variety of hardwoods and conifers and is widely distributed from Europe to North and Central America (Kropp et al. 2013). The other related taxa are all African taxa not yet described, such as *Inosperma* sp. BB3233 from Zambia and the Democratic Republic of Congo, as well as *Inosperma* sp. G1842 distributed in south-eastern Africa, while *I. flavobrunneum* is distributed in West Africa.

Taxonomic key to species of *Inosperma* from West Africa

1 Basidiomata large, pileus 28–38 mm diam., yellow to orange-brown, surface clearly rimose, lamellae adnexed and decurrent, subdistant ..... ***Inosperma flavobrunneum***

– Basidiomata small, pileus 8.5–15 mm diam., fibrillose, lamellae close..... **2**

2 Pileus vinaceous to red, basidiospores 8–10 × 4–7, (sub) globose to cylindrical, sometimes ellipsoid..... ***I. africanum***

– Pileus orange-brown to somewhat cinnamon, greyish-white, basidiospores 8–14 × 4–7 µm, elongate..... ***I. bulbomarginatum***

New combination

For an evolutionarily-consistent taxonomy, we propose the following combination:

Inosperma shawarense **(Naseer & Khalid) Aïgnon & Naseer, comb. nov.**
MycoBank No: 836296

Inocybe shawarensis Naseer & Khalid, Mycotaxon 132: 912. 2018. Basionym.

Notes. This species is placed in the old *Inosperma* clade which became the genus *Inosperma*, but the combination is not made in the study of Matheny et al. (2020). The new combination is based on molecular phylogenetic data and sequencing the type of *Inocybe shawarensis* (Naseer et al. 2018).

Discussion

The new species exhibit the overall characteristics often observed in *Inosperma*. These characters include; pileus radially rimose, fibrillose or squamulose and absence of pleurocystidia (Matheny et al. 2020). They can be distinguished from other *Inosperma* species by their remarkable characteristics. In addition, *I. africanum* is common in West Africa and *I. bulbomarginatum* presents a large distribution and was recognised in Zambia in the collections of Bart Buyck (Matheny et al. 2009). However, the low sequence divergences between the sequences (2.2%–2.5%) of ITS and 0.3% of 28S allows us to confirm the wide distribution of *I. bulbomarginatum.*

Phylogenetically, *I. africanum* is nested in *Inosperma* with full support (99% SH-aLRT values, 100% ML Ultrafast bootstrap, 1 BPP) and *I. bulbomarginatum* is indicated as the sister of Old World Tropical clade 1 with full support (100% SH-aLRT values, 100% ML bootstrap, 1 BPP). Sequences of *Inosperma bulbomarginatum* from West Africa and Zambia formed a subclade. *Inosperma flavobrunneum* is nested in Old World Tropical clade 1 and has sister species undescribed in a collection from Zambia, BB3233, G1842 and PC96013. ML and BI analysis, using 28S and RPB2 sequences data, shows most nodes well resolved; for example, the node uniting Old World Tropical clade 2 with the crown group of *Inosperma* is supported with 0.97 BPP, but with weak ML bootstrap as shown in Pradeep et al. (2016); based also on combined data of 28S and RPB2, this node is with weaker support < 50% ML bootstrap.

The position of each of these new species is confirmed by single data from ITS (Fig. 6). There are several collections from undescribed species in *Inosperma* (e.g. *Inosperma* sp. G1842, *Inosperma* sp. BB3233, *Inosperma* sp. PC 96073, *Inosperma* sp. PC96013, *Inosperma* sp. PC96082, *Inosperma* sp. PC96080 and *Inosperma* sp. Zam07) that are of African origin, thereby attesting the need for further studies of this genus on this continent. Previously, in *Inosperma*, only one species, *Inosperma*

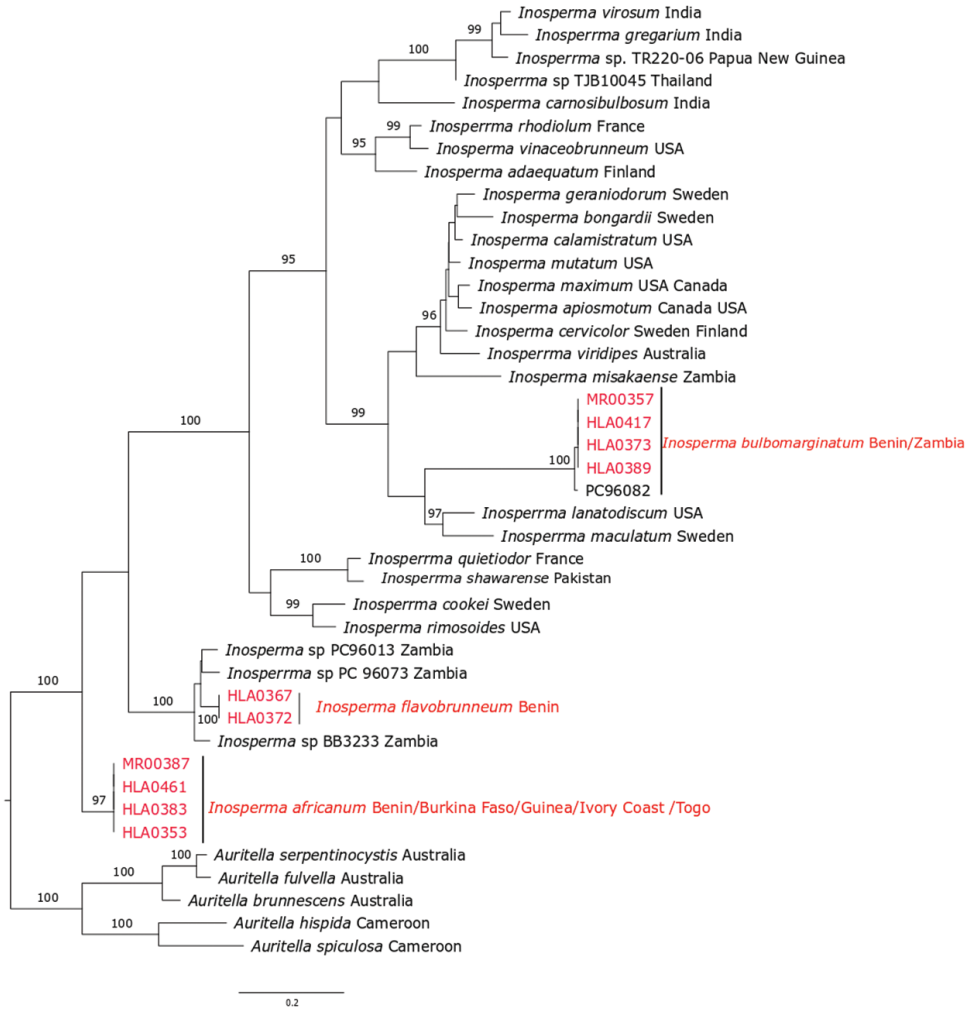

Figure 6. ML phylogeny of *Inosperma africanum*, *I. bulbomarginatum* and *I. flavobrunneum* based on ITS dataset.

misakaense, has been described from Africa before this study (Matheny and Watling 2004). So, this study reinforces the diversity of *Inosperma* in Tropical Africa which now amounts to four described species.

Acknowledgements

We are grateful to the Rufford Small Grants Foundation (grant n° 30738-2) which allowed us to collect some additional samples analysed in this paper, the Swedish Research Council for Environment, Agricultural Sciences and Spatial Planning (grant

n° 226-2014-1109) for funding molecular analysis and the Deutscher Akademischer Austauschdienst (DAAD, grant n° PKZ 300499) for granting the University of Parakou with a microscope, type Leica DM5700, that enabled us to perform microscopic investigations. Anneli SVANHOLM, Bobby SULISTYO and Brandan FURNEAUX (Systematic Biology programme, Department of Organismal Biology, Uppsala University) are thanked for their assistance during molecular analyses. We also thank Kassim TCHAN ISSIFFOU and Evans CODJIA (MyTIPS Research Unit, University of Parakou) for their assistance during field data collection. P. Brandon MATHENY (Department of Ecology and Evolutionary Biology, University of Tennessee, USA) and an anonymous reviewer are thanked for their corrections and suggestions to improve our paper.

References

Aïgnon HL, Naseer A, Matheny PB, Yorou NS, Ryberg M (2021) *Mallocybe africana* (Inocybaceae, Fungi) the first species of *Mallocybe* described from Africa. Phytotaxa 478(1): 049–060. https://doi.org/10.11646/phytotaxa.478.1.3

Alvarado P, Manjón JL, Matheny PB, Esteve-Raventós F (2010) *Tubariomyces*, a new genus of Inocybaceae from the Mediterranean region. Mycologia 102: 1389–1397. https://doi.org/10.3852/10-041

Bauman D, Raspé O, Meerts P, Degreef J, Ilunga Muledi J, Drouet T (2016) Multiscale assemblage of an ectomycorrhizal fungal community: the influence of host functional traits and soil properties in a 10-ha miombo forest. FEMS Microbiology Ecology 92(10): fiw151. https://doi.org/10.1093/femsec/fiw151

Bell JR (2018) A simple way to treat PCR products prior to sequencing using ExoSAP-IT. BioTechniques 44(6): 834–834. https://doi.org/10.2144/000112890

Benson DA, Karsch-Mizrachi I, Lipman DJ, Ostell J, Sayers EW (2010) GenBank. Nucleic Acids Research 38: 46–51. https://doi.org/10.1093/nar/gkp1024

Cubeta M, Echandi E, Albernethy T (1991) Characterization of anastomosis groups of binucleate Rhizoctonia species using restriction analysis of an amplified ribosomal RNA gene. Phytopathology 81: 1395–1400. https://doi.org/10.1094/Phyto-81-1395

Drummond AJ, Ashton B, Buxton S, Cheung M, Cooper A, Duran C, Field M, Heled J, Kearse M, Markowitz S, Moir R, Stones-Havas S, Sturrock S, Baroni T, Wilson T (2010) Geneious v5.3. http://www.geneious.com/

Esteve-Raventós F (2014) *Inocybe aureocitrina* (Inocybaceae), a new species of section Rimosae from Mediterranean evergreen oak forests. Plant Biosystems 148: 377–383. https://doi.org/10.1080/11263504.2013.877532

Gardes M, Bruns T (1993) ITS primers with enhanced specificity for basidiomycetes – application to the identification of mycorrhizae and rusts. Molecular Ecology 2(2): 113–118. https://doi.org/10.1111/j.1365-294X.1993.tb00005.x

Hoang DT, Chernomor O, von Haeseler A, Minh BQ, Vinh LS (2017) UFBoot2: Improving the Ultrafast Bootstrap Approximation. Molecular Biology and Evolution 35: 518–522. https://doi.org/10.1093/molbev/msx281

Horak E, Matheny PB, Desjardin DE, Soytong K (2015) The genus *Inocybe* (Inocybaceae, Agaricales, Basidiomycota) in Thailand and Malaysia. Phytotaxa 230: 201–238. https://doi.org/10.11646/phytotaxa.230.3.1

Jabeen S, Khalid AN (2020) *Pseudosperma flavorimosum* sp. nov. from Pakistan. Mycotaxon 135: 183–193. https://doi.org/10.5248/135.183

Kalyaanamoorthy S, Minh BQ, Wong TKF, von Haeseler A, Jermiin LS (2017) ModelFinder: fast model selection for accurate phylogenetic estimates. Nature Methods 14: 587–589. https://doi.org/10.1038/nmeth.4285

Katoh K, Rozewicki J, Yamada KD (2019) MAFFT online service: multiple sequence alignment, interactive sequence choice and visualization. Briefings in Bioinformatics 20: 1160–1166.

Kornerup A, Wanscher JH (1978) Methuen Handbook of Colour. 3d ed. E. Methuen, London, 252 pp. https://doi.org/10.3852/12-185

Kropp BR, Matheny PB, Hutchison LJ (2013) *Inocybe* section *Rimosae* in Utah: phylogenetic affinities and new species. Mycologia 105: 728–747.

Larsson E, Ryberg M, Moreau PA, Mathiesen ÅD, Jacobsson S (2009) Taxonomy and evolutionary relationships within species of section Rimosae (*Inocybe*) based on ITS, LSU and mtSSU sequence data. Persoonia: Molecular Phylogeny and Evolution of Fungi 23: 86–98. https://doi.org/10.3767/003158509X475913

Latha KP, Manimohan P (2015) Inocybe griseorubida, a new species of *Pseudosperma* clade from Tropical India. Phytotaxa 221: 166–174. https://doi.org/10.11646/phytotaxa.221.2.6

Latha KPD, Manimohan P (2016) Inocybe gregaria, a new species of the *Inosperma* clade from Tropical India. Phytotaxa 286(2): 107–115. https://doi.org/10.11646/phytotaxa.286.2.5

Matheny P, Ammirati J (2003) *Inocybe angustispora*, *I. taedophila*, and *Cortinarius aureifolius*: an unusual inocyboid Cortinarius. Mycotaxon 88: 401–407.

Matheny P, Watling R (2004) A new and unusual species of *Inocybe* (*Inosperma* clade) from Tropical Africa. Mycotaxon 89: 497–503.

Matheny PB (2005) Improving phylogenetic inference of mushrooms with RPB1 and RPB2 nucleotide sequences (*Inocybe*; *Agaricales*). Molecular Phylogenetics and Evolution 35(1): 1–20. https://doi.org/10.1016/j.ympev.2004.11.014

Matheny PB, Kudzma LV (2019) New species of *Inocybe* (Inocybaceae) from eastern North America. The Journal of the Torrey Botanical Society 146(3): 213–235. https://doi.org/10.3159/TORREY-D-18-00060.1

Matheny PB, Hobbs AM, Esteve-Raventós F (2020) Genera of Inocybaceae: New skin for the old ceremony. Mycologia 112: 83–120. https://doi.org/10.1080/00275514.2019.1668906

Matheny PB, Aime M, Smith ME, Henkel TW (2012) New species and reports of Inocybe (Agaricales) from Guyana. Kurtziana 37(1): 23–39.

Matheny PB, Henkel TW, Séné O, Korotkin HB, Dentinger BTM, Aime MC (2017) New species of *Auritella* (*Inocybaceae*) from Cameroon, with a worldwide key to the known species. IMA Fungus 8: 287–298. https://doi.org/10.5598/imafungus.2017.08.02.06

Matheny PB, Wang Z, Binder M, Curtis JM, Lim YW, Henrik Nilsson R, Hughes KW, Hofstetter V, Ammirati JF, Schoch CL (2007) Contributions of rpb2 and tef1 to the phylogeny of mushrooms and allies (Basidiomycota, Fungi). Molecular Phylogenetics and Evolution 43: 430–451. https://doi.org/10.1016/j.ympev.2006.08.024

Matheny PB, Aime MC, Bougher NL, Buyck B, Desjardin DE, Horak E, Kropp BR, Lodge DJ, Soytong K, Trappe JM, Hibbett DS (2009) Out of the Palaeotropics? Historical biogeography and diversification of the cosmopolitan ectomycorrhizal mushroom family Inocybaceae. Journal of Biogeography 36: 577–592. https://doi.org/10.1111/j.1365-2699.2008.02055.x

Naseer A, Khalid AN, Smith ME (2018) *Inocybe shawarensis* sp. nov. in the *Inosperma* clade from Pakistan. Mycotaxon 132: 909–918. https://doi.org/10.5248/132.909

Nguyen L-T, Schmidt HA, von Haeseler A, Minh BQ (2015) IQ-TREE: A fast and effective stochastic algorithm for estimating maximum-likelihood phylogenies. Molecular Biology and Evolution 32: 268–274. https://doi.org/10.1093/molbev/msu300

Pradeep CK, Vrinda KB, Varghese SP, Korotkin HB, Matheny PB (2016) New and noteworthy species of *Inocybe* (Agaricales) from Tropical India. Mycological Progress 15: 1–25. https://doi.org/10.1007/s11557-016-1174-z

Rehner S, Samuels G (1995) Molecular Systematics of the Hypocreales: a teleomorph gene phylogeny and the status of their anamorph. Canadian Journal of Botany 73(Suppl 1): 816–823. https://doi.org/10.1139/b95-327

Ronquist F, Teslenko M, Van Der Mark P, Ayres DL, Darling A, Höhna S, Larget B, Liu L, Suchard MA, Huelsenbeck JP (2012) Mrbayes 3.2: efficient Bayesian phylogenetic inference and model choice across a large model space. Systematic Biology 61: 539–542. https://doi.org/10.1093/sysbio/sys029

Ryberg M, Matheny PB (2012) Asynchronous origins of ectomycorrhizal clades of Agaricales. Proceedings of the Royal Society B – Biological Sciences 279: 2003–2011. https://doi.org/10.1098/rspb.2011.2428

Ryberg M, Nilsson RH, Kristiansson E, Töpel M, Jacobsson S, Larsson E (2008) Mining metadata from unidentified ITS sequences in GenBank: A case study in *Inocybe* (Basidiomycota). BMC Evolutionary Biology 8: 1–14. https://doi.org/10.1186/1471-2148-8-50

Tedersoo L, Põlme S (2012) Infrageneric variation in partner specificity: multiple ectomycorrhizal symbionts associate with Gnetum gnemon (Gnetophyta) in Papua New Guinea. Mycorrhiza 22: 663–668. https://doi.org/10.1007/s00572-012-0458-7

Tedersoo L, Bahram M, Jairus T, Bechem E, Chinoya S, Mpumba R, Leal M, Randrianjohany E, Razafimandimbison S, Sadam A, Naadel T, Koljalg U (2011) Spatial structure and the effects of host and soil environments on communities of ectomycorrhizal fungi in wooded savannas and rainforests of Continental Africa and Madagascar. Molecular Ecology 20(14): 3071–3080. https://doi.org/10.1111/j.1365-294X.2011.05145.x

Vilgalys R, Hester M (1990) Rapid genetic identification and mapping of enzymatically amplified ribosomal DNA from several Cryptococcus species. Journal of Bacteriology 172: 4238–4246. https://doi.org/10.1128/JB.172.8.4238-4246.1990

White TJ, Bruns T, Lee S, Taylor J (1990) Amplification and direct sequencing of fungal ribosomal RNA genes for phylogenetics. In: Innis MA, Gelfand DH, Sninsky JJ, White TJ (Eds) PCR protocols: a guide to methods and applications. Academic Press, New York, 315–322. https://doi.org/10.1016/B978-0-12-372180-8.50042-1

Supplementary material 1

Partition for phylogeny analysis

Authors: Hyppolite L. Aïgnon, Sana Jabeen, Arooj Naseer, Nourou S. Yorou, Martin Ryberg

Data type: phylogeny data

Link: https://doi.org/10.3897/mycokeys.77.60084.suppl1

MycoKeys 77: 117–141 (2021)
doi: 10.3897/mycokeys.77.57394
https://mycokeys.pensoft.net

RESEARCH ARTICLE

A peer-reviewed open-access journal
MycoKeys
Launched to accelerate biodiversity research

Hebeloma in the Malay Peninsula: Masquerading within *Psathyrella*

Ursula Eberhardt[1], Nicole Schütz[1], Henry J. Beker[2,3,4], Su See Lee[5], Egon Horak[6]

1 *Staatliches Museum für Naturkunde Stuttgart, Rosenstein 1, 70191, Stuttgart, Germany* **2** *Rue Père de Deken 19, B-1040, Bruxelles, Belgium* **3** *Royal Holloway College, University of London, Egham, UK* **4** *Plantentuin Meise, Nieuwelaan 38, B-1860, Meise, Belgium* **5** *Forest Health and Conservation Programme, Biodiversity Division, Forest Research Institute, Kepong, Malaysia* **6** *Schlossfeld 17, A-6020, Innsbruck, Austria*

Corresponding author: Ursula Eberhardt (ursula.eberhardt@smns-bw.de)

Academic editor: M.P. Martín | Received 8 August 2020 | Accepted 7 January 2021 | Published 28 January 2021

Citation: Eberhardt U, Schütz N, Beker HJ, Lee SS, Horak E (2021) *Hebeloma* in the Malay Peninsula: Masquerading within *Psathyrella*. MycoKeys 77: 117–141. https://doi.org/10.3897/mycokeys.77.57394

Abstract

In 1994 Corner published five new species within the genus *Psathyrella*, all having been collected on the Malay Peninsula between 1929 and 1930. Three of these species belong to the genus *Hebeloma* and with their vinaceous colored lamellae and spore print, when fresh, they belong to *H.* sect. *Porphyrospora*. Of these three species, only one, *P. flavidifolia*, was validly published and thus we herewith recombine it as *H. flavidifolium*. The other two species, *P. splendens* and *P. verrucispora*, are synonyms of *H. parvisporum* and *H. lactariolens*, respectively. We also describe a new Malayan species, *H. radicans*, which also belongs to *H.* sect. *Porphyrospora.* These findings confirm the western Pacific Rim as a diversity hotspot for *H.* sect. *Porphyrospora*. The records described within this paper, represent the first recognition that the genus *Hebeloma*, and indeed that members of the ectomycorrhizal Hymenogastraceae, are present on the Malay Peninsula.

Keywords

Anamika, Agaricales, Dipterocarpaceae, ectomycorrhiza, Fagaceae, taxonomy, tropical forests

Introduction

Only a small number of *Hebeloma* species have been described from Asia, most recently *H. parvisporum* from Laos (Eberhardt et al. 2020). In the same paper, *H.* sect. *Porphyrospora* was proposed to include species originally described in *Anamika*. This

decision was based on morphological and molecular data. The most distinctive features of the section are the predominantly dry cap surface and a spore deposit that is vinaceous red when fresh, but changes to brown without any reddish hue within one year in the herbarium. This color of the fresh spores, and as a result of the spore deposit, also normally causes the fresh mature lamellae to exhibit at least tinges of vinaceous red. This spore deposit color, and the subsequent color change when dried, appears to be restricted to this one section within *Hebeloma*.

The geographical distribution of species within *H.* sect. *Porphyrospora* is remarkable. The majority of the species occur in the western Pacific Rim region, with the exception of two species, *H. porphyrosporum*, to date only known from Europe, and *H. sarcophyllum*, to date only recorded from eastern North America (Beker et al. 2016; Eberhardt et al. 2020).

During the course of this research, and our efforts to find relevant information about *Hebeloma* recorded from the Malay Peninsula, we came across a paper by E.J.H. Corner (1993), effectively published 1994 (Corner 1994 ["1993"]), where he described five new *Psathyrella* species from the Malay Peninsula. These taxa have ornamented spores, and Corner followed Pegler and Young (1992), who also included a few species with ornamented spores in *Psathyrella.* Furthermore, *P. splendens* has a membranous persisting veil forming a conspicuous annulus, a feature excluding its position in the current circumscription of genus *Psathyrella* (Örstadius et al. 2015). This and two other of the new species, according to Corner (1994 ["1993"]), do not fit well within the genus. On the one hand, their robust stature might suggest they should be placed in *Lacrymaria* Pat. (which Voto (2019) did for all five of the Corner (1994 ["1993"]) taxa), but while the spores of *Lacrymaria* are black or certainly very dark in mass, at least the three collections with ornamented spores have fuscous purple or vinaceous brown spores. Also, *Lacrymaria* spores have a germ pore, not seen in these collections.

It is now clear that these three species belong to the genus *Hebeloma.* Based on the spore color in fresh material, they are members of *H.* sect. *Porphyrospora.* Unfortunately, the publication of two of these species is invalid under Art. 40.7 of the International Code (Turland et al. 2018), as the published description does not specify the herbarium in which the types are conserved.

It does appear that two of these three species, *Psathyrella splendens* and *P. verrucispora*, have been described and classified within *Hebeloma* since Corner's publication, as *H. parvisporum* and *H. lactariolens*, originally published as *Alnicola lactariolens*. The third taxon, *P. flavidifolia* is recombined here as *H. flavidifolium.* Within this paper we cite seven new *Hebeloma* collections from the Malay Peninsula, collected by one of the authors (E. H.) during 2009 and 2010. Three of these collections are referred to *H. lactariolens*, one to *H. parvisporum*, two to *H. flavidifolium* and one to a species here described as new, *H. radicans.* All collections are from mixed tropical lowland forests dominated by *Dipterocarpus*, *Quercus* and *Lithocarpus*.

Corner (1994 ["1993"]) published detailed descriptions and excellent drawings of *P. splendens* and *P. verrucispora*. However, his description of *P. flavidifolia* is rather brief

and has very little microscopic detail. He writes: "*P. flavidifolia*, is imperfectly known from one collection and is included in order that it may be rediscovered". He goes on to say: "I describe this fungus, even though my notes on microscopic details are so imperfect, because it indicates an ally of *P. splendens*. It may be rare because I found it but once and, then, it puzzled me and became *Hebeloma* in my notes". It appears that Corner already guessed that perhaps this taxon belonged within *Hebeloma*. Based on two new collections from the Malay Peninsula, we can now provide a much more detailed description and photographs of this mushroom. The description of *Hebeloma radicans* is based on a single collection. Although this is unfortunate, we have decided to go ahead with the description of this new species, anticipating that the knowledge of this species will advance its rediscovery and that of related taxa.

Materials and methods

Basidiomes were collected, dried and accessioned at the fungus herbarium of the Forest Research Institute Malaysia (**FRIM**) with duplicates in the collection of E. Horak at the herbarium of the Eidgenössische Technische Hochschule Zürich (**ZT**). Type material of the Corner species was obtained from the herbarium of the Royal Botanic Garden of Edinburgh (**E**).

Sequence data were obtained from dried specimens by direct sequencing following methods detailed in Eberhardt et al. (2016) and Cripps et al. (2019) for ITS and Vesterholt et al. (2014) for *MCM7* (a DNA replication licensing factor). Sequence data were generated by LGC Genomics (Berlin, Germany). Sequences were edited using Sequencher vs. 4.8 (Gene Codes Corp., Ann Arbor, Michigan). Newly generated sequences were accessioned to GenBank (MT832016–MT832022 and MT832328–MT832331).

Flammula alnicola was used for rooting, and two species of *Alnicola* [*Naucoria* fide Species Fungorum (Index Fungorum Partnership 2019) accessed 13 Dec 2019] (*A. amarescens* and *A. salicis*) were used as additional outgroups. Members of the genus *Hebeloma* are represented by material, including type material, used in earlier publications (Beker et al. 2016; Eberhardt et al. 2020) and listed in Table 1. Material of all sequenced collections (apart from MEL 2382694) was available for examination.

Sequence alignments were done online in MAFFT using the E-INS-i option (Katoh et al. 2017) for ITS and 'auto' for *MCM7 data*. Alignments were viewed and reformatted using ALIVIEW 1.24 (Larsson 2014). Maximum likelihood (ML) analyses of single locus alignments were calculated in RAXML 8.2.10 (Stamatakis 2014) using the raxml-Gui interface 2.0 (Silvestro and Michalak 2012; Edler et al. 2019), with the GTRGAMMA option, 10 searches for the best ML tree, using the MRE option to limit the number of rapid bootstrap replicates.

The compatibility of the two loci was accessed following the principle of Kauff and Lutzoni (2002), assuming a conflict to be significant if two different relationships for the same set of taxa, one being monophyletic and the other non-monophyletic, are supported by bootstrap with more than 75% in ML analyses.

Table 1. Sequences used in the analysis. Herbarium abbreviations follow Index Herbariorum and are given in capital letters followed by a space or hyphen and the herbarium number. Private collections are indicated by the lack of a space between the letters and numbers. MO refers to https://mushroomobserver.org/

Species	Country	HJB database reference	Voucher	GenBank acc. no. ITS	GenBank acc. no. MCM7
Alnicola amarescens (Quél.) R. Heim & Romagn.	Switzerland	HJB11116	HJB11116	MK961996†	MK961952†
Alnicola salicis (P.D. Orton) Bon	U.K.	HJB14745	HJB14745	MK962001†	MK961960†
Flammula alnicola (Fr.) P. Kumm.	Germany	–	GLM-F045994	MK957190†	MK961971†
Hebeloma aestivale Vesterh.	U.K.	HJB9291	HJB9291	KT218221‡	MK961944†
H. alboerumpens Vila & al.	Spain	HJB13021	JVG1090114-15	JQ751220§	JQ751104§
H. alpinum (J. Favre) Bruchet	Switzerland	HJB11132	HJB11132	KM390590|	KM390046|
H. aminophilum R.N. Hilton & O.K. Mill.	New Zealand	HJB10682	PDD 102982 (PL14504)	MK961993†	MK961949†
H. aminophilum	Australia	HJB16823	HO 586929	MK962007†	MK961966†
H. aminophilum f. *hygrosarx* B.J. Rees	Australia	HJB1000297	PERTH 06659152	MK962016†	MK961969†
H. angustilamellatum (Zhu L. Yang & Z.W. Ge) B.J. Rees	China	HJB1000408	HKAS 42927	AY575919¶	–
H. angustilamellatum	Thailand	HJB12251	GENT RW07-470	MK961997†	MK961953†
H. angustilamellatum	Laos	HJB14851	HNL 501000	MK962003†	MK961962†
H. angustilamellatum	Laos	HJB17006	HNL 501053	MK962010†	–
H. bulbiferum Maire	Croatia	HJB13083	TUR-A 177060	KT218422‡	MK961956†
H. cavipes Huijsman	Spain	HJB9433	HJB9433	KT217362#	KT216685#
H. celatum Grilli, U. Eberh. & Beker	Germany	HJB13621	BR 5020184119676	KT218446‡	MK961957†
H. crustuliniforme (Bull.) Quél.	Spain	HJB11237	HJB11237	JN943870††	KF309440|
H. cylindrosporum Romagn.	Spain	HJB11427	C-F-44748	FJ769365‡‡	MT832328
H. cylindrosporum	France	HJB12763	HJB12763	JQ751210§	JQ751106§
H. dunense L. Corb. & R. Heim	Belgium	HJB14141	AdH11031	KY271835§§	MK961959†
H. flavidifolium	Malaysia	HJB13504	E. Horak 13404 (ZT)	MT832021	–
H. flavidifolium	Malaysia	HJB13505	E. Horak 13406 (ZT)	MT832022	–
H.ifeleletorum Kropp	American Samoa	HJB1000386	UTC 00235643	MK962019†	MK961970†
H. indicum (K.A. Thomas & al.) B.J. Rees	India	HJB1000384	IB 19971307	AF407163||	–
H. indicum	India	HJB12902	IB 19991200	MK961999†	MK961955†
H. khogianum Bresinsky	New Caledonia	HJB1000388	M-0124631	GU591635¶¶	–
H. lactariolens Clémençon & Hongo) B.J. Rees & Orlovich	Japan	–	LAU HC88/95	AY818352¶	–
H. lactariolens	China	–	HMAS 280191	KX513590†††	–
H. lactariolens	Malaysia	HJB13363	E. Horak 12796 (ZT)	MT832017	MT832330
H. lactariolens	Malaysia	HJB13365	E. Horak 13287 (ZT)	MT832019	–
H. lactariolens	Malaysia	HJB13503	E. Horak 13381 (ZT)	MT832020	MT832331
H. laterinum (Batsch) Vesterh.	France	HJB13703	HJB13703	MK962000†	MK961958†
H. mediorufum Soop	New Zealand	HJB10689	PDD 102983 (PL51404)	KM390552|	KM390037|
H. mediorufum	New Zealand	HJB10688	PDD102995 (PL167404)	KM390572|	KM390042|
H. mesophaeum (Pers.) Quél.	Iceland	HJB11050	HJB11050	MK961995†	MK961951†
H. parvisporum Sparre Pedersen & al.	Laos	HJB14850	HNL 501009	MK962002†	MK961961†
H. parvisporum	Laos	HJB14852	HNL 500968	MK962004†	MK961963†
H. parvisporum	Laos	HJB17004	HNL 500914	MK962008†	–
H. parvisporum	Laos	HJB17005	HNL 500984	MK962009†	–
H. parvisporum	Laos	HJB17007	HNL 500884	MK962011†	–
H. parvisporum	Malaysia	HJB13362	E. Horak 12795 (ZT)	MT832016	–
H. plesiocistum Beker & al.	Spain	HJB11514	JVG1021214-5	EU570170‡‡‡	JQ751115§
H. porphyrosporum Maire	Italy	HJB10344	HJB10344	MK961992†	MK961947†
H. porphyrosporum	Spain	HJB10767	HJB10767	MK961994†	MK961950†
H. radicans	Malaysia	HJB13364	E. Horak 13265 (ZT)	MT832018	–
H. radicosum (Bull.) Ricken	Belgium	HJB10262	HJB10262	MK961990†	MK961945†
H. radicosum	Italy	HJB10314	HJB10314	MK961991†	MK961946†
H. sarcophyllum (Peck) Sacc.	U.S.A.	HJB15696	DPL 10569	MK962005†	MK961964†
H. sarcophyllum	U.S.A.	HJB17783	MO301904	MK962014†	–
H. sinapizans (Paulet) Gillet	U.K.	HJB10628	HJB10628	JQ751191§	JQ751119§
H. sinapizans	U.K.	HJB10751	HJB10751	JQ751193§	JQ751121
H. subvictoriense B.J. Rees	Australia	HJB1000299	MEL 2331640	MK962017†	–

Species	Country	HJB database reference	Voucher	GenBank acc. no. ITS	GenBank acc. no. MCM7
H. syrjense (P. Karst.) P. Karst.	France	HJB12064	HJB12064	JQ751206§	JQ751122§
H. syrjense	Finland	HJB12396	C 26197F	JQ751218§	JQ751123§
H. theobrominum Quadr.	Estonia	HJB10009	HJB10009	EU570181‡‡‡	JQ751124
H. theobrominum	Belgium	HJB10063	HJB10063	FJ816623§§§	JQ751125§
H. vaccinum Romagn.	Belgium	HJB9965	HJB9965	KT217371#	KT216689#
H. velutipes Bruchet	France	HJB10547	HJB10547	EU570174‡‡‡	MK961948†
H. velutipes	U.K.	HJB10483	HJB10483	EU570175‡‡‡	MT832329
H. vesterholtii Beker & U. Eberh.	Italy	HJB10339	HJB10339	FJ816629, FJ816630§§§	JQ751132
H. vesterholtii	Italy	HJB11869	HJB11869	FJ943239, FJ943240§§§	JQ751135§
H. victoriense A.A. Holland & Pegler	New Zealand	HJB12401	PDD 93802 (PL3408)	MK961998†	MK961954†
H. victoriense	Australia	HJB16704	HO 586713	MK962006†	MK961965†
H. vinosophyllum Hongo	Japan	HJB17411	MO287712 (UK323)	MK962012†	MK961967†
H. vinosophyllum	Japan	HJB17413	MO299315 (UK347)	MK962013†	MK961968†
H. westraliense Bougher & al.	Australia	HJB1000134	PERTH 01012665	MK962015†	–
H. youngii B.J. Rees	Australia	–	MEL 2382694	KP012873|||	–
H. youngii	Australia	HJB1000343	BRI AQ669300	MK962018†	–

† Eberhardt et al. (2020); ‡ Grilli et al. (2016); § Eberhardt et al. (2013); | Eberhardt et al. (2015); ¶ Yang et al. (2005); # Eberhardt et al. (2016); †† Schoch et al. (2012); ‡‡ Vesterholt et al. (2009); §§ Beker et al. (2018); || Thomas et al. (2002); ¶¶ Rees et al. (2013); ††† Wei et al. 06 Jul 2016, no reference found; ‡‡‡ Eberhardt et al. (2009); §§§ Eberhardt and Beker (2010); ||| Bonito et al. 19 Oct 2014, no reference found.

The datasets were then concatenated and subdivided into five partitions, ITS and four *MCM7* partitions, the exon in three partitions by codon position and the intron. In IQ TREE 2.0.6, the best partitioning scheme and the best likelihood models were determined under the Bayesian information criterion (Lanfear et al. 2012, 2014: Kalyaanamoorthy et al. 2017). This scheme and the selected models were used for ML tree construction (Nguyen et al. 2015; Chernmor et al. 2016). A bootstrap analysis was run in 500 replicates.

A Bayesian inference (BI) analysis was run with MRBAYES 3.2.6 (Ronquist et al. 2012) on CIPRES (Miller et al. 2012). The BI analysis was done unpartitioned in two runs with four chains including one heated chain each using the GTRINVGAMMA model and a uniform prior and sampling one tree of each run every 10,000 generations. The analysis was stopped automatically after 4.28 mio generations. The first 25% of trees were discarded as burnin for calculating posterior probabilities.

Trees were visualized using FigTree 1.4.4 (Rambaut 2006–2018) and submitted to TreeBASE (http://purl.org/phylo/treebase/phylows/study/TB2:S26715). Relationships between species are termed "fully supported", if bootstrap support is 100% or posterior probability is 1, respectively; and "supported" if bootstrap support ≥ 75% and posterior probabilities ≥ 0.95.

Details of morphological analyses were provided in Beker et al. (2016). For each collection at least 50 spores were measured in Melzer's reagent, excluding the apiculus. The maximum length and width of each spore was measured, and its Q value (ratio of length to width) calculated. Average length, width, and Q value were calculated and recorded alongside the median, standard deviation, and 5% and 95% percentiles. The assessment and coding of spore characters followed Beker et al. (2016) and Vesterholt (2005). The average width of the widest part of the cheilocystidium in the vicinity of

the apex appears to be an important character in the separation of species within *Hebeloma* (Vesterholt 2005). It is also important, when determining this average width near the apex, not to be selective with regard to the cystidia chosen for measurement. To determine the average width at the apex, about 100 cheilocystidia were measured on the lamella edge. For other measurements, around 20 cheilocystidia, separated from the lamella edge, were measured from each collection. Because of the complex shapes of the cheilocystidia, four measurements were made: length, width at apex (A), width at narrowest point in central region (M), and maximum width in lower half (B). The measurements were given in this order, and an average value was calculated for each of these measurements. For each cheilocystidium the ratios A/M, A/B, and B/M were calculated and averaged across all cheilocystidia measured. Measurements were made in 5% KOH and Melzer's reagent. For all other details with regard to our methodology, see Beker et al. (2016). Each collection studied has a database record number associated with that collection; we give these numbers as we intend to make the database publicly available.

Results

We obtained ITS data for all recent collections from Malaysia and in addition *MCM7* data for Malaysian *H. lactariolens*. No sequence information could be obtained from Corner's material. The datasets included 68 ITS and 49 *MCM7* sequences (Table 1). Bootstrap support was based on 350 or 300 replicates, respectively. The single locus ML results obtained under the GTRGAMMA model (See TreeBase submission) were fully compatible.

The concatenated dataset included 1439 sites that were analyzed in three partitions with three different models (ITS: GTR+F+I+G4; MCM7 1st and 3rd position: K3P+I; MCM7 2nd and intron: K2P+I) in the ML tree reconstruction. Bootstrap support was based on 500 replicates. The topology of the ML tree is shown in Fig. 1. The consensus tree resulting from the BI analysis differed from the depicted ML tree only at few supported parts of the tree (see TreeBase submission). Posterior probabilities were based on 642 trees and included in Fig. 1.

All of the Malaysian collections are included in the clade corresponding to *H.* sect. *Porphyrospora* and there within the western Pacific rim clade. The clade of the species *H. flavidifolium* received full bootstrap and posterior probability support as does the clade of *H. parvisporum*. In the ML reconstruction, *Hebeloma lactariolens* is paraphyletic in relation to the sequences of the Oceanic species *H. youngii*, which are monophyletic and receive full support. In the BI result, *H. lactariolens* is monophyletic, but unsupported and in a weakly (0.96 posterior probability) supported sister clade relationship with the clade of *H. angustilamellatum*, *H. flavidifolium*, *H. ifeleleretorum* and the *H. indicum* clade. The Malaysian collections that we refer to as *H. flavidifolium*, *H. lactariolens*, and *H. parvisporum* (Fig. 2) are morphologically and molecularly congruous with each other and other collections from the respective species. The only representative of *H. radicans* is morphologically and molecularly incongruous with all other known species of fungi.

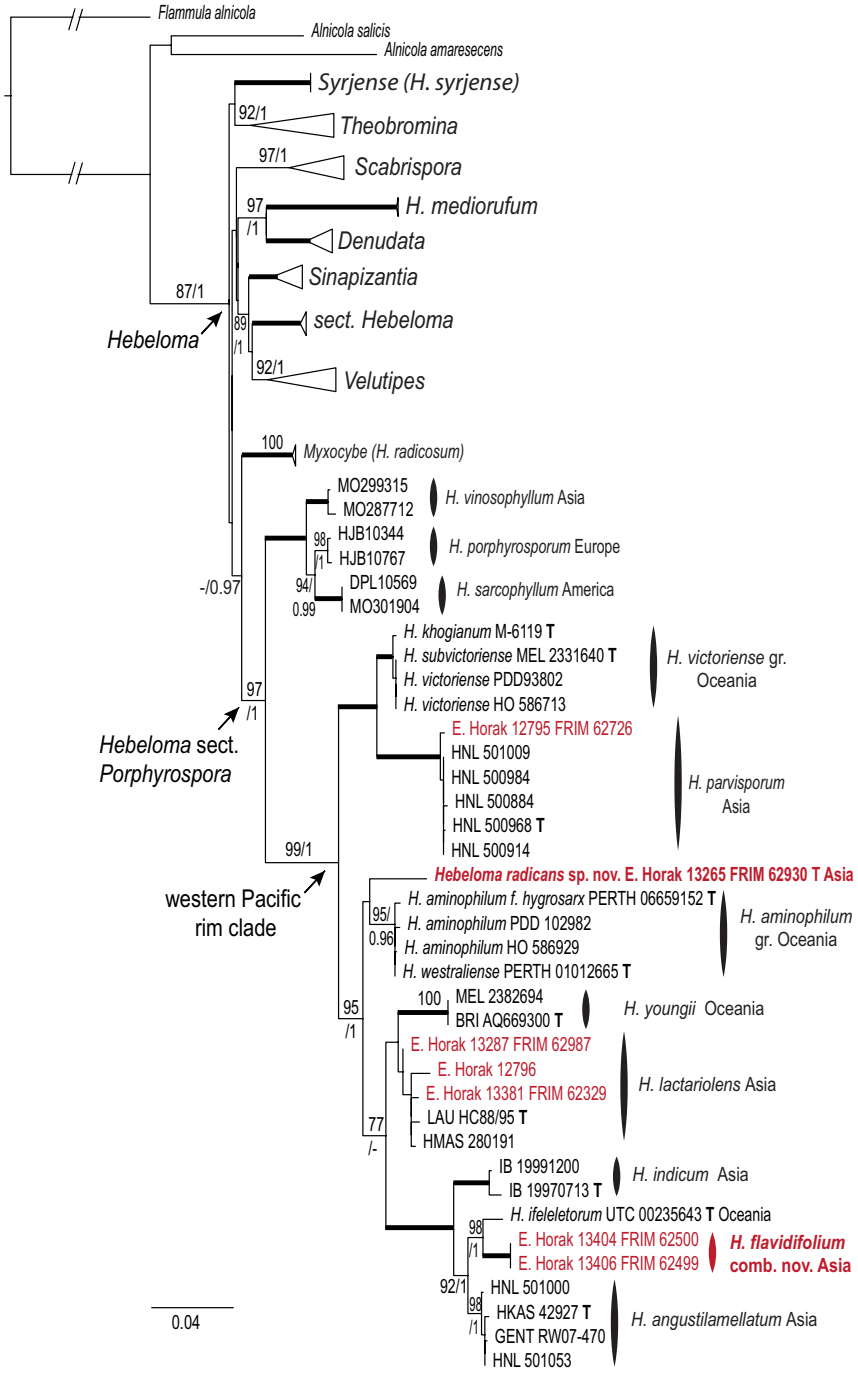

Figure 1. ML topology of concatenated ITS and *MCM7* sequences of *Hebeloma* and *Alnicola*. *Flammula alnicola* is used for rooting purposes. Bootstrap support based on 500 replicates and posterior probabilities based on a BI analysis are indicated at the branches. Assignment of species to sections follows Beker et al. (2016). Sequences in red are from Malaysian collections discussed in this paper. **T** indicates type collections. Thick branches indicate full support. AS – Asia, EU – Europe, NA – North America, O – Oceania, gr. – group.

Taxonomy

We include four species collected from the Malay Peninsula. Three of these have previously been described as *Psathyrella.* Two of these species, *P. splendens* and *P. verrucispora*, were invalidly published but have since been validly published within *Hebeloma*, as *H. parvisporum* and *H. lactariolens*, respectively. The third of these species, *Psathyrella flavidifolia* was validly published and here we recombine it as a *Hebeloma*. Finally, we describe a fourth *Hebeloma* from the Malay Peninsula, *Hebeloma radicans*, as new.

Hebeloma flavidifolium **(Corner) Beker & U. Eberh., comb. nov.**
MycoBank No: 838406
Figures 2A, 3–5

Basionym. *Psathyrella flavidifolia* Corner, Gdns' Bull., Singapore 45(2): 339 (1994) ["1993"].

Homotypic synonym. *Lacrymaria flavidifolia* (Corner) Voto, Boll. Assoc. micol. ecol. Romana 107(2): 94 (2019).

Type. Malaysia. Pahang State: Raub district, Bukit Fraser (Fraser's Hill), ca. 1200 m a.s.l., *Quercus* woodland, 25 Nov 1930, E.J.H. Corner (holotype: E! [E 00204812]; database reference HJB19600).

Description. Basidiomes scattered. Pileus 35–105 mm wide, convex to broadly umbonate; surface dry, sometimes rugulose, occasionally striate at the margin, usually with veil remnants on the margin; cuticle color predominantly cinnamon brown to orange brown (6C5, 7C7) in the center with paler margin, dark beige to tan (5B3); pileus margin strongly involute when young, hygrophanous. Lamellae adnate, often with decurrent tooth, 2–3 mm broad, crowded, thin, with approx. 80–90 full length lamellae and 2–3 lamellules between the lamellae, off-white to cream or yellow-grey when young, later becoming more pinkish or grayish red to purplish and eventually vinaceous to purple-brown or brown following spore maturity; edges weakly fimbriate and white; the white edge remains when the basidiome is dried but the reddish brown color of the lamellae disappears with time. Stipe 50–120 mm long and with central width 5–12 mm, cylindrical sometimes tapering or clavate towards the base, not rooting, occasionally with mycelial cords at the base; white or alutaceous; surface dry, fibrillose, pruinose in the upper part, not discoloring with handling, becoming hollow with age. Flesh whitish, hardly discoloring where bruised. Odor indistinct to raphanoid; taste bitter. Spore vinaceous cinnamon becoming chocolate brown. Exsiccata with no particular characteristics.

Basidiospores based on at least 50 spores from each of three collections, 5% to 95% percentile range 8.9–11.4 × 5.6–7.1 µm, with median 9.7–10.6 × 6.1–6.7 µm and av. 9.6–10.6 × 6.1–6.6 µm with av. S. D. length 0.47 µm and width 0.33 µm; Q value 5% to 95% percentile range 1.43–1.72, with median 1.53–1.58 and av. 1.53–1.59 with av. S. D. 0.07; amygdaloid, occasionally limoniform with small apiculus and

Figure 2. Macroscopic features **A** *Hebeloma flavidifolium* (E. Horak 13406) **B** *H. lactariolens* (E. Horak 13381) **C** *H. parvisporum* (E. Horak 12796) **D** *H. radicans* holotype (E. Horak 13265). Photographs E. Horak.

rounded apically, with a distinct thinning of the apical wall, without guttules, usually very strongly ornamented, warty, with a strongly and distinctly loosening perispore on almost every mature spore and strongly dextrinoid, becoming medium brown in Melzer's reagent, sometimes deep brown, ((O3) O4; P3; D3 (D4)); spore color under the light microscope distinctly brown. Basidia av. dimensions 19–33 × 6–9 µm, cylindrical to clavate, without pigmentation, 4-spored. Cheilocystidia irregular, cylindrical to ventricose, often pyriform or napiform often mucronate or rostrate, even lanceolate (as shown in Fig. 3c for example) sometimes septate with width near apex (excluding any rostrum) 5% to 95% percentile range 5.4–10.2 µm, with median 5.6–8.4 µm and av. 5.7–8.6 µm with av. S.D. 0.94; and av. overall measurements 26–29 × 5.7–8.6 × 6.6–9.7 × 5.8–7.5 µm av. Cheilocystidium av. ratios A/M: 0.9–0.91, A/B: 0.77–1.6, B/M: 0.61–1.35. Pleurocystidia present, and abundant, and similar to cheilocystidia, but more often mucronate. Caulocystidia resembling the cheilocystidia but tending to be more cylindrical and longer up to 60 µm. Pileipellis an ixocutis with a very thin epicutis only about 30 µm thick, with gelatinized hyphae, sometimes encrusted, up to 6 µm wide. Subcutis, below the epicutis, orange-brown and the trama below the cutis made up of isodiametric cells up to 17 µm wide. Clamp connections at septa present throughout the basidiome.

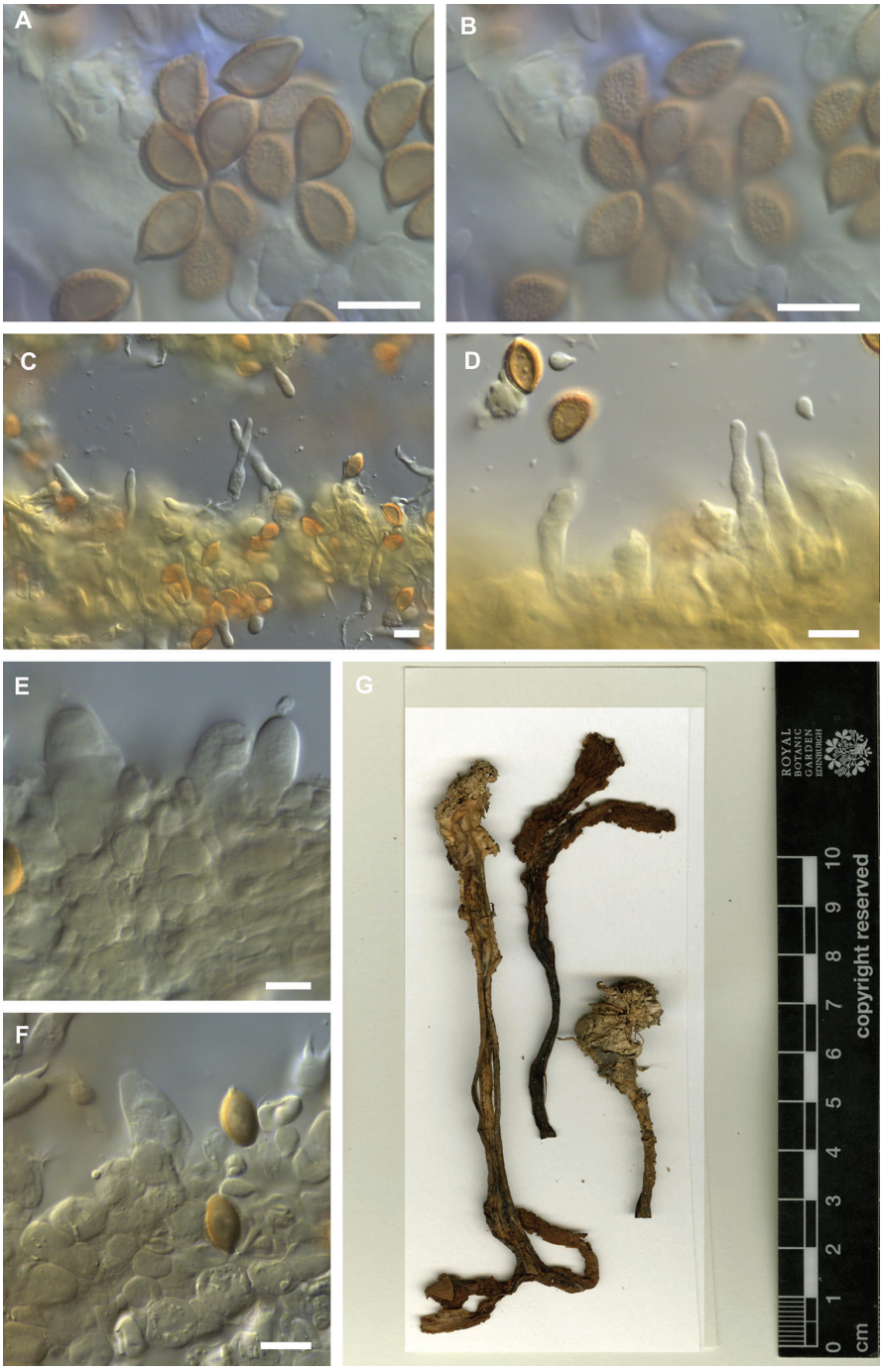

Figure 3. Microscopic features of *Hebeloma flavidifolium* holotype (E 00204812) **A** spores in Melzer's reagent ×1600 **B** spore ornamentation in Melzer's reagent ×1600 **C** cheilocystidia in Melzer's reagent ×500 **D** cheilocystidia in Melzer's reagent ×1000 **E** cheilocystidia in KOH ×1000 **F** pleurocystidia in KOH ×1000. Scale bars: 10 µm (**A–F**). Photographs H.J. Beker. **G** Exsiccata (a section of photograph from http://data.rbge.org.uk/herb/ E 00204812 provided by the Royal Botanic Garden Edinburgh).

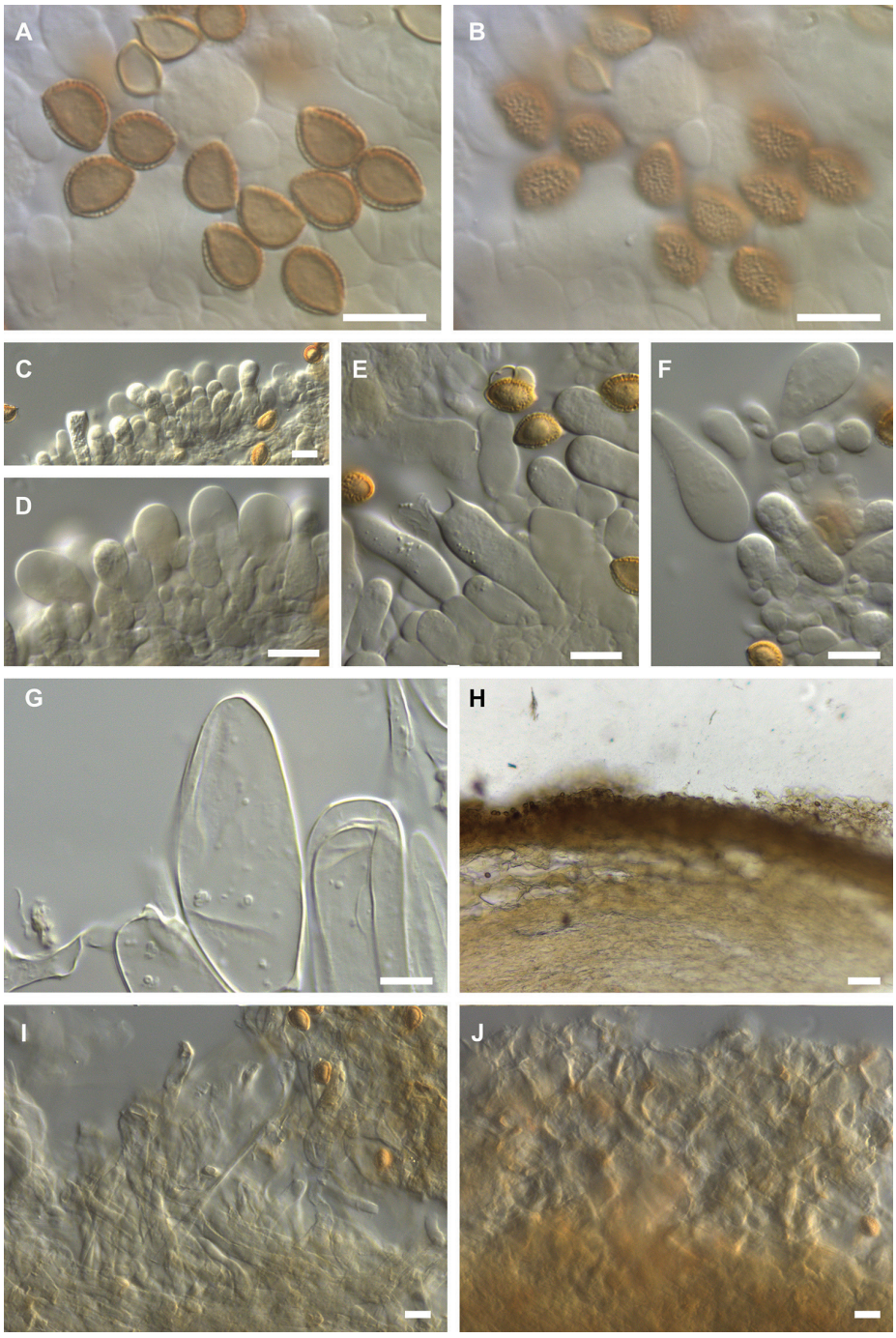

Figure 4. Microscopic features of *Hebeloma flavidifolium* (E. Horak 13406) **A** spores in Melzer's reagent ×1600 **B** spore ornamentation in Melzer's reagent ×1600 **C** cheilocystidia in KOH ×500 **D** cheilocystidia in KOH ×1000 **E** basidium in KOH ×1000 **F** pleurocystidia in KOH ×1000 **G** caulocystidium in KOH ×1000 **H** ixocutis section (showing thin gelatinous epicutis) in KOH ×125 **I** epicutis hyphae in KOH ×500 **J** subcutis below epicutis in KOH ×500. Scale bars: 10 µm, 100 µm (**H**). Photographs H.J. Beker.

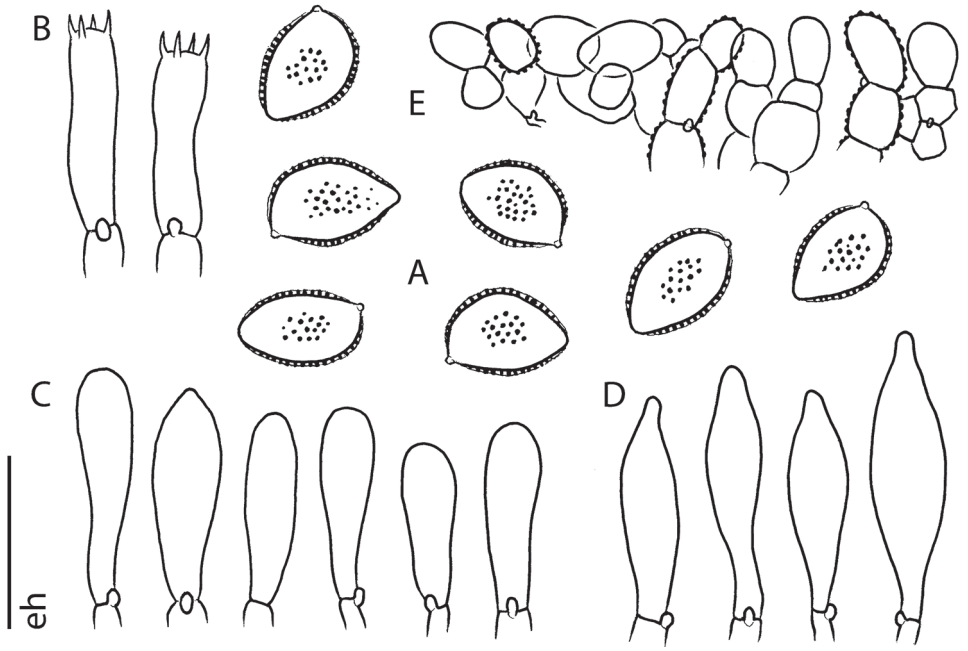

Figure 5. Microscopic features of *Hebeloma flavidifolium* (E. Horak 13406) **A** spores ×2000 **B** basidia ×1000 **C** cheilocystidia ×1000 **D** pleurocystidia ×1000 **E** pileipellis (section of subcutis below epicutis) ×500. Scale bar: 10 µm ×2000, 20 µm ×1000 and 40 µm ×500. Drawing E. Horak.

Distribution. So far known only from Bukit Fraser (Fraser's Hill), Malaysia.

Ecology. The recent collections were found scattered in lowland dipterocarp-oak woodland on the side of the path in tropical rain forest with *Quercus*.

Additional material examined. Malaysia. Pahang State: Raub district, Bukit Fraser (Fraser's Hill), Jalan Girdle, ca. 1000 m a.s.l., 3.71°N, 101.74°E, *Quercus* woodland, 26 Apr. 2010, E. Horak 13406 (collection E. Horak at ZT, FRIM [FRIM 62499]; database reference HJB13505); Pahang State: Raub district, Bukit Fraser (Fraser's Hill), Jalan Girdle, ca. 1000 m alt., 3.71°N, 101.74°E, *Quercus* woodland, 26 Apr. 2010, E. Horak 13404 (collection E. Horak at ZT, FRIM [FRIM 62500]; database reference HJB13504).

Remarks. Given Corner's original description almost totally lacked any microscopic information, we present a full description here based on the holotype plus two more recent collections from roughly the same location, both collected by E. Horak. Morphologically, this species most closely resembles *Hebeloma angustilamellatum*, originally described from the Yunnan province of China (Yang et al. 2005) and also recorded from northern Thailand and Laos (Table 1, Fig. 1), from which it can be distinguished morphologically by the very strongly ornamented spores (O4), conspicuous even without immersion (those of *H. angustilamellatum* are O3, so distinctly ornamented but not conspicuous without immersion) and the less conspicuous annulus on the fibrillose stipe of mature basidiomes (*H. angustilamellatum* has a more persistent

annulus, always present, and a stipe, with scattered fibrillose scales, consistently present.) Phylogenetically, based on ITS and *MCM7*, *H. flavidifolium* is a sister species of *H. ifeleleretorum* described from Samoa, but all three form a cluster in Fig. 1 that received full posterior probability and 92% bootstrap support.

***Hebeloma lactariolens* (Clémençon & Hongo) B.J. Rees & Orlovich, Mycologia 105: 1055 (2013).**
Figures 2B, 6

Type. Japan. Shiga-ken: Otsu-shi, Tomikawa, ca. 180 m a.s.l., 34.9001°N, 135.9489°E, *Pinus* sp., *Quercus* sp., 15 Aug 1988, T. Hongo, H. Clémençon HC88/95 (holotype TNS! [TNS-F-237670]; isotype LAU; database reference HJB1000383; ITS GenBank acc. no. AY818352).

Homotypic synonyms. *Alnicola lactariolens* Clémençon & Hongo, Mycoscience 35(1): 25 (1994). *Anamika lactariolens* (Clémençon & Hongo) Matheny, Mycol. Res. 109(11): 1262 (2005).

Heterotypic synonyms. *Psathyrella verrucispora* Corner, Gdns'Bull., Singapore 45(2): 344 (1994) [1993], nom. inval., Art. 40.7 ≡ *Lacrymaria verrucispora* (Corner) Voto, Boll. Assoc. micol. ecol. Romana 107(2): 95 (2019), nom. inval., Art. 40.7. Type: Singapore. Malay Peninsula, Aug. 1929, E.J.H. Corner (holotype E! [E 00204780]; database reference HJB19598).

Other material examined. Malaysia. Johor State: Mersing district, Endau-Rompin Selai, Endau-Rompin (Johor) National Park, Camp Lubuk Tapah, ca. 130 m a.s.l., 2.2976°N, 103.1351°E, with *Dipterocarpus*, 19 Mar. 2009, E. Horak 12796 (collection E. Horak at ZT, FRIM [FRIM 62726]; database reference HJB13363); Johor State: Kluang district, Endau-Rompin Peta, Endau-Rompin (Johor) National Park, trail to Upeh Guling, ca. 40 m a.s.l., 2.5230°N, 103.3611°E, in woodland with *Dipterocarpus* and *Quercus*, 4 Sept. 2009, E. Horak 13287 (collection E. Horak at ZT, FRIM [FRIM 62987]; database reference HJB13365); Negeri Sembilan State: Jelebu district, Simpang Pertang, Pasoh Forest Reserve, ca. 165 m a.s.l., 2.7264°N, 102.0783°E, in woodland, 20 Apr. 2010, E. Horak 13381 (collection E. Horak at ZT, FRIM [FRIM 62329]; database reference HJB13503). SINGAPORE. Malay Peninsula, (E! [E 002048240]; database reference HJB19652), this is just a spore print collected by E.J.H. Corner that may be from the intended type of *Psathyrella verrucispora*.

Remarks. Clémençon and Hongo (1994) originally published this taxon as *Alnicola lactariolens* in the April issue of Mycoscience, apparently published on 1 Apr 1994; it appears Corner had effectively published the paper including the same taxon one day earlier, on 31 Mar 1994 as *Psathyrella verrucispora*. Both are morphologically clearly members of *Hebeloma* section *Porphyrospora*. The authors of both papers comment on the purple-brown (vinaceous) spore print, Corner (1994 ["1993"], p. 345) notes that the spore deposit color is fuscous purple, which is why he described his species in *Psathyrella* rather than *Lacrymaria*. Clémençon and Hongo (1994) commented on

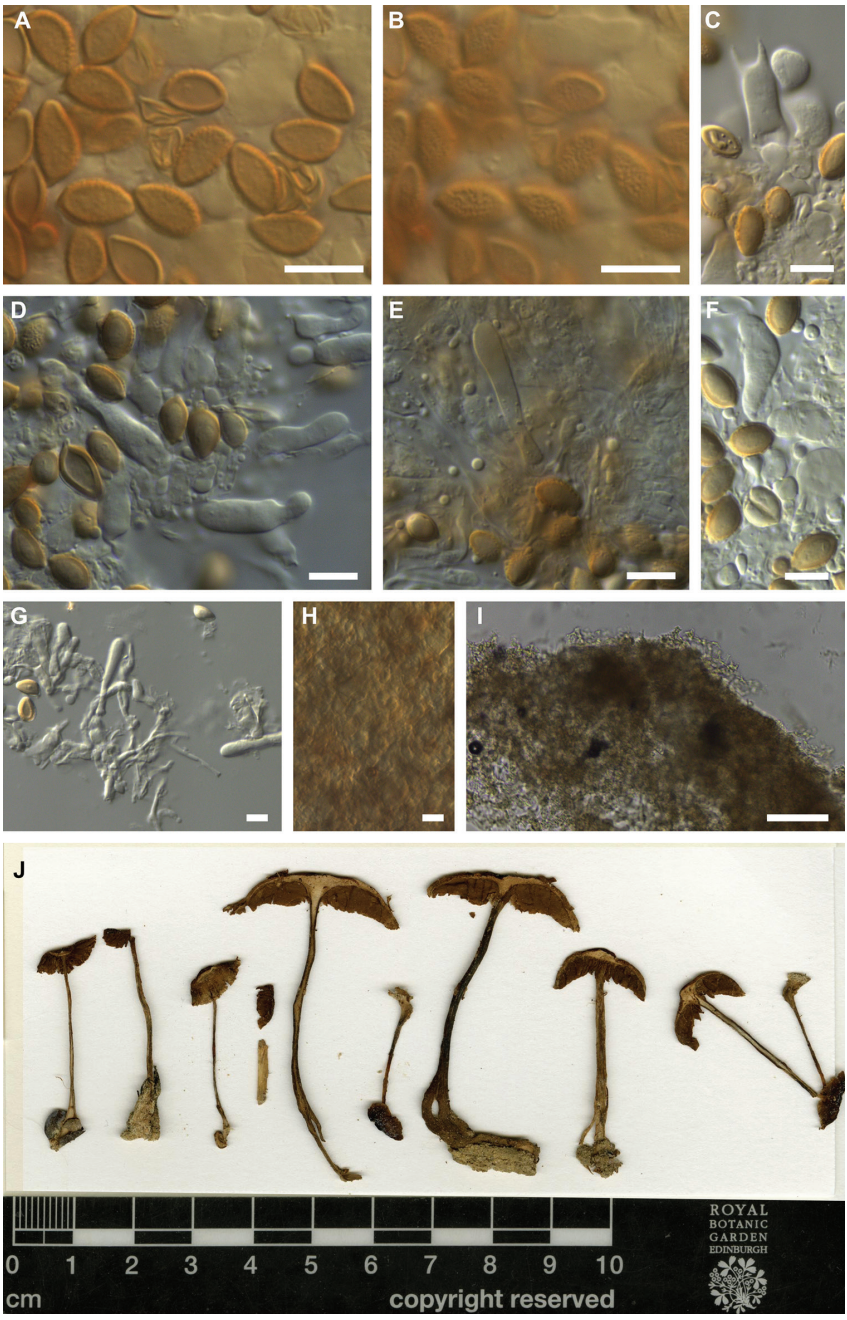

Figure 6. Microscopic features of *Hebeloma lactariolens* (E 00204780); intended holotype of *Psathyrella verrucispora* nom. inval.) **A** spores in Melzer's reagent ×1600 **B** spore ornamentation in Melzer's reagent ×1600 **C** basidium in KOH ×1000 **D** cheilocystidia in KOH ×1000 **E, F** pleurocystidium in KOH ×1000 **G** caulocystidia in KOH ×500 **H** sectional view of cutis below the gelatinous epicutis in KOH ×500 **I** sectional view of ixocutis showing thin gelatinous epicutis in KOH ×125. Scale bars: 10 μm (**A–H**), 100 μm (**I**). Photographs H.J. Beker. **J** Exsiccata (a section of photograph from http://data.rbge.org.uk/herb/E00204780 provided by the Royal Botanic Garden Edinburgh).

the spore deposit being a dark purple-brown color, an unknown feature of *Alnicola.* In Yang et al. (2005) *Alnicola lactariolens* was recombined into *Anamika* and later by Rees et al. (2013) into *Hebeloma*. The spore deposit color and its typical color change upon storage is the most striking feature of members of *H.* sect. *Porphyrospora* (Eberhardt et al. 2020). Good descriptions and further illustrations of *H. lactariolens* can be found in Corner (1994 ["1993"]) and Clémençon and Hongo (1994). Figure 6, shows various macro and micro characters of Corner's intended type of *Psathyrella verrucispora*.

This species is rather variable molecularly and in the ML reconstruction forms a clade together with *H. youngii*, an Australian species growing with *Eucalyptus* and *Corymbia*, to our knowledge only known from the type locality (Rees et al. 2013). Even though the monophyly of *H. lactariolens* in relation to *H. youngii* is not bootstrap-supported within this analysis (Fig. 1), although it is in the BI results (see TreeBase), the molecular distance, the occurrence on different continents, the different host associations, and morphologically, the cheilocystidia which for *H. youngii* are more consistently lanceolate and the number of full length lamellae which for *H. youngii* is in the range 50–60 while for *H. lactariolens* is always less than 40, clearly separate these taxa. The Malaysian and Singapore records are from lowland tropical forests while the type has been described from a subtropical habitat from Japan, thus hinting at a wide climatic and geographical range. *Hebeloma lactariolens* is according to observations of S. S. L. not uncommon in Malaysia. The FRIM database includes additional records of this species (not studied) from Hutan Simpan Semangkuk, Fraser's Hill, Pahang and the Pasoh Forest Reserve, Negeri Sembilan, from hill respective lowland dipterocarp forests.

***Hebeloma parvisporum* Sparre Pedersen, Læssøe, Beker & U. Eberh., Mycologia 112: 179 (2020)**

Figures 2C, 7

Type. Laos. Xieng Khouang: Phoukhout, Laethong, ca. 1135 m a.s.l., 19.742408°N, 103.258102°E, on soil under Fagaceae, 18 Aug 2015, T. Læssøe, O.S. Pedersen (holotype: HNL [HNL 500968]; isotype: C! [C-F-122153]; database reference HJB14852; ITS GenBank Acc. No.: MK962004).

Heterotypic synonyms. *Psathyrella splendens* Corner, Gdns' Bull., Singapore 45(2): 341 (1994) ["1993"], nom. inval., Art. 40.7 ≡ *Lacrymaria splendens* (Corner) Voto, Boll. Assoc. micol. ecol. Romana 107: 95 (2019), nom. inval., Art. 40.7. Type. Singapore. Malay Peninsula, 9. Mar 1930, E.J.H. Corner (holotype: E! [E 00204835]; database reference HJB19597).

Other material examined. Laos. Xiang Khouang: Khoun, Thoum, ca.1130 m a.s.l.**,** 19.314945°N, 103.409749°E, under Fagaceae, 20 Aug. 2015, T. Læssøe, O.S. Pedersen (HNL [HNL 501009]; database reference HJB14850); Xiang Khouang: Paek, Phonekham, ca.1125 a.s.l.**,** 19.494286°N, 103.269110°E, under Fagaceae, 16 Aug. 2015, T. Læssøe, O.S. Pedersen (HNL [HNL 500914]; database reference HJB17004); Xieng Khouang, Phoukhout, Ban Bong, ca.1150 m a.s.l., 19.672180°N, 103.135841°S, under Fagaceae 15 Aug. 2015, T. Læssøe, O.S. Pedersen (HNL [HNL

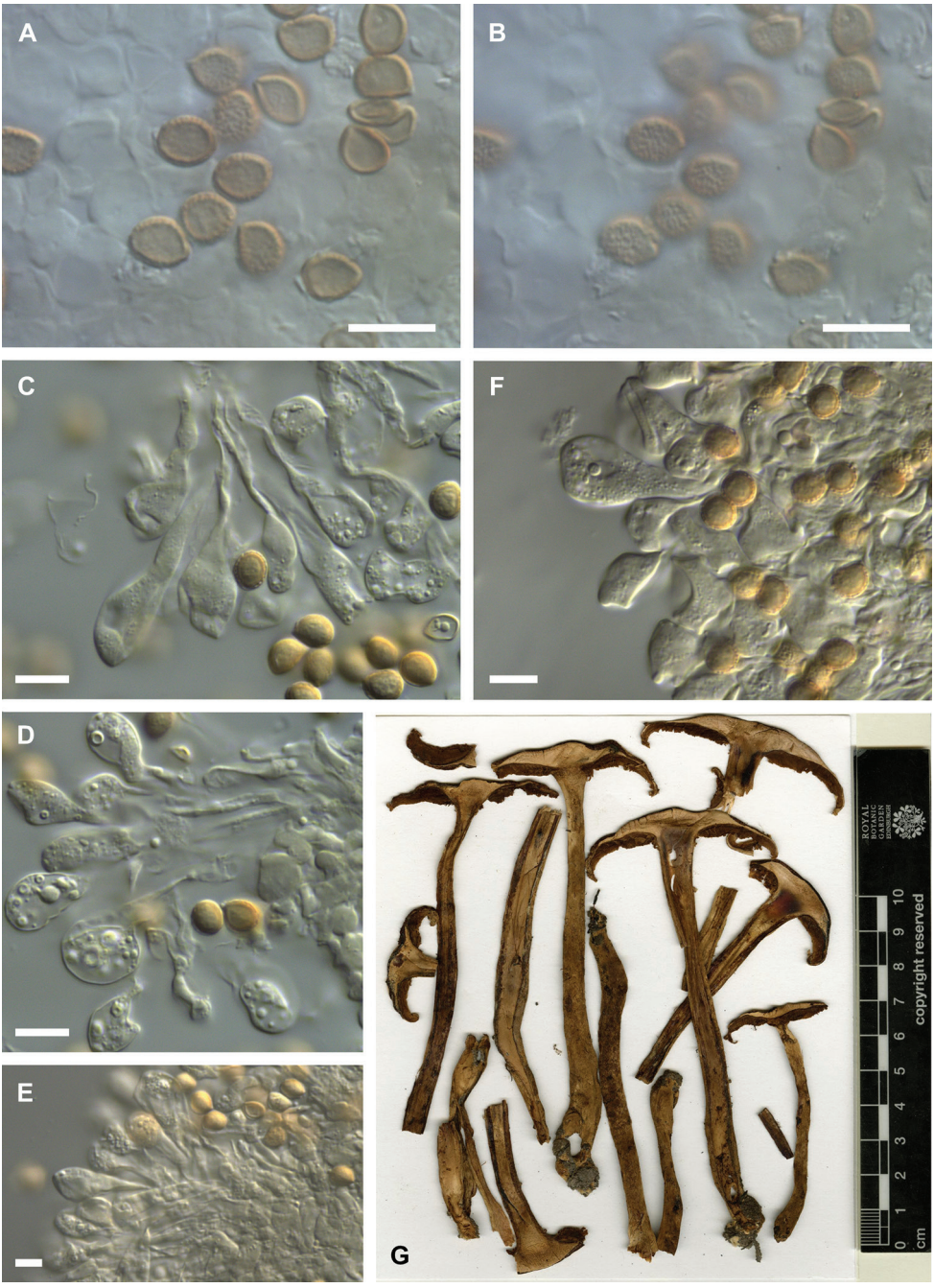

Figure 7. Microscopic features of *Hebeloma parvisporum* (E 00204835; intended holotype of *Psathyrella splendens* nom. inval.) **A** spores in Melzer's reagent ×1600 **B** spore ornamentation in Melzer's reagent ×1600 **C, D** cheilocystidia in KOH ×1000 **E** cheilocystidia and basidium in KOH ×500 **F** caulocystidia, in KOH ×1000. Scale bars: 10 µm. Photos H.J. Beker. **G** Exsiccata (a section of photograph from http://data.rbge.org.uk/herb/E00204835, provided by the Royal Botanic Garden Edinburgh).

500884]; database reference HJB17007); Xieng Khouang, Phoukhout, Sui, ca. 1150 m a.s.l., 19.530514°N, 102.8659°E, under Fagaceae, 19 Aug. 2015, T. Læssøe, O.S. Pedersen (HNL [HNL 500984]; database reference HJB17005). MALAYSIA. Johor State, Mersing district, Endau-Rompin Selai, Endau-Rompin (Johor) National Park, Camp Lubuk Tapah, ca. 130 m alt., 2.2976°N, 103.1351°E, with *Dipterocarpus*, 19 Mar 2009, E. Horak 12795 (collection E. Horak at ZT; database reference HJB13362).

Remarks. The description of this species (Eberhardt et al. 2020) was based upon the above collections from Laos. The intended holotype of *P. splendens* was examined and is micro- and macromorphologically in agreement with *H. parvisporum*; this is illustrated in Fig. 7 which shows the main micro characters of Corner's intended type. The collection from Malaysia is monophyletic with the Laos material. Molecularly, the species is most closely related to the Australian/New Zealand *H. victoriense* species group.

The collection cited as holotype for *P. splendens* was collected in Singapore while Corner also cites other collections from Singapore and Malaysia (Corner 1994 ["1993"]), to which we can add the Malaysian collection above. Plate 3 of Corner (1994 ["1993"]) illustrates the species macroscopically; Lee (2017) includes a photograph of *P. splendens* from the FRIM forest and comments that it often grows in large clusters and is common in the FRIM forest and other parts of the country. The FRIM database includes additional records of this species (not studied) from: Endau-Rompin National Park, Johor; Fraser's Hill, Pahang; the FRIM grounds, Kepong, Selangor; Pasoh, Negeri Sembilan and Tasik Bera, Pahang from lowland and hill dipterocarp forests and a planted dipterocarp forest. S.S.L. observed this species also in degraded hill dipterocarp forest in Janda Baik, Pahang. The species is not listed on the checklist of mushrooms in Thailand (Chandrariskul et al. 2011), but Felix Hampe (oral communication, 21 Jan 2020) reported it from Thailand (Chiang Mai Prov.). Thus, it appears that this species may be widespread within tropical Asia, associated with Fagaceae and dipterocarps (*Dipterocarpus*). In Laos, *H. parvisporum* is found for sale in the local markets for human consumption, but its synonym *P. splendens* is not listed among the species consumed in Malaysia (Chang and Lee 2004; Samsudin and Abdullah 2019).

***Hebeloma radicans* E. Horak, Beker & U. Eberh., sp. nov.**
MycoBank No: 838407
Figures 2D, 8, 9

Diagnosis. The combination of a deeply rooting stipe, about 60 full length lamellae (from stipe to margin of pileus) and spores where almost every spore has a strongly loosening perispore forming a clear layer around the spore, separate this taxon from all other members of *H.* sect. *Porphyrospora*, as does the ITS-sequence.

Type. Malaysia. Johor State: Kluang district, Endau-Rompin Peta, Endau-Rompin (Johor) National Park, Kampung-Peta, trail to Kuala Marong, ca. 50 m a.s.l., 2.52°N, 103.36°E, on soil in lowland dipterocarp-oak forest, 3 Sept 2009, E. Horak,

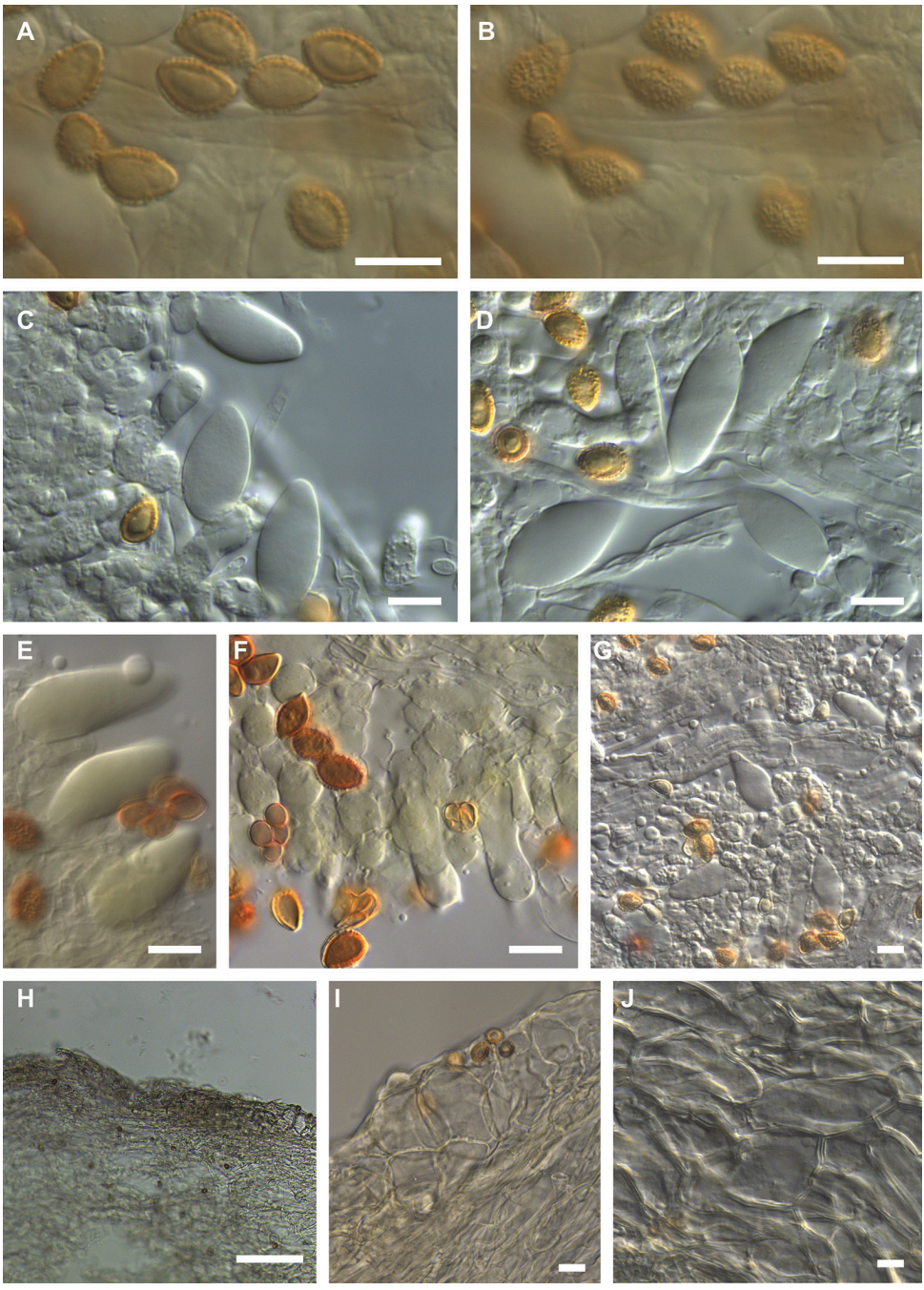

Figure 8. Microscopic features of *Hebeloma radicans* holotype (E. Horak 13265) **A** spores in KOH ×1600 **B** spore ornamentation in KOH ×1600 **C** cheilocystidia and basidium in KOH ×1000 **D** cheilocystidia and basidium in KOH ×1000 **E** pleurocystidia in Melzer's reagent ×1000 **F** basidia in KOH ×1000 **G** pleurocystidia in KOH ×500 **H** sectional view of ixocutis showing thin gelatinous epicutis in KOH ×125 **I** sectional view of subcutis and trama below subcutis in KOH ×500 **J** sectional view of trama below subcutis in KOH ×500. Scale bars: 10 µm, 100 µm (**H**). Photographs H.J. Beker.

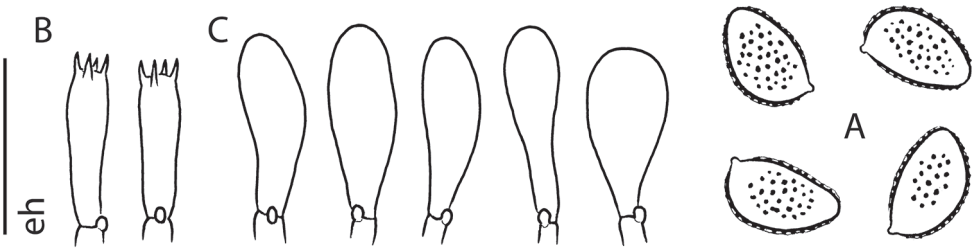

Figure 9. Microscopic features of *Hebeloma radicans* holotype (E. Horak 13265) **A** spores ×2000 **B** basidia ×1000 **C** cheilocystidia ×1000. Scale bar: 10 µm ×2000, 20 µm ×1000 and 40 µm ×500. Drawing E. Horak.

13265 (holotype: collection E. Horak at ZT; isotype: FRIM [FRIM 62930]; database reference HJB13364, ITS GenBank Acc. No.: MT832018).

Description. Basidiomes scattered. Pileus 37–64 mm wide, convex to broadly umbonate; surface dry or slightly viscid, without veil remnants on the pileus; cuticle color predominantly cream to pale buff (4A3, 4A4) in the center with paler margin, off-white to pale cream (4A2); pileus margin entire, hygrophanous. Lamellae adnate, moderately dense, thin, with approx. 60 full length lamellae and 2–3 lamellulae between the lamellae, off-white to cream when young, later pinkish or grayish red to purplish and eventually vinaceous to purple-brown following spore maturity; edges weakly fimbriate and white; the white edge remains when the basidiome is dried but the reddish brown color of the lamellae disappears with time. Stipe 160–194 mm long (including the 'root') and with central width 4–9 mm, cylindrical, distinctly and deeply rooting, white or alutaceous; surface dry, fibrillose, pruinose in the upper part, discoloring with handling and age. Flesh whitish, hardly discoloring where bruised. Smell fragrant; taste bitter. Spore deposit porphyry-brown (10E4). Exsiccata with no particular characteristics.

Basidiospores based on n = 94 spores of the holotype, 5% to 95% percentile range 8.7–10.2 × 5.6–6.6 µm, with median 9.5 × 6.2 µm and av. 9.5 × 6.2 µm with S. D. length 0.47 µm and width 0.34 µm; Q value 5% to 95% percentile range 1.43–1.65, with median 1.53 and av. 1.54 with S. D. 0.07; amygdaloid, with small apiculus and rounded apically, with a distinct thinning of the apical wall and never any sign of papilla, without guttules, usually very strongly ornamented, warty, with a strongly and distinctly loosening perispore on almost every mature spore (almost forming a uniform layer around the spore and making measurement quite difficult at times) and very strongly dextrinoid, immediately becoming deep and intensely red-brown in Melzer's reagent, (O4; P3; D4); spore color under the light microscope distinctly brown. Basidia 21–29 × 6–8 µm, with av. 24.3 × 7.2 µm, cylindrical to clavate, without pigmentation, 4-spored. Cheilocystidia ventricose, primarily pyriform often mucronate or rostrate with width near apex (excluding any rostrum) 5% to 95% percentile range 5–8 µm, with median 6.4 µm and av. 6.5 µm with S.D. 1.06; and av. overall measurements 24 × 6.5 × 9.9 × 8.3 µm av. Cheilocystidium av. ratios A/M: 0.66, A/B: 0.79, B/M: 0.84. Pleurocystidia present, and abundant, and similar to cheilocystidia. Caulocystidia resembling the pleurocystidia but tending to be more cylindrical and longer.

Pileipellis an ixocutis with a very thin epicutis only about 20 µm thick, with gelatinized hyphae up to 5 µm wide. The cutis below the epicutis is orange-brown and the trama below the cutis is made up of isodiametric cells up to 25 µm wide. Clamp connections at septa present throughout the basidiome.

Distribution. Only known from the type locality in Endau-Rompin (Johor) National Park, Malaysia.

Ecology. Scattered in lowland dipterocarp-oak woodland on the side of the path.

Etymology. From 'radicans', meaning rooting, to emphasize this character of the species.

Remarks. *Hebeloma radicans* with its vinaceous colored lamellae when mature and the porphyry colored spore print which turns brown with time, is a typical member of *H.* sect. *Porphyrospora.* The highly ornamented and highly dextrinoid spores are often seen in taxa of this section; while the consistently loosening perispore is also a common feature of a number of the taxa within this section, the regularity and presentation of the perispore is atypical and very distinctive. The rooting stipe is also unusual; while we have recorded rooting stipes in other members of this section, namely: *H. lactariolens*, *H. parvisporum*, and *H. victoriense*, in these cases it is a shallow root occurring infrequently and not on every basidiome. The rooting stipe of *H. radicans* is deep and more reminiscent of *H. radicosum.* This long rooting stipe should be sufficient to distinguish this species from other described members of this section, but taken together with the spore properties and also the moderately dense (but not crowded) lamellae (approx. 60 full length lamellae), assuming these characters are constant, this taxon is clearly distinct. In Fig. 1 as in the BI reconstruction, *H. radicans* is sister to the Oceanic *H. aminophilum* group clade, but this relationship is not supported. The ITS differs by at least 2.2% from other members of *H.* sect. *Porphyrospora*; there are many species in *Hebeloma* that are less distant from each other (Beker et al. 2016).

While, to date, we only have one collection of this species, given its morphological differences and molecular distinctness, we are confident that this taxon is different from any other described within *Hebeloma* and we hope that its publication will encourage its rediscovery. It is of course possible that it has been confused with other genera, e.g. *Psathyrella*, as was the case with other Malay Peninsula collections as described here, but thus far we have not been able to find any evidence of this.

Discussion

Had the describers of *Hebeloma parvisporum* been aware of *Psathyrella splendens*, they would have used that epithet for *H. parvisporum*. When describing the species, other genera like *Alnicola*, *Naucoria*, and even *Pholiota* were checked for misplaced *Hebeloma* species (Eberhardt et al. 2020), but it did not occur to the authors to investigate *Psathyrella* names – nor, it seems, to the authors who reclassified *Alnicola lactariolens* (Yang et al. 2005; Rees et al. 2013) without referring to *P. verrucispora*.

We here demonstrate the presence of four, presumably endogenous species, of *Hebeloma* in tropical forests of the Malay Peninsula, a genus previously overlooked in this region. In the checklist for Malaysia (Lee et al. 2012) the genus *Hebeloma* is missing. In fact, the entire group of ectomycorrhizal Hymenogastraceae is missing, unless one considers *Naucoria periniana*, adopted from Chipp's checklist for the Malay Peninsula (Chipp 1921). This species was recombined into *Galerina* by Pegler (1975), thus outside of the ectomycorrhizal Hymenogastraceae, although it appears unlikely that Pegler and Chipp refer to the same taxon (Chipp, 1921 p. 383, "King's collector"). *Hebeloma* is also missing from checklists for Singapore fungi (Tham and Watling 2017a–d). The ectomycorrhizal Hymenogastraceae are missing, if assuming that *Wakefieldia striaespora*, described from Singapore, does not represent the same genus as the Greek collections referred to as *Wakefieldia macrospora* (Kaounas et al. 2011), which are members of the Hymenogastraceae and have been sequenced from ectomycorrhizal root samples (Tedersoo and Smith 2013; Richard et al. 2011). *Hebeloma* and *Hymenogaster* records from Thailand (Chandrasrikul et al. 2011) appear to be from northern Thailand and are comprised of names of species that are presumably not native to Thailand (*H. albidulum*, *H. crustuliniforme*, *H. hiemale*, *H. radicosum*, *H. sacchariolens*, *H. sarcophyllum*); the single record of *Hymenogaster* cf. *albellus* (originally described from Tasmania by Massee 1898) would currently be referred to as *Descolea albella* and was moved to the Bolbitaceae (Kuhar et al. 2017). The cited collection of *H. angustilamellatum* from Thailand is not from the Malay Peninsula (the species is not listed by Chandrasrikul et al. 2011). Thus, it is a safe assumption that these are the first literature records of *Hebeloma* under this name from the Malay Peninsula, almost certainly endogenous species, and possibly also the first reliable records of ectomycorrhizal Hymenogastraceae. *Hebeloma* is considered rare in tropical forests. Apart from the records presented here, the only confirmed record is of *H. ifeleleretorum* (American Samoa, Kropp 2015).

Having said this, it should be noted that the authors of checklists for the Malay Peninsula (Lee et al. 2012; Tham and Watling 2017a–d) do state that these lists are not exhaustive, but represent the state of knowledge at the time of publication. Lack of opportunity and the generally overwhelming biodiversity has often prevented the investigation of less commercially important and generally less well-studied fungi. Those of us with field experience in the area have been aware of the presence of members of *Alnicola*, *Hebeloma* and *Hymenogaster* (probably also in the strict sense) on the Malay Peninsula for some time.

The molecular results support earlier results of Eberhardt et al. (2020) that the members of *H.* sect. *Porphyrospora*, originating from the western Pacific Rim, apart from *H. vinosophyllum*, form a well-supported clade. Within this clade, however, closely related species may be of Oceanic or southeast Asian origin, and may be associated with Fagaceae and/or dipterocarps or Myrtaceae. How this pattern came about, and even whether it will be supported when more data become available, is at this point an open question.

Acknowledgements

The collections were made in the context of the Forest Research Institute Malaysia (FRIM) project "Survey, Inventory and Documentation of the Flora and Fauna Biological Diversity of Malaysia" funded by the Malaysian government. We are very much obliged to A. Bogaerts and P. Ballings of the Botanic Garden Meise (BR) for help with handling various loans from a variety of herbaria. We also thank these herbaria for their help: C, E, HNL, IB, TNS and ZT. The Royal Botanic Garden Edinburgh is acknowledged for allowing us to reproduce photographs. We are grateful for the help of K. Bensch of Mycobank in a number of nomenclatural and taxonomic questions. We thank the reviewers for their improvements of the manuscript.

References

Beker HJ, Eberhardt U, Vesterholt J (2016) Hebeloma (Fr.) P. Kumm. Fungi Europaei 14. Edizioni Tecnografica, Lomazzo, 1232 pp.

Beker HJ, Eberhardt U, Schütz N, Gulden G (2018) A review of the genus *Hebeloma* in Svalbard. Mycoscience 59: 303–309. https://doi.org/10.1016/j.myc.2017.12.001

Chandrasrikul A, Suwanarit P, Sangwanit U, Lumyong P, Payapanon A, Sanoamuang N, Pukahuta C, Petcharat V, Sardsud U, Duengkae K, Klinhom U, Thongkantha S, Thongklam S (2011) Checklist of mushrooms (Basidiomycetes) in Thailand. Office of Natural Resources and Environmental Policy and Planning, Bangkok. https://www.phakhaolao.la/en/publications/check-list-mushrooms-basidiomycetes-thailand

Chang YS, Lee SS (2004) Utilisation of macrofungi species in Malaysia. Fungal Diversity 15: 15–22. http://www.fungaldiversity.org/fdp/sfdp/15-2.pdf

Chernomor O, von Haeseler A, Minh BQ (2016) Terrace aware data structure for phylogenomic inference from supermatrices. Systematic Biology 65: 997–1008. https://doi.org/10.1093/sysbio/syw037

Chipp TF (1921) A list of the fungi of the Malay Peninsula. The Gardens' Bulletin Straits Settlements 2: 311–418.

Clémençon H, Hongo T (1994) Notes on three Japanese Agaricales. Mycoscience 35: 21–27. https://doi.org/10.1007/BF02268524

Corner EJH (1994 ["1993"]) *Psathyrella* (Agaricales) with ornamented spores in the Malay Peninsula. Gardens Bulletin Singapore 45: 337–357. https://www.nparks.gov.sg/sbg/research/publications/gardens-bulletin-singapore/-/media/sbg/gardens-bulletin/4-4-45-2-02-y1993-v45p2-gbs-pg-337.pdf

Cripps C, Eberhardt U, Schütz N, Beker HJ, Evenson VS, Horak E (2019) The genus *Hebeloma* in the Rocky Mountain alpine zone. MycoKeys 46: 1–54. https://doi.org/10.3897/mycokeys.46.32823

Eberhardt U, Beker HJ (2010) *Hebeloma vesterholtii*, a new species in section *Theobromina*. Mycological Progress 9: 215–223. https://doi.org/10.1007/s11557-009-0627-z

Eberhardt U, Beker HJ, Schütz N, Pedersen OS, Sysouphanthong P, Læssøe T (2020) Adventurous cuisine in Laos: *Hebeloma parvisporum*, a new species in *Hebeloma* section *Porphyrospora*. Mycologia 112(1): 172–184. https://doi.org/10.1080/00275514.2019.1680220

Eberhardt U, Beker HJ, Vesterholt J, Schütz N (2016) The taxonomy of the European species of *Hebeloma* section *Denudata* subsections *Hiemalia*, *Echinospora* subsect. nov. and *Clepsydroida* subsect. nov. and five new species. Fungal Biology 120: 72–103. https://doi.org/10.1016/j.funbio.2015.09.014

Eberhardt U, Beker HJ, Vesterholt J (2015) Decrypting the *Hebeloma crustuliniforme* complex: European species of *Hebeloma* section *Denudata* subsection *Denudata*. Persoonia 35: 101–147. https://doi.org/10.3767/003158515X687704

Eberhardt U, Beker HJ, Vesterholt J, Dukik K, Walther G, Vila J, Fernández Brime S (2013) European species of *Hebeloma* section *Theobromina*. Fungal Diversity 58: 103–126. https://doi.org/10.1007/s13225-012-0188-3

Eberhardt U, Beker HJ, Vila J, Vesterholt J, Llimona X, Gadjieva R (2009) *Hebeloma* species associated with *Cistus*. Mycological Research 113: 153–162. https://doi.org/10.1016/j.mycres.2008.09.007

Edler D, Klein J, Antonelli A, Silvestro D (2019) raxmlGUI 2.0 beta: a graphical interface and toolkit for phylogenetic analyses using RAxML. bioRxiv. https://doi.org/10.1101/800912

Grilli E, Beker HJ, Eberhardt U, Schütz N, Leonardi M, Vizzini A (2016) Unexpected species diversity and contrasting evolutionary hypotheses in *Hebeloma* sections *Sinapizantia* and *Velutipes* in Europe. Mycological Progress 15: 1–46. https://doi.org/10.1007/s11557-015-1148-6

Kalyaanamoorthy S, Minh BQ, Wong TKF, von Haeseler A, Jermiin LS (2017) Fast model selection for accurate phylogenetic estimates. Nature Methods 14: 587–589. https://doi.org/10.1038/nmeth.4285

Kaounas V, Assyov B, Alvarado P (2011) New data on hypogeous fungi from Greece with special reference to *Wakefieldia macrospora* (Hymenogasteraceae, Agaricales) and *Geopora clausa* (Pyronemataceae, Pezizales). Mycologia Balcanica 8: 105–113.

Katoh K, Rozewicki J, Yamada KD (2017) MAFFT online service: multiple sequence alignment, interactive sequence choice and visualization. Briefings in Bioinformatics bbx108: 1–7. https://doi.org/10.1093/bib/bbx108

Kauff F, Lutzoni F (2002) Phylogeny of the Gyalectales and Ostropales (Ascomycota, Fungi): among and within order relationships based on nuclear ribosomal RNA small and large subunits. Molecular Phylogenetics and Evolution 25: 138–156. https://doi.org/10.1016/S1055-7903(02)00214-2

Kropp BR (2015) A Samoan *Hebeloma* with phylogenetic ties to the western Pacific. Mycologia 107: 149–156. https://doi.org/10.3852/14-047

Kuhar F, Smith ME, Mujic A, Truong C, Nouhra E (2017) A systematic overview of (Agaricales) in the Nothofagaceae forests of Patagonia. Fungal Biology 121: 876–889. https://doi.org/10.1016/j.funbio.2017.06.006

Lanfear R, Calcott B, Kainer D, Mayer C, Stamatakis A (2014) Selecting optimal partitioning schemes for phylogenomic datasets. BMC Evolutionary Biology14: e82. https://doi.org/10.1186/1471-2148-14-82

Lanfear R, Calcott B, Ho SYW, Guindon S (2012) PartitionFinder: combined selection of partitioning schemes and substitution models for phylogenetic analyses. Molecular Biology and Evolution 29: 1695–1701. https://doi.org/10.1093/molbev/mss020

Larsson A (2014) AliView: a fast and lightweight alignment viewer and editor for large data sets. Bioinformatics 30: 3276–3278. https://doi.org/10.1093/bioinformatics/btu531

Lee SS (2017) A Field Guide to the Larger Fungi of FRIM. Forest Research Institute Malaysia, Kepong, Selangor, Malaysia.

Lee SS, Alias SA, Jones EGB, Zainuddin N, Chan HT (2012) Checklist of Fungi from Malaysia. Forest Research Institute Malaysia, Kepong, Selangor.

Massee GE (1898) Fungi exotici, I. Bulletin of Miscellaneous Informations of the Royal Botanical Gardens Kew 1898: 113–136. https://doi.org/10.2307/4115483

Miller MA, Pfeiffer W, Schwartz T (2010) Creating the CIPRES science gateway for inference of large phylogenetic trees. In: Xavier J (Ed.) 2010 Gateway Computing Environments Workshop (GCE) Proceedings of a meeting held 14 Nov 2010, New Orleans, Louisiana, USA. Institute of Electrical and Electronics Engineers (IEEE), Piscataway, New Jersey, 8 pp. https://doi.org/10.1109/GCE.2010.5676129

Nguyen L-T, Schmidt HA, von Haeseler A, Minh BQ (2015) IQ-TREE: A fast and effective stochastic algorithm for estimating Maximum Likelihood phylogenies. Molecular Biology and Evolution 32: 268–274. https://doi.org/10.1093/molbev/msu300

Örstadius L, Ryberg M, Larsson E (2015) Molecular phylogenetics and taxonomy in Psathyrellaceae (Agaricales) with focus on psathyrelloid species: introduction of three new genera and 18 new species. Mycological Progress 14(25): 1–42. https://doi.org/10.1007/s11557-015-1047-x

Paul V, Sudin M, Fui FS, Kassim MHS, Seelan JSS (2019) Macrofungi of Imbak Canyon-Batu Timbang Area, Sabah. Journal of Tropical Biology and Conservation 16: 107–117. https://jurcon.ums.edu.my/ojums/index.php/jtbc/article/view/2031/1325

Pegler DN (1975) A revision of the Zanzibar Agaricales described by Berkeley. Kew Bulletin 30: 429–442. https://doi.org/10.2307/4103067

Rambaut A (2006–2018) FigTree. Tree figure drawing tool version 14.4.4. Institute of Evolutionary Biology, University of Edinburgh, Edinburgh. http://tree.bio.ed.ac.uk/software/figtree/

Rees BJ, Midgley DJ, Marchant A, Lerkins A, Orlovich DA (2013) Morphological and molecular data for Australian *Hebeloma* species do not support the generic status of *Anamika*. Mycologia 105: 1043–1058. https://doi.org/10.3852/12-404

Richard F, Roy M, Shahin O, Sthultz C, Duchemin M, Joffre R, Selosse M-A (2011) Ectomycorrhizal communities in a Mediterranean forest ecosystem dominated by *Quercus ilex*: seasonal dynamics and response to drought in the surface organic horizon. Annals of Forest Science 68: 57–68. https://doi.org/10.1007/s13595-010-0007-5

Ronquist F, Huelsenbeck JP, Teslenko M (2011) Draft MrBayes version 3.2 Manual: Tutorials and Model Summaries. http://mrbayes.sourceforge.net/mb3.2_manual.pdf

Ronquist F, Teslenko M, Van der Mark P, Ayres DL, Darling A, Höhna S, Larget B, Liu L, Sucharard MA, Huelsenbeck JP (2012) MrBayes 3.2: Efficient Bayesian phylogenetic inference and model choice across a large model space. Systematic Biology 61: 539–542. https://doi.org/10.1093/sysbio/sys029

Samsudin NIP, Abdullah N (2019) Edible mushrooms from Malaysia; a literature review on their nutritional and medicinal properties. International Food Research Journal 26: 11–31. http://www.ifrj.upm.edu.my/

Schoch CL, Seifert KA, Huhndorf S, Robert V, Spouge JL, Levesque CA, Chen W, Fungal Barcoding Consortium (2012) Nuclear ribosomal internal transcribed spacer (ITS) region as a universal DNA barcode marker for Fungi. Proceedings of the National Academy of Sciences 109: 6241–6246. https://doi.org/10.1073/pnas.1117018109

Silvestro D, Michalak I (2012) raxmlGUI: a graphical front-end for RAxML. Organisms Diversity and Evolution 12: 335–337. https://doi.org/10.1007/s13127-011-0056-0

Stamatakis A (2014) RAxML Version 8: a tool for phylogenetic analysis and post-analysis of large phylogenies. Bioinformatics 30: 1312–1313. https://doi.org/10.1093/bioinformatics/btu033

Tedersoo L, Smith ME (2013) Lineages of ectomycorrhizal fungi revisited: Foraging strategies and novel lineages revealed by sequences from belowground. Fungal Biology 27: 83–99. https://doi.org/10.1016/j.fbr.2013.09.001

Tham FY, Watling R (2017a) Annotated checklist of macrofungi recorded from Singapore: Singapore Botanic Gardens. The authors, Singapore.

Tham FY, Watling R (2017b) Annotated checklist of macrofungi recorded from Singapore: MacRitchie-Pierce. The authors, Singapore.

Tham FY, Watling R (2017c) Annotated checklist of macrofungi recorded from Singapore: Bukit Timah. The authors, Singapore.

Tham FY, Watling R (2017d) Annotated checklist of macrofungi recorded from Singapore: Mandai-Seletar. The authors, Singapore.

Thomas KA, Peintner U, Moser MM, Manimohan P (2002) *Anamika*, a new mycorrhizal genus of Cortinariaceae from India and its phylogenetic position based on ITS and LSU sequences. Mycological Research 106: 245–251. https://doi.org/10.1017/S0953756201005445

Turland NJ, Wiersema JH, Barrie FR, Greuter W, Hawksworth DL, Herendeen PS, Knapp S, Kusber W-H, Li D-Z, Marhold K, May TW, McNeill J, Monro AM, Prado J, Price MJ, Smith GF [Eds] (2018) International Code of Nomenclature for algae, fungi, and plants (Shenzhen Code) adopted by the Nineteenth International Botanical Congress Shenzhen, China, July 2017. Koeltz Botanical Books, Glashütten. https://doi.org/10.12705/Code.2018

Vesterholt J (2005) The Genus *Hebeloma*. Fungi of Northern Europe 3. Svampetryk, Tilst.

Vesterholt J, Eberhardt U, Beker HJ (2014) Epitypification of *Hebeloma crustuliniforme*. Mycological Progress 13: 553–562. https://doi.org/10.1007/s11557-013-0938-y

Vesterholt J, Gryta H, Marmeisse R, Beker HJ, Eberhardt U, Grilli E, Boyle H (2009) (1899) Proposal to conserve the name *Hebeloma cylindrosporum* against *Hebeloma angustispermum* (Basidiomycota). Taxon 58: 1005. https://doi.org/10.1002/tax.583034

Voto P (2019) Novelties in the family Psathyrellaceae. Part I. Rivista Micologica Romana, Bolletino dell'Associazione Micologica Ecologica Romana 107: 94–95.

Yang ZL, Matheny PB, Ge Z-W, Slot JC, Hibbett DS (2005) New Asian species of the genus *Anamika* (Euagarics, hebelomatoid Clade) based on morphology and ribosomal DNA sequences. Mycological Research 109: 1259–1267. https://doi.org/10.1017/S0953756205003758